

Total synthesis of Epicoccolide A & B and two related analogs

Dissertation

zur

Erlangung des Doktorgrades (Dr. rer. nat.)

der

Mathematisch-Naturwissenschaftlichen Fakultät

der

Rheinischen Friedrich-Wilhelms-Universität Bonn

vorgelegt von

Tim Treiber

aus El Paso, Texas

Bonn 2025

Angefertigt mit der Genehmigung der Mathematisch-Naturwissenschaftlichen Fakultät der Rheinischen Friedrich-Wilhelms-Universität Bonn

Gutachter/Betreuer: Prof. Dr. Dirk Menche Gutachterin: Junior Prof. Dr. Ala Bunescu

Tag der Promotion: 23.10.2025

Erscheinungsjahr: 2025

Erklärung
Ich versichere, dass ich die vorliegende Arbeit unter Einhaltung der Regeln guter wissenschaftlicher Praxis selbstständig verfasst, keine anderen als die angegebenen Quellen und Hilfsmittel benutzt, sowie die Zitate kenntlich gemacht habe. Bonn, 2025
Tim Treiber

Acknowledgements

I want to thank many people for their continuous support throughout the years. Without your help this thesis would not have been possible!

First and foremost, I want to thank Prof. Dr. Dirk Menche for providing me with this interesting and exciting topic. The possibility to continue the total synthesis and finally bring it to an end resulted in a great journey over the last few years. Thank you for allowing me to work at my own pace without ever pressuring for results and making it possible to explore a wide variety of synthetic opportunities. You were always there for useful tips and new insights on the topic whenever I asked for help.

Next, I want to thank Junior Prof. Dr. Ala Bunescu for being the second reviewer of this thesis, Prof. Dr. Moritz Sokolowski for accepting the role of chair of the examination committee and Prof. Dr. Michael Gütschow for being the non-specialist member of the committee. Thank you for your participation in my examination board.

I also want to thank the entire working group I was a part of in addition to the *Krbek* group that worked in the same laboratory wing. You were always there for advice or just casual conversations whenever I came around to chat. Namely I want to thank Jonas, my former mentor, who always provided excellent advice at every point. Our coffee breaks together were a great time to regularly catch up and talk about many different topics. Furthermore, I want to thank Max G., my lab partner for many years, for a pleasant time working next to each other and I want to thank Torben for lots of conversations inside and outside of the lab that did not always have to be about work. I want to thank my bachelor and master interns Tim and Felicitas for their motivated and independent working style during their respective thesis.

I want to thank the teams of the central analytics department of the university of Bonn for their continuous work in the NMR- and mass spectrometry department. A very special thanks is for Andreas Schneider from the HPLC pool. Thanks to your your expertise and finesse the purification of my final compounds turned out to be excellent. Furthermore, your introductory course into the world of HPLC showed the amount of effort you invested into the purification steps.

Finally, I want to thank my family for their everlasting encouragement and interest in my work.

I appreciate your constant support over all the years and thank you for motivating me and

always believing in me. Thank you to my friends for also providing support and distractions when I needed them. Much love and cuddles go out to my cute pet rats that eagerly waited for my return every single day to play and snuggle up.

The biggest thanks of all goes to my fiancée Wing-Si, who was by my side for the entire time. You encouraged me, gave me motivation and provided support no matter the situation. Thank you for standing by me during all the highs and lows of the PhD, constantly loving me with all your heart. You always believed in me and provided valuable insights whenever I asked for your help.

Thank you everybody very much for all your support!

Summary

The family of epicoccolides has been known for over a decade now and show remarkable biological properties in a variety of fields. Different groups have reported antibacterial, antifungal and antitumor reactivity. More recently, an inhibition of galactosylceramide sulfotransferase by epicoccolide B was patented. This sulfotransferase is involved in the very rare but deadly disease metachromatic leukodystrophy. To be able to use the mentioned biological activities it is essential to gain access to large amounts of the desired natural product. Extraction from nature is a costly and time-consuming venture and no reliable source for the required material. To provide a solution for this problem a successful total synthesis of the natural products epicoccolide A and epicoccolide B was the goal of this thesis.

Efforts into the total synthesis of epicoccolide B have been invested by previous members of our working group and were continued. The first total synthesis of epicoccolide B was achieved after investigating several different routes with varying outcomes and a multitude of challenges that needed to be overcome. In the course of these investigations two structural analogs were synthesized as well.

After the final step of the total synthesis epicoccolide B showed interesting and unprecedented reactivity under mild aqueous conditions. The outcome and reproducibility of this reaction was examined in detail leading to the first total synthesis of epicoccolide A. Comparison of synthetic epicoccolide A to reported literature resulted in structural reassignment and questioning of the previously proposed biosynthetic pathways. To clear up these problems, plausible answers have been provided including a newly proposed biosynthesis.

First attempts at the total synthesis of epicocconigrone A were also initiated but exceeded the final scope of this thesis. The project was handed off to a new member of our working group with the current plans presented herein. Finally, initial testing of the bioactivity of the two structural analogs synthesized during the course of this project revealed valuable data that is worthwhile to be pursued further.

Table of contents

1.	Introduction	1
	1.1 Natural products and their importance for pharmaceuticals and beyond	1
	1.2 The importance of total synthesis	2
	1.3 The family of epicoccolides and their bioactivity	3
	1.4 A unique tetracyclic core	7
2.	Past accomplishments	. 11
	2.1 Synthesis of the tetracyclic core of epicoccolide A (1) and integrastatin B (8)	. 11
	2.2 Contributions to the total synthesis of epicoccolide B by Simon Dedenbach	. 14
	2.3 Contributions to the total synthesis of epicoccolide B by Wing-Si Li	. 16
3.	Objectives	. 19
4.	Results and discussion	. 21
	4.1 Continuing the route established by Wing-Si Li	. 21
	4.1.1 Reproducing the boronic ester synthesis and modifying the sequence	. 22
	4.1.2 Finishing the benzofurane fragment	. 23
	4.1.3 Coupling of borane and benzofurane followed by the final steps	. 27
	4.2 New retrosynthetic approach to epicoccolide B	. 33
	4.2.1 Synthesis of the new fragments	. 34
	4.2.2 Sonogashira coupling and establishing key cyclisation	. 36
	4.3 Final adaptation to the total synthesis of epicoccolide B	. 39
	4.3.1 Synthesis of the adjusted fragments	. 39
	4.3.2 Finishing the total synthesis of epicoccolide B	. 41
	4.4 Unexpected reaction of epicoccolide B observed	. 45
	4.4.1 Oxidation of epicoccolide B under controlled environment	. 47
	4.4.2 Comparing synthetic epicoccolide A to the literature	. 49
	4.4.3 Detailed NMR-analysis of synthetic epicoccolide A	. 53
	4.5 A very fast route to the core structure	. 54
	4.6 First attempts of synthesizing epicocconigrone A	. 55

	4.6.1 Fragment synthesis and coupling	55
	4.6.2 Revised approach to epicocconigrone A	57
	4.6.3 Different cyclisation attempts for core structure	59
	4.7 Bioactivity assays of epicoccolide A & B and the two analogs	61
5.	Conclusion and outlook	63
6.	Experimental part	67
	6.1 Materials and methods	67
	6.2 Experimental procedures	69
	6.2.1 Relevant to chapter 4.1	69
	6.2.2 Relevant to chapter 4.2	93
	6.2.3 Relevant to chapter 4.3	. 100
	6.2.4 Relevant to chapter 4.4	. 108
	6.2.5 Relevant to chapter 4.5	. 110
	6.2.6 Relevant to chapter 4.6	. 112
7.	List of abbreviations	. 115
8.	References	. 119
Αp	ppendix	. 127
	NMR-Spectra	127

1. Introduction

1.1 Natural products and their importance for pharmaceuticals and beyond

Natural products are every single compound that can be isolated from nature. This can be from edible things like apples, inedible things like dirt and wood or even microscopic organisms such as bacteria or fungi. The list of places where one can find natural products is endless. Many of these compounds are thoroughly researched or even commercially available, e.g. simple citric acid. In the case of organic natural products, they can be classified as either primary or secondary metabolites. Primary metabolites are essential for life of the organism and basically needed every single day. Some of the most common and known primary metabolites are amino acids, sugars and lipids.¹

Secondary metabolites however are not directly essential for the metabolism of the organism they are found in. For many compounds their purpose within an organism is still unclear and needs in-depth research. The biosynthesis and mode of operation for the majority of the representatives of these compounds has yet to be clarified presenting a fascinating research area. Many known secondary metabolites show interesting antibacterial or other bioactive properties.¹

Two of the known applications of secondary metabolites for an organism are as a defense mechanism against external threats or as a signaling substance.² The antibacterial properties of some secondary metabolites can be used to fend off diseases for an organism. Instead of antibacterial properties some secondary metabolites have presented antifungal properties such as extracts of an endophytic fungus of the genus *Epicoccum*.³ This particular fungus has a symbiotic relation with the cocoa tree *Theobroma cacao*. The fungus is harbored in the tree but in return some of its secondary metabolites protect the tree from phytopathogenic fungi and other dangers. This kind of symbiotic system can be used as an inspiration for the development of new natural fungicides and pesticides.

In case of antibacterial compounds, the oldest known natural antibiotic is penicillin. It is formed as a secondary metabolite by a fungus of the genus *Penicillium*.⁴ This discovery of antibiotics led to the possibility to treat bacterial infections for the first time. This in turn caused a significant increase in life expectancy for humans and animals. In livestock farming antibiotics are used as a precaution before any infections can start spreading. Additionally, some antibiotics are used as growth-promoting agents in large quantities. This overuse of antibiotics in livestock farming, in many cases due to missing regulations or controls, leads to an absorption of residual amounts through the consumption as food. As a result, a habituation effect of these antibiotics can be observed reducing their effectiveness, even up to a point of complete ineffectiveness. Furthermore, an overuse or misuse in human medicine carries a large risk of developing multi-resistant bacteria strains.⁵ The constant increase of multi-

1. Introduction

resistant bacteria and other pathogens is a rising concern all across the world.⁶ This problem cannot be solved by regulation of existing antibiotics alone but rather has to be addressed differently. New compounds have to be found, researched and optimized yield further options in battling this global challenge.

Sadly, bacteria are not the only type of pathogen that can infect humans and animals. Another major class of pathogens are fungi. Before it was common knowledge to only treat bacteria with antibiotics they were also used for many other kinds of infections, e.g. also for fungal infections. This was also a cause for the problems mentioned above. Only few targeted medicines that can be used for fungal infections exist compared to the number of available antibiotics. Compared to the amount of resistant pathogens the quantity of therapeutically used antifungals is negligible. Not only humans can be infected with fungi but especially plants can be vulnerable without proper fungicides. Many phytopathogenic fungi exist that can devastate crops and obliterate entire harvests. Combined with a constantly growing world population and the resulting increase in demand for food the development of new fungicides and antifungals for plants and humans is of great interest.

Lastly another disease that plagues humankind are tumors. They exist in many different forms and places making it very difficult to target therapy and research in general. A widely used method is chemotherapy, which targets the cancer cells directly or sometimes indirectly to reduce or even revers growth. One kind of chemotherapeutic drugs are protein kinase inhibitors. Many secondary metabolites are tested regarding their activity as protein kinase inhibitors in the hope of finding new potential structures for the development of novel chemotherapeutics.

All of the fields mentioned above and more are constantly expanding and evolving. With increasing demand due to resistances and growing population the need for new, suitable drugs is continuously rising. To meet this demand already isolated secondary metabolites are investigated and the search for novel compounds that exhibit relevant bioactivity is never ending. Still, the discovery is just the first step on a long road for the development of new therapeutically active substances.

1.2 The importance of total synthesis

Once a secondary metabolite of interest is found extensive testing of bioactivity and cytotoxicity needs a reasonably large amount of the compound. These substances are usually extracted as a mixture of several compounds that need to be separated and purified. The process of separation and purification is extremely tedious and expensive while only yielding a very small amount of the desired secondary metabolite. Often the other isolated materials are not even of any interest and are considered waste product. In many cases this small amount of extract is enough for an initial analysis and activity testing but not a sufficient amount for detailed *in vitro* and *in vivo* testing.

Additionally, the function and mode of operation of the new compounds in the human body are of major interest. Knowledge of the interaction at a cellular level can help improve the structure by molecular modification to reduce undesired cytotoxicity and increase the desired bioactivity and stability within a living organism. The (quantitative) analysis of the structure-activity relationships (Q)SAR of a compound can be used to identify the pharmacophore of a specific active substance. The pharmacophore encompasses all the steric and orderly alignments of an active substance in relation to a pharmacological target structure, while ensuring optimized supramolecular interactions. The term pharmacophore is often used synonymously, but incorrectly, to describe certain structural elements within an active substance. These elements should alternatively be named the lead structure of the active substance.

The bioactive secondary metabolites mentioned before have some kind of lead structure that results in their desired activity, but only in very rare cases that encompasses the entire molecular structure. Usually, the lead structure is only part of the natural product and other parts are irrelevant or even hindering. The determination of the lead structure and eventual modifications thereof can only be done after SAR-studies are carried out. This process generally requires more material than the extraction from nature can provide, especially when the access is limited.

To supply enough material for extensive activity and SAR studies a successful total synthesis of the desired compound is crucial. The goal of natural product synthesis is to provide a way to produce the active compound starting from industrially available, ideally cheap substances using efficient reactions. Additionally, a modular route provides easier access to structure modification and the synthesis of analogs, a pivotal part of SAR studies. This shows that the research area of natural product synthesis is of key importance for the development of new active substances.

In conclusion, many secondary metabolites that exhibit antibiotic or other useful activity are cytotoxic as well making them unsuitable for use as pharmaceutical products. Their structure needs to be modified accordingly to shift their biological activity, which is only possible after the lead structure has been identified. This is made possible by a modular total synthesis of the natural product.

1.3 The family of epicoccolides and their bioactivity

A promising and potent family of substances for tackling the aforementioned challenges (chapter 1.1) are the epicoccolides, which were found in different strains of the endophytic fungus *Epicoccum*. Epicoccolide A (1) and epicoccolide B (2) together with epicolactone (3) and their postulated biosynthetic precursor flavipin (4) were found in *Epicoccum* sp. CAFTBO in 2013 by *Laatsch*.³ Additionally, epicocconigrone A (5) and epicocconigrone B (6), together with some of the other compounds, were found in *Epicoccum nigrum* in 2014 by *Proksch* (Figure 1).¹⁰ Epicoccolide B (2)

1. Introduction

however was already known since 2005 after being isolated from the fungus *Aspergillus flavipes* ST003878 (DSM 15290)¹³ and presents the main target of this work. It demonstrates the most divers biological activity of the epicoccolide family.

Figure 1: All relevant compounds isolated from two different strains of *Epicoccum* fungus.

1, **2** and **3** showed antimicrobial activities against *E. coli* and multiresistant strains of *B. subtilis* and *S. aureus* (Table 1).³

Table 1: Antimicrobial activities of 1-3 (diameters of growth inhibition zone [mm])[a].3

compound	E. coli	B. subtilis	S. aureus
1	10	8	n.a.
2	14	n.a.	16
3	16	13	n.a.

[[]a] 40 µg per paper disk with 9 mm diameter. n.a.: not active at 40 µg per paper disk.

E. coli is one of the most common causes for bacterial infections for humans. ¹⁴ *B. subtilis* can also cause infections but only in very rare cases. ¹⁵ *S. aureus* usually leads to an asymptomatic colonization of the host (humans and animals). In case of a weak immune system however some severe or even lethal infections can occur like Pyomyositis ¹⁶, Mastitis ¹⁷ or sepsis. Especially strains which are multiresistant against common antibiotics cause major complications in the treatment of these occurrences.

The same compounds also showed significant growth inhibition of two different tested peronosporomycete phytopathogens (*P. ultimum* and *A. cochlioides*) and another plant pathogenic fungus (*R. solani*) (Table 2).³ All three of these plant pathogenic fungi can be the source of major croploss and ruin an entire harvest.

Table 2: Antifungal activities of 1-3 in agar diffusion tests (estimated MICs in μg per paper disk).³

compound	P. ultimum	A. cochlioides	R. solani
1	40	40	80
2	40	>40	20
3	40	20	40

Furthermore, epicocconigrone A (5) and epicoccolide B (2) were tested *in vitro* for their protein kinase inhibition as well as histone deacetylase inhibition (Table 3 & Table 4).¹⁰

Table 3: Protein kinase inhibition activities of compounds 2 & 5 (IC $_{50}$ [μ M]) $^{[a]}$. 10

compound	AKT1	ALK	ARK5	Aurora-B	AXL	FAK	IGF1-R	MEK1 wt
2	4.07	0.25	3.77	7.29	0.22	0.80	0.15	>30
5	2.15	0.18	2.51	2.51	.016	0.42	0.07	>30
	MET wt	NEK2	NEK6	PIM1	PLK1	PRK1	SRC	VEGF-R2
2	1.12	3.78	1.85	4.44	6.31	9.00	0.49	0.39
5	0.58	1.83	0.52	3.10	3.18	4.48	0.37	0.32

 $^{^{[}a]}$ IC₅₀ values were calculated from the inhibitory dose-response curves using the solvent DMSO set to 100% activity and the negative control without enzyme set to 0% activity.

Table 4: Inhibitory effects of compounds 2 & 5 on HDAC activities (IC₅₀ [μM])^[a].¹⁰

		class I				clas	ss IIb	class IV
compound	total	HDAC1	HDAC2	HDAC3	HDAC8	HDAC6	HDAC10	HDAC11
2	14.2±3.9	8.8±1.7	9.1±0.6	6.9±0.0	2.1±0.2	6.5±0.2	8.1±0.6	12.9±1.5
5	9.8±3.0	8.6±0.8	10.0±1.2	12.4±1.0	1.6±0.1	4.6±0.1	8.4±2.0	11.7±1.6

 $^{^{[}a]}$ IC₅₀ values were calculated from the inhibitory dose-response curves using the solvent DMSO set to 100% activity. Values are the mean \pm SD of three independent experiments.

Both of these kinds of inhibition can play a role in anticancer therapy development. For example, ALK is a receptor tyrosine kinase, which is known to be involved in several human tumors. AXL overexpression is connected to myelogenous leukemia and other carcinomas, for example colon, breast and lung cancer. An increased expression of FAK shows correlation with an increased invasiveness and malignancy for some human tumors. The link of most of these protein kinases to some form of human tumor and their progression was already thoroughly researched.

By regulating the acetylation levels of various proteins, histone deacetylase enzymes play a vital role in numerous cellular processes, including gene expression, cell mobility, and the modulation of transcription factor activities. An alteration of their activity, especially an overactivity, can be connected to the aggressiveness of a tumor as well as their general development. Hence, the compounds that show the ability to inhibit these functions are promising candidates for anticancer research.^{30–34}

The most recent and most relevant discovery was the very potent inhibition (1.1±0.1 μM) of the galactosylceramide-sulfotransferase by epicoccolide B (2).³⁵ This sulfotransferase is a potential target for substrate reduction therapy of metachromatic leukodystrophy, a rare lysomal storage disease.^{36,37} Metachromatic leukodystrophy (MLD) is a disease caused by a deficient activity of arylsulfatase A (ASA). ASA is responsible for the degradation of 3-O-sulfogalactosyl ceramide (sulfatide). An impairment of the ASA function causes an accumulation of sulfatide which clinically leads to a progressive demyelination (destruction of the central nervous system) and ensuing neurological

1. Introduction

symptoms. Every form of MLD results in a progressive deterioration of neurodevelopment and consequently a decrease of neurocognitive function.³⁸ This deterioration vastly impacts the quality of life and often causes death within a few years depending on the age of onset.³⁹

Regarding treatment many advances have been made in the past few years but the possibilities are far from exhausted. The most commonly encountered treatment for MLD is a rather new gene therapy approved by the FDA.⁴⁰ The success of this gene therapy does not come without its downsides. Although the treatment is comparably safe and very effective for patients in a presymptomatic stage the criteria for being eligible are very hard to fulfill. For the late-infantile subtype MLD has to be diagnosed in a presymptomatic stage, which is not without its challenges. In later onset stages (e.g. early-juvenile subtype) the patient needs to be in a pre/early symptomatic stage with no evidence of cognitive decline, among other things. 41 An alternative treatment option is providing the deficient ASA to combat the reduced activity. This method and variations of it all run into the same difficulty, which is the poor permeability of the blood-brain barrier (BBB). 35,39 The alternative to circumvent this problem is small-molecule therapy. Small molecules can cross the BBB more easily and don't need to target the deficient ASA but can reduce the production of sulfatides directly. The sulfatide mentioned before is produced by the enzyme galactosylceramide-sulfotransferase, which can be inhibited by epicoccolide B (2). So rather than targeting the accumulation of sulfatide and their deficient degradation the proposed small-molecule therapy relies on the inhibition of the production of the sulfatide itself.35

1.4 A unique tetracyclic core

Epicoccolide A (1) and epicocconigrone A (5) have a very rare, almost unique core structure consisting of a [6,6,6,6]-tetracycle with two oxygen bridges forming an acetal at C-1 (Figure 2).

Figure 2: All known natural products with the unique tetracyclic core (highlighted in red). 3,10,42,43

The same tetracyclic core can only be found in the structurally close Integrastatin A (7) and B (8) and the non-related chartarolides A (9) and B (10). 42,43 To this date no other natural products with the same core have been reported, showing the uniqueness of the structural motif. The proposed absolute and relative configuration shown above have been determined by NOE- & ROESY correlations together with various modeling and calculations. 3,10,42,43 These configurations have however not been confirmed by crystal structure analysis for any of the compounds since crystallizing these compounds poses significant challenges. The relative configuration of H-1 and H-9 was determined to be *cis* for all natural products. This was confirmed by simple NOE/ROESY experiments and can also be explained by the massive ring strain the *anti*-conformation would inherit. For compounds 1, 9 and 10 ECD-spectra were measured and compared to model calculations with defined absolute configurations. These comparisons were used to assign the absolute configurations shown above. The configuration for the tetracyclic core will be omitted in the remainder of the thesis unless specifically relevant. This is intended to give a clear differentiation between stereospecific and non-stereospecific reactions. The relative configuration between H-1 and H-9 will always be assumed to be *cis* unless stated otherwise.

1. Introduction

A confirmed biosynthesis for any of these compounds has not yet been reported but several different pathways were proposed. For **1** an unsymmetrical benzoin condensation of two flavipin (**4**) molecules is postulated forming intermediate **11** followed by an acetal formation to **12** and cyclization (Scheme 1).³

Scheme 1: Proposed biosynthesis for epicoccolide A (1) via an unsymmetrical benzoin condensation.3

The proposed biosynthesis for **9** and **10** is very similar. Instead of a benzoin condensation a pinacol coupling of two aldehydes (**13a** & **14**) and an acetalization are the first step leading to **15**, which then cyclizes to **9** (Scheme 2).⁴³ Only one isomer is shown, although the other one works analog to this with inverted stereochemistry.

Scheme 2: Proposed biosynthesis for chartarolides A (9) and B (10). Only one isomer shown here. 43

The suggested biosynthesis for integrastatin A (7) and B (8) takes a completely different approach starting with the condensation of nine acetate units (16). Following aromatization to 17 and further cyclization to 18 gives a potential precursor for the integrastatins (Scheme 3).⁴²

Scheme 3: Proposed biosynthesis for integrastatins A (7) and B (8).42

Finally, I propose a new biosynthetic route for **1** via an oxidative benzofurane rearrangement of **2** in a single step. The benzofurane is oxidized to epoxide **19** which opens leading to a brief dearomatization (**20**) followed by a 4+2 cycloaddition resulting in the tetracyclic core and epicoccolide A (Scheme 4).

Scheme 4: Proposed biosynthesis of epicoccolide A (1) via an oxidative benzofurane rearrangement.

This theory would be supported by the fact that both **1** and **2** were isolated from the same strain of *Epicoccum* and the same reaction was used for the total synthesis of integrastatin B (**8**) albeit with protecting groups (chapter 2.1).⁴⁴ Hence, one of the goals of this work is to achieve this reaction in a possibly biomimetic way giving further insights into the potential biosynthesis.

All four of these postulated biosynthetic pathways to the tetracyclic core are plausible but none of them have been verified so far. Considerable efforts have been invested in the synthesis of this unique core structure but no total synthesis of 1 has been reported so far.

2. Past accomplishments

2.1 Synthesis of the tetracyclic core of epicoccolide A (1) and integrastatin B (8)

Considerable efforts have been invested into the synthesis of the unique [6,6,6,6]-tetracycle but no total synthesis has been reported so far for epicoccolide A (1) and epicocconigrone A (5). The total synthesis of integrastatin B (8) was accomplished and reported by *Ramana et al.* in 2016 after extensive research.⁴⁴ All accomplishments for the unique core structure will be presented in a chronological fashion starting with the oldest publication.

Shortly after the discovery of integrastatins A (**7**) and B (**8**) in 2002⁴² the first synthesis of the tetracyclic core was already reported in 2003 by *Taylor*. Key steps include a *Ramberg-Bäcklund* reaction followed by a *Lewis* acid promoted cyclization (Scheme 5).⁴⁵

Scheme 5: First synthesis of the tetracyclic core by a *Ramberg-Bäcklund* reaction and *Lewis* acid mediated cyclization.⁴⁵

Sulfone **21** is transformed to the desired *Z*-olefin **22** via a *Ramberg-Bäcklund* reaction. Only the *Z*-olefin reacts in the following cyclization. Interestingly, the oxidation state of the acetophenone has an impact on the ratio of E/Z for the double bond. The benzylic alcohol gives significantly better yields and ratio (88%, E/Z = 1:16) compared to the ketone (50%, E/Z = 1:8). Subjecting **22** to tin(II) chloride leads to the deprotection of the benzyl protecting group and hemi-acetal formation with the ketone to intermediate **23**. The hemi-acetal then reacts with the double bond to form the tetracyclic core **24** without the ketone at C-8. Subsequent oxidation completes the desired core **25** in an efficient manner.⁴⁵

A few years later in 2008 *Ramana* published a synthesis of the tetracyclic core by using a pinacol coupling and an intramolecular acetal formation (Scheme 6).⁴⁶

2. Past accomplishments

Scheme 6: Second synthesis of the tetracyclic core by a pinacol coupling of an aldehyde (13b) with a ketone (26).⁴⁶

The pinacol coupling was done with *o*-phthalaldehyde (**13b**) and *o*-hydroxy acetophenone (**26**) resulting in the intermediate **27** that immediately undergoes acetal formation to **28**. Finally, **28** can be oxidized to ketone **29** finishing the tetracycle with one of the two methyl groups present in the integrastatins. ⁴⁶ The same sequence was also done without the methyl group present resulting in the tetracyclic core of epicoccolide A (**1**) and epicocconigrone (**5**), however, **1** and **5** were not known yet at the time. It is possible that this route inspired the postulated biosynthesis of chartarolides A and B as the reaction path is identical (Scheme **2**). ⁴³

In 2011 Stoltz reported a palladium-based Wacker-type cyclization of diol 30 (Scheme 7).⁴⁷

Scheme 7: Third synthesis of the tetracyclic core by a Wacker-type cyclization.⁴⁷

The diol **30** is subjected to catalytic amounts of PdCl₂ and CuCl₂ under an oxygen atmosphere which leads to a cyclization, most likely through intermediate **31**. Phenol **31** can then in turn cyclize intramolecular onto the enol ether giving the core structure **24**.⁴⁷ The oxidation of **24** was already published by *Taylor* before (Scheme 5).⁴⁵

Later on, *Ramana* published another possible route to the tetracyclic core utilizing an oxidative benzofurane dearomatization cascade (Scheme 8).⁴⁸

Scheme 8: Synthesis of the tetracyclic core by a single-step oxidative benzofurane rearrangement.⁴⁸

Benzofurane **32** was treated with Oxone® and sodium bicarbonate in a mixture of acetone and water directly rearranging to the desired tetracyclic core (**25/33**). This was done both with and without the methyl groups present giving direct access to the core of epicoccolide A as well.⁴⁸ Shortly after, *Ramana* used this reaction for the successful total synthesis of integrastatin B (**8**) as presented in Scheme 9.⁴⁴

Scheme 9: Total synthesis of integrastatin B using the oxidative benzofurane rearrangement. 44

Starting from phenol **34** an esterification with eudesmic acid (**35**) provides the precursor for the first cyclization. Ester **36** is cyclized through a *Fürstner-McMurry* coupling and subjected to *Friedel-Craft* acetylation conditions giving benzofurane **37** in an efficient sequence. Three out of the five phenols are deprotected selectively (**38**) and reprotected with acetate groups (**39**). Following this, the key reaction, namely the oxidative rearrangement, was accomplished in the presence of the acetate protecting groups finishing the tetracyclic core (**40**) through the same route published before. Introduction of the aldehyde and removal of the protecting groups completes the total synthesis of integrastatin B (**8**) in a mere 8 steps with an overall yield of 18%.⁴⁴

2. Past accomplishments

Finally, *Brimble* published an entirely new strategy for composing the tetracyclic core in 2019 employing an umpolung alkylation as the key step (Scheme 10).⁴⁹

Scheme 10: Latest synthesis of the tetracyclic core by an umpolung alkylation reaction of a dithiane (41).49

The basis of the strategy is the umpolung alkylation of dithiane **41** and coupling with aldehyde **42** to give ester **43**. The ester is reduced to the lactol **44** which undergoes an acid-catalyzed cyclization with the *in-situ* deprotected phenol to close the final ring (**45**). The complete tetracyclic core **33** is released by dithiane removal as the last step.⁴⁹

This concludes the current reported pathways to construct the unique [6,6,6,6]-tetracyclic core. Considerable efforts from many different groups have shown success for the total synthesis of integrastatin B (8) but to date no total synthesis has been reported for epicoccolide A (1) and epicocconigrone A (5).

2.2 Contributions to the total synthesis of epicoccolide B by Simon Dedenbach

Another pathway of the postulated biosynthesis of epicoccolide A (1) also leads to epicoccolide B (2). Starting from the asymmetrical benzoin condensation 11 a reductive dehydration followed by acetalization with the ketone (46) instead of immediate acetal formation with the aldehyde leads to 2 (Scheme 11).³

Scheme 11:Biosynthetic proposal for epicoccolide B (2).3

A biomimetically inspired total synthesis was designed our working group based on eudesmic acid (35) and the asymmetrical benzoin condensation. Planning and execution were done by *Simon Dedenbach*,

part of our working group, in the scope of his doctoral thesis. However, a selective asymmetric benzoin condensation is not effective under laboratory conditions since a statistical distribution of the products is highly likely and rather inefficient. Instead, a synthesis inspired by the benzofurane formation in integrastatin B by a *McMurry* reaction was sought after. Sadly, the esterification between fragments **47** and **48** to form **49** was not possible resulting in a stop for this route (Scheme 12).⁵⁰

Scheme 12: First attempt to build the benzofurane by McMurry coupling.⁵⁰

An entirely new route was designed breaking epicoccolide B into two fragments which were combined by a *Suzuki* cross-coupling reaction (Scheme 13).⁵⁰

Scheme 13: Second route for the synthesis of 2.50

Eudesmic acid (35) was transformed into the common precursor 50 by esterification and methylation of the aromatic ring. The benzofurane fragment 51 was synthesized from the precursor 50 by a sequence of steps, namely formylation, selective *o*-deprotection, *Ramirez* homologation and

2. Past accomplishments

cyclization. The boronic ester fragment **52** in turn was assembled by saponification of the ester followed by decarboxylative iodination and *Miyaura*-borylation. Fragment union was achieved by *Suzuki*-coupling and the methyl ester was converted into the aldehyde by reduction and selective oxidation to obtain **53**. For the final steps of the synthesis a global deprotection and late-stage formylation to arrive at epicoccolide B **(2)** were envisioned. Despite testing a broad range of conditions for the deprotection the desired global removal of the methyl groups remained unsuccessful.⁵⁰

At this point the topic was handed over to Wing-Si Li with a small change in strategy.⁵¹

2.3 Contributions to the total synthesis of epicoccolide B by Wing-Si Li

After the difficulties with the deprotection of the methyl groups, the strategy was adjusted to the use of benzyl protection groups. Although being electronically rather different the steric influence of the added phenyl ring on the main aromatic ring is surprisingly small due to the distance caused by -O-CH₂- in between. The cleavage of the benzyl groups in the end can be achieved by reduction with H₂ or using *Lewis* acids.

Following the synthetic plan laid out in Scheme 13 the forward synthesis commenced with slight deviations to accommodate for the change in reactivity (Scheme 14).⁵¹

HO OME
$$K_2CO_3$$
, KI BNO OME $AgCO_2CF_3$ BNO OME BNO OBN BNO OBN BNO OME $AgCO_2CF_3$ BNO OME BNO OME

Scheme 14: Adapted synthesis of the benzyl protected general precursor 57.51

Starting with phenol **54** benzyl protection proceeded smoothly to **55** with a 93% yield in a decagram scale. Several *ortho*-lithiation conditions applied to **55** did not result in the desired product so a two-step sequence was applied. Single iodination to **56** in 84% yield followed by *Negishi* cross-coupling with 66% yield completed the general precursor **57** efficiently and in a gram scale. ⁵¹

The boronic ester fragment was prepared without deviation from the original route (Scheme 15).51

Scheme 15: Synthesis of boronic ester 60.51

Saponification of precursor **57** to acid **58** was successful (95% yield) after temperature elevation (50 °C) compared to the methyl-protected compound **50** (rt.). The crucial decarboxylative iodination of the acid **58** resulted in iodide **59** with a very good yield of 91%. Lastly, fragment **60** is completed by *Miyaura* reaction to introduce pinacol borane onto the aromatic ring. Avoiding the formation of the homo-coupling product boronic ester **60** was obtained in 85% yield. Again, all reactions were performed on a gram scale showing high efficiency and scalability of the route.⁵¹

Synthesis of the benzofurane fragment caused major complications and significant effort had to be invested (Scheme 16).⁵¹

Scheme 16: Partial synthesis of the benzofurane fragment 65.51

Formylation of precursor **57** via various conditions proved to be quite difficult and ultimately was moderately successful using a *Gross-Riche*-formylation giving aldehyde **61** in 43% yield after HPLC-purification. Next, a selective deprotection of C-5 was envisioned but screening of a wide range of conditions either gave no conversion or decomposition with only minor amounts of desired product (<11%). A slight change in the order of reactions was necessary so the *Wittig* reaction was done before any deprotection. Wittig product **62** was isolated in 40% yield and subsequently globally deprotected by TFA (**63**) in a quantitative yield. To finish the fragment cyclization needed to be accomplished (**64**) in addition to the reprotection of the remaining phenols (**65**). An initial attempt of the cyclization was unsuccessful and the reserve of **63** was fully depleted. Resynthesizing the required material was beyond the scope of the project hence the master thesis was concluded.⁵¹

2. Past accomplishments

Significant progress has been made in the synthesis of the required fragments holding benzyl protection groups. Precursor **57** and boronic ester **60** were synthesized in a gram scale with (very) good yields. Preparation of the benzofurane fragment had many difficulties that were ultimately overcome to progress the route several steps up to deprotected geminal dibromide **63**. ⁵¹

3. Objectives

The scope of this thesis includes three different objectives. The first and most important one is the successful total synthesis of epicoccolide B. To achieve this the established route from *Simon Dedenbach* with protecting group changes by *Wing-Si Li* will be continued. An initial synthesis of the building blocks was necessary as the bulk of reserves was depleted by the research of *Wing-Si Li*.⁵¹ A decagram scale of precursor **57** was planned, potentially increasing efficiency and yield of the route. Following this the boronic ester **60** needed to be reproduced, again with reaction optimization if possible (Scheme 17).

Scheme 17: Planned large scale reproduction of building blocks 57 and 60.

The final and more challenging part consisted of finishing the synthesis of benzofurane **65**. After assembling all necessary building blocks the coupling (**66**) and subsequent last steps needed to be examined (Scheme 18).

Scheme 18 Mapped out synthesis of benzofurane 65 and finishing the total synthesis.

After a successful total synthesis of epicoccolide B a single step oxidation of the unprotected natural product to obtain epicoccolide A was envisioned as shown in Scheme 4 (chapter 1.4). This reaction can then in turn be used to potentially verify our proposed biosynthesis and give a protecting group free alternative to the conditions shown by *Ramana* in the total synthesis of integrastatin B (Scheme 9).⁴⁴

Lastly a modular route with potential for diversification is essential for SAR studies later on. Therefore, a flexible and adaptable total synthesis is very advantageous. Following the completion of the total synthesis of epicoccolide B a synthesis of simplified analogs is planned to discover the lead structure of this class of natural products. The exact composition of the simplified analog is not determined yet as the final route for the total synthesis has a big impact on possible variations.

4. Results and discussion

4.1 Continuing the route established by Wing-Si Li

As mentioned before several fragments needed to be synthesized in a large scale to provide enough material for the remaining steps. This started with the synthesis of the general precursor **57** (Scheme 19).

$$\begin{array}{c} \text{BnCl } (3.03 \ \text{eq}), \ \text{K}_2\text{CO}_3 \ (6.01 \ \text{eq}), \\ \text{HO} \\ \text{OMe} \\ \text{HO} \\ \text{OH} \\ \end{array} \\ \begin{array}{c} \text{St} \ (6 \ \text{mol}\%), \ \text{acetone, reflux, 20 h} \\ \\ \text{quant.}^a \ (97\%) \\ \\ \text{largest scale: 7.51 g (40.8 \ \text{mmol})} \\ \end{array} \\ \begin{array}{c} \text{Sp} \\ \text{OBn} \\ \end{array} \\ \begin{array}{c} \text{Sp} \\ \text{OMe} \\ \\ \text{Sp} \ (89\%) \\ \\ \text{largest scale: 20.0 g (44.0 \ \text{mmol})} \\ \end{array} \\ \begin{array}{c} \text{CHCl}_3, \ \text{rt., 4 h} \\ \\ \text{89\% (89\%)} \\ \\ \text{largest scale: 20.0 g (44.0 \ \text{mmol})} \\ \end{array} \\ \begin{array}{c} \text{CHCl}_3, \ \text{rt., 4 h} \\ \\ \text{89\% (89\%)} \\ \\ \text{largest scale: 20.0 g (44.0 \ \text{mmol})} \\ \end{array} \\ \begin{array}{c} \text{OMe} \\ \\ \text{BnO} \\ \end{array} \\ \begin{array}{c} \text{OMe} \\ \\ \text{Sp} \\ \end{array} \\ \begin{array}{c} \text{OMe} \\ \\ \text{OMe} \\ \end{array} \\ \begin{array}{c} \text{OMe} \\ \\ \text{Sp} \\ \end{array} \\ \begin{array}{c} \text{OMe} \\ \\ \text{OMe} \\ \end{array} \\ \begin{array}{c} \text{OMe} \\ \\ \text{Sp} \\ \end{array} \\ \begin{array}{c} \text{OMe} \\ \\ \text{OMe} \\ \end{array} \\ \begin{array}{c} \text{OMe} \\ \\ \end{array} \\ \begin{array}{c}$$

Scheme 19: Synthesis of the precursor **57** in large scale. Conditions and yield shown for the largest scale. Best isolated yield given in parentheses, sometimes from a different scale. ^a crude yield slightly over quantitative because of remaining solvent. ^b 90% *brsm* based on recovered **55**

The first reaction to 55 is a *Williamson* ether synthesis with the addition of potassium iodide (KI). The potassium iodide increases the reactivity of benzyl chloride (BnCl) through chloride to iodide exchange providing a better leaving group for the following S_N2 reaction with the phenolates. The yield of this benzyl protection could be consistently improved by a small amount from 93% to 97%, mostly due to a simplified workup and purification. The initial purification was tedious column chromatography on a large scale which has an inherit loss of material in most cases. Replacing the column by simple filtration over a plug of silica removes any remaining inorganic salts (K_2CO_3 , KI). Residue of benzyl chloride or organic solvents in the crude product does not hinder the following reaction making further purification unnecessary.

The iodination of **55** to **56** is an electrophilic aromatic substitution (S_EAr) reaction. The electrophile I⁺ is generated by heterolytic cleavage of iodine (I_2) by the silver salt ($AgCO_2CF_3$) and precipitation of silver iodide.⁵³ This reaction proceeded smoothly, again with nearly identical yield (84% vs. 89%). There are two important factors for this reaction to succeed with high reproducibility and yield. First, the precise measurement of silver salt and iodine to exactly 1.00 equivalents to avoid over-iodination or incomplete conversion is crucial. Second, the chloroform used as a solvent for the reaction needs to be as dry as possible. This can be easily achieved by buying pre-dried chloroform that is stored over

4. Results and discussion

molecular sieve (MS) and under argon. Further optimization is not needed as the yield is very good for large scale reactions and purification is very simple recrystallization.

The third reaction to complete the precursor **57** is a *Negishi* cross-coupling of the aromatic iodide with dimethyl zinc (ZnMe₂). The catalyst Pd(dppf)Cl₂ is reduced to its active state by a small excess of dimethyl zinc.⁵⁴ The best improvement in regards to the yield was achieved for this reaction of the sequence (66% to 84%). Iodide **56** needs to be very dry, both in terms of water content and remaining organic solvent. If the recrystallization from methanol is done correctly the product is obtained in a very pure and dry fashion after removal of the methanol and other solvents *in vacuo*. The other optimization was an adjustment of the eluent for the column chromatography including applying a slower gradient. This change resulted in less mixed fractions and a cleaner isolation of the desired product. Additionally, it facilitated a better re-isolation of deiodinated starting material (**55**). The yield of the largest scale shown in Scheme 19 is slightly lower than expected due to insufficient purity of iodide **56** showing the importance of the mentioned optimizations.

All three reactions were performed on a decagram scale (7.51 - 21.1 g, 36.3 - 44.0 mmol) with very good yields (84 - 97%). The purification of the first two steps is very fast and simple removing the need for additional tedious column chromatography. With large amounts of **57** on hand the synthesis of the other fragments could commence.

4.1.1 Reproducing the boronic ester synthesis and modifying the sequence

The reproduction of the boronic ester **60** proved to be difficult and some changes were made to accompany that fact (Scheme 20).

Scheme 20: Synthesis of the boronic ester **60**. Conditions and yield shown for the largest scale. Best isolated yield given in parentheses, sometimes from a different scale.

The first reaction in this sequence is the saponification of the methyl ester using lithium hydroxide (LiOH) in a wet solvent mixture to provide water (H_2O), solubility of the compound (DCM) and

miscibility of the solvents (MeOH). The yield is practically identical to that of *Wing-Si Li* (95% vs. *quant*.) leaving no room for improvement. Straightforward aqueous workup provides acid **58** in a very pure fashion with no further purification.

Following the saponification a decarboxylative iodination to **59** is performed. Contrary to the *Hunsdiecker* reaction this method does not need a silver salt and supposedly follows a concerted mechanism opposed to a radical pathway. ⁵⁵ It was not possible to reproduce the very high yields of *Wing-Si Li* and only moderate yields of up to 59% were achieved. In all cases conversion was incomplete and starting material **58** could be partially isolated. The *brsm* yields reached up to 90% but purification and separation of the two compounds was tedious. With decent amounts of **59** on hand the *Miyaura* reaction was carried out.

The *Miyaura* reaction of **59** to **60** is a borylation to introduce a boronic ester onto the aromatic system by cleavage of a bis-boronic ester.⁵⁶ Through the use of a mild base (KOAc)⁵⁷ and low catalyst loading the homo-coupling can be avoided to obtain the product with high selectivity and good yields (87%). Both the saponification and *Miyaura* reaction were reproducible with almost identical yields but the decarboxylative iodination remained elusive. To avoid this step the acid **58** was directly converted to the boronic ester **60** by a rather uncommon decarboxylative *Miyaura* reaction.⁵⁸

The first two attempts at the decarboxylative *Miyaura* were successful with a moderate to good isolated yield of 46-66%. At this point further optimization was omitted because the total amount of **60** that was obtained during all performed reactions including reserves of *Wing-Si Li* were more than enough to continue. The new route has a slightly lower overall yield (66% vs. 73%) but is one step shorter and still needs to be optimized. Hence, the decarboxylative *Miyaura* borylation has its merits and can be considered an improvement to the two-step sequence of iodination and *Miyaura* reaction from before.

With sufficient amounts of precursor **57** and boronic ester **60** in hand the key synthesis of benzofurane **65** had to be completed next.

4.1.2 Finishing the benzofurane fragment

To complete the synthesis of benzofurane **65** significant improvements needed to be made to the first two steps. The first reaction is a rather mild *Gross-Rieche* formylation⁵⁹ but due to the methyl ester *ortho* to the formylated position the side product **67** can be formed during the reaction and workup.⁶⁰ This side product is very difficult to remove by standard column chromatography and had to be separated by tedious HPLC-purification.⁵¹ To simplify the step and remove the need for time consuming purifications the goal for the following optimization was the avoidance of the side product entirely in addition to improving the yield (Table 5).

4. Results and discussion

Table 5: Optimization of the formylation from **57** to **61**.

entry	T [°C]	t [h]	AgOTf [eq]	yield	comment
1	-78	2	2.77	-	decomposition in the rotary evaporator (40 °C bath)
2	-78	2	3.00	56%	mixture of product 61 and side product 67
3	-78	1.5	3.00	23-26%	crude product stored overnight (-20 °C), slower column gradient
4	-78	2	2.15	51%	same day column, 79% brsm calculated
5	-78	5	3.04	45%	
6	-78	2	4.00	31%	qNMR yield
7	-78	2	4.98	25%	qNMR yield
8	-78	2	6.06	30%	qNMR yield
9	-90	4	3.02	76%	adjusted reaction time to lower temperature
10	-90	4	3.01	quant	very fast column due to residual Et ₂ O from workup
11	-90	4.75	3.02	64-72%	75-97% brsm isolated, wet AgOTf, no column
12	-90	3.75	3.22	quant	no column, fully optimized conditions

Initial reproduction of the reaction conditions only gave total decomposition as the crude product is not stable in the rotary evaporator at 40 °C (entry 1). Adjusting the workup resulted in the expected mixture of product and undesired side product (entry 2). The next attempts were to separate 61 from 67 by changing the eluent for column chromatography parallel to improving the ratio of product to side product in the crude reaction mixture. A few relevant observations were made: The crude product is not stable for longer periods of time even while stored under argon in a freezer (entry 3). Reducing the equivalents of silver triflate (AgOTf) to two and doing the column chromatography directly after aqueous workup improved the isolated yield slightly (entry 4), while increasing the reaction time or the equivalents of AgOTf had no positive effect on the outcome (entry 5-8).

At this point I theorized that the reactivity of the reaction was still too high so I lowered the temperature to -90 °C which increased the yield drastically and reduced side product to barely traceable amounts (entry 9). Repeating the same conditions on a larger scale resulted in remaining diethyl ether (Et₂O) in the crude product from aqueous workup. Due to this the column afterwards was significantly faster than intended but surprisingly gave a quantitative yield of pure product (entry 10). The only thing remaining at this point was the reproducibility of the excellent yield, which proved to be harder than expected. The AgOTf used was from different suppliers and had noticeable impact on the reaction. Some batches of AgOTf contained visible chunks implying the presence of moisture. Employing this partially wet AgOTf reduced the yield significantly even when pre-drying was attempted (entry 11). After developing a thorough drying protocol applicable for any batch of silver triflate the

optimized reaction conditions were reproducible in a multigram scale (4.98 g, 10.6 mmol). In addition to the aforementioned changes the column chromatography was omitted and instead the crude product was merely filtered over a plug of silica to obtain pure aldehyde **61** after removal of the solvent *in vacuo* (entry 12).

The *Ramirez* homologation⁶¹ of **61** to **62** was very unreliable but the yield could be improved nonetheless (Scheme 21).

Scheme 21: Ramirez homologation of aldehyde 61 to geminal dibromide 62.

In the master thesis of *Wing-Si Li* she described difficulties removing the triphenylphosphine oxide (OPPh₃) after the reaction through the means of column chromatography. Small changes in the aqueous workup and filtering the crude product through a tall plug of silica with DCM alleviated this problem while also improving isolated yields. Sadly, the yield of the reaction was subject to large fluctuations (55-91%) with unknown origin. The best yield of 91% was obtained from the largest scale reaction (3.00 g, 6.04 mmol) but there was no causal connection between scale and yield for the other attempts. With a moderate minimum yield and a large amount of **62** on hand further optimization was put on hold and the next steps were investigated.

As with both reactions before the deprotection presented complications that needed to be addressed with extensive testing (Table 6). Trying to reproduce the conditions set by *Wing-Si Li* resulted in the global deprotection but only with bad to moderate yields (entry 1).^{51,62} Using other deprotection methods did not seem promising either (entry 2-4).⁶³ The good news was that the cyclized product **64** could be observed during the deprotection with aluminum trichloride (AlCl₃). Removing the benzyl protecting groups through boron trichloride (BCl₃) seemed to be the most promising candidate so the conditions and the workup were adjusted to obtain **63** in very good yields (entry 5-8).⁶⁴ Interestingly the yield showed medium fluctuations (73-98%) with no clear correlation to the reaction handling or size. With a good minimum yield of 73% and sufficient amounts of pure **63** the final steps could be tested.

Table 6: Different screened conditions for the global deprotection of 62.

entry	conditions	result
1	TFA (excess), PhMe ₅ (3.04-4.69 eq), DCM, rt. 20-22 h	20-50% qNMR yield
2	AlCl ₃ (3-9 eq), PhNMe ₂ (30.0 eq), DCM, rt40 °C, 0.5-22 h	30-36% yield, 4:1 ratio 63:64
3	Pd/C (3.00 eq), H ₂ (1 atm), MeOH, 30 min	no reaction
4	BCl ₃ (6.03 eq), PhMe ₅ (4.92-9.74 eq), DCM, -78 °C, 20 min	15-46% qNMR yield
5	BCl_3 (6.14 eq), PhMe ₅ (3.37 eq), DCM, -78 °C, 30 min, filter over plug of silica (CH/EA 9:1) to remove scavenger, 850 mg scale	98% isolated yield
6	BCl_3 (3.91 eq), PhMe ₅ (4.93 eq), DCM, -78 °C, 30 min, filter over plug of silica (CH/EA 9:1) to remove scavenger, 1.25 g scale	76% isolated yield
7	BCl ₃ (4.04 eq), PhMe ₅ (4.09 eq), DCM, -78 °C, 15 min, column chromatography, 2.34 g scale	73% isolated yield
8	BCl_3 (3.60 eq), PhMe ₅ (3.27 eq), DCM, -78 °C, 15 min, column chromatography, ~4 g scale	61% over 3 steps starting from 57

As a key reaction of this route the cyclization of the benzofurane is crucial to introduce the second ring. The successful cyclization was already observed during the deprotection with AlCl₃ but could not be separated from the non-cyclized product. Attempting the reaction with pure $\bf 63$ and the conditions set beforehand, including slight variations (2 eq K_3PO_4 , 0.2-1 eq Cul)⁶¹, decomposition or no reaction occurred. It has been reported that different ligands support the reaction and can drastically increase reactivity and selectivity. Two of these ligands tested are dipivaloyl methane and picolinic acid. ^{65,66} Employing these ligands and increasing the reaction time drastically resulted in the wrong product for the former ligand while the latter gave the desired product (Scheme 22).

Scheme 22: Synthesis of the benzofurane **64**. Conditions and yield shown for the largest scale. Best isolated yield given in parentheses from a different scale.

Varying equivalents of base (1-2 eq) as well as different solvents (DMSO, DMF) showed no effect on the yield. Just like the two reactions before an unusually large fluctuation of the yield could be observed for different batches (45-76%), again with no clear correlation to the reaction handling or size. Accepting this trend of unpredictability in the route, the fragment was almost finished. Only the reprotection with benzyl protection groups was necessary.

To reprotect the phenols with benzyl groups the same conditions as in the very first step were used.⁵² The first attempts showed small signs of product but also large amounts of unknown side product were obtained. Initial characterization of the side product was more confusing than helpful. Later on, I realized that the side product was actually the dibrominated and protected benzofurane. Reducing the temperature but in turn increasing reaction time improved the yield to 63% (Scheme 23).

$$\begin{array}{c} \text{HO} \\ \text{HO} \\ \text{OMe} \\ \\ \text{HO} \\ \\ \text{OMe} \\ \\ \text{Iargest scale: 175 mg (582 \ \mu mol)} \\ \\ \text{65} \\ \text{Br} \\ \\ \end{array} \\ \begin{array}{c} \text{BnO} \\ \text{OMe} \\ \\ \text{BnO} \\ \\ \text{OMe} \\ \\ \text{OMe} \\ \\ \text{OMe} \\ \\ \text{BnO} \\ \\ \text{OMe} \\ \\ \\ \text{OMe} \\ \\ \text{OMe} \\ \\ \text{OMe} \\ \\ \\ \text{OMe} \\ \\ \text{OMe} \\ \\$$

Scheme 23: Final protection to complete fragment 65.

The debromination most likely occurs due to the base potassium carbonate (K_2CO_3). Alternative deprotonation by sodium hydride (NaH) prevented the debromination but gave less yield overall (46%). This concludes the synthesis of benzofurane **65**.

To summarize, the formylation could be improved drastically with high reproducibility and significantly less purification effort. For the *Ramirez* homologation to the geminal dibromide **62** the best-case yield improved significantly but large fluctuations of the yield were observed for different batches. The sequence of deprotection, cyclization and reprotection to complete the fragment **65** suffered from the same phenomenon. Using the highest obtained outcomes **65** was synthesized in 5 steps with 43% yield starting from the precursor **57**. With both fragments **60** and **65** in hand the coupling could finally be tested followed by the remaining last few steps.

4.1.3 Coupling of borane and benzofurane followed by the final steps

The envisioned coupling of the fragments is a standard *Suzuki-Miyaura* cross-coupling with no particularly challenging substituents.⁶⁷ Therefore, a catalyst that is easy to handle and is used for a wide variety of applications can be employed. In this case I chose XPhos Pd G4 because of its stability under air and in aqueous environments in addition to a generally high reactivity even at low temperatures. With a very low catalyst loading of 1.5 mol% (0.6 mol% also tested successfully) and a low temperature (compared to most other cross-couplings) the fragment union to acquire **66** proceeded smoothly in a quantitative manner (Scheme 24).

Scheme 24: Coupling of fragments 65 and 60 to obtain the core structure 66.

Finally, having completed the core structure only a few steps remained. The second aldehyde needs to be introduced, the methyl ester has to be converted into the aldehyde and the protection groups have to be removed. For the order of the steps the deprotection was chosen as the final step since five free phenols will have a significant impact on the solubility and reactivity of the compound. Formylation to **68** is possibly the most difficult step of the remaining and will be done next with the conversion of the methyl ester in between.

Going back to the originally employed temperature of -78 °C with a reaction time of 2 h but increasing the equivalents of reagent instantly gave an excellent yield (Scheme 25).

Scheme 25: Formylation of **66** to synthesize **68** but purely **69** was obtained.

Interestingly the obtained product was exclusively **69** and not the desired aldehyde **68**. This is very surprising since it is expected that the free aromatic position C-14 would react more readily than the heterocycle. But apparently, in this case, the benzofurane has drastically higher reactivity towards electrophiles than the other aromatic position, which has three protected phenols to increase electron density. It is also possible that the methyl ester has a directing effect for approaching electrophiles. This outcome was not predictable but highly reproducible and always gave a single product. This shows the vast difference in reactivity for the two free aromatic positions.

I decided to finish the synthesis even though the aldehyde was at the wrong aromatic position as it would be the first synthesized analog of epicoccolide B. Next, a reduction and selective oxidation need to transform the methyl ester into the corresponding aldehyde. The second aldehyde will react as well

so the equivalents need to be adjusted accordingly. To obtain diol **70** a standard reduction protocol was used (Scheme 26). ⁶⁸

Scheme 26: Reduction of 69 to diol 70.

The use of an excess of reduction agent (DIBAI-H) ensures the complete reduction of both carbonyl groups to the benzylic alcohols. When lithium aluminum hydride (LAH)⁶⁹ was used, a much stronger reducing agent, the yields were very inconsistent (36-94%) compared to the conditions shown above.

As the deprotection caused problems before, several different pathways were investigated in parallel: the deprotection of **70**, the oxidation of **70** and the development of a simplified test system to screen reaction conditions that are hopefully transferable. Since it is impossible to describe multiple pathways at once without confusing some readers I will elaborate on the test systems first and then their application to diol **70**, even if some of the following reactions were done in parallel.

For a simplified test system, the general precursor **57** was chosen. It bears most of the functional groups that can be found in diol **70**. To be a more accurate representation the methyl ester was reduced to the benzylic alcohol as well (**71**).⁶⁸ Subsequent oxidation to aldehyde **72** presents another test system for the oxidation of **70** and the following deprotection. The synthesis of **71** and **72** is shown in Scheme **27**.

Scheme 27: Synthesis of benzylic alcohol 71 and aldehyde 72.

For the reduction of **57** to **71** both DIBAI-H and LAH resulted in excellent and reproducible yields with minimal synthetic effort. Oxidation of alcohol **71** to aldehyde **72** was achieved by the use of IBX, a cheap and selective oxidant. This reaction gave an excellent yield as well and needed no tedious purification making for an efficient two-step sequence. A selective reduction is plausible as well but poses significantly higher synthetic effort and needs a precise temperature control, while this sequence is very simple and easy to handle. During the period of a practical course under my supervision a bachelor student performed this sequence on a gram scale (1.63 g, 3.48 mol) with a very good yield of 95% over two steps.

With three different test compounds in hand (57, 71, 72) the most common deprotection for benzyl groups was tested, namely the reductive removal using Pd/C and a hydrogen source resulting in the deprotected compounds 73, 74 and 75 (Table 7).

Table 7: Deprotection testing for compounds 57, 71 and 72.71

entry	starting material	product	Pd/C [eq]	'H ₂ ' source	solvent	T [°C]	t [min]	result
1	57	73	0.3-0.8	HCO ₂ H	MeOH, DCM	rt.	120	no reaction
2	71	74	0.69	HCO ₂ H	MeOH	rt.	20 h	no reaction
3	71	74	1.34	<i>i</i> PrOH	<i>i</i> PrOH	100	20 h	no reaction
4	71	74	3.35	TES-H	MeOH	rt.	15	44%
5	71	74	3.72	H_2	MeOH	rt.	50	84%
6	72	75	2.90	H ₂	MeOH	rt	25	97%

First, transfer-hydrogenations were tested as they generate the reactive hydrogen *in situ* and directly at the reaction sites. Most of the reactions showed no conversion with standard to high amounts of Pd/C (entry 1-3). Once the amount of Pd/C was increased drastically the benzyl groups were finally removed with a moderate yield (entry 4). Swapping to pure hydrogen (H₂) bubbling through the reaction in combination with the very high amounts of Pd/C very good yields were achieved for the deprotection (entry 5-6).

Applying the deprotection conditions to diol **70** provided globally deprotected **76** in good yields. Sadly the following oxidation of the benzylic alcohols did not work so the analog **77** could not be obtained (Scheme 28).

Scheme 28: Global deprotection of diol 70 to 76. No oxidation to 77 could be achieved.

Since the deprotection of the test system also worked in the presence of the aldehyde (entry 6) diol **70** was oxidized to the dialdehyde **78** with IBX and attempted to deprotect with Pd/C (Scheme 29).⁷⁰

Scheme 29: Oxidation of diol 70 to dialdehyde 78 and attempted deprotection.

As these reactions were not done in the exact order they are presented here the optimized conditions for the IBX oxidation shown in Scheme 27 were not used here. Therefore, a large excess of IBX was needed compared to the optimized lower amount in addition to small amounts of DMSO. Nevertheless, a good yield was achieved obtaining dialdehyde 78 with good purity after simple filtration. The deprotection conditions established before (~1 eq Pd/C per protection group) showed no effect and the starting material was reisolated entirely. Increased reaction time or temperature showed no different effect until at some point the starting material decomposed completely.

At this point I was very sure that the aldehydes are the major cause of complications so I decided to protect them as acetals in hopes of facilitating any deprotection afterwards. I tested the acetalizations and subsequent deprotections on aldehyde **72** for easier access (Table 8).

Table 8: Formation and deprotection of (thio)acetals.

entry	conditions 1	product, yield	conditions 2	result
1	TMOF (1.2 eq), MeOH, HCl (4 м), rt. 17 h	79 , 93%	Pd/C (3.92 eq), H ₂ , MeOH, rt. 1 h	94% 75 , 0% 80
2	TMOF (excess), ethylene glycol, DCM, HCl (4 M), rt. 23 h	81 , 83%	Pd/C (4.58 eq), H ₂ , MeOH, rt. 1 h	quant. 75 , 0% 82
3	Amberlyst (2.0 eq), 1,2-ethane dithiol (1.96 eq), MgSO ₄ , THF, rt. 20 h	83 , quant.	Pd/C (5.02 eq), H ₂ , MeOH, rt. 1 h	no reaction
4	Amberlyst (2.0 eq), 1,2-ethane dithiol (1.96 eq), MgSO ₄ , THF, rt. 20 h	83 , quant.	BCl ₃ (5.39 eq), PhMe ₅ (5.95 eq), DCM, -78 °C, 45 min	complete deprotection to 75 ^a
5	Amberlyst (2.0 eq) , $1,2\text{-ethane}$ dithiol (1.96 eq) , MgSO ₄ , THF, rt. 20 h	83 , quant.	$BF_3 \cdot OEt_2$ (8.01eq), 1,2-ethane dithiol, rt. 45 min	87% 84

^a crude yield >>quant., no isolated yield determined.

The simplest acetal is the dimethoxy acetal **79** formed by trimethyl orthoformate (TMOF) and catalytic amounts of dry acid.⁷² Deprotection of **79** directly resulted in **75** rather than **80** showing the low stability of this acetal (entry 1). Increasing the stability of the acetal by synthesizing the dioxolane **81** also works in good yields.⁷² Interestingly also this deprotection results in the removal of both the benzyl groups as well as the acetal giving **75** again instead of the expected **82** (entry 2). Since the most stable acetal **81** was not enough under the given conditions I decided to try thioacetals, known for their even higher stability. Synthesis of **83** proceeded smoothly⁷³ but deprotection with Pd/C showed no reaction (entry 3). This was not unexpected as sulfur is a known catalyst poison completely inhibiting any reactions including palladium.⁷⁴ Instead, *Lewis* acids were tested. Boron trichloride (BCl₃)⁶⁴ also resulted in a complete deprotection of both the benzyl groups and the dithiolane, again giving **75** (entry 4). Employing boron trifluoride (BF₃)⁷⁵ in 1,2-ethane dithiol finally achieved the desired deprotection of the benzyl groups while not removing the dithiolane (**84**, entry 5).

Before I got around to testing the dithiolane for **78** I managed to remove the protection groups through a different method tested in the meantime (Scheme 30).⁷⁶

Scheme 30: Successful global deprotection of dialdehyde 78 to obtain the first analog 77 of epicoccolide B.

This concludes the route that resulted in the first analog of epicoccolide B **77** instead of the planned total synthesis. The longest linear sequence (LLS) consists of 13 steps and has a total yield of 21%. This yield is calculated with the best-case outcomes, if more realistic yields are applied it is roughly half, which is still a very good total yield.

There are several options for new approaches from this point onward. The first option is to try different formylation methods in an attempt to arrive at **68**. This would be very challenging as the current formylation through an electrophilic mechanism shows remarkable selectivity for the heterocycle. Alternatively, the aldehyde can be introduced to the boronic ester fragment before coupling, eliminating the problem of selectivity later on. The third option consists of an entirely new route with a different cyclization to build the benzofurane.

Even though scalability is good for the fragments and the few steps following I decided to pursue a new route. This is mostly to avoid the synthesis of the benzofurane fragment **65**, which was very unreliable in many batches. Even though the best-case yields are very good for several steps it is very difficult to reproduce them consistently. This problem can be seen for the *Ramirez* homologation (**62**),

the deprotection (63) and the cyclization (64). The reprotection with benzyl groups as the last step can very likely be optimized for very high and consistent yields if the time were to be invested to avoid the debromination. The new cyclization and retrosynthetic approach will be presented in the next chapter.

4.2 New retrosynthetic approach to epicoccolide B

Extensive literature research revealed several possibilities for benzofurane generation. The introduction of the benzofurane motif too early caused problems with the first route and opened up the possibility for the formylation of the heterocycle. To avoid both problems the plan is to introduce the heterocycle as late as possible while preparing the remaining substituents beforehand. The most promising option is the cyclization of an alkyne with a phenol in *ortho* position (85) to the corresponding benzofurane 86.^{77–80} By the use of the internal alkyne 87 both substituted benzyl rings can be introduced before the cyclization (88) occurs (Scheme 31).

Scheme 31: Left: Cyclization of an *ortho*-phenol alkyne **85** to the corresponding benzofurane **86**. Right: Planned cyclization of an internal alkyne **87**.

Since the proposed reaction requires free phenols, it is envisioned to do the cyclization as the very last step of the synthesis, in accordance with the plan. Through the versatile design of the precursor the retrosynthetic approach has several options (Scheme 32).

Scheme 32: Retrosynthetic approach to the alkyne cyclisation via two possible pathways.

The targeted alkyne for the final deprotection and cyclization is dialdehyde **89**. It can be accessed through two different routes. The first possibility is to introduce the alkyne to the precursor **57** to obtain alkyne **90**. This in turn would be coupled with iodide **59**. Alternatively, the iodide **91** can be coupled with the alkyne on the other benzyl ring (**92**). All new fragments can be derived from the general precursor **57**.

4.2.1 Synthesis of the new fragments

Many compounds from the first route can be reused minimizing the synthetic effort for the new route. First, efforts were invested installing a terminal alkyne to the left side. A very common and simple method for installing terminal alkynes is the *Ohira-Bestmann* reaction (Scheme 33).⁸¹

Scheme 33: Ohira-Bestmann reaction of aldehyde 61 to obtain alkyne 90.

Aldehyde **61** is easily accessible and presents a good starting point. Sadly, the *Ohira-Bestmann* reaction did not result in the desired product **90**. A mixture of two products was observed. Both of which with neither an aldehyde, nor the desired terminal alkyne. Starting only from previously synthesized

compounds the following attempts were to introduce the alkyne onto the other aromatic ring (Scheme 34).

Scheme 34: Three different pathways to synthesize alkyne 92.

Three different options were investigated. Starting with iodide **59** a *Sonogashira* cross-coupling to alkyne **92** works perfectly well with a yield of 94%.⁸² The next option was a decarboxylative *Sonogashira* reaction, similar to the Miyaura borylation from before, using acid **58**.^{83–85} Although it was successful the yield is rather low with only 38%. The last option was again an *Ohira-Bestmann* reaction of aldehyde **72**,⁸¹ originally only synthesized as a test fragment. With a yield of 98% this reaction was the best out of the three options. Additionally, this reaction avoids the need for iodide **59**, which caused issues in regards to reproducibility before.

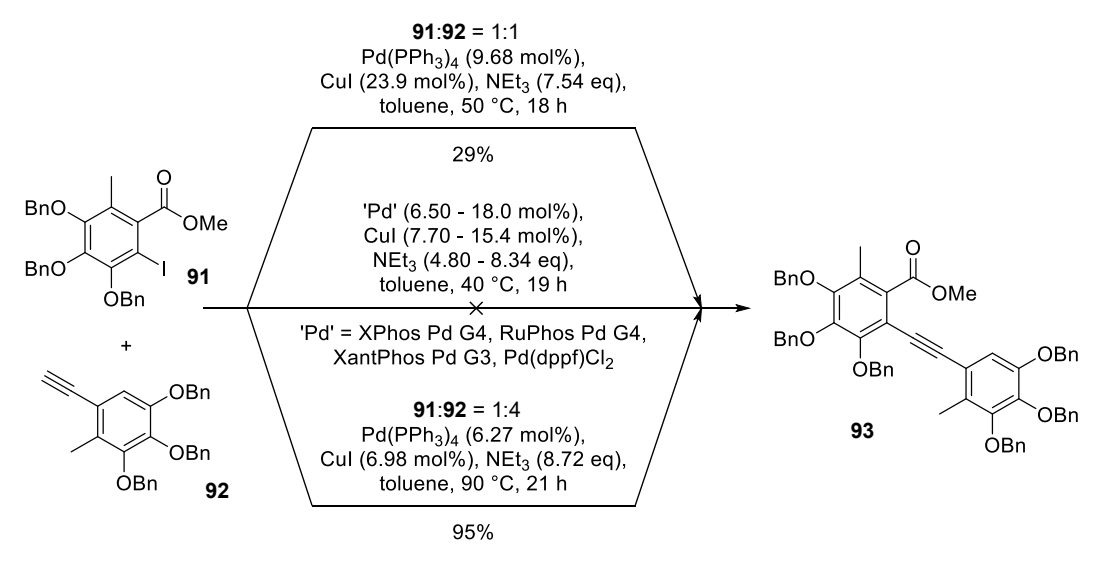
With the alkyne successfully synthesized in very good yields (98% over 3 steps from precursor **57**) the coupling partner **91** needed to be obtained. Applying the same iodination conditions⁵³ used for **56** gave **91** with an excellent yield (Scheme 35).

Scheme 35: Synthesis of iodide 91 in a single step from precursor 57.

With both fragments obtained the coupling could be investigated next.

4.2.2 Sonogashira coupling and establishing key cyclisation

The first try for the coupling showed the importance of degassing a reaction properly as only *Glaser* product was obtained instead of the desired alkyne **93**. With a ratio of iodide **91** to alkyne **92** of 1:1 and properly degassed solvents resulted in 29% of the desired coupling product **93** (Scheme 36, top).⁸² Testing of various different ligands for palladium catalysts gave valuable insight regarding the challenges of the reaction. Highly reactive catalysts like 'XPhos Pd G4', 'RuPhos Pd G4' and 'XantPhos Pd G4' purely gave the *Glaser* product, even after very thorough degassing of the reaction beforehand (Scheme 36, middle). Less reactive catalysts like Pd(PPh₃)₄ and Pd(P(tBu)₃)₄ (but not Pd(dppf)Cl₂) were the best candidates giving up to 95% yield for optimized conditions (Scheme 36, bottom).



Scheme 36: Different coupling conditions for the fragments 91 and 92.

For a successful reaction it was necessary to increase the amount of alkyne to 4 equivalents for high yields and good reaction times. Reducing the equivalents of alkyne **92** to 2.5 also resulted in a reduced yield of 72%. The alkyne seems to be used up faster than iodide **91** even though no *Glaser* product was observed. Interestingly, a different side product (**94**) was isolated explaining some of the loss of alkyne (Scheme 37).

Scheme 37: Asymmetric homocoupling of two alkynes to enyne 94.

The enyne **94** was observed in several batches of this reaction but only accounts for a fraction of the lost alkyne. Another part of the excess of alkyne can be recovered through column chromatography but a large amount cannot be recovered and most likely decomposes. In an attempt to optimize the reaction and reduce the needed amount of alkyne the addition of alkyne took place over time instead of all at once. The amount of alkyne was reduced to 1.7 eq and the yield was still very good with 76%.

However, the reaction time was drastically higher and the constant addition of alkyne reintroduced oxygen into the system leading to the formation of *Glaser* product. As a result, I concluded that the tested optimization is not worth the synthetic effort since the alkyne fragment itself can be produced in large amounts with very good yields. A reduction of the amount of alkyne can be investigated at a later time if necessary.

Before completing the remaining functional groups, the validity of the strategy itself needed to be tested. A variety of deprotection conditions were applied, one of which was successful in several attempts. Removing the benzyl protection groups with BF₃·Et₂O⁷⁵ in ethane (di)thiol globally deprotected all six groups while already cyclizing the alkyne to the benzofurane. With initial low to moderate yields of 20-51% in small scales (20-30 mg) the only observed product was cyclized **95**. Repeating the reaction on a much larger scale (462 mg) resulted in a mixture of the cyclized (**95**) and non-cyclized product **96** with a very good combined yield of 90% (Scheme 38). The exact ratio was not determined but can be estimated to roughly **95:96** 2:1.

Scheme 38: Deprotection of 93 with partial or complete cyclisation depending on the scale.

The most important take-away is that the cyclization itself works and can be observed during the deprotection without any metal catalysts present. Due to these results the completion of the functional groups was targeted next. This includes the introduction of the second aldehyde and transformation of the methyl ester to the aldehyde, just like before. This time there is no heterocycle present so there is only one free aromatic position left.

For the formylation the same *Gross-Rieche* reaction as before was used.⁵⁹ Several batches were done with varying temperature (-90 - -70 °C), different amounts of silver triflate (AgOTf, 3.55 - 4.58 eq), different amounts of dichloromethyl methyl ether (MeOCHCl₂, 6.20 - 9.78 eq) and adjusted reaction times (2 – 26 h). Every single variation resulted in a mixture of product **97**, starting material **93** and unidentified side products (Scheme 39). The ratio varied depending on the conditions but never achieved acceptable results. Instead of isolating and separating the compounds a two-step sequence was applied, directly reducing⁶⁸ the entire mixture. Alcohol **98** could be isolated in 29% after two steps (Scheme 39).

Scheme 39: Formylation and reduction of 93.

These very low yields explain the observed selectivity of the first route where only the heterocycle is formylated. The free aromatic position seems to be very inaccessible and hardly reacts. Similar results were obtained when the small amounts of **98** were oxidized to the aldehyde with IBX (Scheme 40).⁷⁰

Scheme 40: Attempted oxidation of diol 98 to dialdehyde 89.

Both attempts lead to total decomposition of the starting material and no dialdehyde **89** could be found. At this point I decided to change the plan to adjust to these new findings. The introduction of the aldehyde has to occur before any fragment coupling to avoid the problems of the first two routes. The alkyne cyclization works and remains the most promising approach so this route is adjusted to fit the needs.

4.3 Final adaptation to the total synthesis of epicoccolide B

The new retrosynthetic plan is shown in Scheme 41.

Scheme 41: New retrosynthetic plan introducing the (protected) aldehydes before the coupling.

The new planned fragments are iodide **99** and alkyne **100**. Since aldehydes caused problems in many different cases before I decided to introduce the aldehyde on the alkyne in a protected form that does not interfere with cross-coupling reactions. The vinyl group can be cleaved to the aldehyde both before and after the fragment coupling, depending on reactivity and yields.

4.3.1 Synthesis of the adjusted fragments

lodide **99** can be synthesized by either reducing methyl ester **91** to the aldehyde or performing an iodination of aldehyde **72** (Scheme 42).

Scheme 42: Synthesis of iodide 99.

The reduction of the methyl ester **91** to the alcohol **101** was not successful but the iodination of aldehyde **72** works flawlessly on a gram scale. Increasing to a decagram scale (15.2 g) still gives very good results (91%).

For the synthesis of **100** there are two options as well. To introduce the vinyl group iodide **102** is the first target followed by a *Suzuki* reaction. Iodide **102** can be obtained by iodination of alkyne **92** or *Ohira-Bestmann* reaction of aldehyde **99** (Scheme *43*).

Scheme 43:Synthesis of alkyne 102.

Alkyne **92** did not react using different iodination methods. Aldehyde **99** could be transformed to alkyne **102** by an *Ohira-Bestmann* reaction after drastically increasing the reaction time. The *Ohira-Bestmann* reagent is thermally labile so an increase of temperature for a faster reaction is not an option. On a gram scale (0.80 - 1.48 g) the yield is very good and reproducible (89 - 94%). To finish fragment **100** a *Suzuki* reaction of iodide **102** with vinyl pinacol boronic ester (Bpin viny) was performed (Scheme 44).

$$\begin{array}{c} \text{K}_3\text{PO}_4 \ (5.08 \ \text{eq}), \\ \text{Pd} \ (\text{PPh}_3)_2\text{Cl}_2 \ (3.70 \ \text{mol}\%), \\ \text{Bpin vinyl} \ (2.02 \ \text{eq}), \\ 1,4\text{-dioxane}, \ H_2\text{O}, \ \text{reflux}, \ 18 \ \text{h} \\ \hline \\ \text{PoBn} \\ \\ \text{OBn} \\ \\ \end{array}$$

Scheme 44: Synthesis of fragment 100.

A good isolated yield of 79% was achieved on a gram scale (1.31 g) after column chromatography (purity >95%). Trying different purification methods for a decagram scale (13.5 g) reaction only resulted in ~90% purity of the obtained product. Even though the obtained yield was better than 79% it will not be listed due to the insufficient purity. Finally, the oxidative cleavage of the vinyl group to the aldehyde **103** was tested. The simplest methodology is the cleavage by ozonolysis (Scheme 45).⁸⁷

Scheme 45: Ozonolysis of 100 to obtain aldehyde 103.

Only a low yield of 35% could be isolated and other methods were not tested at that point. Optimization was put on hold until the fragment coupling of iodide **99** and alkyne **100** was successful.

4.3.2 Finishing the total synthesis of epicoccolide B

To achieve fragment union of aldehyde **99** and alkyne **100** to obtain alkyne **104** the optimized conditions of the first *Sonogashira* reaction were applied (Scheme *46*).

Scheme 46: Fragment union of iodide 99 and alkyne 100 to 104.

As with the coupling beforehand an increased amount of alkyne was necessary to ensure a fast reaction and high yields. As long as three or more equivalents (3.01 - 4.34 eq) of alkyne **100** were used the yield was very consistent (85 - 88%), no matter the scale of the reaction (0.26 - 2.23 g).

Next, the oxidative cleavage of the vinyl group needs to be optimized after the rather disappointing results from the first attempt. Three different methods were tested (Table 9).

Table 9: Oxidative cleavage of 104.87-90

entry	conditions	yield 89	comment
1	O ₃ , DCM, pyridine (3.0 eq), -78 °C, 3 min	35%	
2	OsO ₄ (3.70 mol%), NalO ₄ (3.97 eq), 2,6-lutidine (2.01 eq), 1,4-dioxane, H_2O , rt., 22 h	44%	
3	1. OsO ₄ (5.58 mol%), NMO·H ₂ O (3.04 eq), acetone, H ₂ O, rt., 26 h 2. Pb(OAc) ₄ (1.51 eq), toluene, rt., 35 min	94%	no isolation or purification of diol 105
4	1. OsO ₄ (3.59 mol%), NMO·H ₂ O (3.11 eq), acetone, H ₂ O, rt., 17 h 2. Pb(OAc) ₄ (1.53 eq), toluene, rt., 1 h	88%	diol 105 isolated: 65%

First, ozonolysis was tested again with identical bad results (entry 1).⁸⁷ Next, a dihydroxylation followed by glycol cleavage through osmium tetroxide (OsO₄) and sodium periodate (NaIO₄) was applied.⁸⁸ This sequence is a one-pot reaction with low synthetic effort but very toxic compared to the ozonolysis. Slightly better yields were obtained but nothing satisfactory (entry 2). I theorized that the combination of both reactions as a one-pot method was the main reason for the moderate yield. To avoid this problem the sequence was separated into two steps. The glycol cleavage was now done by

lead acetate Pb(OAc)₄.⁹⁰ This change increased the yield to very good results (entry 3) and can still be handled on a gram scale (949 mg). Isolating the diol **105** before the glycol cleavage drastically reduced the total yield, most likely due to losses during column chromatography (entry 4).

The final steps were the deprotection and cyclization of dialdehyde **89**. To obtain phenol **106** many different conditions were examined. Preliminary testing revealed that deprotection with BBr₃ shows the most promising results.⁷⁶ Optimization through the variation of conditions was thoroughly screened (Table 10).

Table 10: Optimization of the deprotection of dialdehyde 89.

entry	BBr ₃ [eq]	T [°C]	workup	yield 106+2 [%] ^a	combined yield [%] ^a
1	6.0	rt.	H ₂ O	35+4	39
2	6.0	0	acid/base	51+3	54
3	6.0	-41	acid/base	58+4	62
4	6.0	-78	acid/base	40+0	40
5	3.0	0	acid/base	7+13	20
6	3.0	-41	acid/base	7+7	14
7	6.0 ^b	-78	acid/base	44+6	50
8	12.0	-41	acid/base	50+7	57

^a qNMR yield. ^b PhMe₅ (6.49 eq) added as a cation scavenger.

All reactions, except entry 4, gave a mixture of the deprotected alkyne (106) and epicoccolide B (2). Since the mixture can be cyclized without separation (vide infra) the combined yield is more relevant than the ratio of cyclized to non-cyclized product. The first step to reduce reactivity and increase selectivity to avoid potential decomposition is the reduction of the reaction temperature (entry 1-4). A maximum in regards to the yield can be observed around -41 °C (entry 3). Since a reduction of the reactivity had a generally positive effect the next option to reduce it further is lowering the amount of *Lewis* acid (entry 5-6). The yield was drastically lower so other possibilities had to be investigated. During the deprotection of the geminal dibromide 62 a cation scavenger (PhMe₅) was crucial. Adding the same scavenger to this reaction at -78 °C increased the yield slightly (entry 7) compared to no scavenger (entry 4) but showed no significant effect at -41 °C (not shown). With an optimal reaction temperature of -41 °C the last variation was an increase of BBr₃ giving similar results within the accuracy of qNMR (entry 8).

The crude product still had significant amounts of benzyl bromide (BnBr) and other unidentified impurities. Purification by column chromatography or preparative TLC resulted in the loss of most of the material. This is very likely due to the very high adsorption of the very polar product on silica gel. Recrystallisation by vapor diffusion gave very pure **106** but also lost a lot of the material. This was sufficient for clean analytical data but inadequate for continuing the route. The optimal purification to proceed with the next step was acid-base workup. For this the crude product is dissolved in alkaline water (saturated aqueous NaHCO₃) and other organic impurities are washed out with EA. After acidifying the aqueous phase, the product could be extracted with drastically increased purity compared to no acid-base workup.

Finally, as the last step the cyclization of **106** to epicoccolide B needs to be tested further. The cyclization itself could already be observed during most deprotection reactions as a minor product. Two options are prominent in literature for this kind of cyclization. First, the variation using copper chloride (CuCl) and cesium carbonate (Cs₂CO₃) was examined (Scheme 47, top). Doing the reaction at room temperature resulted in mostly cyclized product but showed no full conversion, even after long reaction times (72 h). Increasing the reaction temperature to 70 °C and adjusting the time gave full conversion and an isolated yield of 38%. The reaction requires an excess of both copper chloride and cesium carbonate.⁸⁰ As a more atom economic possibility the cyclization using catalytic amounts of platinum chloride (PtCl₂) was pursued (Scheme 47, bottom).⁷⁷

Scheme 47: Final cyclisation of alkyne 106 to epicoccolide B (2).

Interestingly, the isolated amount of product was always very close to a quantitative yield but qNMR experiments revealed a low purity of the obtained product. The purity was in the range of 25-47% for different batches giving an actual yield for the reaction of up to 42%. Combining the best yields for the deprotection (62%) and cyclization (42%) the two steps have an expected yield of 26%. If the isolation of highly pure **106** is omitted and the cyclization is performed immediately afterwards a qNMR yield

of 23-26% can be observed for several batches, even up to a gram scale (974 mg). The purity of the crude product was still insufficient so several different purification methods were tested. Again, silica gel adsorbs high amounts of the highly polar product resulting in significant loss of material. Acid-base workup showed an unexpected reactivity resulting in a new product (chapter 4.4). In an attempt to avoid tedious HPLC purification gel chromatography with Sephadex LH-20 was performed. A twofold increase of purity could be observed (qNMR) from 34% to 73% for the tested batch. Sadly, the obtained purity was not sufficient so HPLC purification was applied. The increased purity from gel chromatography was helpful for the HPLC but not necessary.

After obtaining highly pure epicoccolide B by HPLC the synthesized compound could be compared to the natural product (Table 11).

Table 11: NMR-comparison of synthetic and natural 2. Sorted by chemical shift, OH-signals omitted, in DMSO-d₆.³

δ _H (synthetic 2)	δ _н (natural 2)³	Δδ	δ_c (synthetic 2)	δ _c (natural 2) ³	Δδ
[ppm]	[ppm]	[ppm]	[ppm]	[ppm]	[ppm]
10.42 (s)	10.41(s)	0.01	194.8	194.7	0.1
9.48(s)	9.48(s)	0.00	190.2	190.1	0.1
7.47(s)	7.46(s)	0.01	151.6	151.6	0.0
2.58(s)	2.58(s)	0.00	151.5	151.5	0.0
2.01(s)	2.01(s)	0.00	150.2	150.2	0.0
			142.4	142.4	0.0
			140.9	141.0	0.1
			136.4	136.7	0.3
			132.7	132.7	0.0
			127.6	127.5	0.1
			124.9	124.9	0.0
			122.9	122.9	0.0
			118.7	118.7	0.0
			117.2	117.1	0.1
			112.6	112.6	0.0
			109.0	108.9	0.1
			12.7	12.6	0.1
			11.1	11.0	0.1

The analytical data is practically identical for both ¹H- and ¹³C-NMR with deviations within standard measurement inaccuracy. This perfect match of the analytical data in addition to the confirmation by mass spectrometry confirms the complete and correct structure of my synthetic epicoccolide B (2). This concludes the first total synthesis of epicoccolide B with a mere 13 steps LLS and a total yield of 11%. All steps are highly scalable and were successfully completed on a (deca)gram scale without significant loss of yield.

4.4 Unexpected reaction of epicoccolide B observed

As mentioned before an unexpected reaction of epicoccolide B was observed during attempted acid-base purification of the crude product. The unknown product could sometimes be observed when crude epicoccolide B was dissolved in alkaline water (saturated aqueous NaHCO₃) and washed with ethyl acetate in a separation funnel with vigorous shaking. After acidifying the aqueous phase and extracting the remaining organic compounds small amounts of the new product could be seen in ¹H-NMR. Repeating the process with the same mixture of epicoccolide B and the new product increased the ratio in favor of the new compound. Interestingly, this reaction did not occur with every batch that was tested. In rare cases no reaction was observed and only epicoccolide B was isolated. In some other cases complete decomposition was the only result. It was not possible to find any correlation between the reaction handling and the consecutive result of the acid-base workup. The observed reaction never resulted in complete conversion and only gave very small amounts that could barely be seen in ¹H-NMR. To be able to obtain complete analytical data this reaction needed to be reproduced in a controlled environment instead of the unreliable conditions in the separation funnel.

Even without extensive analytical data some assumptions can be made in regards to the product. It can be observed that one of the aldehyde signals and the benzofurane signal are no longer present in the unknown compound. Instead, two new signals appeared in the range of 6-7 ppm, both singlets with an integral of one. The aldehyde of the left/upper ring and both methyl groups still exist. These observations are consistent with my proposed biosynthesis for epicoccolide A (1). An air oxidation of the benzofurane with a subsequent intramolecular reaction with the right-side aldehyde directly forms 1. According to the proposed mechanism in Scheme 48 the only possible product of this reaction is epicoccolide A. No other product is possible without resulting in massive ring strain or instable compounds.

Scheme 48: Proposed air oxidation of **2** to form **1** in a single step.

This result is very unexpected since the shown oxidation and rearrangement have neither been reported under such mild conditions before, nor on a completely unprotected natural product. So far this type of reaction was only published in 1993 for very low substituted benzofuranes⁹¹ and in the total synthesis of integrastatin B (8).^{44,48} Both literature known procedures use dimethyl dioxirane

(DMDO) as the oxidant, either prepared in advance or *in situ*. Additionally, during the total synthesis of integrastatin B this reaction is performed on the acetylated compound, protecting the remaining phenols. To my knowledge, this constitutes the first occurrence of this reaction under very mild conditions on an unprotected, highly substituted natural product.

To confirm this theory and provide reproducible reaction conditions thorough testing was done.

4.4.1 Oxidation of epicoccolide B under controlled environment

A wide variety of conditions were applied to epicoccolide B under a controlled environment to attempt a reproduction of this oxidation (Table 12).

Table 12: Optimization for the oxidative benzofurane rearrangement.

entry	oxidant	solvent	additives	time [min]	yield 1 [%]ª	unreacted 2 [%] ^a	comment
1	air (O ₂)	H ₂ O	excess NaHCO ₃ , 1% acetone	20	-	5	10% side product ^b
2	air (O ₂)	EtOH	10 eq NaHCO₃, 3% H₂O	10	-	100	
3	air (O ₂)	EtOH	10 eq $NaHCO_3$, 3% H_2O , $PtCl_2$	20	-	71	
4	O ₂	DMF	excess NaHCO₃	5	-	100	
5	O ₂	DMF	10 eq NaHCO₃, 4% H₂O	5	-	48	
6	O ₂	DMF/H₂O 1:1	excess NaHCO₃	15	-	15	15% side product ^b
7	O_2	DMF	salcomine	50	-	10	
8	mCPBA	EtOH	-	30	-	100	
9	Oxone® 2 eq	acetone/H₂O 2:1	9 eq NaHCO₃	30	-	50	
10	DMDO 1.4 eq	acetone	-	55	-	80	-41 °C
11	DMDO 1.4 eq	acetone	-	15	-	80	
12	DMDO 10 eq	acetone	-	15	5	73	
13	DMDO 10 eq	acetone	-	60	8	26	
14	DMDO 10 eq	acetone	-	120	6	7	
15	DMDO 100 eq	acetone	-	18	3-4	54	
16	DMDO 11 eq	acetone	12 eq NaHCO₃	15	-	-	total decomposition
17	DMDO 1.4 eq	acetone	-	30	-	11	Ac protected 2
18	Oxone® 2 eq	acetone/H₂O 2:1	6 eq NaHCO₃	120	-	12	Ac protected 2

^a qNMR yield. ^b unknown side product, not isolated.

The initial attempt was to recreate the conditions in the separation funnel by dissolving crude 2 in a large excess of alkaline water (saturated aqueous NaHCO₃) with minimal amounts of acetone for better solubility. A short reaction time and air, instead of pure oxygen, were chosen to simulate the duration

and atmosphere of the initial acid-base workup. Only decomposition and small amounts of a new unknown side product could be observed (entry 1). More mild conditions with reduced amounts of base and even small amounts of PtCl₂ also showed no conversion towards 1 (entries 2-3). Switching the solvent to DMF with varying amounts of water content and the atmosphere to pure oxygen had no impact on the desired reaction (entries 4-6). It continued to be only partial or no decomposition. Alternative oxidants for the epoxidation were tested as well. A more reactive state of oxygen, the singlet oxygen, was generated by the addition of salcomine and seemed to be too reactive for the system (entry 7).⁹² Other standard oxidation conditions like mCPBA showed no reactivity as well (entry 8).⁹³

The most promising results were obtained with DMDO, the oxidant used in literature. ^{44,48,91} Generating DMDO *in situ* or using small amounts of freshly distilled DMDO still gave no different results than before (entries 9-11). Increasing the amount of oxidant drastically gave the same product as it was observed in the separatory funnel, also as a mixture with unreacted **2** (entries 12-15). The best outcome was a short reaction time of 15 minutes with 10 equivalents of DMDO at room temperature resulting in a qNMR yield of 5% (entry 12). A large amount of unreacted **2** remained (73%). Increasing the reaction time or the amount of oxidant had no significant effect on the yield of **1** and only reduced the amount of reisolated starting material (entries 13-15). Also, the addition of base caused total decomposition (entry 16).

To compare the reaction to the sequence in the total synthesis of integrastatin B⁴⁴ all phenols were protected with acetate groups (Scheme 49).

Scheme 49: Acetate protection of all phenols of 2.

Acetate protected epicoccolide B **107** was obtained in a good yield following a standard protection protocol. ⁹⁴ Applying both freshly distilled and *in situ* generated DMDO to **107** only caused major decomposition (entries 17-18). The method published by *Ramana*⁴⁸ was not applicable for this compound. ⁴⁸

After obtaining enough material purification by HPLC was necessary again. Luckily, the developed method for **2** was suitable with a minor change of the gradient. Having barely enough material on hand detailed analytical data could be measured.

4.4.2 Comparing synthetic epicoccolide A to the literature

Mass spectrometry was able to confirm the absolute mass of the compound to perfectly fit the sum formula of epicoccolide A. Comparing the measured ¹H- and ¹³C-NMR to the literature³ caused serious confusion. The difference in chemical shift for most of the signals is way higher than measurement inaccuracy or residual solvent influences can explain. Furthermore, my NMR-data also does not match that of epicocconigrone A (5), an almost identically substituted tetracycle with the same sum formula introduced earlier. While comparing the data of my compound to the literature of epicoccolide A and epicocconigrone A I noticed remarkable similarity between the published analytical data. A comparison of all data sets sorted by chemical shift paints a very clear picture (Table 13).

Table 13: Comparison of epicoccolide A^3 , epicocconigrone A^{10} and synthesized 1 sorted by chemical shift δ [ppm].

entry		¹H			¹³ C	
	isolated 1	Laatsch ³	Proksch ¹⁰	isolated 1	Laatsch³	Proksch ¹⁰
1	2.29	2.25	2.25	11.9	10.1	10.1
2	2.33	2.32	2.31	12.7	11.7	11.8
3	6.11	6.33	6.35	71.0	68.7	68.7
4	6.75	6.79	6.80	89.3	90.0	90.0
5	10.32	10.35	10.35	113.8	104.1	104.0
6				115.6	112.8	112.9
7				119.1	115.4	115.4
8				120.2	121.6	121.6
9				121.1	121.7	121.6
10				121.9	126.6	126.6
11				135.9	132.5	132.5
12				138.2	135.8	135.8
13				140.0	138.3	138.4
14				141.4	144.2	144.2
15				144.0	148.6	148.6
16				145.0	152.8	153.0
17				191.3	191.1	191.2
18				193.3	196.9	196.9

The biggest discrepancies in the ¹H-NMR can be seen at 6.11 ppm vs. 6.33 ppm (entry 3). The other four signals are a near fit but still show a larger difference in chemical shift than the NMR data of *Laatsch* and *Proksch*. Further comparison of ¹³C-NMR data presents a continuation of this trend. While several signals are a near fit (e.g. entries 4,9,17) many others are vastly different (e.g. entries 5,7,16). However, when comparing the published NMR data, it can be seen that they are nearly identical with all differences well within measurement inaccuracy. Due to these observations, I formulated the theory that *Laatsch et. al* actually isolated epicocconigrone A but misassigned the structure. This would fully explain the findings regarding the NMR data. If this theory is correct that would also mean that the actual compound epicoccolide A was not isolated from nature so far. This in turn implies that epicoccolide A is not a natural product itself.

The co-occurrence of epicoccolide B and epicocconigrone A in the investigated fungi *Epicoccum sp. CAFTBO* (*Laatsch et. al.*) and *Epicoccum nigrum* (*Proksch et. al.*) clearly contradicts and questions both proposed biosynthetic pathways. The common intermediate **11** proposed by *Laatsch* does not result in epicoccolide A but only gives epicoccolide B. A possible explanation for the occurrence of epicocconigrone A might be a divergent benzoin addition of flavipin (**4**, Scheme 51).

Scheme 50: New proposed biosynthesis via a divergent benzoin addition of flavipin (4).

The initially proposed unsymmetrical addition (red) leads to the intermediate 11 while a symmetrical benzoin addition (blue) would result in 108. Formation of epicoccolide B (2) may be explained by a selective addition of the C-5 hydroxyl to the C-10 ketone giving 109. On the other side hemiacetal formation of the C-9 hydroxyl with the C-18 aldehyde instead of the C-10 ketone would result in the intermediate 110 and following cyclization to epicocconigrone A (5). The selectivity of the different pathways can be explained by the substitution pattern. Both cyclizations can be classified as 5/6 exo trig cyclizations according to the *Baldwin* rules. 95 For cyclizations at a trigonal center the *Bürgi-dunitz* angle of 109° for the attacking nucleophile is crucial for a successful reaction. 95 This angle is not possible for every reaction and can be shown by 3D modelling for both intermediates.

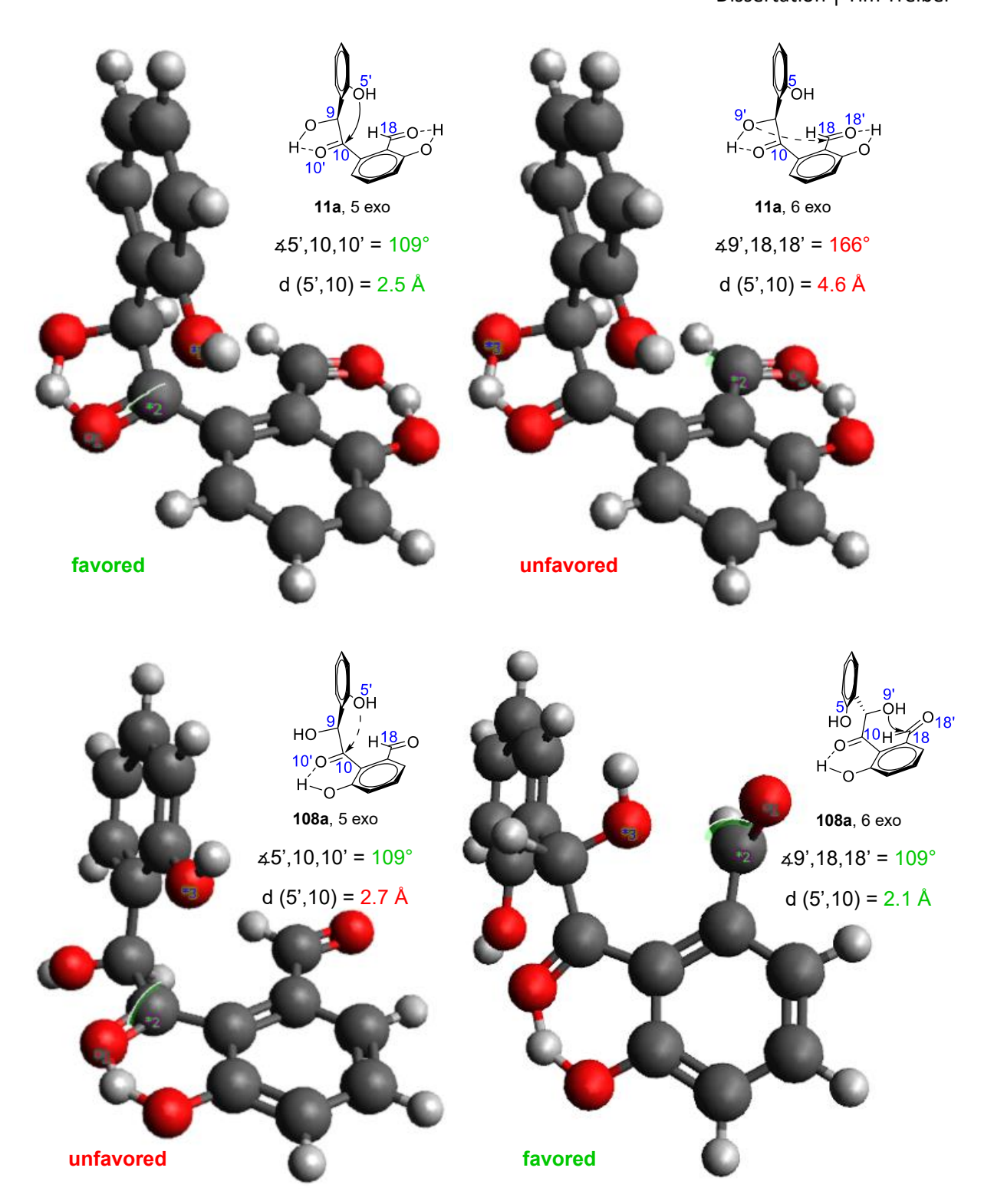


Figure 3: Modelling of the 5 exo cyclization (left) and 6 exo cyclization (right) for **11a** (top) and **108a** (bottom). Non participating functional groups were omitted to improve visibility. Carbon atoms: dark grey; Hydrogen atoms: light grey; Oxygen atoms: red. Relevant angles and distances shown.

Intermediate **11** forms two favored hydrogen bonds. These are between aldehyde C-18 and the *ortho*-hydroxyl group and between ketone C-10 and the hydroxyl at C-9. The 3D model (Figure 3, top) shows the fixed formation of this intermediate allowing only a single kind of cyclization. The hydrogen bond located at the bridge of the two aromatic rings brings the phenol at C-5 to the perfect angle and at a relatively short distance (Figure 3, top left). It is noteworthy that the ketone is rotated out of the

plane of the neighboring aromatic ring. The hydroxyl group at C-9 however is not even close to the aldehyde C-18 and at a completely different angle (Figure 3, top right). Furthermore, the aldehyde C-18 is fixed in the plane of the aromatic ring and can barely rotate out of it. If the hydroxyl group at C-9 were not engaged in a hydrogen bond it is still not possible to arrive at the optimal angle (not shown). The required free rotation of the aldehyde is shown below. These presented differences for the 5 exo and 6 exo cyclization show that it is basically impossible to form the previously proposed intermediate 12.

The difference for intermediate **108** is not as drastic but can still explain the observed cyclization. Ketone C-10 preferably forms a hydrogen bond with the *ortho*-phenol instead of the C-9 hydroxyl group on the bridge because the formed 6-ring is more stable and has a higher overlap of the involved orbitals. This introduces a rigidity that can also be observed for the aldehyde in intermediate **11**. The hydroxyl at C-5 can still reach the optimal attack angle of 109° but the distance to C-10 is slightly longer and it has to break apart a more rigid structure (Figure 3, bottom left). On the other hand, the hydroxyl at C-9 can move into the perfect position to attack aldehyde C-18 which rotates out of the aromatic plane (Figure 3, bottom right). This 6 exo cyclization has more degrees of freedom for finding the best possible attack angle and distance than the 5 exo cyclization. Additionally, it is possible that the C-9 hydroxyl can form a hydrogen bond with aldehyde C-18 fixing it in place for the attack (not shown). The different cyclizations can potentially both occur but the 6 exo cyclization is clearly more favored and results in the only observed benzofurane **2**.

The shown new proposed biosynthesis explains the co-occurrence of epicoccolide B(2) and epicocconigrone A(5) while no epicoccolide A (1) was ever isolated. Additionally, a detailed rational is presented to explain the difference in selectivity and cyclization behavior of the intermediates.

4.4.3 Detailed NMR-analysis of synthetic epicoccolide A

Finally, the last step to prove the structure of isolated epicoccolide A and the theory regarding *Laatsch* isolating epicocconigrone A is a detailed analysis of 2D-NMR experiments (HSQC, HMBC and NOESY). The final assignment and the most relevant correlations are shown in Table 14.

Table 14: NMR-assignment of epicoccolide A by 2D experiments in DMSO-d6. Only the most relevant correlations are shown.

position	δ(¹H) [ppm]	δ(¹³ C) [ppm]
1	6.75	89.3
2		119.1
3		140.0
4		141.4
5		145.0
6		120.2
7		115.6
8		193.3
9	6.11	71.0
10		113.8
11		121.9
12		121.1
13		144.0
14		138.2
15		135.9
16	2.33	12.7
17	10.32	191.3
18	2.29	11.9

The best starting point for the assignment is aldehyde H-17 with the unambiguous chemical shift of 10.32 ppm. The HSQC correlation to 191.3 ppm reveals the other carbonyl carbon (193.3 ppm) as C-8. The methyl groups were differentiated by NOE correlation of aldehyde H-17 with 2.29 ppm, which can only occur with H-18. Similarly, H-9 was assigned to 6.11 ppm by another NOE correlation to aldehyde H-17. The carbons C-10 to C-13 can be assigned by HMBC couplings of aldehyde H-17 and methyl group H-18. Hydrogens H-1, H-9 and H-16 all have HMBC couplings to 115.6 ppm assigning it to C-7, the only possible carbon seen by all three positions in a normal distance. Carbons C-5 and C-6 can be seen by methyl group H-16 and differentiated by their chemical shift. Similarly, C-2 and C-3 were assigned through H-1. Lastly, C-15 is allocated via HMBC couplings of H-1 and H-9 to 135.9 ppm. The only remaining unassigned carbons are C-4 and C-14 which are potentially exchangeable in their assignment because no couplings are visible for both carbons in DMSO-d6. The 2D experiments were repeated in acetone-d6 which showed very weak couplings of the methyl groups to the corresponding hydroxyl carbons, leading to the assignment shown above.

The three HMBC couplings that are connected to C-7 in addition to the coupling of H-1 to C-3 prove the configuration of epicoccolide A since this is not possible when methyl group H-16 and C-3 hydroxyl are swapped.

4.5 A very fast route to the core structure

With the first total synthesis of epicoccolide B completed the access to a simplified analog is crucial for SAR studies. Due to the success of the alkyne cyclization the simplest possible fragments were chosen without impacting the core aromatic structure. To reduce the synthetic effort both chosen fragments need to be easily accessible, ideally already synthesized before. Luckily, this is true for the iodide **99** and alkyne **92**. Both fragments are readily available and can be synthesized from **54** in six steps with a total yield of 70% and 71% respectively. Since reserves of both fragments were available the coupling could be tested immediately (Scheme 51).

Scheme 51: Coupling of iodide 99 and alkyne 92 to obtain 111.

Using the optimized reactions conditions established before coupling product **111** was obtained with an excellent yield. As with the other reactions before an excess of alkyne (3.56 eq) was needed and the side product **94** could be observed again. Next, the deprotection was tested (Table 15).

Table 15: Optimization of the deprotection of aldehyde 111.

entry	BBr ₃ [eq]	T [°C]	yield 112[%] ^a
1	6.0	0	26
2	6.0	-41	28
3	3.0	0	0
4	3.0	-41	5
5	6.0 ^b	-78	39
6	12.0 ^b	-78	40

^a qNMR yield. ^b PhMe₅ (6.22-6.71 eq) added as a cation scavenger.

Similar conditions as for the deprotection of **89** were applied. Varying temperature and equivalents of BBr₃ again the best result this time was achieved at -78 °C with the addition of the cation scavenger (entry 5-6). The most notable difference is that this time the alkyne immediately cyclizes during the deprotection to directly obtain **112** in moderate yields. Since no cyclization has to be done afterwards the yields is better than the 26% from the two-step sequence for epicoccolide B.

Analog **112** was synthesized in merely eight steps with a total yield of 28%. The scalability of the last two steps was not tested extensively but can be assumed to be very good, following trends observed before. For purification an acid-base workup of the reaction provided decently clean product which was further purified by HPLC, applying a similar protocol as for **2**, to give highly pure **112**. The successful coupling and cyclization using established or slightly modified protocols shows the high versatility of the route and possible access to more analogs. It is important to note that any adaptations to the substitution pattern should be done before the coupling of the fragments and final cyclisation. As shown in the first two attempts for the total synthesis the reactivity is drastically reduced for several reaction types once the conjugated π -system is built.

4.6 First attempts of synthesizing epicocconigrone A

With the success of the alkyne cyclization for two different routes and no total synthesis available for epicocconigrone A (5) the next step was to adapt the synthetic plan to also make 5. The well thought out construction of the fragments makes the initial planning very easy. lodide 99 can be used in a symmetric coupling to obtain dialdehyde 113 in a single step. Deprotection and cyclization leads to 114, another analog of epicoccolide B, which can then in turn be rearranged to 5 by the method developed before (Scheme 52).

Scheme 52: Planned synthesis for epicocconigrone A (5) using the alkyne cyclization.

4.6.1 Fragment synthesis and coupling

First, the symmetric coupling of iodide **99** was tested but various conditions only gave deiodinated product **72** (Scheme 53).

Scheme 53:Several attempts to couple iodide 99 with an alkyne.

Even the introduction of a terminal alkyne to obtain **115** was unsuccessful in several attempts. This behavior is consistent with the observations made before for every single coupling attempt of iodide **99** and was already expected. To avoid this problem the aldehyde was protected as a vinyl group (**116**) to drastically change the reactivity of the system (Scheme 54).⁹⁶

Scheme 54: Protection of the aldehyde with a vinyl group. Best isolated yield in parentheses.

The symmetric coupling of iodide **116** was achieved by *Stille* coupling with bis(trimethylstannyl) acetylene to get **117** (Table 16).⁹⁷

Table 16: Symmetric coupling if iodide 116 to internal alkyne 117. The acetylene linker is set to 1.00 equivalents.

entry	catalyst	eq 116	116 [%]	117 [%]	118 [%]
1	Pd(PPh ₃) ₂ Cl ₂ (8.7 mol%)	1.58	0	58	23
2	Pd(PPh ₃) ₄ (8.5 mol%)	2.00	0	83	17
3	Pd(PPh ₃) ₂ Cl ₂ (9.9 mol%)	2.30	12	68	0

For entries 1 and 2 incomplete conversion could be observed leading to remaining terminal alkyne **118**. The separation of **117** and **118** through standard column chromatography was not possible due to nearly identical polarity. The separation of product and starting material however was possible leading to an isolated yield of 68%. There are further options to improve the yield and conversion of this

reaction but they were beyond the time scope of this project. The amount obtained so far was sufficient to continue investigating the route.

Next, the oxidative cleavage of the vinyl groups was performed to release the aldehydes (Scheme 55).

Scheme 55: Oxidative cleavage of the vinyl groups to obtain dialdehyde 113.

Applying the conditions established before the oxidative cleavage gave dialdehyde **113** in a very good yield over 2 steps. The deprotection of **113** was attempted with all kinds of conditions, including the optimized ones from the other routes. However, every tested condition only resulted in partial or total decomposition. The same is true for the vinyl bearing compound **117**. All reserves of dialdehyde **113** were depleted during deprotection testing and I came to the conclusion that this route will not lead to the desired end products **114** and **5**. Therefore, this marks the end of my attempts for a total synthesis of epicocconigrone A **(5)**.

4.6.2 Revised approach to epicocconigrone A

The following results were obtained in the course of the master thesis of *Felicitas Wagner*, who was working under my supervision. Since the deprotection of **117** and **113** was not successful bearing benzyl groups the plan was to change the protection groups at an earlier stage to facilitate easier removal. Sufficient amounts of iodide **99** were provided to be deprotected and subsequently reprotected with different groups (Scheme 56). 98

Scheme 56: Planned swap of the protection groups for $\bf 99$.

As the first step a variety of deprotection methods were tested to obtain 119 (Table 17).

Table 17: Deprotection attempts of iodide 99.98

entry	conditions	time [min]	qNMR [%]	comment
1	Pd/C (2.30 eq), H₂ (1 bar), MeOH	30	-	no reaction
2	Pd/C (3.00 eq), H_2 (1 bar), MeOH	90	-	no reaction
3	Pd/C (3.00 eq), H₂ (20 bar), MeOH	60	-	no reaction
4	TMSI (5.00 eq), MeCN	120	-	no reaction
5	AlCl ₃ (12.0 eq), N,N-dimethylaniline (9.00 eq), DCM	60	-	decomposition
6	BF ₃ ·Et ₂ O (10.0 eq), 1,2-ethane dithiol	45	-	47% dithiolane
7	BBr ₃ (3.05 eq), DCM	20	39%	19% side product

Standard reductive deprotection did not show any reaction, even under very high pressure (entries 1-3). While some conditions also showed no reaction or even decomposition (entries 4-5)^{63,99} boron trifluoride resulted in complete deprotection. As expected, the aldehyde formed the respective dithiolane under these conditions but the thiol is crucial for the reaction and cannot be exchanged (entry 6). Using the established deprotection with boron tribromide showed some desired product but also an unidentified side product (entry 7). As this deprotection was the only one that worked without the formation of a dithiolane and showed moderate amounts of product it was investigated further (Table 18).⁹⁸

Table 18: Detailed screening of the deprotection using BBr₃ (3.00 eq).⁹⁸

entry	T [°C]	t [min]	work-up	119 [%]ª	75 [%]ª
1	20	20	aqueous	39	19
2	0	15	aqueous	42	18
3 ^b	0	15	aqueous	37	23
4	-41	15	aqueous	35	23
5 ^b	-41	15	aqueous	43	17
6	-78	15	aqueous	42	16
7 ^b	-78	15	aqueous	66	9
8 ^b	-78	15	acid-base	7	-

^a qNMR yield. ^b PhMe₅ (3.00 eq) added as a cation scavenger.

Temperature control and the addition of a cation scavenger showed barely any effect on the yield (entries 1-6) except for entry 7. The side product was identified as the deprotected and deiodinated

75, which was visible for all reactions with aqueous workup. When switching to an acid-base workup for purification major decomposition occurred and only a fraction of the expected yield remained (entry 8). Other purification methods also failed and it was not possible to isolate any desired product in a pure fashion.⁹⁸

At this point the plan was adapted to restart the entire synthesis from phenol **54** with different protection groups (Scheme 57).

Scheme 57: Currently ongoing plan for the total synthesis of 5.98

This endeavor is currently still ongoing and will be published at a later date once it is completed.

4.6.3 Different cyclisation attempts for core structure

In the course of the bachelor thesis of *Felicitas Wagner* she investigated the alternative cyclization of the tetracyclic core published by *Brimble* (Scheme 10).⁴⁹ Since the synthesis of the complete substitution pattern was beyond the scope of the project simplified fragments (**72** & **120**) were targeted (Figure 4).¹⁰⁰ The targeted tetracycle was that of epicocconigrone A.

Figure 4: Original fragments of *Brimble* (left)⁴⁹ vs. adapted fragments (right).¹⁰⁰

At the time of the bachelor thesis no reserves of material could be provided so the majority of the work consisted of the synthesis of known compounds. General precursor **57** was successfully synthesized and transformed to aldehyde **72**. Fragment **120** was obtained from **57** in two steps (Scheme 58).¹⁰⁰

Scheme 58: Synthesis of fragment 120 from general precursor 57.100

The sequence was not optimized but provided fragment **120** in a moderate yield through an efficient route. With both fragments in hand the first step of the coupling to **121** was tested under literature conditions (Scheme 59).

Scheme 59: Attempted coupling of the fragments. 100

Interestingly, the literature conditions did not provide the desired coupling product **121** but rather showed signs of a single decomposition side product of **120**. Later it was found that under strong basic conditions dithiolanes can decompose which does not occur with the respective dithiane.¹⁰¹

Scheme 60: Fragmentation of dithiolane 120 under basic conditions. 100

The observed fragmentation product turned out to be the internal cyclization product **122**. This explains the choice of dithianes in the literature instead of the more common dithiolanes. Due to time constraints, it was not possible to resynthesize fragment **120** with the respective dithiane. The project was ended at this point and further investigations put on hold. Even with the setback of the fragmentation the general plan might be worthwhile to pursue in the future as it provides an entirely different approach to the tetracyclic core and does not rely on the synthesis of the benzofurane.

4.7 Bioactivity assays of epicoccolide A & B and the two analogs

With the successful synthesis of epicoccolide A (1), epicoccolide B (2), analog 77 and simplified analog 112 first bioactivity studies were done in cooperation with *Matthias Eckhardt*. The sulfotransferase inhibitory potency was evaluated for all four compounds. The galactosylceramide-sulfotransferase was not available for testing so SULT1A1 was analyzed instead to test for general inhibitory activity (Table 19).

Table 19: IC50 values of the tested compounds for the inhibition of SULT1A1.

compound	ІС50 [μм]		
epicoccolide A (1)	13.46		
epicoccolide B (2)	4.81		
analog 77	> 50		
analog 112	16.38		

Epicoccolide B showed high potency confirming the previous results.³⁵ Furthermore, epicoccolide A and analog **112** retained inhibitory activity even with the different core or substitution pattern. Analog **77** however was not active in the given concentration range. The difference between the aldehydes in **2**, **77** and **112** seem to have a significant impact on the inhibitory potency. While the shift of the aldehyde from the second aromatic ring to the heterocycle completely removes activity for **77** the absence of that aldehyde entirely (**112**) only has a small impact and retains most of the activity.

These observations are very important for further SAR studies and give valuable insight into the lead structure. Furthermore, the analog **112** is much more readily available with a shorter route and better yields providing an excellent starting point for more in-depth studies in the future.

5. Conclusion and outlook

In conclusion the results presented in this thesis are a major advancement for the natural product family of epicoccolides. The first total synthesis of epicoccolide A (1) and epicoccolide B (2) was achieved in addition to the synthesis of two structural analogs (77 & 112). The synthetic routes for these compounds gave access to adequate amounts of product for important bioactivity studies. The focus of these studies was set on the sulfotransferase inhibition as this topic is of highest importance for the development of a new potential small molecule therapy to treat metachromatic leukodystrophy. The observed bioactivity of all four isolated compounds gives first insights into the SAR and a possible lead structure for further diversification.

The late-stage oxidation of unprotected epicoccolide B gave access to epicoccolide A, which then could be compared to the literature published by *Laatsch et al.* in 2013. Surprisingly the NMR-data did not match and later on it was found that the metabolite reported by *Laatsch* has to be reassigned to the structure of epicocconigrone A, originally reported by *Proksch et al.* in 2014. This unexpected correction questions both proposed biosynthetic pathways as epicoccolide A was, to my knowledge, never reported as a natural product so far. A revised biosynthetic pathway is proposed with a possible explanation for the unusual selectivity of the divergent benzoin addition.

Careful and thorough planning of the fragments and the routes made a divergent approach possible where everything emerges from a general precursor. Additionally, several fragments, including compounds originally synthesized for testing purpose, are used in different routes, minimizing synthetic efforts and waste. A detailed overview of all routes combined, highlighting the versatility of the successful and divergent approach, can be seen in Scheme 61.

5. Conclusion and outlook

Scheme 61: Complete overview of the synthesis of 1, 2, 77 and 112.

Starting from cheap and commercially available phenol **54** the general precursor **57** was synthesized in three steps with a cumulative yield of 73%. From here, two pathways emerge. The first option is to synthesize boronic ester **60** and benzofurane **65** separate from each other combining them to the core structure **66**. The benzofurane, synthesized midway through the complete route, presents interesting and unexpected reactivity regarding the formylation, introducing the aldehyde solely at the

heterocycle. Completing the route by transforming the methyl ester to the aldehyde and removing the protection groups gives the first analog of epicoccolide B **77**. The LLS consists of 13 steps with a combined yield of 21%, although fragment **65** displayed large inconsistencies regarding the reproducibility.

The second branch employs a new precursor **72** made from the general precursor **57** with an excellent cumulative yield over 2 steps. For the total synthesis of epicoccolide B aldehyde **72** is transformed to the fragments **99** and **100** with very good yields in an efficient sequence. Union of the fragments provides **104**. The final steps consist of the release of the aldehyde, removal of the benzyl protection groups and an alkyne cyclization to complete the first total synthesis of epicoccolide B **(2)**. The LLS consists of 13 steps with a combined yield of 11% with all steps being highly reproducible.

Analytical data of synthetic epicoccolide B is in full agreement with the reported data of the natural product confirming the complete architecture of this highly substituted aromatic compound. Initially during aqueous purification, a new product was observed under very mild conditions. The structure turned out to be that of epicoccolide A (1) and the reaction could be reproduced under controlled conditions with unprotected 2.

Another direction for the second branch is the synthesis of a simplified analog only bearing a single aldehyde. Aldehyde 72 is converted to the alkyne 92 and coupled with previously synthesized iodide 99 with very good yields, again in an efficient sequence. Deprotection of 111 directly facilitated the cyclisation to 112 in a single step revealing another interesting impact of the second aldehyde regarding reactivity. This analog's LLS consists of mere eight steps with a combined yield of 28% providing a highly efficient and reproducible route to access the simplified analog 112.

The scalability of most steps has been discussed in detail before and will not be repeated here. In summary a trend can be seen that all steps are highly scalable, once optimized, giving the desired products in a (deca)gram scale without significant or any loss of yield compared to a smaller lab scale. Purification methods have been adjusted and optimized to reduce effort and remove tedious and expensive column chromatography where possible. In many cases simple recrystallization or filtration over small amounts of silica gave pure products.

The goals of this thesis mentioned in chapter 3 were all completed successfully and first investigations into the total synthesis of epicocconigrone A were already started. Even with the vast number of results presented here, several topics are worthwhile to be researched further by other scientists.

Detailed mechanistic studies and optimization of the oxidative benzofurane rearrangement from 2 to 1 can significantly improve the yield and provide an established method to build further products bearing the unique [6,6,6,6]-tetracycle. This would be most relevant for the total synthesis of epicocconigrone A or other analogs. On the topic of epicocconigrone A, the alkyne route needs to be

5. Conclusion and outlook

investigated further to finish the first total synthesis. Alternatively, the cyclization presented in chapter 4.6.3 is a promising approach to build the tetracyclic core by a completely different route.

The simplified analog **112** can be derivatized for important SAR studies. The introduction of different functional groups, both on the heterocycle or the other aromatic position seem to have a very important effect for the bioactivity. Other possibilities consist of the removal or exchange of existing functional groups to increase reactivity and selectivity for the desired applications.

Finally, more testing of the bioactivity needs to be done in regards to antibacterial and antifungal properties. The published data is slim but shows promising activity for epicoccolide B. The lead structure can be very different compared to the results before and requires further investigation.

6.1 Materials and methods

Solvents and reagents:

All reagents and solvents were purchased from commercial suppliers (*Sigma Aldrich, TCI, Acros, Alfa Aesar, abcr, Carbolution*) in the highest purity grade available and used without further purification except noted otherwise. Anhydrous solvents (THF, toluene, CH₂Cl₂, MeCN) were obtained from a solvent drying system MB SPS-800 (MBraun) and stored over molecular sieves (4 Å). Dry acetone, 1,4-dioxane, CHCl₃, MeOH and DMF were bought from *Acros Organics* and were used as received. Degassed solvents were obtained by using standard freeze-pump-thaw methods on anhydrous solvents for 3 cycles.

Silver triflate (AgOTf) was dried and stored under argon in a glovebox. For drying the larger chunks were pulverized with a mortar and pestle and the resulting powder was dried in a desiccator over P_2O_5 for up to 2 weeks. If any chunks remain repeat this process until only a fine powder remains. Fresh dimethyl dioxirane (DMDO) was prepared and distilled according to literature and stored in the freezer (-20 °C). The concentration of the batch was also determined according to literature and was 60 mM. For *in situ* obtained DMDO Oxone was added to a mixture of acetone and water with the following reaction in the same mixture and vessel. IBX was prepared according to literature and stored in the freezer (-20 °C). The freezer (-20 °C).

Reaction handling:

The reactions in which dry solvents were used were performed under an argon atmosphere in flame-dried glassware, which had been flushed with argon unless stated otherwise. The reactants were handled using standard *Schlenk* techniques. Drying under vacuum refers to a pressure of <1 mbar at rt for at least 15 min to remove any residual solvents or air prior to the reaction. Temperatures above rt (23 °C) refer to oil bath temperatures which were controlled by a temperature modulator. For cooling, the following baths were used: acetone/dry ice (–78 °C), acetonitrile/dry ice (–41 °C), water/ice (0 °C). Reactions were magnetically stirred and monitored by TLC, unless otherwise noted.

Analytical Thin Layer Chromatography (TLC) monitoring was performed with silica gel 60_{F254} pre-coated polyester sheets (0.2 mm silica gel, *Macherey-Nagel*) and for reversed phase TLC silica gel 60 RP-18 F_{254} S pre-coated aluminum sheets (*Merck*). The spots were visualized using UV light and stained with a solution of CAM (1.0 g Ce(SO₄)₂), 2.5 g (NH₄)₆Mo₇O₂₄, 8 mL conc. H₂SO₄ in 100 mL H₂O) and

subsequent heating. Concentrations and removal of solvents *in vacuo* were performed by rotary evaporation at 40 °C at the respective pressure, unless otherwise noted.

Purification methods:

Flash column chromatography was accomplished using silica gel (pore size 60 Å; 0.040-0.063 mm) purchased from *Merck Millipore*, Massachusetts (USA). Compounds were eluted using the stated mixtures under a positive pressure of argon or air. Solvents for column chromatography (CH, EA) were distilled over a *Vigreux* column prior to use. Semi-preparative and analytical HPLC were performed on *Knauer Wissenschaftliche Geräte GmbH* systems by Andreas J. Schneider. The solvents for HPLC were purchased in HPLC grade. The chromatograms were recorded by UV-detection.

Analytical methods:

NMR spectra were recorded at room temperature (298 K) on a *Bruker* DPX-300 spectrometer with a 1 H operating frequency of 300 MHz, a *Bruker* DPX-400 spectrometer with a 1 H operating frequency of 400 MHz, a *Bruker* DSX-500 spectrometer with a 1 H operating frequency of 500 MHz and a 13 C operating frequencies of 126 MHz and a *Bruker* Avance III 700 spectrometer with a 1 H operating frequency of 700 MHz a 13 C operating frequencies of 176 MHz in deuterated solvents obtained from *Deutero, Carl Roth* or *Sigma Aldrich*. Spectra were measured at room temperature unless stated otherwise and chemical shifts are reported in ppm relative to $Si(Me)_4$ (d = 0.00 ppm) and were calibrated to the residual signal of undeuterated solvents. 105 Data for 1 H-NMR spectra are reported as follows: chemical shift (multiplicity, coupling constants, number of hydrogens, assignment). Abbreviations used are: s (singlet), d (doublet), m (multiplet). The spectra are zoomed to 0 - 13 ppm (1 H) and -10 – 240 ppm (1 C) with no signals outside of this range. Coupling constants through n bonds (1 J) are given in Hertz [Hz]. For quantitative NMR (qNMR) spectra the d_1 relaxation time was increased to 30 s. 1,3-Dichloro-4,6-dinitrobenzene or 1,1,2,2-tetrachloroethane were added as internal standards.

Mass spectra (MS) and High-resolution-mass spectra (HRMS) were recorded on a MAT 95 XL sector field device from *Thermo Finnigan* (Bremen) and microTOF-Q from *Bruker Daltonik* (Bremen) at the University Bonn under supervision of *Dr. Marianne Engeser*. Ionization processes and mol peaks are given.

Molecular modelling method:

3D modeling was done using Avogadro version 1.2.0n. The models were force field optimized with 'UFF' using a 'steepest descent' algorithm. After force field optimization minor rotations, well within regular molecule flexibility, were applied to improve visibility.

6.2 Experimental procedures

6.2.1 Relevant to chapter 4.1

Synthesis of ester 55

HO OMe
HO OMe
HO OH
$$54$$
 $C_{29}H_{26}O_{5}$
 $M = 454.52 \text{ g/mol}$

 K_2CO_3 (400 mg, 2.89 mmol, 6.11 eq) was flame-dried under vacuum before phenol **54** (87.3 mg, 474 mmol, 1.00 eq) and KI (26.4 mg, 159 mmol, 34 mol%) were added. The solids were suspended in dry acetone (10 mL) and stirred at room temperature for 15 min. BnCl (170 μL, 1.48 mmol, 3.12 eq) was added and the reaction was stirred at reflux for 20 h. After completion the reaction was cooled to room temperature, filtered and concentrated *in vacuo*. Flash column chromatography (SiO₂, CH/EA 19:1 \rightarrow 9:1) gave **55** (209 mg, 460 mmol, 97%) as a white amorphous solid.

¹H-NMR (500 MHz, CD₂Cl₂, 298 K): δ (ppm) = 7.47-7.44 (m, 4 H, H-Ph), 7.42-7.39 (m, 4 H, H-Ph), 7.39 (s, 2 H, H-2), 7.38-7.34 (m, 4 H, H-Ph), 7.28-7.25 (m, 3 H, H-Ph), 5.14 (s, 4 H, H-7), 5.09 (2, 2 H, H-8), 3.86 (s, 3 H, H-5). ¹³C-NMR (126 MHz, CD₂Cl₂, 298 K): δ (ppm) = 166.8 (C-6), 153.0 (C-3), 142.5 (C-4), 138.0 (C-Ph), 137.2 (C-Ph), 128.9 (C-Ph), 128.9 (C-Ph), 128.5 (C-Ph), 128.4 (C-Ph), 128.3 (C-Ph), 128.0 (C-Ph), 125.8 (C-1), 109.0 (C-2), 75.4 (C-8), 71.5 (C-7), 52.5 (C-5). **MS (EI, 70.0 eV)** m/z: [M⁻⁺] calcd. for C₂₉H₂₆O₅⁻⁺ 454.1780, found 454.1777.

Synthesis of iodide 56

BnO OMe Ph 9 0 3 2 8 7 OMe Ph 9 0 3 56
$$\frac{10}{6}$$
 56 $\frac{11}{10}$ Ph $\frac{10}{5}$ $\frac{11}{6}$ Ph $\frac{10}{5}$ $\frac{11}{6}$ Ph $\frac{10}{5}$ $\frac{11}{6}$ Ph $\frac{10}{5}$ $\frac{11}{6}$ $\frac{11}{6}$ Ph $\frac{10}{5}$ $\frac{11}{6}$ $\frac{11}{6}$ Ph $\frac{10}{5}$ $\frac{11}{6}$ $\frac{11}{6}$ Ph $\frac{10}{5}$ $\frac{11}{6}$ $\frac{11}{6}$

Ester **55** (20.0 g, 44.0 mmol, 1.00 eq) and AgCO₂CF₃ (9.71 g, 44.0 mmol, 1.00 eq) were dried under vacuum and I_2 (11.2 g, 44.0 mmol, 1.00 eq) was added. The solids were dissolved in dry CHCl₃ (100 mL) and the reaction was stirred at room temperature for 4 h. After completion the reaction was quenched with aqueous $Na_2S_2O_3$ (1 M, 100 mL). The phases were separated and the organic phase was concentrated *in vacuo*. Recrystallisation from MeOH (400 mL) gave iodide **56** (22.8 g, 39.2 mmol, 89%) as a white amorphous solid.

¹H-NMR (700 MHz, CD₂Cl₂, 298 K): δ (ppm) = 7.54-7.51 (m, 2 H, H-Ph), 7.47-7.44 (m, 2 H, H-Ph), 7.43-7.40 (m, 2 H, H-Ph), 7.40-7.35 (m, 7 H, H-Ph), 7.32-7.28 (m, 2 H, H-Ph), 7.31 (2, 1 H, H-6), 5.13 (s, 2 H, H-11), 5.10 (s, 2 H, H-10), 5.03 (s, 2 H, H-9), 3.90 (s, 3 H, H-7). ¹³C-NMR (176 MHz, CD₂Cl₂, 298 K): δ (ppm) = 167.2 (C-8), 153.6 (C-3), 153.3 (C-5), 144.9 (C-4), 137.4 (C-Ph), 137.2 (C-Ph), 136.6 (C-Ph), 132.1 (C-1), 129.2 (C-Ph), 129.0 (C-Ph), 128.7 (C-Ph), 128.7 (C-Ph), 128.7 (C-Ph), 128.6 (C-Ph), 128.1 (C-Ph), 112.6 (C-6), 84.6 (C-2), 76.0 (C-10), 75.6 (C-9), 71.7 (C-11), 52.8 (C-7). **MS (ESI-TOF)** m/z: [M+H]⁺ calcd. for C₂₉H₂₆IO₅⁺ 581.0819, found 581.0815.

Synthesis of the common precursor 57

lodide **56** (8.33 g, 14.4 mmol, 1.00 eq) and Pd(dppf)Cl₂ (310 mg, 424 μ mol, 2.95 mol%) were dissolved in dry 1,4-dioxane (30 mL) and ZnMe₂ (10.5 mL, 10% in hexane, 15.25 mmol, 1.06 eq) was added. The reaction was stirred at reflux for 3.25 h. After completion the reaction was cooled to room temperature and filtered over a short plug of silica (Et₂O). Et₂O (50 mL) and HCl (1.2 M, 100 mL) were added and the phases were separated. The aqueous phase was extracted with Et₂O (3×50 mL) and the combined organic phases were washed with H₂O (50 mL) and brine (50 mL). The organic phase was dried over MgSO₄ and concentrated *in vacuo*. Flash column chromatography (SiO₂, CH/EA 19:1 \rightarrow 9:1) gave common precursor **57** (5.62 g, 12.0 mmol, 84%) as a white amorphous solid.

¹H-NMR (500 MHz, CD₂Cl₂, 298 K): δ (ppm) = 7.48-7.45 (m, 2 H, H-Ph), 7.43-7.39 (m, 6 H, H-Ph), 7.38 (s, 1 H, H-6), 7.38-7.34 (m, 4 H, H-Ph), 7.31-7.28 (m, 3 H, H-Ph), 5.12 (s, 2 H, H-12), 5.11(s, 2 H, H-11), 4.97(s, 2 H, H-10), 3.85(s, 3 H, H-7), 2.40(s, 3 H, H-9). ¹³C-NMR (126 MHz, CD₂Cl₂, 298 K): δ (ppm) = 167.9 (C-8), 152.0 (C-3), 150.5 (C-5), 145.8 (C-4), 137.9 (C-Ph), 137.9 (C-Ph), 137.3 (C-Ph), 128.9 (C-Ph), 128.9 (C-Ph), 128.8 (C-Ph), 128.8 (C-Ph), 128.7 (C-Ph), 128.5 (C-Ph), 128.4 (C-Ph), 128.4 (C-Ph), 128.4 (C-Ph), 125.9 (C-1), 112.1 (C-6), 75.7 (C-11), 75.6 (C-10), 71.5 (C-12), 52.2 (C-7), 13.5 (C-9). **MS (ESI-TOF)** m/z: [M+H]⁺ calcd. for C₃₀H₂₉O₅⁺ 469.2010, found 469.2008.

Synthesis of acid **58**

Common precursor **57** (1.00 g, 2.15 mmol, 1.00 eq) and LiOH H_2O (455 mg, 10.8 mmol, 5.02 eq) were dissolved in a mixture of MeOH/ H_2O /DCM (7:3:5, 30 mL) and the mixture was stirred at 60 °C for 46 h. After completion the reaction was cooled to room temperature and HCl (2.5 M, 10 mL) and Et_2O (15 mL) were added. The phases were separated and the aqueous phase was extracted with Et_2O (3×10 mL). The combined organic phases were dried over MgSO₄ and concentrated *in vacuo* giving acid **58** (977 mg, 2.15 mmol, *quant*.) as a white amorphous solid.

¹H-NMR (500 MHz, CD₂Cl₂, 298 K): δ (ppm) = 7.52 (s, 1 H, H-6), 7.49-7.45 (m, 2 H, H-Ph), 7.43-7.39 (m, 7 H, H-Ph), 7.37-7.34 (m, 3 H, H-Ph), 7.32-7.29 (m, 3 H, H-Ph), 5.14 (s, 4 H, H-10, H-11), 4.98 (s, 2 H, H-9), 2.46 (s, 3 H, H-8). ¹³C-NMR (126 MHz, CD₂Cl₂, 298 K): δ (ppm) = 170.2 (C-7), 152.0 (C-3), 150.5 (C-5), 146.7 (C-4), 137.8 (C-Ph), 137.8 (C-Ph), 137.1 (C-Ph), 129.8 (C-2), 129.0 (C-Ph), 128.9 (C-Ph), 128.8 (C-Ph), 128.7 (C-Ph), 128.5 (C-Ph), 128.5 (C-Ph), 128.5 (C-Ph), 128.1 (C-Ph), 123.9 (C-1), 112.8 (C-6), 75.7 (C-4), 75.6 (C-3), 71.5 (C-5), 13.6 (C-8). **MS (ESI-TOF)** m/z: [M+NH₄]⁺ calcd. for $C_{29}H_{30}O_5N_1^+$ 472.2118, found 472.2118.

Synthesis of iodide 59

Acid **58** (586 mg, 1.29 mmol, 1.00 eq), I_2 (990 mg, 3.90 mmol, 3.02 eq) and K_3PO_4 (290 mg, 1.36 mmol, 1.06 eq) were dissolved in dry MeCN (20 mL). The mixture was stirred at reflux for 23 h before being cooled to 0 °C. The reaction was quenched with $Na_2S_2O_8$ (15 mL, 15 wt%), H_2O_2 (15 mL, 30 wt%) and aqueous $NaHCO_3$ (sat., 30 mL). The aqueous phase was extracted with Et_2O (3×40 mL) and CH_2CI_2 (1×40 mL). The combined organic phases were dried over Na_2SO_4 and the solvent was removed in vacuo. Flash column chromatography (SiO_2 , CH/EA 4:1) gave iodide **59** (406 mg, 766 µmol, 59%) as a red oil.

¹H-NMR (500 MHz, CD₂Cl₂, 298 K): δ (ppm) = 7.46-7.44 (m, 2 H, H-Ph), 7.43-7.34 (m, 11 H, H-Ph), 7.31-7.30 (m, 2 H, H-Ph), 7.29 (s, 1 H, H-6), 5.06 (s, 2 H, H-10), 5.04 (s, 2 H, H-9), 4.99 (s, 2 H, H-8), 2.29 (s, 3 H, H-7). ¹³C-NMR (126 MHz, CD₂Cl₂, 298 K): δ (ppm) = 151.9 (C-5), 151.2 (C-3), 143.0 (C-4), 138.0 (C-Ph), 137.8 (C-Ph), 137.1 (C-Ph), 129.3 (C-2), 128.9 (C-Ph), 128.9 (C-Ph), 128.9 (C-Ph), 128.9 (C-Ph), 128.8 (C-Ph), 128.7 (C-Ph), 128.5 (C-Ph), 128.5 (C-Ph), 128.4 (C-Ph), 128.1 (C-Ph), 120.4 (C-Ph), 93.8 (C-1), 75.8 (C-8), 75.7 (C-9), 71.7 (C-10), 21.8 (C-7). **MS (ESI-TOF)** m/z: [M+NH₄]⁺ calcd. for C₂₈H₂₉O₃I₁N₁⁺ 554.1187, found 554.1188.

Synthesis of boronic ester 60 through decarboxylative Miyaura borylation

Acid **58** (55.3 mg, 122 μ mol, 1.00 eq), (Bpin)₂ (47.8 mg, 188 μ mol, 1.55 eq), Pd(OAc)₂ (3.8 mg, 16.9 μ mol, 14 mol%) and dppb (7.7 mg, 18.1 μ mol, 15 mol%) were dried under vacuum. NEt₃ (25 μ L, 180 μ mol, 1.48 eq) and piv₂O (37 μ L, 182 μ mol, 1.5 eq) were added and the mixture was dissolved in dry 1,4-dioxane (5 mL). The reaction was stirred at reflux for 23 h. After completion the reaction was cooled to room temperature and filtered over a short plug of silica (CH₂Cl₂). Concentration *in vacuo* and flash column chromatography (SiO₂, CH/EA 19:1) gave boronic ester **60** (42.9 mg, 80.0 μ mol, 66%) as a white amorphous solid.

¹H-NMR (700 MHz, CD₂Cl₂, 298 K): δ (ppm) = 7.53-7.50 (m, 2 H, H-Ph), 7.48-7.35 (m, 11 H, H-Ph), 7.33-7.31 (m, 2 H, H-Ph), 7.28 (s, 1 H, H-6), 5.15 (s, 2 H, H-12), 5.12 (s, 2 H, H-11), 5.00 (s, 2 H, H-10), 2.45 (s, 3 H, H-9), 1.38 (s, 12 H, H-8). ¹³C-NMR (176 MHz, CD₂Cl₂, 298 K): δ (ppm) = 151.5 (C-3), 150.6 (C-5), 144.9 (C-4), 138.4 (C-Ph), 138.3 (C-Ph), 137.8 (C-Ph), 132.6 (C-1), 128.9 (C-Ph), 128.9 (C-Ph), 128.8 (C-Ph), 128.7 (C-Ph), 128.6 (C-Ph), 128.3 (C-Ph), 128.3 (C-Ph), 128.3 (C-Ph), 128.2 (C-Ph), 128.2 (C-2), 117.0 (C-6), 84.0 (C-7), 75.6 (C-11), 75.3 (C-10), 71.5 (C-12), 25.1 (C-8), 14.9 (C-9). **MS (ESI-TOF)** m/z: [M+H]⁺ calcd. for C₃₄H₃₈B₁O₅⁺ 537.2813, found 537.2805.

Synthesis of boronic ester 60 through regular Miyaura borylation

lodide **59** (385 mg, 717 μ mol, 1.00 eq), (Bpin)₂ (193 mg, 759 μ mol, 1.06 eq), Pd(OAc)₂ (5.2 mg, 23.2 μ mol, 3.2 mol%) and KOAc (217 mg, 2.21 mmol, 3.08 eq) were dissolved in dry DMF (11 mL) and degassed. The reaction was stirred at 85 °C for 5 h. After completion the reaction was cooled to room temperature and H₂O was added (30 mL). The aqueous phase was extracted with EA (3×30 mL) and the combined organic phases were dried over Na₂SO₄. Filtration over a plug of silica (EA) and removal of the solvent *in vacuo* gave crude **60**. Flash column chromatography (SiO₂, CH/EA 4:1) gave boronic ester **60** (336 mg, 626 μ mol, 87%) as a yellow oil.

For analytical data see above (decarboxylative route).

Synthesis of aldehyde 61

Common precursor **57** (2.40 g, 5.12 mmol, 1.00 eq) and dry AgOTf (3.96 g, 15.4 mmol, 3.00 eq) were dissolved in dry CH₂Cl₂ (40 mL) and cooled to -90 °C for 1 h. MeOCHCl₂ (1.37 mL, 15.4 mmol, 3.00 eq) was added and the reaction was stirred at -90 °C for 4 h. After completion the reaction was quenched with aqueous NaHCO₃ (sat., 20 mL) and stirred vigorously while thawing to room temperature. Et₂O (30 mL) was added and the reaction mixture was filtered. The phases were separated and the aqueous phase was extracted with Et₂O (3×50 mL). The combined organic phases were dried over MgSO₄ and concentrated *in vacuo* (room temperature, 300 mbar). Flash column chromatography (SiO₂, CH/EA 19:1) gave aldehyde **61** (2.54 g, 5.12 mmol, *quant*.) as a colorless oil.

¹H-NMR (300 MHz, CD₂Cl₂, 298 K): δ (ppm) = 10.11 (s, 1 H, H-13), 7.48-7.43 (m, 2 H, H-Ph), 7.41-7.34 (m, 13 H, H-Ph), 5.22 (s, 2 H, H-12), 5.18 (s, 2 H, H-10), 5.13 (s, 2 H, H-11), 3.84 (s, 3 H, H-7), 2.09 (s, 3 H, H-9). ¹³C-NMR (126 MHz, CD₂Cl₂, 298 K): δ (ppm) = 188.5 (C-13), 169.4 (C-8), 157.4 (C-3), 155.2 (C-5), 146.1 (C-4), 137.3 (C-Ph), 137.1 (C-Ph), 136.5 (C-Ph), 130.5 (C-1), 129.2 (C-Ph), 129.1 (C-Ph), 129.0 (C-Ph), 128.9 (C-Ph), 128.8 (C-Ph), 128.8 (C-Ph), 126.5 (C-2), 123.5 (C-6), 77.5 (C-12), 76.4 (C-11), 75.8 (C-10), 52.8 (C-7), 12.7 (C-9). **MS (EI, 70.0 eV)** m/z: [M⁺] calcd. for $C_{31}H_{28}O_6$ ⁺ 496.1886, found 496.1887.

Synthesis of geminal dibromide 62

PPh₃ (9.51g, 36.2 mmol ,6.00 eq) was dissolved in dry CH₂Cl₂ (20 mL) and cooled to 0 °C. CBr₄ (6.01 g, 18.1 mmol, 3.00 eq) was added and the mixture was stirred at 0 °C for 15 min. A solution of aldehyde **61** (3.00 g, 6.04 mmol, 1.00 eq) in dry CH₂Cl₂ (15 mL) was added and the reaction was stirred at room temperature for 19 h. After completion the reaction was quenched with aqueous Na₂S₂O₃ (sat., 50 mL). The phases were separated and the aqueous phase was extracted with CH₂Cl₂ (3×50 mL). The combined organic phases were washed with aqueous NaHCO₃ (50 mL), H₂O (50 mL) and brine (50 mL) and dried over Na₂SO₄. Filtration over a short plug of silica (CH₂Cl₂) and removal of the solvent *in vacuo* gave geminal dibromide **62** (3.60 g, 5.52 mmol, 91%) as a yellow oil.

¹H-NMR (500 MHz, CD₂Cl₂, 298 K): δ (ppm) = 7.44-7.33 (m, 15 H, H-Ph), 7.26 (s, 1 H, H-13), 5.13 (s, 2 H, H-11), 5.05 (s, 2 H, H-10), 5.00 (s, 2 H, H-12), 3.85 (s, 3 H, H-7), 2.20 (s, 3 H, H-9). ¹³C-NMR (126 MHz, CD₂Cl₂, 298 K): δ (ppm) = 168.4 (C-8), 152.0 (C-3), 148.4 (C-5), 147.7 (C-4), 137.6 (C-Ph), 137.5 (C-Ph), 134.1 (C-13), 129.1 (C-1), 129.0 (C-Ph), 128.9 (C-Ph), 128.8 (C-Ph), 128.8 (C-Ph), 128.8 (C-Ph), 128.6 (C-Ph), 127.3 (C-2), 126.0 (C-6), 94.1 (C-14), 76.1 (C-11), 76.1 (C-12), 75.6 (C-10), 52.6 (C-7), 13.6 (C-9). **MS (ESI-TOF)** m/z: [M+NH₄]⁺ calcd. for C₃₂H₃₂Br₂O₅N₁⁺ 668.0642/670.0624/672.0612, found 668.0645/670.0620/672.0597.

Synthesis of phenol 63

Dibromide **62** (850 mg, 1.30 mmol, 1.00 eq) and PhMe₅ (650 mg, 4.38 mmol, 3.37 eq) were dried under vacuum before being dissolved in dry CH₂Cl₂ (10 mL). The mixture was cooled to -78 °C and BCl₃ (8.0 mL, 1 M in CH₂Cl₂, 8.00 mmol, 6.14 eq) was added dropwise. After stirring at -78 °C for 30 min the reaction was quenched with a mixture of CHCl₃/MeOH (10:1, 5 mL). The reaction was thawed to room temperature and Celite (2.00 g) was added. The suspension was concentrated *in vacuo* and loaded onto a short plug of silica. The plug of silica was purged with CH (200 mL) and CH/EA (9:1, 200 mL) before extracting the product with EA (200 mL) into a different flask. Removal of the solvent *in vacuo* gave phenol **63** (490 mg, 1.28 mmol, 98%) as a green amorphous solid.

¹**H-NMR** (500 MHz, acetone-d6, 298 K): δ (ppm) = 7.95 (s, 1 H, H-OH), 7.86 (s, 1 H, H-OH), 7.71 (s, 1 H, H-OH), 7.38 (s, 1 H, H-10), 3.80 (s, 3 H, H-7), 2.17 (3 H, H-9). ¹³**C-NMR** (126 MHz, acetone-d6, 298 K): δ (ppm) = 169.1 (C-8), 145.0 (C-3), 141.3 (C-5), 135.9 (C-4), 135.1 (C-10), 124.9 (C-1), 116.5 (C-2), 115.7 (C-6), 94.2 (C-11), 52.0 (C-7), 12.9 (C-9). **MS** (ESI-TOF) m/z: [M-H]⁻ calcd. for C₁₁H₉Br₂O₅⁺ 378.8822/380.8804/382.8781, found 378.8823/380.8802/382.8782.

Synthesis of benzofurane 64

Phenol **63** (50.0 mg, 131 μ mol, 1.00 eq), K₃PO₄ (56.0 mg, 264 μ mol, 2.02 eq), CuI (25.0 mg, 131 μ mol, 1.00 eq) and picolinic acid (18.0 mg, 146 μ mol, 1.12 eq) were dried under vacuum before being dissolved in dry THF (2.0 mL). The reaction mixture was stirred at 80 °C for 24 h. After completion the reaction was cooled to room temperature and filter over a short plug of silica (EA). Removal of the solvent *in vacuo* gave benzofurane **64** (29.9 mg, 99.3 μ mol, 76%) as a white amorphous solid.

¹H-NMR (500 MHz, acetone-d6, 298 K): δ (ppm) = 9.38 (s, 1 H, H-OH), 7.78 (s, 1 H, H-OH), 7.12 (s, 1 H, H-10), 3.90 (2, 3 H, H-7), 2.54 (s, 3 H, H-9). ¹³C-NMR (126 MHz, acetone-d6, 298 K): δ (ppm) = 167.6 (C-8), 143.8 (C-5), 142.2 (C-3), 133.8 (C-4), 127.6 (C-11), 126.9 (C-1), 124.4 (C-6), 113.4 (C-2), 111.2 (C-10), 51.7 (C-7), 13.8 (C-9). **MS (ESI-TOF)** m/z: [M+H]⁺ calcd. for C₁₁H₁₀Br₁O₅⁺ 300.9706/302.9687, found 300.9722/302.9701.

Synthesis of benzofurane 65

Benzofurane **64** (175 mg, 582 μ mol, 1.00 eq), K₂CO₃ (506 mg, 3.66 mmol, 6.29 eq) and KI (15.0 mg, 90.4 μ mol, 16 mol%) were dried under vacuum and dissolved in dry acetone (10 mL). BnCl (135 μ L, 1.17 mmol, 2.20 eq) was added and the reaction was stirred at reflux for 52 h. After completion the reaction was cooled to room temperature and filtered over a plug of silica (CH₂Cl₂). Removal of the solvent *in vacuo* and flash column chromatography (SiO₂, CH/EA 19:1) gave benzofurane **65** (177 mg, 367 μ mol, 63%) as a white amorphous solid.

¹H-NMR (700 MHz, CD₂Cl₂, 298 K): δ (ppm) = 7.51-7.48 (m, 2 H, H-Ph), 7.42-7.33 (m, 8 H, H-Ph), 7.09 (s, 1 H, H-12), 5.51 (s, 2 H, H-11), 4.94 (s, 2 H, H-10), 3.91 (s, 3 H, H-7), 2.51 (s, 3 H, H-9). ¹³C-NMR (176 MHz, CD₂Cl₂, 298 K): δ (ppm) = 167.3 (C-8), 146.5 (C-3), 145.8 (C-5), 140.2 (C-4), 137.7 (C-Ph), 137.3 (C-Ph), 132.7 (C-1), 129.2 (C-13), 128.9 (C-Ph), 128.9 (C-Ph), 128.8 (C-Ph), 128.8 (C-Ph), 128.7 (C-Ph), 128.5 (C-6), 127.9 (C-Ph), 115.9 (C-2), 110.5 (C-12), 75.8 (C-10), 75.3 (C-11), 52.0 (C-7), 14.3 (C-9). **MS (APCI)** m/z: [M+H]⁺ calcd. for C₂₅H₂₁Br₁O₅⁺ 481.0645/483.0627, found 481.0632/483.0611.

Synthesis of coupling product 66

Benzofurane **65** (327 mg, 679 μ mol, 1.00 eq), boronic ester **60** (533 mg, 994 μ mol, 1.46 eq), XPhos Pd G4 (8.3 mg, 9.6 μ mol, 1.4 mol%) and K₃PO₄ (302 mg, 1.42 mmol, 2.09 eq) were dissolved in degassed THF/H₂O (4:1, 30 mL). The reaction was stirred at room temperature for 23 h. Filtration over a plug of silica (CH₂Cl₂) and removal of the solvent *in vacuo* gave crude coupling product **66** (613 mg). The crude product was purified by flash column chromatography (SiO₂, CH/EA 19:1) to obtain pure **66** (551 mg, 679 mol, *quant*.) as a red amorphous solid.

¹H-NMR (700 MHz, CD₂Cl₂, 298 K): δ (ppm) = 7.53-7.50 (m, 2 H, H-Ph), 7.48-7.41 (m, 9 H, H-Ph), 7.40-7.31 (m, 14 H, H-Ph), 7.25 (s, 1 H, H-14), 7.16 (s, 1 H, H-7), 5.58 (s, 2 H, H-19), 5.17 (s, 2 H, H-23), 5.14 (s, 2 H, H-22), 5.06 (s, 2 H, H-21), 4.97 (s, 2 H, H-18), 3.95 (s, 3 H, H-15), 2.53 (s, 3 H, H-17), 2.41 (s, 3 H, H-20). ¹³C-NMR (176 MHz, CD₂Cl₂, 298 K): δ (ppm) = 167.8 (C-16), 156.8 (C-8), 152.2 (C-13), 151.1 (C-11), 146.4 (C-3), 144.3 (C-5), 143.4 (C-12), 140.6 (C-4), 138.1 (C-Ph), 138.0 (C-Ph), 137.9 (C-Ph), 137.6 (C-Ph), 137.4 (C-Ph), 131.8 (C-1), 129.0 (C-Ph), 128.9 (C-Ph), 128.9 (C-Ph), 128.9 (C-Ph), 128.8 (C-Ph), 128.8 (C-Ph), 128.7 (C-Ph), 128.6 (C-Ph), 128.5 (C-Ph), 128.4 (C-Ph), 128.4 (C-6), 128.0 (C-Ph), 125.8 (C-9), 124.4 (C-10), 116.6 (C-2), 110.3 (C-14), 106.8 (C-7), 75.8 (C-22), 75.8 (C-18), 75.7 (C-21), 75.3 (C-19), 71.6 (C-23), 51.9 (C-15), 14.3 (C-17), 14.2 (C-20). **MS (ESI-TOF)** m/z: [M+H]⁺ calcd. for C₅₃H₄₇O₈⁺ 811.3265, found 811.3260.

Synthesis of aldehyde 69

Coupling product **66** (99.2 mg, 122 μ mol, 1.00 eq) and dry AgOTf (95.3 mg, 371 μ mol, 3.03 eq) were dissolved in dry CH₂Cl₂ (5.0 mL) and cooled to -78 °C for 40 min. MeOCHCl₂ (34.0 μ L, 383 μ mol, 3.13 eq) was added and the reaction was stirred at -78 °C for 3 h. After completion the reaction was quenched with aqueous NaHCO₃ (sat., 4.0 mL) and stirred vigorously while thawing to room temperature. Et₂O (5.0 mL) was added and the reaction mixture was filtered. The phases were separated and the aqueous phase was extracted with Et₂O (3×20 mL). The combined organic phases were dried over MgSO₄ and filtered over a tall plug of silica (Et₂O). Removal of the solvent *in vacuo* (room temperature, 300 mbar) gave aldehyde **69** (103 mg, 122 μ mol, *quant.*) as a yellow amorphous solid.

¹H-NMR (500 MHz, CD₂Cl₂, 298 K): δ (ppm) = 9.67 (2, 1 H, H-24), 7.47-7.43 (m, 6 H, H-Ph), 7.43-7.39 (m, 6 H, H-Ph), 7.38-7.32 (m, 13 H, H-Ph), 6.93 (s, 1 H, H-14), 5.41 (s, 2 H, H-19), 5.18 (s, 2 H, H-22), 5.13 (s, 2 H, H-23), 5.09 (s, 2 H, H-21), 5.04 (s, 2 H, H-18), 3.96 (s, 3 H, H-15), 2.29 (s, 3 H, H-17), 2.15 (s, 3 H, H-20). ¹³C-NMR (126 MHz, CD₂Cl₂, 298 K): δ (ppm) = 185.9 (C-24), 168.8 (C-16), 168.1 (C-8), 152.2 (C-11), 151.1 (C-13), 147.8 (C-3), 145.6 (C-5), 145.1 (C-12), 138.4 (C-4), 137.9 (C-Ph), 137.8 (C-Ph), 137.7 (C-Ph), 137.3 (C-Ph), 128.9 (C-Ph), 129.0 (C-Ph), 128.9 (C-Ph), 128.9 (C-Ph), 128.9 (C-Ph), 128.8 (C-Ph), 128.8 (C-Ph), 128.8 (C-Ph), 128.7 (C-Ph), 128.6 (C-Ph), 128.6 (C-Ph), 128.5 (C-Ph), 128.1 (C-1), 126.9 (C-9), 122.9 (C-10), 122.7 (C-2), 118.9 (C-7), 118.5 (C-6), 113.8 (C-14), 75.9 (C-22), 75.9 (C-18), 75.8 (C-19), 75.7 (C-21), 71.7 (C-23), 52.5 (C-15), 14.0 (C-20), 13.8 (C-17). **MS (APCI)** m/z: [M+H]⁺ calcd. for C₅₄H₄₇O₉⁺ 839.3215, found 839.3215.

Synthesis of diol 70

Aldehyde **69** (254 mg, 302 μ mol, 1.00 eq) was dissolved in dry THF (10 mL) and cooled to 0 °C. DIBAl-H (1.6 mL, 1 M in hexane, 1.60 mmol, 5.30 eq) was added dropwise and the reaction was stirred for 2 h while warming to room temperature. After completion the reaction was quenched with aqueous *Rochelle* salt (sat., 10 mL). The phases were separated and the aqueous phase was extracted with Et₂O (3×20 mL). The combined organic phases were dried over MgSO₄ and filtered over a short plug of silica (Et₂O). Removal of the solvent *in vacuo* gave diol **70** (240 mg, 295 μ mol, 98%) as a white amorphous solid.

¹H-NMR (700 MHz, CD₂Cl₂, 298 K): δ (ppm) = 7.49-7.43 (m, 10 H, H-Ph), 7.41-7.31 (m, 15 H, H-Ph), 6.90 (s, 1 H, H-14), 5.40 (s, 2 H, H-18), 5.16 (s, 4 H, H-21, H-22), 5.09 (s, 2 H, H-20), 5.01 (s, 2 H, H-15), 5.00 (s, 2 H, H-17), 4.71 (s, 2 H, H-23), 2.39 (s, 3 H, H-15), 2.15 (s, 3 H, H-19). ¹³C-NMR (176 MHz, CD₂Cl₂, 298 K): δ (ppm) = 155.1 (C-8), 152.0 (C-11), 150.8 (C-13), 146.9 (C-3), 145.8 (C-12), 143.8 (C-5), 138.1 (C-Ph), 138.1 (C-Ph), 138.0 (C-Ph), 137.9 (C-Ph), 137.6 (C-4), 137.4 (C-Ph), 128.9 (C-Ph), 128.9 (C-Ph), 128.8 (C-Ph), 128.8 (C-Ph), 128.8 (C-Ph), 128.8 (C-Ph), 128.8 (C-Ph), 128.6 (C-Ph), 128.6 (C-Ph), 128.6 (C-Ph), 128.4 (C-Ph), 128.4 (C-Ph), 128.0 (C-Ph), 127.6 (C-6), 126.4 (C-9), 126.2 (C-2), 125.1 (C-1, C-10), 124.9 (C-7), 117.1, 113.0 (C-14), 75.9 (C-17), 75.8 (C-21), 75.6 (C-20), 75.4 (C-18), 71.5 (C-22), 59.3 (C-15), 57.2 (C-23), 13.9 (C-19), 12.2 (C-16). **MS (ESI-TOF)** m/z: [M+NH₄]⁺ calcd. for C₅₃H₅₂O₈N₁⁺ 830.3687, found 830.3692.

Global deprotection of diol 70 to 76

Diol **70** (15.4 mg, 18.9 μ mol, 1.00 eq) and Pd/C (18.0 mg, 169 μ mol, 8.93 eq) were suspended in dry MeOH (2.0 mL) and H₂ gas was bubbled through the reaction mixture at room temperature for 1.75 h. After completion of the reaction the mixture was filtered over a plug of silica (EA) and the solvent was removed *in vacuo* to obtain **76** as a white amorphous solid (5.5 mg, 15.2 μ mol, 80%).

¹H-NMR (400 MHz, acetone-d6, 298 K): δ (ppm) = 7.11 (s, 1 H, H-14), 3.92 (s, 2 H, H-15), 3.78 (s, 2 H, H-17), 2.56 (s, 3 H, H-16), 2.24 (s, 3 H, H-19). **MS (ESI-TOF)** m/z: [M+H-H₂O]⁺ calcd. for C₁₈H₁₇O₇⁺ 345.0969, found 345.0965.

Synthesis of dialdehyde 78

Diol **70** (16.2 mg, 19.9 μ mol, 1.00 eq) and IBX (68.2 mg, 244 μ mol, 12.2 eq) were suspended in EA (2.0 mL) and stirred at 85 °C for 2.7 h. After completion the reaction mixture was cooled to 2 °C (fridge, 60 min). Filtration over a short plug of silica (EA) and removal of the solvent *in vacuo* gave dialdehyde **78** (13.2 mg, 16.3 μ mol, 82%) as a white amorphous solid.

¹H-NMR (300 MHz, CD₂Cl₂, 298 K): δ (ppm) = 10.95 (s, 1 H, H-15), 9.77 (s, 1 H, H-23), 7.48-7.32 (m, 25 H, H-Ph), 6.95 (s, 1 H, H-14), 5.52 (s, 2 H, H-18), 5.19 (s, 2 H, H-21), 5.15 (s, 2 H, H-22), 5.10 (s, 2 H, H-20), 5.00 (s, 2 H, H-17), 2.58 (s, 3 H, H-16), 2.13 (s, 3 H, H-19). ¹³C-NMR (126 MHz, CD₂Cl₂, 298 K): δ (ppm) = 194.7 (C-15), 186.5 (C-23), 169.8 (C-8), 152.1 (C-11), 151.1 (C-13), 147.8 (C-3), 145.5 (C-5), 145.2 (C-12), 141.3 (C-4), 137.8 (C-Ph), 137.7 (C-Ph), 137.4 (C-Ph), 137.0 (C-Ph), 136.9 (C-Ph), 133.1 (C-2), 129.0 (C-Ph), 128.9 (C-Ph), 128.9 (C-Ph), 128.9 (C-Ph), 128.8 (C-Ph), 128.8 (C-Ph), 128.7 (C-Ph), 128.7 (C-Ph), 128.6 (C-Ph), 128.6 (C-Ph), 128.6 (C-Ph), 128.1 (C-6), 127.1 (C-9), 124.1 (C-1), 123.3 (C-7), 123.0 (C-10), 120.1, 113.8 (C-14), 75.9 (C-17, C-21), 75.7 (C-18), 75.7 (C-20), 71.8 (C-22), 14.0 (C-19), 13.6 (C-16). **MS (APCI)** m/z: [M+H]⁺ calcd. for C₅₃H₄₅O₈⁺ 809.3109, found 809.3103.

Synthesis of first analog 77

Dialdehyde **78** (8.4 mg, 10.4 μ mol, 1.00 eq) was dissolved in dry CH₂Cl₂ (1.0 mL) and BBr₃ (120 μ L, 1.0 μ M in CH₂Cl₂, 120 μ mol, 11.6 eq) was added dropwise. The reaction was stirred at room temperature for 25 min. After completion H₂O (5.0 mL) and brine (5.0 mL) were added. The phases were separated and the aqueous phase was extracted with EA (3×10 mL). The combined organic phases were washed with brine (10 mL) and dried over Na₂SO₄. CH (15 mL) was added and the solution was filtered over a short plug of silica. Purging the plug of silica with generous amounts of EA into a different flask and removal of the solvent *in vacuo* gave the first analog **77** (3.2 mg, 8.9 μ mol, 86%) as a white amorphous solid.

¹H-NMR (400 MHz, acetone-d6, 298 K): δ (ppm) = 11.11 (s, 1 H, H-15), 9.84 (s, 1 H, H-18), 9.74 (s, 1 H, H-OH), 8.48 (s, 1 H, H-OH), 8.11 (s, 1 H, H-OH), 8.03 (s, 1 H, H-OH), 7.74 (s, 1 H, H-OH), 6.68 (s, 1 H, H-14), 2.63 (s, 3 H, H-16), 2.17 (s, 3 H, H-17). ¹³C-NMR (176 MHz, acetone-d6, 298 K): δ (ppm) = 195.4 (C-15), 187.1 (C-18), 171.7 (C-8), 145.5 (C-11), 143.8 (C-13), 143.3 (C-3), 143.1 (C-5), 136.6 (C-12), 135.0 (C-4), 126.4 (C-2), 121.7 (C-1), 120.9 (C-6), 120.4 (C-7), 119.2 (C-9), 118.3 (C-10), 111.6 (C-14), 13.3 (C-16), 13.2 (C-17). **MS (APCI)** m/z: [M+H]⁺ calcd. for C₁₈H₁₅O₈⁺ 359.0761, found 359.0758.

Synthesis of alcohol 71

Common precursor **57** (1.20 g, 2.56 mmol, 1.00 eq) was dissolved in dry THF (10 mL) and cooled to 0 °C. DIBAl-H (5.5 mL, 1.0 M in hexanes, 5.50 mmol, 2.15 eq) was added and the reaction was stirred at 0 °C for 45 min. After completion the reaction was quenched with aqueous *Rochelle* salt (sat., 20 mL). The phases were separated and the aqueous phase was extracted with Et_2O (3×20 mL). The combined organic phases were dried over MgSO₄ and filtered over a short plug of silica (Et_2O). Removal of the solvent *in vacuo* gave alcohol **71** (1.13 g, 2.56 mmol, *quant*.) as a white amorphous solid.

¹H-NMR (700 MHz, CD₂Cl₂, 298 K): δ (ppm) = 7.48-7.46 (m, 2 H, H-Ph), 7.44-7.38 (m, 6 H, H-Ph), 7.38-7.33 (m, 4 H, H-Ph), 7.31-7.29 (m, 2 H, H-Ph), 6.90 (s, 1 H, H-6), 5.12 (s, 2 H, H-11), 5.05 (s, 2 H, H-10), 5.00 (s, 2 H, H-9), 4.61 (d, ${}^{2}J_{7,7}$ = 5.4 Hz, 2 H, H-7), 2.16 (s, 3 H, H-8). ¹³C-NMR (176 MHz, CD₂Cl₂, 298 K): δ (ppm) = 151.7 (C-3), 151.0 (C-5), 141.7 (C-4), 138.3 (C-Ph), 138.3 (C-Ph), 137.7 (C-Ph), 135.3 (C-1), 128.9 (C-Ph), 128.9 (C-Ph), 128.8 (C-Ph), 128.7 (C-Ph), 128.6 (C-Ph), 128.3 (C-Ph), 128.3 (C-Ph), 128.3 (C-Ph), 128.0 (C-Ph), 123.2 (C-2), 109.7 (C-6), 75.7 (C-10), 75.5 (C-9), 71.5 (C-11), 63.6 (C-7), 11.3 (C-8). MS (EI, 70.0 eV) m/z: [M⁻⁺] calcd. for C₂₉H₂₈O₄ 440.1988, found 440.1988.

Synthesis of aldehyde 72

BnO OH Ph 9 O 3 2 77 H Ph O 5 6 72 Ph
$$C_{29}H_{26}O_4$$
 M = 438.52 g/mol

Alcohol **71** (15.7 mg, 35.6 μ mol, 1.00 eq) and IBX (16.0 mg, 57.1 μ mol, 1.60 eq) were suspended in EA (1.0 mL) and stirred at 85 °C for 2 h. After completion the reaction mixture was cooled to 2 °C (fridge, 60 min). Filtration over a short plug of silica (EA) and removal of the solvent *in vacuo* gave aldehyde **72** (15.6 mg, 35.6 μ mol, *quant.*) as a white amorphous solid.

¹H-NMR (700 MHz, CD₂Cl₂, 298 K): δ (ppm) = 10.21 (s, 1 H, H-7), 7.48-7.46 (m, 2 H, H-Ph), 7.41-7.39 (m, 7 H, H-Ph); 7.38-7.34 (m, 4 H, H-Ph), 7.31 (s, 1 H, H-6), 7.31-7.29 (m, 2 H, H-Ph), 5.17 (s, 2 H, H-10), 5.16 (s, 2 H, H-11), 4.99 (s, 2 H, H-9), 2.47 (s, 3 H, H-8). ¹³C-NMR (176 MHz, CD₂Cl₂, 298 K): δ (ppm) = 191.1 (C-7), 151.9 (C-3), 151.4 (C-5), 147.7 (C-4), 137.7 (C-Ph), 137.7 (C-Ph), 137.1 (C-Ph), 130.2 (C-1), 129.6 (C-2), 129.0 (C-Ph), 128.9 (C-Ph), 128.8 (C-Ph), 128.7 (C-Ph), 128.5 (C-Ph), 128.5 (C-Ph), 128.5 (C-Ph), 128.1 (C-Ph), 110.7 (C-6), 75.7 (C-9), 75.7 (C-10), 71.4 (C-11), 10.8 (C-8). **MS (ESI-TOF)** m/z: [M+H]⁺ calcd. for C₂₉H₂₇O₄⁺ 439.1904, found 439.1901.

Deprotection of alcohol 71 to 74

BnO OH HO 3
$$\frac{2}{7}$$
 7
HO $\frac{3}{5}$ $\frac{2}{6}$ 74

 $\frac{C_8H_{10}O_4}{M}$ M = 170.16 g/mol

Alcohol **71** (123 mg, 280 μ mol, 1.00 eq) and Pd/C (112 mg, 1.04 mmol, 3.72 eq) were suspended in dry MeOH (5.0 mL) and H₂ gas was bubbled through the reaction mixture at room temperature for 50 min. After completion the reaction mixture was filtered over a plug of silica (EA) and the solvent was removed *in vacuo* to obtain **74** as a white amorphous solid (40.2 mg, 236 μ mol, 84%).

¹**H-NMR** (300 MHz, acetone-d6, 298 K): δ (ppm) = 6.46 (s, 1 H, H-6), 4.45 (s, 2 H, H-7), 2.10 (s, 3 H, H-8).

Deprotection of aldehyde 72 to 75

Aldehyde **72** (14.2 mg, 32.4 μ mol, 1.00 eq) and Pd/C (10.0 mg, 94.0 μ mol, 2.90 eq) were suspended in dry MeOH (1.0 mL) and H₂ gas was bubbled through the reaction mixture at room temperature for 25 min. After completion the reaction mixture was filtered over a plug of silica (EA) and the solvent was removed *in vacuo* to obtain **75** as a white amorphous solid (5.3 mg, 31.5 μ mol, 97%).

¹**H-NMR** (300 MHz, acetone-d6, 298 K): δ (ppm) = 10.06 (s, 1 H, H-7), 6.95 (s, 1 H, H-6), 2.47 (s, 3 H, H-8).

Synthesis of dimethoxy acetal 79

Aldehyde **72** (50.0 mg, 114 μ mol, 1.00 eq) was dissolved in dry MeOH (2.0 mL) and dry CH₂Cl₂ (0.5 mL). CH(OMe)₃ (30 μ L, 29.1 mg, 274 μ mol, 2.41 eq) and dry HCL (4.0 μ m in 1,4-dioxane, 2 drops) were added and the reaction was stirred at room temperature for 2.5 h. After completion the reaction was quenched with aqueous NaHCO₃ (sat., 5.0 mL). The aqueous phase was extracted with CH₂Cl₂ (3×20 mL) and the combined organic phases were dried over Na₂SO₄. Removal of the solvent *in vacuo* gave dimethoxy acetal **79** as a white amorphous solid (52.2 mg, 108 μ mol, 94%).

¹**H-NMR** (300 MHz, CD₂Cl₂, 298 K): δ (ppm) = 7.49-7.28 (m, 15 H, H-Ph), 7.04 (s, 1 H, H-6), 5.12 (s, 2 H, H-12) 5.06 (s, 2 H, H-11) 4.98 (s, 2 H, H-10), 4.92 (s, 1 H, H-7), 3.28 (s, 3 H, H-8), 3.27 (s, 3 H, H-8), 2.15 (s, 3 H, H-9).

Synthesis of dioxolane 81

Aldehyde **72** (24.2 mg, 55.2 μ mol, 1.00 eq) was dissolved in dry ethylene glycol (3 mL) and dry CH₂Cl₂ (1.0 mL). CH(OMe)₃ (0.5 mL) and dry HCL (4.0 M in 1,4-dioxane, 2 drops) were added and the reaction was stirred at room temperature for 23 h. After completion the reaction was quenched with aqueous NaHCO₃ (sat., 5.0 mL). The aqueous phase was extracted with CH₂Cl₂ (3×10 mL) and the combined organic phases were dried over MgSO₄. Filtration over a plug of silica (CH₂Cl₂) and removal of the solvent *in vacuo* gave dioxolane **81** as a white amorphous solid (22.2 mg, 46.0 μ mol, 83%).

¹**H-NMR** (300 MHz, CD₂Cl₂, 298 K): δ (ppm) = 7.50-7.28 (m, 15 H, H-Ph), 7.07 (s, 1 H, H-6), 5.87 (s, 1 H, H-7) 5.12 (s, 2 H, H-12) 5.06 (s, 2 H, H-11), 4.99 (s, 2 H, H-10), 4.10-4.17 (m, 2 H, H-8), 4.03-3.99 (m, 2 H, H-8), 2.22 (s, 3 H, H-9).

Synthesis of dithiolane 83

Aldehyde **72** (107 mg, 243 μ mol, 1.00 eq), Amberlyst® (153 mg, 487 μ mol, 2.00 eq) and MgSO₄ (178 mg) were dried under vacuum and dissolved in dry THF (4.0 mL).1,2-Ethane dithiol (40 μ L, 44.8 mg, 477 μ mol, 1.96 eq) was added and the reaction was stirred at room temperature for 20 h. After completion the reaction mixture was filtered over a plug of silica (CH₂Cl₂) and removal of the solvent *in vacuo* gave crude dithiolane **83**. Flash column chromatography (SiO₂, CH/EA 19:1) provides pure dithiolane **83** (125 mg, 243 μ mol, *quant*.) as a white amorphous solid.

¹**H-NMR** (500 MHz, CD₂Cl₂, 298 K): δ (ppm) = 7.49-7.46 (m, 2 H, H-Ph), 7.43-7.34 (m, 10 H, H-Ph), 7.33 (s, 1 H, H-6), 7.31-7.29 (m, 3 H, H-Ph), 5.83 (s, 1 H, H-7), 5.14 (s, 2 H, H-12), 5.04 (s, 2 H, H-11), 4.97 (s, 2 H, H-10), 3.44-3.38 (m, 2 H, H-8), 3.35-3.29 (m, 2 H, H-8), 2.23 (s, 3 H, H-9). ¹³**C-NMR** (126 MHz, CD₂Cl₂, 298 K): δ (ppm) = 151.3 (C-3), 150.9 (C-5), 141.9 (C-4), 138.3 (C-Ph), 138.1 (C-Ph), 137.7 (C-Ph), 134.3 (C-1), 128.9 (C-Ph), 128.8 (C-Ph), 128.7 (C-Ph), 128.6 (C-Ph), 128.3 (C-Ph), 128.1 (C-Ph) (C-Ph), 123.5 (C-2), 109.7 (C-6), 75.7 (C-11), 75.6 (C-10), 71.4 (C-12), 53.5 (C-7), 40.1 (C-8), 11.9 (C-9). **MS** (**ESI-TOF**) m/z: [M+H]⁺ calcd. for C₃₁H₃₁O₃S₂⁺ 515.1709, found 515.1710.

Deprotection of dithiolane 83 to 84

Dithiolane **83** (101 mg, 197 μ mol, 1.00 eq) was dissolved in 1,2-ethane dithiol (4.0 mL) and cooled to 0 °C. BF₃·OEt₂ (200 μ L, 1.58 mmol, 8.01 eq) was added and the reaction was stirred at room temperature for 45 min. After completion the reaction was quenched with H₂O (20 mL) and the aqueous phase was extracted with Et₂O (3×20 mL). The combined organic phases were washed with brine (20 mL) and dried over Na₂SO₄ and concentrated *in vacuo*. Flash column chromatography (SiO₂, CH/EA 9:1 \rightarrow 1:1) gave deprotected dithiolane **84** (41.8 mg, 171 μ mol, 87%) as a white amorphous solid.

¹**H-NMR** (700 MHz, acetone-d6, 298 K): δ (ppm) = 6.92 (s, 1 H, H-6), 5.84 (s, 1 H, H-7), 3.46-3.41 (m, 2 H, H-8), 3.33-3.30 (m, 2 H, H-8), 2.20 (s, 3 H, H-9). ¹³**C-NMR** (176 MHz, acetone-d6, 298 K): δ (ppm) = 144.7 (C-3), 143.7 (C-5), 133.1 (C-4), 129.1 (C-1), 115.2 (C-2), 107.2 (C-6), 54.2 (C-7), 40.0 (C-8), 11.2 (C-9).

6.2.2 Relevant to chapter 4.2

Synthesis of alkyne 92 by Sonogashira reaction of iodide 59 (route 1)

lodide **59** (52.0 mg, 96.9 μ mol, 1.00 eq), Pd(PPh₃)₂Cl₂ (5.65 mg, 8.05 μ mol, 8.3 mol%), PPh₃ (4.22 mg, 16.1 μ mol, 16.6 mol%) and CuI (1.53 mg, 8.05 μ mol, 8.3 mol%) were dried under vacuum before NEt₃ (100 μ L, 721 μ mol, 7.44 eq) was added. The compounds were dissolved in dry and degassed toluene (2.0 mL) and the reaction was stirred at 40 °C for 22 h. After completion the reaction mixture was filtered over a plug of silica (CH₂Cl₂) and the solvent was removed *in vacuo*. K₂CO₃ (49.6 mg, 359 μ mol, 3.70 eq) was added and the mixture was suspended in dry MeOH (5.0 mL) and dry CH₂Cl₂ (5.0 mL). The reaction was stirred at room temperature for 1.5 h. After completion the reaction mixture was filtered over a plug of silica (CH₂Cl₂) and the solvent was removed *in vacuo*. Flash column chromatography (SiO₂, CH/EA 19:1) gave alkyne **92** (39.8 mg, 91.6 μ mol, 94%) as a white amorphous solid.

¹H-NMR (500 MHz, CD₂Cl₂, 298 K): δ (ppm) = 7.47-7.44 (m, 2 H, H-Ph), 7.43-7.34 (m, 10 H, H-Ph), 7.32-7.30 (m, 3 H, H-Ph), 6.94 (s, 1 H, H-6), 5.09 (s, 2 H, H-12), 5.08 (s, 2 H, H-11), 5.01 (s, 2 H, H-10), 3.29 (s, 1 H, H-8), 2.29 (s, 3 H, H-9). ¹³C-NMR (126 MHz, CD₂Cl₂, 298 K): δ (ppm) = 151.6 (C-3), 151.0 (C-5), 143.8 (C-4), 138.0 (C-Ph), 138.0 (C-Ph), 137.3 (C-Ph), 128.9 (C-2), 128.9 (C-Ph), 128.9 (C-Ph), 128.8 (C-Ph), 128.7 (C-Ph), 128.4 (C-Ph), 128.0 (C-Ph), 117.5 (C-1), 113.9 (C-6), 82.6 (C-7), 80.5 (C-8), 75.8 (C-11), 75.5 (C-10), 71.5 (C-12), 14.2 (C-9). **MS (APCI)** m/z: [M+H]⁺ calcd. for C₃₀H₂₇O₃⁺ 435.1955, found 435.1956.

Synthesis of alkyne 92 by decarboxylative Sonogashira reaction of acid 58 (route 2)

BnO OH OH Ph 10 O 3
$$\frac{2}{2}$$
 7 8 Ph 10 O 3 $\frac{2}{2}$ 7 8 Ph 10 O 3 $\frac{2}{2}$ 7 8 Ph 10 O 3 $\frac{2}{2}$ 7 8 Ph $\frac{11}{2}$ 9 92 Ph $\frac{12}{2}$ O 92 P

Acid **58** (56.1 mg, 123 µmol, 1.00 eq), XantPhos Pd G3 (12.8 mg, 13.5 µmol, 10.9 mol%) and DMAP (90.3 mg, 739 µmol, 5.99 eq) were dried under vacuum before piv₂O (40.0 µL, 197 µmol, 1.60 eq) and TIPS acetylene (150 µL, 669 µmol, 5.42 eq) were added. The compounds were dissolved in dry and degassed 1,4-dioxane (2.0 mL) and the reaction was stirred at reflux for 19 h. After completion the reaction mixture was filtered over a plug of silica (CH₂Cl₂) and the solvent was removed *in vacuo*. TBAF (1.0 M in THF, 1.0 mL, 1.00 mmol, 8.10 eq) was added and the mixture was suspended in dry THF (5.0 mL). The reaction was stirred at room temperature for 1.5 h. After completion the reaction was quenched with aqueous NH₄Cl (sat., 20 mL) and the aqueous phase was extracted with CH₂Cl₂ (3×15 mL). The combined organic phases were dried over Na₂SO₄ and filtered over a plug of silica (CH₂Cl₂). Removal of the solvent *in vacuo* and flash column chromatography (SiO₂, CH/EA 100:1 \rightarrow 24:1) gave alkyne **92** (20.4 mg, 46.9 µmol, 38%) as a white amorphous solid.

For analytical data see route 1 above.

Synthesis of alkyne 92 by Ohira-Bestmann reaction of aldehyde 72 (route 3)

BnO
$$\frac{9}{Ph}$$
 $\frac{9}{10.03}$ $\frac{7}{2}$ $\frac{7}{8}$ $\frac{11}{9}$ $\frac{4}{9}$ $\frac{1}{10.03}$ $\frac{9}{2}$ $\frac{7}{10.03}$ $\frac{9}{2}$ $\frac{7}{10.03}$ $\frac{9}{2}$ $\frac{12}{Ph}$ $\frac{12}{$

Aldehyde **72** (434 mg, 990 μ mol, 1.00 eq) and K₂CO₃ (277 mg, 2.00 mmol, 2.02 eq) were dried under vacuum before *Ohira-Bestmann* reagent (225 μ L, 1.49 mmol, 1.51 eq) was added. The compounds were dissolved in dry MeOH (5.0 mL) and dry THF (5.0 mL) and the reaction was stirred at room temperature for 23 h. After completion Et₂O (30 mL) was added and the organic phase was washed with aqueous NaHCO₃ (sat., 20 mL). The organic phase was dried over MgSO₄ and filtered over a plug of silica (Et₂O). Removal of the solvent *in vacuo* gave alkyne **92** (421 mg, 970 μ mol, 98%) as a white amorphous solid.

For analytical data see route 1 above.

Synthesis of iodide 91

Precursor **57** (615 mg, 1.31 mmol, 1.00 eq) and $AgCO_2CF_3$ (306 mg, 1.39 mmol, 1.06 eq) were dried under vacuum and I_2 (365 mg, 1.44 mmol, 1.10 eq) was added. The solids were dissolved in dry CHC I_3 (10 mL) and the reaction was stirred at room temperature for 23 h. After completion the reaction was quenched with aqueous $Na_2S_2O_3$ (1.0 M, 20 mL). The phases were separated and the organic phase was concentrated *in vacuo*. Flash column chromatography (SiO₂, CH/EA 9:1) gave iodide **91** (780 mg, 1.31 mmol, *quant*.) as a white amorphous solid.

¹H-NMR (500 MHz, CD₂Cl₂, 298 K): δ (ppm) = 7.53-7.50 (m, 2 H, H-Ph), 7.43-7.34 (m, 13 H, H-Ph), 5.09 (s, 2 H, H-11), 5.05 (s, 2 H, H-12), 5.04 (s, 2 H, H-10), 3.91 (s, 3 H, H-7), 2.15 (s, 3 H, H-9). ¹³C-NMR (126 MHz, CD₂Cl₂, 298 K): δ (ppm) = 169.3 (C-8), 152.4 (C-3), 151.4 (C-5), 146.9 (C-4), 137.5 (C-Ph), 137.4 (C-Ph), 137.2 (C-1), 137.1 (C-Ph), 129.2 (C-Ph), 128.9 (C-Ph), 128.9 (C-Ph), 128.8 (C-Ph), 128.7 (C-Ph), 128.7 (C-Ph), 127.3 (C-Ph), 84.8 (C-6), 76.3 (C-11), 75.8 (C-12), 75.7 (C-10), 53.0 (C-7), 14.1 (C-9). **MS (APCI)** m/z: [M+H]⁺ calcd. for C₃₀H₂₈IO₅⁺ 595.0976, found 595.0976.

Synthesis of alkyne 123

lodide **91** (49.2 mg, 82.8 µmol, 1.00 eq) and alkyne **92** (158 mg, 364 µmol, 4.39 eq) were dried under vacuum. Pd(PPh₃)₄ (6.00 mg, 5.19 µmol, 6.27 mol%) and CuI (1.10 mg, 5.78 µmol, 6.98 mol%) were added in the glovebox to ensure air-free conditions. NEt₃ (100 µL, 721 µmol, 8.72 eq) was added and the mixture was dissolved in dry and degassed toluene (4.0 mL). The reaction was stirred at 90 °C for 21 h. After completion the reaction mixture was filtered over a plug of silica (CH₂Cl₂) and the solvent was removed *in vacuo*. Flash column chromatography (SiO₂, CH/EA 100:1 \rightarrow 9:1) gave alkyne **93** (70.7 mg, 78.5 µmol, 95%) as an orange amorphous solid.

¹H-NMR (500 MHz, CD₂Cl₂, 298 K): δ (ppm) = 7.51-7.48 (m, 2 H, H-Ph), 7.44-7.29 (m, 28 H, H-Ph), 6.79 (s, 1 H, H-14), 5.20 (s, 2 H, H-20), 5.12 (s, 2 H, H-19), 5.08 (s, 2 H, H-23), 5.06 (s, 2 H, H-18), 5.00 (s, 2 H, H-22), 4.97 (s, 2 H, H-24), 3.86 (s, 3 H, H-15), 2.25 (s, 3 H, H-21), 2.14 (s, 3 H, H-17). ¹³C-NMR (126 MHz, CD₂Cl₂, 298 K): δ (ppm) = 168.7 (C-16), 152.6 (C-5), 152.2 (C-3), 151.6 (C-11), 151.1 (C-13), 147.2 (C-4), 143.5 (C-12), 138.0 (C-Ph), 137.8 (C-Ph), 137.6 (C-Ph), 137.6 (C-Ph), 137.3 (C-Ph), 133.4 (C-1), 128.9 (C-Ph), 128.9 (C-Ph), 128.9 (C-Ph), 128.8 (C-Ph), 128.8 (C-Ph), 128.6 (C-Ph), 128.7 (C-Ph), 128.6 (C-Ph), 128.6 (C-Ph), 128.5 (C-Ph), 128.4 (C-Ph), 128.3 (C-10), 128.0 (C-Ph), 126.2 (C-2), 118.6 (C-9), 113.3 (C-14), 112.2 (C-6), 95.5 (C-8), 86.5 (C-7), 76.2 (C-19), 76.2 (C-20), 75.8 (C-18), 75.7 (C-23), 75.5 (C-22), 71.5 (C-24), 52.8 (C-15), 14.5 (C-21), 13.5 (C-17). **MS (MALDI)** m/z: [M+K]⁺ calcd. for C₆₀H₅₂O₈K⁺ 939.3294, found 939.3324.

Synthesis of benzofurane 95

Alkyne **93** (462 mg, 513 µmol, 1.00 eq) was dissolved in EtSH (10 mL) and BF₃·Et₂O (780 µL, 6.16 mmol, 12.0 eq) was added dropwise. The reaction was stirred at room temperature for 1.25 h. After completion the reaction was quenched with H₂O (40 mL) and the aqueous phase was extracted with EA (3×50 mL). The combined organic phases were dried over Na₂SO₄ and the solvent was removed *in vacuo*. Flash column chromatography (SiO₂, CH/EA 3:1 \rightarrow 1:1) gave a mixture of non-cyclized **96** and cyclized **95** (combined yield, 167 mg, 461 µmol, 90%). Analytical data was obtained from a smaller, earlier batch that only gave cyclized **95** (51%, see chapter 4.2.2).

¹H-NMR (500 MHz, acetone-d6, 298 K): δ (ppm) = 7.08 (s, 1 H, H-7), 6.88 (s, 1 H, H-14), 3.91 (s, 3 H, H-15), 2.55 (s, 3 H, H-17), 2.35 (s, 3 H, H-18). ¹³C-NMR (176 MHz, acetone-d6, 298 K): δ (ppm) = 168.3 (C-16), 157.0 (C-8), 145.3 (C-11), 143.9 (C-13), 142.0 (C-5), 141.7 (C-3), 134.7 (C-12), 134.0 (C-4), 125.7 (C-1), 125.5 (C-6), 122.3 (C-9), 115.7 (C-10), 113.6 (C-2), 108.0 (C-14), 106.5 (C-7), 51.5 (C-15), 13.9 (C-17), 13.4 (C-18). MS (EI, 70.0 eV) m/z: [M⁻⁺] calcd. for C₁₈H₁₆O₈⁺⁻ 360.0845, found 360.0853.

Synthesis of aldehyde 97

Alkyne **93** (104 mg, 115 μ mol, 1.00 eq) and AgOTf (127 mg, 494 μ mol, 4.30 eq) were dissolved in dry CH₂Cl₂ (4.0 mL) and cooled to -70 °C. The mixture was stirred at this temperature for 1 h before MeOCHCl₂ (80 μ L, 901 μ mol, 7.84 eq) was added slowly and the reaction was stirred at -70 °C for 26 h. After completion the reaction was quenched with aqueous NaHCO₃ (sat., 10 mL) and the aqueous phase was extracted with Et₂O (3×10 mL). The combined organic phases were dried over MgSO₄ and filtered over a plug of silica (CH₂Cl₂). Removal of the solvent *in vacuo* gave crude aldehyde **97** (97.1 mg), which was used immediately in the following reduction (see below). For pure analytical data preparative TLC (SiO₂, CH/EA 9:1) was performed.

¹H-NMR (400 MHz, CD₂Cl₂, 298 K): δ (ppm) = 10.43 (s, 1 H, H-15), 7.49-7.45 (m, 2 H, H-Ph), 7.44-7.34 (m, 26 H, H-Ph), 7.29-7.27 (m, 2 H, H-2), 5.22 (s, 2 H, H-21), 5.12 (s, 2 H, H-23), 5.12 (s, 2 H, H-25), 5.12 (s, 2 H, H-20), 5.11 (s, 2 H, H-24), 5.06 (s, 2 H, H-19), 3.88 (s, 3 H, H-16), 2.25 (s, 3 H, H-22), 2.14 (s, 3 H, H-18). ¹³C-NMR (176 MHz, CD₂Cl₂, 298 K): δ (ppm) = 190.2 (C-15), 168.6 (C-17), 155.8 (C-11), 152.9 (C-13), 152.8 (C-5), 152.7 (C-3), 147.1 (C-4), 146.9 (C-12), 137.5 (C-Ph), 137.5 (C-Ph), 137.5 (C-Ph), 137.5 (C-Ph), 137.3 (C-Ph), 137.2 (C-Ph), 133.5 (C-1), 132.9 (C-10), 129.3 (C-Ph), 129.0 (C-Ph), 129.0 (C-Ph), 128.9 (C-Ph), 128.9 (C-Ph), 128.8 (C-Ph), 128.8 (C-Ph), 128.8 (C-Ph), 128.7 (C

Synthesis of diol 98

Crude aldehyde **97** (97.1 mg) was dissolved in dry THF (10 mL) and DIBAI-H (1.0 M in CH, 600 μ L, 600 μ mol, 5.74 eq) was added. The reaction was stirred at room temperature for 19 h. After completion the reaction was quenched with aqueous *Rochelle* salt (sat., 10 mL) and the aqueous phase was extracted with Et₂O (3×10 mL). The combined organic phases were dried over MgSO₄ and filtered over a plug of silica (Et₂O). Removal of the solvent *in vacuo* and flash column chromatography (SiO₂, CH/EA 19:1 \rightarrow 4:1) gave diol **98** (29.6 mg, 32.8 μ mol, 29% over 2 steps) as a white amorphous solid.

¹H-NMR (400 MHz, CD₂Cl₂, 298 K): δ (ppm) = 7.48-7.46 (m, 2 H, H-Ph), 7.44-7.33 (m, 26 H, H-Ph), 7.29-7.27 (m, 2 H, H-2), 5.23 (s, 2 H, H-20), 5.14 (s, 2 H, H-23), 5.10 (s, 2 H, H-24), 5.09 (s, 2 H, H-19), 5.04 (s, 2 H, H-22), 5.03 (s, 2 H, H-18), 4.83 (s, 2 H, H-16), 4.71 (s, 2 H, H-15), 2.30 (s, 3 H, H-21), 2.28 (s, 3 H, H-17). ¹³C-NMR (176 MHz, CD₂Cl₂, 298 K): δ (ppm) = 152.4 (C-3), 152.3 (C-5), 151.3 (C-11), 149.4 (C-13), 146.8 (C-4), 145.7 (C-12), 137.8 (C-Ph), 137.8 (C-Ph), 137.8 (C-Ph), 137.8 (C-Ph), 137.8 (C-Ph), 137.8 (C-Ph), 138.9 (C-Ph), 128.9 (C-Ph), 128.9 (C-Ph), 128.9 (C-Ph), 128.9 (C-Ph), 128.8 (C-Ph), 128.6 (C-Ph), 128.5 (C-Ph), 128.5 (C-Ph), 128.3 (C-2), 120.1 (C-9), 115.1 (C-6), 93.6 (C-8), 92.2 (C-7), 76.7 (C-24), 76.1 (C-23), 76.1 (C-19), 76.1 (C-20), 75.7 (C-18), 75.5 (C-22), 61.1 (C-16), 58.8 (C-15), 14.9 (C-21), 12.3 (C-17). **MS (ESI-TOF)** m/z: [M+NH₄]⁺ calcd. for C₆₀H₅₈O₉N₁⁺ 920.4168, found 920.4156.

6.2.3 Relevant to chapter 4.3

Synthesis of iodide 99

Aldehyde **72** (1.19 g, 2.72 mmol, 1.00 eq) and AgCO₂CF₃ (611 mg, 2.76 mmol, 1.02 eq) were dried under vacuum and I₂ (706 mg, 2.78 mmol, 1.02 eq) was added. The solids were dissolved in dry CHCl₃ (40 mL) and the reaction was stirred at room temperature for 46 h. After completion the reaction was quenched with aqueous Na₂S₂O₃ (1.0 M, 40 mL). The phases were separated and the aqueous phase was extracted with Et₂O (2×40 mL). The combined organic phases were dried over MgSO₄ and filtered over a short plug of silica (Et₂O). Removal of the solvent *in vacuo* gave iodide **99** (1.48 g, 2.63 mmol, 97%) as a white amorphous solid.

¹H-NMR (500 MHz, CD₂Cl₂, 298 K): δ (ppm) = 10.20 (s, 1 H, H-7), 7.54-7.51 (m, 2 H, H-Ph), 7.42-7.33 (m, 13 H, H-Ph), 5.17 (s, 2 H, H-10), 5.07 (s, 2 H, H-11), 5.01 (s, 2 H, H-9), 2.39 (s, 3 H, H-8). ¹³C-NMR (126 MHz, CD₂Cl₂, 298 K): δ (ppm) = 197.9 (C-7), 152.5 (C-3), 150.8 (C-5), 149.5 (C-4), 137.3 (C-Ph), 137.1 (C-Ph), 136.9 (C-Ph), 132.8 (C-2), 130.9 (C-1), 129.3 (C-Ph), 129.0 (C-Ph), 128.9 (C-Ph), 128.8 (C-Ph), 128.8 (C-Ph), 128.7 (C-Ph), 95.5 (C-6), 76.3 (C-10), 75.7 (C-9), 75.7 (C-11), 12.7 (C-8). **MS (EI, 70.0 eV)** m/z: [M⁻⁺] calcd. for C₂₉H₂₅lO₄⁻⁺ 564.0798, found 564.0792.

Synthesis of alkyne 102

lodide **99** (797 mg, 1.41 mmol, 1.00 eq) and K_2CO_3 (788 mg, 5.70 mmol, 4.40 eq) were dried under vacuum. *Ohira-Bestmann* reagent (430 μ L, 2.85 mmol, 2.02 eq) was added and the mixture was suspended in MeOH/THF (1:1, 20 mL). The reaction was stirred at room temperature for 94 h. After completion Et_2O (20 mL), aqueous NaHCO₃ (sat. 10 mL) and H_2O (5.0 mL) were added. The phases were separated and the aqueous phase was extracted with Et_2O (2×10 mL). The combined organic phases were dried over MgSO₄ and filtered over a short plug of silica (Et_2O). Removal of the solvent *in vacuo* gave alkyne **102** (747 mg, 1.33 mmol, 94%) as a white amorphous solid.

¹H-NMR (500 MHz, CD₂Cl₂, 298 K): δ (ppm) = 7.54-7.50 (m, 2 H, H-Ph), 7.43-7.33 (m, 13 H, H-Ph), 5.10 (s, 2 H, H-11), 5.04 (s, 2 H, H-12), 5.02 (s, 2 H, H-10), 3.64 (s, 1 H, H-8), 2.36 (s, 3 H, H-9). ¹³C-NMR (126 MHz, CD₂Cl₂, 298 K): δ (ppm) = 151.9 (C-3), 151.5 (C-5), 147.3 (C-4), 137.5 (C-Ph), 137.4 (C-Ph), 137.1 (C-Ph), 133.7 (C-2), 129.3 (C-Ph), 128.9 (C-Ph), 128.9 (C-Ph), 128.9 (C-Ph), 128.8 (C-Ph), 128.7 (C-Ph), 128.7 (C-Ph), 128.6 (C-Ph), 128.6 (C-Ph), 128.6 (C-Ph), 124.7 (C-1), 94.4 (C-6), 85.1 (C-8), 84.4 (C-7), 76.3 (C-11), 75.6 (C-12), 75.5 (C-10), 16.0 (C-9). **MS (APCI)** m/z: [M+H]⁺ calcd. for C₃₀H₂₆IO₃⁺ 561.0921, found 561.0917.

Synthesis of fragment 100

Alkyne **102** (1.31 g, 2.33 mmol, 1.00 eq) K_3PO_4 (2.51 g, 11.8 mmol, 5.08 eq) and $Pd(PPh_3)_2Cl_2$ (60.5 mg, 86.2 µmol, 3.7 mol%) were dried under vacuum before being dissolved in 1,4-dioxane/ H_2O (4:1, 50 mL). Vinyl Bpin (800 µL, 4.72 mmol, 2.02 eq) was added and the reaction was stirred at reflux for 18 h. After completion the reaction was quenched with HCl (6.0 M, 40 mL). The phases were separated and the aqueous phase was extracted with Et_2O (3×50 mL). The combined organic phases were dried over MgSO₄, filtered over a short plug of silica (Et_2O) and concentrated *in vacuo*. Flash column chromatography (SiO_2 , CH/EA 30:1) gave fragment **100** (853 mg, 1.85 mmol, 79%) as an orange oil.

¹H-NMR (700 MHz, CD₂Cl₂, 298 K): δ (ppm) = 7.44-7.39 (m, 6 H, H-Ph), 7.38-7.33 (m, 9 H, H-Ph), 7.00 (dd, ${}^3J_{13,14a}$ = 17.9 Hz, ${}^3J_{13,14b}$ = 11.8 Hz, 1 H, H-13), 6.16 (dd, ${}^3J_{13,14a}$ = 17.9 Hz, ${}^2J_{14a,14b}$ = 2.0 Hz, 1 H, H-14a), 5.51 (dd, ${}^3J_{13,14b}$ = 11.8 Hz, ${}^2J_{14a,14b}$ = 2.0 Hz, 1 H, H-14b), 5.12 (s, 2 H, H-11), 5.02 (s, 2 H, H-10), 4.99 (s, 2 H, H-12), 3.56 (s, 1 H, H-8), 2.33 (s, 3 H, H-9). ¹³C-NMR (176 MHz, CD₂Cl₂, 298 K): δ (ppm) = 150.5 (C-3), 149.5 (C-5), 147.6 (C-4), 137.8 (C-Ph), 137.8 (C-Ph), 137.7 (C-Ph), 132.3 (C-2), 131.6 (C-13), 130.8 (C-6), 128.9 (C-Ph), 128.9 (C-Ph), 128.8 (C-Ph), 128.8 (C-Ph), 128.7 (C-Ph), 128.5 (C-Ph), 128.4 (C-Ph), 120.4 (C-14), 117.5 (C-1), 86.1 (C-8), 81.2 (C-7), 76.1 (C-11), 75.6 (C-10), 75.2 (C-12), 14.8 (C-9). MS (EI, 70.0 eV) m/z: [M⁻⁺] calcd. for C₃₂H₂₈O₃ + 460.2038, found 460.2035.

Synthesis of coupling product 104

lodide **99** (300 mg, 531 μ mol, 1.00 eq), alkyne **100** (761 mg, 1.65 mmol, 3.1 eq), Pd(PPh₃)₄ (32.1 mg, 27.8 μ mol, 5.2 mol%) and CuI (10.0 mg, 52.5 μ mol, 9.9 mol%) were dried under vacuum before being dissolved in dry degassed toluene (20 mL). NEt₃ (650 μ L, 4.69 mmol, 8.82 eq) was added and the reaction was stirred at 100 °C for 2 h. After completion the reaction was cooled to room temperature and filtered over a short plug of silica (Et₂O). Concentration *in vacuo* and flash column chromatography (SiO₂, CH/EA 100:1 \rightarrow 30:1) gave internal alkyne **104** (419 mg, 467 μ mol, 88%) as an orange amorphous solid.

¹H-NMR (500 MHz, CD₂Cl₂, 298 K): δ (ppm) = 10.73 (s, 1 H, H-15), 7.45-7.39 (m, 11 H, H-Ph), 7.38-7.33 (m, 17 H, H-Ph), 7.29-7.26 (m, 2 H, H-Ph), 7.04 (dd, ${}^{3}J_{24,25a}$ = 17.8 Hz, ${}^{3}J_{24,25b}$ = 11.8 Hz, 1 H, H-24), 6.09 (dd, ${}^{3}J_{24,25a}$ = 17.8 Hz, ${}^{2}J_{25a,25a}$ = 2.0 Hz, 1 H, H-25a), 5.41 (dd, ${}^{3}J_{24,25b}$ = 11.8 Hz, ${}^{2}J_{25a,25a}$ = 2.0 Hz, 1 H, H-25b), 5.23 (s, 2 H, H-19), 5.19 (s, 2 H, H-22), 5.15 (s, 2 H, H-18), 5.02 (s, 2 H, H-21), 5.00 (s, 2 H, H-23), 4.99 (s, 2 H, H-17), 2.44 (s, 3 H, H-16), 2.31 (s, 3 H, H-20). ¹³C-NMR (126 MHz, CD₂Cl₂, 298 K): δ (ppm) = 193.5 (C-15), 152.5 (C-5), 152.1 (C-3), 150.6 (C-11), 150.4 (C-12), 149.6 (C-13), 147.6 (C-4), 137.8 (C-Ph), 137.8 (C-Ph), 137.7 (C-Ph), 137.4 (C-Ph), 137.3 (C-Ph), 131.9 (C-24), 131.8 (C-10), 131.6 (C-1), 131.2 (C-2), 130.6 (C-14), 129.0 (C-Ph), 128.9 (C-Ph), 128.9 (C-Ph), 128.9 (C-Ph), 128.6 (C-Ph), 128.6 (C-Ph), 128.8 (C-Ph), 128.8 (C-Ph), 128.8 (C-Ph), 128.4 (C-Ph), 128.4 (C-Ph), 120.7 (C-25), 120.3 (C-6), 118.4 (C-9), 98.4 (C-8), 90.3 (C-7), 76.2 (C-19), 76.2 (C-18, C-22), 75.8 (C-17), 75.6 (C-21), 75.2 (C-23), 15.1 (C-20), 12.9 (C-16). MS (ESI-TOF) m/z: [M+Na]* calcd. for C₆₁H₅₂O₇Na* 919.3605, found 919.3604.

Synthesis of diol 105

Alkyne **104** (949 mg, 1.06 mmol, 1.00 eq) and NMO·H₂O (435 mg, 3.22 mmol, 3.04 eq) were dissolved in acetone/H₂O (20:1, 40 mL) and THF (5 mL). OsO₄ (4 wt% in H₂O, 375 μ L, 59.0 μ mol, 5.6 mol%) was added and the reaction was stirred at room temperature for 26 h. After completion the reaction was quenched with aqueous Na₂S₂O₃ (sat., 40 mL) and the aqueous phase was extracted with EA (2×30 mL). The combined organic phases were dried over MgSO₄ and filtered. Removal of the solvent *in vacuo* gave crude diol **105** (1.10 g) as a yellow amorphous solid, which was immediately used in the following reaction without purification. This step can be purified by flash column chromatography (SiO₂, CH/EA 4:1) for analytical data.

¹H-NMR (500 MHz, CD₂Cl₂, 298 K): δ (ppm) = 10.62 (s, 2 H, H-15), 7.45-7.33 (m, 27 H, H-Ph), 7.29-7.23 (m, 3 H, H-Ph), 5.34-5.28 (m, 1 H, H-24), 5.26 (s, 2 H, H-19), 5.23 (d, ${}^2J_{23,23}$ = 10.8 Hz, 1 H, H-23), 5.19 (s, 2 H, H-22), 5.14 (s, 2 H, H-18), 5.11 (d, ${}^2J_{23,23}$ = 10.8 Hz, 1 H, H-23), 5.08-5.02 (m, 2 H, H-21), 5.02-4.96 (m, 2 H, H-17), 3.82 (dd, ${}^2J_{25,25}$ = 11.3 Hz, ${}^3J_{25,OH}$ = 8.7 Hz, 1 H, H-25), 3.76 (d, ${}^3J_{25,OH}$ = 10.1 Hz, 1 H, H-OH), 3.60 (d, ${}^2J_{25,25}$ = 11.3 Hz, 1 H, H-25), 2.42 (s, 3 H, H-16), 2.31 (s, 3 H, H-20). ¹³C-NMR (126 MHz, CD₂Cl₂, 298 K): δ (ppm) = 192.9 (C-15), 152.6 (C-5), 152.3 (C-3), 151.1 (C-11), 150.3 (C-12), 149.6 (C-13), 147.1 (C-4), 137.7 (C-Ph), 137.5 (C-Ph), 137.3 (C-Ph), 137.2 (C-Ph), 137.1 (C-Ph), 132.3 (C-10), 132.2 (C-14), 132.1 (C-2), 131.1 (C-1), 129.0 (C-Ph), 129.0 (C-Ph), 129.0 (C-Ph), 128.9 (C-Ph), 128.9 (C-Ph), 128.8 (C-Ph), 128.8 (C-Ph), 128.8 (C-Ph), 128.6 (C-Ph), 128.6 (C-Ph), 128.6 (C-Ph), 128.6 (C-Ph), 175.9 (C-17), 75.6 (C-21), 73.3 (C-24), 66.8 (C-25), 14.9 (C-20), 12.6 (C-16). MS (MALDI) m/z: [M+Na]⁺ calcd. for C₆₁H₅₄O₉Na⁺ 953.3660, found 953.3688.

Synthesis of dialdehyde 89

Crude diol **105** (1.10 g) and Pb(OAc)₄ (708 mg, 1.60 mmol, 1.51 eq) were dissolved in dry toluene (40 mL) and stirred at room temperature for 35 min. After completion the reaction was filtered over a short plug of silica (EA) and the solvent was removed *in vacuo* giving dialdehyde **89** (894 mg, 995 μ mol, 94% over 2 steps) as a yellow amorphous solid.

¹H-NMR (500 MHz, CD₂Cl₂, 298 K): δ (ppm) = 10.80 (s, 1 H, H-15), 10.40 (s, 1 H, H-24), 7.47-7.33 (m, 27 H, H-Ph), 7.28-7.24 (m, 3 H, H-Ph), 5.22 (s, 2 H, H-19), 5.19 (s, 2 H, H-22), 5.16 (s, 2 H, H-23), 5.15 (s, 2 H, H-18), 5.13 (s, 2 H, H-21), 5.00 (s, 2 H, H-17), 2.45 (s, 3 H-16), 2.28 (s, 3 H, H-20). ¹³C-NMR (126 MHz, CD₂Cl₂, 298 K): δ (ppm) = 194.3 (C-15), 189.7 (C-24), 156.2 (C-11), 154.1 (C-13), 152.8 (C-5), 152.5 (C-3), 150.3 (C-12), 146.7 (C-4), 137.4 (C-Ph), 137.3 (C-Ph), 137.3 (C-Ph), 137.2 (C-Ph), 136.9 (C-Ph), 133.3 (C-10), 131.7 (C-1), 131.6 (C-2), 129.3 (C-Ph), 129.0 (C-Ph), 129.0 (C-Ph), 129.0 (C-Ph), 128.9 (C-Ph), 128.9 (C-Ph), 128.8 (C-Ph), 128.8 (C-Ph), 128.8 (C-Ph), 128.7 (C-Ph), 128.6 (C-Ph), 128.4 (C-Ph), 127.4 (C-14), 119.8 (C-6, C-9), 96.6 (C-8), 91.8 (C-7), 77.2 (C-23), 76.3 (C-18), 76.3 (C-19), 76.2 (C-22), 75.8 (C-17), 75.7 (C-21), 14.6 (C-20), 12.9 (C-16). **MS (ESI-TOF)** m/z: [M+H]⁺ calcd. for C₆₀H₅₁O₈⁺ 899.3578, found 899.3580.

Synthesis of phenol 106

Dialdehyde **89** (974 mg, 1.08 mmol, 1.00 eq) was dissolved in dry CH_2Cl_2 (20 mL) and cooled to -41 °C. BBr₃ (6.6 mL, 1.0 M in CH_2Cl_2 , 6.60 mmol, 6.09 eq) was added dropwise and the reaction was stirred at -41 °C for 10 min. After completion the reaction was quenched with aqueous $NaHCO_3$ (sat., 40 mL) and brine (40 mL). The phases were separated and the aqueous phase was washed with EA (3×40 mL). Afterwards the aqueous phase was acidified with HCl (12 M, dropwise and slowly) until pH < 1 and extracted with EA (3×50 mL). The combined organic phases were dried over Na_2SO_4 and filtered. Removal of the solvent *in vacuo* gave crude phenol **106**, which was immediately used in the following reaction without purification. The crude product can be purified by vapor diffusion recrystallisation (EtOH/pentane) for analytical data.

¹H-NMR (700 MHz, acetone-d6, 298 K): δ (ppm) = 10.68 (s, 1 H, H-15), 10.50 (s, 1 H, H-18), 2.49 (s, 3 H, H-16), 2.41 (s, 3 H, H-17). ¹³C-NMR (176 MHz, acetone-d6, 298 K): δ (ppm) = 197.1 (C-18), 192.4 (C-15), 151.7 (C-11), 150.9 (C-13), 146.4 (C-5), 145.9 (C-3), 139.2 (C-4), 133.1 (C-12), 127.3 (C-1), 121.9 (C-10), 121.4 (C-2), 119.4 (C-9), 114.6 (C-14), 108.5 (C-6), 94.4 (C-8), 92.2 (C-7), 13.6 (C-17), 11.8 (C-16). **MS** (APCI) m/z: [M+H]⁺ calcd. for $C_{18}H_{15}O_8^+$ 359.0761, found 359.0753.

Synthesis of epicoccolide B (2)

Crude phenol **106** and PtCl₂ (57.3 mg, 215 μ mol, 19.9 mol%) were dissolved in dry THF/toluene/1,4-dioxane (1:1:1, 30 mL) and stirred at 80 °C for 19 h. After completion the reaction was cooled to room temperature and filtered. Removal of the solvent *in vacuo* gave crude epicoccolide B (**2**, 26% qNMR over 2 steps). The crude product can be purified by HPLC (MACHERY-NAGEL Nucleodur 100-5 Gravity C18 250 × 16 mm, 0.1 Vol% TFA in both solvents, 0-20 min 25:75 \rightarrow 40:60 MeCN/H₂O, product elution after 15 min) to obtain pure **2** as a yellow amorphous solid.

¹H-NMR (700 MHz, DMSO-d6, 298 K): δ (ppm) = 12.08 (s, 1 H, H-OH C-13), 10.81 (s, 1 H, H-OH C-4), 10.42 (s, 1 H, H-15), 10.18 (s, 1 H, H-OH C-11), 9.53 (s, 1 H, H-OH), 9.48 (s, 1 H, H-18), 8.80 (s, 1 H, H-OH), 7.47 (s, 1 H, H-7), 2.58 (s, 3 H, H-16), 2.01 (s, 3 H, H-17). ¹³C-NMR (176 MHz, DMSO-d6, 298 K): δ (ppm) = 194.8 (C-18), 190.2 (C-15), 151.6 (C-8), 151.5 (C-11), 150.2 (C-13), 142.4 (C-5), 140.9 (C-3), 136.4 (C-4), 132.7 (C-12), 127.6 (C-2), 124.9 (C-9), 122.9 (C-6), 118.7 (C-10), 117.2 (C-1), 112.6 (C-14), 109.0 (C-7), 12.7 (C-17), 11.1 (C-16). **MS (APCI)** m/z: [M+H]⁺ calcd. for C₁₈H₁₅O₈⁺ 359.0761, found 359.0758.

6.2.4 Relevant to chapter 4.4

Synthesis of epicoccolide A (1)

Epicoccolide B (**2**, 1.98 mg, 5.53 μmol, 1.00 eq) was dissolved in dry acetone (0.5 mL) and fresh DMDO (1.0 mL, 60 mm in acetone, 60 μmol, 10.8 eq) was added. The reaction was stirred at room temperature for 15 min before quenching with aqueous $Na_2S_2O_3$ (sat., 4.0 mL). The aqueous phase was extracted with EA (3×4.0 mL), the combined organic phases were dried over Na_2SO_4 and filtered. Removal of the solvent *in vacuo* gave a crude mixture of epicoccolide A (**1**, 5% qNMR) and epicoccolide B (**2**, 73% qNMR). The crude mixture can be purified by HPLC (MACHERY-NAGEL Nucleodur 100-5 Gravity C18 250 × 16 mm, 0.1 Vol% TFA in both solvents, 0-20 min 20:80 \rightarrow 40:60 MeCN/H₂O, product elution after 12.5 min) to obtain **1** as a yellow amorphous solid.

¹H-NMR (700 MHz, DMSO-d6, 298 K): δ (ppm) = 10.32 (s, 1 H, H-17), 6.75 (s, 1 H, H-1), 6.11 (s, 1 H, H-9), 2.33 (s, 3 H, H-16), 2.29 (s, 3 H, H-18). ¹³C-NMR (176 MHz, DMSO-d6, 298 K): δ (ppm) = 193.3 (C-8), 191.3 (C-17), 145.0 (C-5), 143.9 (C-13), 141.4 (C-4), 140.0 (C-3), 138.2 (C-14), 135.9 (C-15), 121.9 (C-11), 121.1 (C-12), 120.2 (C-6), 119.1 (C-2), 115.6 (C-7), 113.8 (C-10), 89.3 (C-1), 71.0 (C-9), 12.7 (C-16), 11.9 (C-18). MS (APCI) m/z: [M+H]⁺ calcd. for C₁₈H₁₅O₉⁺ 375.0711, found 375.0705.

Synthesis of acetylated epicoccolide B (107)

HO H ACO
$$\frac{16}{2}$$
 $\frac{16}{15}$ H ACO $\frac{16}{3}$ $\frac{16}{15}$ H ACO $\frac{17}{10}$ $\frac{18}{12}$ H ACO $\frac{17}{10}$ $\frac{13}{12}$ OACO $\frac{17}{10}$ $\frac{13}{12}$ OACO $\frac{17}{10}$ $\frac{13}{12}$ OACO $\frac{18}{12}$ $\frac{13}{12}$ OACO $\frac{13}{12}$ $\frac{13}$ $\frac{13}{12}$ $\frac{13}{12}$ $\frac{13}{12}$ $\frac{13}{12}$ $\frac{13}{12}$

Epicoccolide B (2) (42.5 mg, 119 μmol, 1.00 eq) was dissolved in dry THF (5 mL). AcCl (1.0 M in CH_2Cl_2 , 600 μL, 600 mol, 5.06 eq) and NEt_3 (165 μL, 1.19 mmol 10.0 eq) were added and the reaction was stirred at room temperature for 1 h. After completion the reaction was quenched with brine (10 mL) and H_2O (10 mL). The aqueous phase was extracted with EA (3×20 mL) and the combined organic phases were dried over Na_2SO_4 . Filtration and removal of the solvent *in vacuo* gave **107** (47.6 mg, 83.7 μmol, 71%) as a white amorphous solid.

¹H-NMR (700 MHz, acetone-d6, 298 K): δ (ppm) = 10.67 (s, 1 H, H-15), 9.81 (s, 1 H, H-18), 7.81 (s, 1 H, H-7), 2.65 (s, 3 H, H-16), 2.44 (s, 3 H, H-Ac), 2.41 (s, 3 H, H-Ac), 2.39 (s, 3 H, H-Ac), 2.38 (s, 3 H, H-Ac), 2.33 (s, 3 H, H-Ac), 2.16 (s, 3 H, H-17). ¹³C-NMR (176 MHz, acetone-d6, 298 K): δ (ppm) = 190.9 (C-15), 188.8 (C-18), 168.9 (C-Ac), 168.5 (C-Ac), 167.9 (C-Ac), 167.6 (C-Ac), 167.4 (C-Ac), 153.8 (C-8), 147.2 (C-11), 146.6 (C-5), 142.5 (C-12), 140.4 (C-3), 139.0 (C-13), 135.3 (C-4), 133.2 (C-2), 132.810), 131.2 (C-9), 128.3 (C-6), 128.2 (C-14), 124.9 (C-1), 111.0 (C-7), 20.4 (C-Ac), 20.2 (C-Ac), 20.2 (C-Ac), 20.2 (C-Ac), 13.8 (C-17), 11.5 (C-16). **MS (APCI)** m/z: [M+Na]⁺ calcd. for C₂₈H₂₄O₁₃Na⁺ 591.1109, found 591.1108.

6.2.5 Relevant to chapter 4.5

Synthesis of coupling product 111

lodide **99** (403 mg, 715 μ mol, 1.00 eq), alkyne **92** (1.11 g, 2.54 mmol, 3.56 eq), Pd(PPh₃)₄ (44.2 mg, 38.2 μ mol, 5.4 mol%) and CuI (13.0 mg, 68.3 μ mol, 9.6 mol%) were dried under vacuum before being dissolved in dry degassed toluene (30 mL). NEt₃ (850 μ L, 6.13 mmol, 8.58 eq) was added and the reaction was stirred at 100 °C for 3 h. After completion the reaction was cooled to room temperature and filtered over a short plug of silica (Et₂O). Concentration *in vacuo* and flash column chromatography (SiO₂, CH/EA 100:1 \rightarrow 30:1) gave internal alkyne **111** (623 mg, 715 μ mol, *quant*.) as a yellow solid.

¹H-NMR (500 MHz, CD₂Cl₂, 298 K): δ (ppm) = 10.75 (s, 1 H, H-15), 7.50-7.46 (m, 2 H, H-Ph), 7.45-7.34 (m, 21 H, H-Ph), 7.32-7.29 (m, 7 H, H-Ph), 6.87 (s, 1 H, H-14), 5.22 (s, 2 H, H-19), 5.21 (s, 2 H, H-18), 5.09 (s, 2 H, H-22), 5.01 (s, 2 H, H-17), 5.00 (s, 2 H, H-21), 4.97 (s, 2 H, H-23), 2.46 (s, 3 H, H-16), 2.29 (s, 3 H, H-20). ¹³C-NMR (126 MHz, CD₂Cl₂, 298 K): δ (ppm) = 193.3, 152.5 (C-5), 152.1 (C-3), 151.7 (C-11), 151.2 (C-13), 150.5 (C-4), 143.8 (C-12), 138.0 (C-Ph), 138.0 (C-Ph), 137.6 (C-Ph), 137.3 (C-Ph), 137.3 (C-Ph), 137.2 (C-Ph), 131.9 (C-2), 131.1 (C-1), 129.0 (C-Ph), 128.9 (C-Ph), 128.9 (C-Ph), 128.9 (C-Ph), 128.9 (C-Ph), 128.7 (C-Ph), 128.5 (C-10), 128.5 (C-Ph), 128.4 (C-Ph), 128.1 (C-Ph), 120.3 (C-Ph), 118.4 (C-9), 113.3 (C-6, C-14), 99.8 (C-8), 85.3 (C-7), 76.2, 76.1, 75.8, 75.8, 75.6, 71.5, 14.6, 12.9. MS (APCI) m/z: [M+H]⁺ calcd. for C₅₉H₅₁O₇⁺ 871.3629, found 871.3623.

Synthesis of analog 112

Alkyne **111** (6.80 mg, 7.8 µmol, 1.00 eq) and PhMe₅ (7.20 mg, 48.6 µmol, 6.22 eq) were dissolved in dry CH₂Cl₂ (1.0 mL) and cooled to -78 °C. BBr₃ (94 µL, 1.0 m in CH₂Cl₂, 94.0 µmol, 12.0 eq) was added dropwise and the reaction was stirred at -78 °C for 10 min. After completion the reaction was quenched with aqueous NaHCO₃ (sat., 3.0 mL) and brine (1.0 mL). The phases were separated and the aqueous phase was washed with EA (3×3.0 mL). Afterwards the aqueous phase was acidified with HCl (12 m, dropwise and slowly) until pH < 1 and extracted with EA (3×5.0 mL). The combined organic phases were dried over Na₂SO₄ and filtered. Removal of the solvent *in vacuo* gave crude analog **112** (40% qNMR). The crude product can be purified by HPLC (MACHERY-NAGEL Nucleodur 100-5 Gravity C18 250 × 16 mm, 0.1 Vol% TFA in both solvents, 0-20 min 25:75 \rightarrow 40:60 MeCN/H₂O, product elution after 9 min) to obtain pure **112** as a yellow solid.

¹H-NMR (700 MHz, acetone-d6, 298 K): δ (ppm) = 10.52 (s, 1 H, H-15), 7.48 (s, 1 H, H-7), 6.94 (s, 1 H, H-14), 2.66 (s, 3 H, H-16), 2.37 (s, 3 H, H-17). ¹³C-NMR (176 MHz, acetone-d6, 298 K): δ (ppm) = 190.4 (C-15), 158.7 (C-8), 145.3 (C-11), 144.0 (C-13), 142.2 (C-5), 141.2 (C-3), 136.3 (C-4), 134.8 (C-12), 127.5 (C-2), 125.5 (C-6), 122.1 (C-9), 118.9 (C-1), 115.6 (C-10), 107.9 (C-14), 104.9 (C-7), 13.4 (C-17), 11.0 (C-16). MS (APCI) m/z: [M+H]⁺ calcd. for C₁₇H₁₅O₇⁺ 331.0812, found 331.0817.

6.2.6 Relevant to chapter 4.6

Synthesis of iodide 116

BrPPh₃Me (472 mg, 1.32 mmol, 2.02 eq) was dissolved in dry THF (10 mL) and NHMDS (1.0 M in THF, 1.31 mL, 1.31 mmol, 2.01 eq) was added. The mixture was stirred at room temperature for 15 min before adding a solution of iodide **99** (369 mg, 653 μ mol, 1.00 eq) in dry THF (10 mL). The reaction was stirred at room temperature for 40 min. After completion the reaction was quenched with aqueous NH₄Cl (sat., 15 mL) and H₂O (5.0 mL). The aqueous phase was extracted with CH₂Cl₂ (3×15 mL) and the combined organic phases were washed with brine (10 mL). Drying over Na₂SO₄, filtration over a short plug of silica (CH₂Cl₂) and removal of the solvent *in vacuo* gave crude **116**. The crude product was adsorbed on Celite (5.0 g) and washed thoroughly with cyclohexane. Isolation of the product by dissolving it in CH₂Cl₂ and filtration of the Celite gave iodide **116** (353 mg, 628 μ mol, 96%) as an amorphous off-white solid.

¹H-NMR (300 MHz, CD₂Cl₂, 298 K): δ (ppm) = 7.75-7.66 (m, 2 H, H-Ph), 7.56-7.32 (m, 13 H, H-Ph), 6.60 (dd, ${}^3J_{7,8b}$ = 17.8 Hz, ${}^3J_{7,8a}$ = 11.3 Hz, 1 H, H-7), 5.53 (dd, ${}^3J_{7,8a}$ = 11.3 Hz, ${}^2J_{8a,8b}$ = 1.7 Hz, 1 H, H-8a), 5.20 (dd, ${}^3J_{7,8b}$ = 17.8 Hz, ${}^2J_{8a,8b}$ = 1.7 Hz, 1 H, H-8b), 5.08 (s, 2 H, H-11), 5.05 (s, 2 H, H-12), 5.03 (s, 2 H, H-10), 2.26 (s, 3 H, H-9). ¹³C-NMR (176 MHz, acetone-d6, 298 K): δ (ppm) = 152.3 (C-3), 150.6 (C-5), 144.9 (C-4), 140.1 (C-7), 138.9 (C-1), 137.8 (C-Ph), 137.7 (C-Ph), 137.5 (C-Ph), 133.7 (C-Ph), 133.2 (C-Ph), 132.6 (C-Ph), 132.5 (C-Ph), 132.0 (C-Ph), 129.2 (C-Ph), 129.0 (C-Ph), 128.9 (C-Ph), 128.9 (C-Ph), 128.8 (C-Ph), 128.8 (C-Ph), 128.7 (C-Ph), 128.6 (C-Ph), 128.5 (C-Ph), 128.5 (C-Ph), 127.7 (C-2), 120.9 (C-8), 92.7 (C-6), 76.2 (C-11), 75.4 (C-10, C-12), 15.5 (C-9). MS (APCI) m/z: [M+H]⁺ calcd. for C₃₀H₂₈IO₃⁺ 563.1078, found 563.1078.

Synthesis of internal alkyne 117

lodide **116** (1.41 g, 2.51 mmol, 2.30 eq), bis(trimethylstannyl) acetylene (384 mg, 1.09 mmol, 1.00 eq) and Pd(PPh₃)₂Cl₂ (76.0 mg, 108 μ mol, 9.9 mol%) were dissolved in dry DMF (22 mL). The reaction was stirred at 100 °C for 19 h. After completion the reaction was quenched with aqueous NH₄Cl (sat., 50 mL) and H₂O (20 mL). The aqueous phase was extracted with CH₂Cl₂ (3×50 mL) and the combined organic phases were washed with brine (50 mL). Drying over Na₂SO₄, filtration over a short plug of silica (CH₂Cl₂) and removal of the solvent *in vacuo* gave crude **117**. Flash column chromatography (SiO₂, CH/EA 49:1) gave pure **117** (664 mg, 742 μ mol, 68%) as a yellow amorphous solid.

¹H-NMR (400 MHz, CD₂Cl₂, 298 K): δ (ppm) = 7.47-7.33 (m, 26 H, H-Ph), 7.26-7.23 (m, 4 H, H-Ph), 6.92 (dd, ${}^{3}J_{8,9b}$ = 17.9 Hz, ${}^{3}J_{8,9a}$ = 11.5 Hz, 2 H, H-8), 5.57 (dd, ${}^{3}J_{8,9b}$ = 17.9 Hz, ${}^{2}J_{9a,9b}$ = 1.7 Hz, 2 H, H-9b), 5.49 (dd, ${}^{3}J_{8,9a}$ = 11.5 Hz, ${}^{2}J_{9a,9b}$ = 1.7 Hz, 2 H, H-9a), 5.18 (s, 4 H, H-13), 5.10 (s, 4 H, H-12), 5.05 (s, 4 H, H-11), 2.25 (s, 6 H, H-10). 13 C-NMR (176 MHz, acetone-d6, 298 K): δ (ppm) = 152.6 (C-5), 152.1 (C-3), 145.1 (C-4), 138.0 (C-Ph), 138.0 (C-Ph), 137.9 (C-Ph), 136.9 (C-1), 134.8 (C-8), 128.9 (C-Ph), 128.9 (C-Ph), 128.8 (C-Ph), 128.7 (C-Ph), 128.5 (C-Ph), 128.4 (C-Ph), 128.4 (C-Ph), 128.1 (C-Ph), 126.7 (C-2), 120.7 (C-9), 114.1 (C-6), 93.0 (C-7), 76.1 (C-12), 76.0 (C-13), 75.6 (C-11), 14.1 (C-10). MS (APCI) m/z: [M+H]⁺ calcd. for $C_{62}H_{55}O_{6}^{+}$ 895.3993, found 895.3998.

Synthesis of dialdehyde 113

Alkyne 117 (537 mg, 600 μ mol, 1.00 eq) and NMO·H₂O (327 mg, 2.42 mmol, 4.03 eq) were dissolved in acetone/THF/H₂O (10:10:1, 21 mL). OsO₄ (4 wt% in H₂O, 200 μ L, 31.5 μ mol, 5.2 mol%) was added and the reaction was stirred at room temperature for 21 h. After completion the reaction was quenched with aqueous Na₂S₂O₃ (sat., 50 mL) and the aqueous phase was extracted with EA (3×25 mL). The combined organic phases were dried over Na₂SO₄ and filtered over a plug of silica (EA). After removal of the solvent *in vacuo* Pb(OAc)₄ (685 mg, 1.54 mmol, 2.57 eq) was added, the mixture was dissolved in dry toluene (40 mL) and stirred at room temperature for 35 min. After completion the reaction was filtered over a short plug of silica (EA) and the solvent was removed *in vacuo* giving dialdehyde 113 (501 mg, 557 μ mol, 93% over 2 steps) as a yellow amorphous solid.

¹H-NMR (700 MHz, CD₂Cl₂, 298 K): δ (ppm) = 10.62 (s, 2 H, H-8), 7.46-7.20 (m, 30 H, H-Ph), 5.20 (s, 4 H, H-11), 5.16 (s, 4 H, H-12), 5.03 (s, 4 H, H-10), 2.44 (s, 6 H, H-9). ¹³C-NMR (176 MHz, CD₂Cl₂, 298 K): δ (ppm) = 193.1 (C-8), 152.9 (C-5), 152.5 (C-3), 150.4 (C-4), 137.3 (C-Ph), 137.1 (C-Ph), 131.8 (C-2), 131.2 (C-1), 129.2 (C-Ph), 129.2 (C-Ph), 129.2 (C-Ph), 129.1 (C-Ph), 129.0 (C-Ph), 129.0 (C-Ph), 129.0 (C-Ph), 128.9 (C-Ph), 128.9 (C-Ph), 128.8 (C-Ph), 128.6 (C-Ph), 128.6 (C-Ph), 128.5 (C-Ph), 119.6 (C-6), 93.1 (C-7), 76.5 (C-12), 76.2 (C-11), 75.8 (C-10), 12.9 (C-9). MS (APCI) m/z: [M+H]⁺ calcd. for C₆₀H₅₁O₈⁺ 899.3578, found 899.3574.

7. List of abbreviations

AcCl acetyl chloride

acetone-d6 deuterated acetone
AgCO₂CF₃ silver trifluoro acetate

AgOTf silver trifluoromethanesulfonate

AlCl₃ aluminum(III) chloride

APCI Atmospheric-pressure chemical ionization

ASA arylsulfatase A

BBB blood brain barrier
BBr₃ boron tribromide

BF₃(·Et₂O) boron trifluoride (diethyl etherate)

boron trichloride

BnBr benzyl bromide
BnCl benzyl chloride

BCl₃

Bpin pinacol boronic ester

BrPPh₃Me methyl tri(phenyl)phosphonium bromide

brsm based on recovered starting material

calcd. calculated

CBr₄ carbon tetrabromide

CD₂Cl₂ deuterated dichloromethane

 $Ce(SO_4)_2$ cerium sulfate CH cyclohexane

CH(OMe)₃ trimethyl orthoformate/trimethoxymethane

CH₂Cl₂ dichloromethane

CHCl₃ chloroform

 Cs_2CO_3 cesium carbonate $CuCl/CuCl_2$ copper(I/II) chloride

Cul copper(I) iodide
DCM dichloromethane

DIBAl-H diisobutylaluminum hydride

DMDO dimethyl dioxirane

DMF dimethylformamide

DMSO dimethylsulfoxide

DMSO-d6 deuterated dimethylsulfoxide

dppb 1,4-bis(diphenylphosphino)butane

7. List of abbreviations

e.g. *exempli gratia* (lat.) = for example

EA ethyl acetate

ECD electronic circular dichroism

El electron ionization

ESI-TOF electrospray ionization-time of flight

Et₂O diethyl ether

et al. et alii (lat.) = and others

eq equivalents

FDA Food and Drug Administration

 H_2 hydrogen H_2O water

H₂O₂ hydrogen peroxide

H₂SO₄ sulfuric acid

HCl hydrochloric acid

HMBC heteronuclear multiple bond correlation
HPLC high performance liquid chromatography

HRMS high resolution mass spectrometry

HSQC heteronuclear single quantum coherence

I₂ iodine

 $\begin{array}{ll} \text{IBX} & \text{2-iodoxybenzoic acid} \\ \text{K}_2\text{CO}_3 & \text{potassium carbonate} \\ \text{K}_3\text{PO}_4 & \text{potassium phosphate} \\ \end{array}$

KI potassium iodide KOAc potassium acetate

LAH lithium aluminum hydride

LiOH(·H₂O) lithium hydroxide (monohydrate)

LLS longest linear sequence

MALDI matrix-assisted laser desorption/ionization

mCPBA meta-chloroperoxybenzoic acid

MeCN acetonitrile

MeOCHCl₂ dichloromethyl methyl ether

MeOH methanol

MgSO₄ magnesium sulfate

MLD metachromatic leukodystrophy

MS mass spectrometry

 $Na_2S_2O_3$ sodium thiosulfate

 $Na_2S_2O_8$ sodium persulfate

Na₂SO₄ sodium sulfate

NaH sodium hydride

NaHCO₃ sodium bicarbonate

NaIO₄ sodium periodate

NEt₃ triethylamine

ammonium chloride NH₄Cl

ammonium heptamolybdate $(NH_4)_6Mo_7O_{24}$

NHMDS sodium bis(trimethylsilyl)amide

 $NMO \cdot H_2O$ N-methylmorpholine-N-oxide

NMR nuclear magnetic resonance (spectroscopy)

NOESY nuclear Overhauser enhancement and exchange spectroscopy

OPPh₃ triphenylphosphine oxide

 OsO_4 osmium tetroxide

 P_2O_5 phosphorus pentoxide

Pb(OAc)₄ lead(IV) acetate

Pd(dppf)Cl₂ [1,1'-bis(diphenylphosphino)ferrocene]palladium(II) dichloride

Pd(OAc)₂ palladium diacetate

 $Pd(P(tBu)_3)_4$ tetrakis(tri-tert-butylphoshpine)palladium(0)

Pd(PPh₃)₂Cl₂ bis(triphenylphosphine)palladium(II) dichloride

Pd(PPh₃)₄ tetrakis(triphenylphosphine)palladium(0)

Pd/C palladium on charcoal $PdCl_2$ palladium dichloride PhMe₅ pentamethyl benzene piv₂O pivaloyl anhydride PPh_3

PtCl₂ platinum dichloride

qNMR quantitative NMR

(Q)SAR (quantitative) structure activity relationship

triphenylphosphine

ROESY rotating frame nuclear Overhauser effect spectroscopy

r.t. room temperature

RuPhos Pd G4 RuPhos palladium precatalyst generation 4

electrophilic aromatic substitution S_EAr

tetramethylsilane Si(Me)₄

silicon dioxide SiO_2

 S_N2 nucleophilic substitution

7. List of abbreviations

TBAF tetrabutylammonium fluoride

TFA trifluoro acetic acid

THF tetrahydrofuran
TIPS triisopropylsilane

TLC thin layer chromatography

TMOF trimethyl orthoformate/trimethoxymethane

XantPhos Pd G3/4 XantPhos palladium precatalyst generation 3/4

XPhos Pd G4 XPhos palladium precatalyst generation 4

ZnMe₂ dimethyl zinc

- (1) McMurry, J.; Begley, T. P. *Organische Chemie der biologischen Stoffwechselwege*, 1. Aufl.; Elsevier Spektrum Akad. Verl., 2006.
- (2) Krug, D.; Garcia, R.; Müller, R. Myxobakterielle Naturstofffabriken. *Biospektrum* **2020**, *26* (1), 32–36. DOI: 10.1007/s12268-020-1334-1.
- (3) Talontsi, F. M.; Dittrich, B.; Schüffler, A.; Sun, H.; Laatsch, H. Epicoccolides: Antimicrobial and Antifungal Polyketides from an Endophytic Fungus Epicoccum sp. Associated with Theobroma cacao. *Eur. J. Org. Chem.* **2013**, *2013* (15), 3174–3180. DOI: 10.1002/ejoc.201300146.
- (4) Alexander Fleming. On the Antibacterial Action of Cultures of a Penicillium, with Special Reference to their Use in the Isolation of B. influenzæ. *Br. J. Exp. Pathol.* **1929** (10), 226–236.
- (5) World Health Organization; Food and Agriculture Organization of the United Nations; International Office of Epizootics. *Report of a joint FAO/OIE/WHO Expert Consultation on antimicrobial use in aquaculture and antimicrobial resistance, Seoul, Republic of Korea, 13–16 June 2006*; World Health Organization, 2006.
- (6) Marino, A.; Maniaci, A.; Lentini, M.; Ronsivalle, S.; Nunnari, G.; Cocuzza, S.; Parisi, F. M.; Cacopardo, B.; Lavalle, S.; La Via, L. The Global Burden of Multidrug-Resistant Bacteria. *Epidemiologia* **2025**, *6* (2), 21. DOI: 10.3390/epidemiologia6020021.
- (7) Braus, G. H. One Health für Pilzpathogene von Pflanze, Tier und Mensch. *Biospektrum* **2020**, *26* (1), 116. DOI: 10.1007/s12268-020-1317-2.
- (8) Deshmukh, S. K.; Gupta, M. K.; Prakash, V.; Saxena, S. Endophytic Fungi: A Source of Potential Antifungal Compounds. *J. Fungi* **2018**, *4* (3). DOI: 10.3390/jof4030077.
- (9) Jacob, S. A.; Ng, W. L.; Do, V. Estimation of an optimal chemotherapy utilisation rate for cancer: setting an evidence-based benchmark for quality cancer care. *Clin. Oncol.* **2015**, *27* (2), 77–82. DOI: 10.1016/j.clon.2014.10.004.
- (10) El Amrani, M.; Lai, D.; Debbab, A.; Aly, A. H.; Siems, K.; Seidel, C.; Schnekenburger, M.; Gaigneaux, A.; Diederich, M.; Feger, D.; Lin, W.; Proksch, P. Protein kinase and HDAC inhibitors from the endophytic fungus Epicoccum nigrum. *J. Nat. Prod.* **2014**, *77* (1), 49–56. DOI: 10.1021/np4005745.
- (11) McKinney, J. D.; Richard, A.; Waller, C.; Newman, M. C.; Gerberick, F. The practice of structure activity relationships (SAR) in toxicology. *Toxicol. Sci.* **2000**, *56* (1), 8–17. DOI: 10.1093/toxsci/56.1.8.
- (12) Langer, T.; Hoffmann, R. D. *Pharmacophores and Pharmacophore Searches*, Vol. 32; Wiley, 2006. DOI: 10.1002/3527609164.
- (13) Vertesy, L.; Kurz, M.; Markus, E. A.; Toti, L. 2-Phenyl-Benzofuran Derivatives, Method for the Production Thereof and Their Use. WO2004EP11695 20041016.

- (14) Kayser, F. H.; Bienz, K. A.; Eckert, J.; Zinkernagel, R. M. *Medical microbiology*, 1st ed.; Thieme flexibook; George Thieme Verlag, 2005.
- (15) Köhler, W., Ed. *Medizinische Mikrobiologie*; 197 Tabellen, 8., völlig neu bearb. Aufl.; Urban & Fischer, 2001.
- (16) Chauhan, S.; Jain, S.; Varma, S.; Chauhan, S. S. Tropical pyomyositis (myositis tropicans): current perspective. *Postgrad. Med. J.* **2004**, *80* (943), 267–270. DOI: 10.1136/pgmj.2003.009274.
- (17) Holmes, M. A.; Zadoks, R. N. Methicillin resistant S. aureus in human and bovine mastitis. *J. Mammary Gland Biol. Neoplasia* **2011**, *16* (4), 373–382. DOI: 10.1007/s10911-011-9237-x.
- (18) Li, R.; Morris, S. W. Development of anaplastic lymphoma kinase (ALK) small-molecule inhibitors for cancer therapy. *Med. Res. Rev.* **2008**, *28* (3), 372–412. DOI: 10.1002/med.20109.
- (19) Roskoski, R. Anaplastic lymphoma kinase (ALK): structure, oncogenic activation, and pharmacological inhibition. *Pharmacol. Res.* **2013**, *68* (1), 68–94. DOI: 10.1016/j.phrs.2012.11.007.
- (20) Verma, A.; Warner, S. L.; Vankayalapati, H.; Bearss, D. J.; Sharma, S. Targeting Axl and Mer kinases in cancer. *Mol. Cancer Ther.* **2011**, *10* (10), 1763–1773. DOI: 10.1158/1535-7163.MCT-11-0116.
- (21) Hauck, C. R.; Hsia, D. A.; Schlaepfer, D. D. The focal adhesion kinase--a regulator of cell migration and invasion. *IUBMB Life* **2002**, *53* (2), 115–119. DOI: 10.1080/15216540211470.
- (22) Jones, H. E.; Goddard, L.; Gee, J. M. W.; Hiscox, S.; Rubini, M.; Barrow, D.; Knowlden, J. M.; Williams, S.; Wakeling, A. E.; Nicholson, R. I. Insulin-like growth factor-I receptor signalling and acquired resistance to gefitinib (ZD1839; Iressa) in human breast and prostate cancer cells. *Endocr.-Relat. Cancer* **2004**, *11* (4), 793–814. DOI: 10.1677/erc.1.00799.
- (23) Wheeler, D. L.; Iida, M.; Dunn, E. F. The role of Src in solid tumors. *Oncologist* **2009**, *14* (7), 667–678. DOI: 10.1634/theoncologist.2009-0009.
- (24) Holmes, K.; Roberts, O. L.; Thomas, A. M.; Cross, M. J. Vascular endothelial growth factor receptor-2: structure, function, intracellular signalling and therapeutic inhibition. *Cell. Signalling* **2007**, *19* (10), 2003–2012. DOI: 10.1016/j.cellsig.2007.05.013.
- (25) Matsumoto, T.; Mugishima, H. Signal transduction via vascular endothelial growth factor (VEGF) receptors and their roles in atherogenesis. *J. Atheroscler. Thromb.* **2006**, *13* (3), 130–135. DOI: 10.5551/jat.13.130.
- (26) Ma, P. C.; Maulik, G.; Christensen, J.; Salgia, R. c-Met: structure, functions and potential for therapeutic inhibition. *Cancer Metastasis Rev.* **2003**, *22* (4), 309–325. DOI: 10.1023/a:1023768811842.
- (27) Gentile, A.; Trusolino, L.; Comoglio, P. M. The Met tyrosine kinase receptor in development and cancer. *Cancer Metastasis Rev.* **2008**, *27* (1), 85–94. DOI: 10.1007/s10555-007-9107-6.
- (28) Peruzzi, B.; Bottaro, D. P. Targeting the c-Met signaling pathway in cancer. *Clin. Cancer Res.* **2006**, *12* (12), 3657–3660. DOI: 10.1158/1078-0432.CCR-06-0818.

- (29) Nassirpour, R.; Shao, L.; Flanagan, P.; Abrams, T.; Jallal, B.; Smeal, T.; Yin, M.-J. Nek6 mediates human cancer cell transformation and is a potential cancer therapeutic target. *Mol. Cancer Res.* **2010**, *8* (5), 717–728. DOI: 10.1158/1541-7786.MCR-09-0291.
- (30) Ruijter, A. J. M. de; van Gennip, A. H.; Caron, H. N.; Kemp, S.; van Kuilenburg, A. B. P. Histone deacetylases (HDACs): characterization of the classical HDAC family. *Biochem. J.* **2003**, *370* (Pt 3), 737–749. DOI: 10.1042/bj20021321.
- (31) Florean, C.; Schnekenburger, M.; Grandjenette, C.; Dicato, M.; Diederich, M. Epigenomics of leukemia: from mechanisms to therapeutic applications. *Epigenomics* **2011**, *3* (5), 581–609. DOI: 10.2217/epi.11.73.
- (32) Seidel, C.; Schnekenburger, M.; Dicato, M.; Diederich, M. Histone deacetylase modulators provided by Mother Nature. *Genes Nutr.* **2012**, *7* (3), 357–367. DOI: 10.1007/s12263-012-0283-9.
- (33) Seidel, C.; Florean, C.; Schnekenburger, M.; Dicato, M.; Diederich, M. Chromatin-modifying agents in anti-cancer therapy. *Biochimie* **2012**, *94* (11), 2264–2279. DOI: 10.1016/j.biochi.2012.05.012.
- (34) Schnekenburger, M.; Diederich, M. Epigenetics Offer New Horizons for Colorectal Cancer Prevention. *Curr. Colorectal Cancer Rep.* **2012**, *8* (1), 66–81. DOI: 10.1007/s11888-011-0116-z.
- (35) Gieselmann, V.; König, G. M.; Eckhardt, M.; Hufendiek, P.; Zech, I. Small Molecule Therapeutics for Treating Metachromatic Leukodystrophy. WO2018EP53652 20180214.
- (36) Singh, N.; Singh, A. K. A comprehensive review on structural and therapeutical insight of Cerebroside sulfotransferase (CST) An important target for development of substrate reduction therapy against metachromatic leukodystrophy. *Int. J. Biol. Macromol.* **2024**, *258* (Pt 1), 128780. DOI: 10.1016/j.ijbiomac.2023.128780.
- (37) Platt, F. M.; d'Azzo, A.; Davidson, B. L.; Neufeld, E. F.; Tifft, C. J. Lysosomal storage diseases. *Nat. Rev. Dis. Primers* **2018**, *4* (1), 27. DOI: 10.1038/s41572-018-0025-4.
- (38) Vanderver, A.; Prust, M.; Tonduti, D.; Mochel, F.; Hussey, H. M.; Helman, G.; Garbern, J.; Eichler, F.; Labauge, P.; Aubourg, P.; Rodriguez, D.; Patterson, M. C.; van Hove, J. L. K.; Schmidt, J.; Wolf, N. I.; Boespflug-Tanguy, O.; Schiffmann, R.; van der Knaap, M. S. Case definition and classification of leukodystrophies and leukoencephalopathies. *Mol. Genet. Metab.* **2015**, *114* (4), 494–500. DOI: 10.1016/j.ymgme.2015.01.006.
- (39) Shaimardanova, A. A.; Chulpanova, D. S.; Solovyeva, V. V.; Mullagulova, A. I.; Kitaeva, K. V.; Allegrucci, C.; Rizvanov, A. A. Metachromatic Leukodystrophy: Diagnosis, Modeling, and Treatment Approaches. *Front. Med.* **2020**, *7*, 576221. DOI: 10.3389/fmed.2020.576221.
- (40) FDA. FDA Approves First Gene Therapy for Children with Metachromatic Leukodystrophy, 2024.
- (41) Wolf, N. I.; van der Knaap, M. S.; Engelen, M. Treatment of leukodystrophies: Advances and challenges. *Eur. J. Paediatr. Neurol.* **2025**, *56*, 46–50. DOI: 10.1016/j.ejpn.2025.03.016.

- (42) Singh, S. B.; Zink, D. L.; Quamina, D. S.; Pelaez, F.; Teran, A.; Felock, P.; Hazuda, D. J. Integrastatins: structure and HIV-1 integrase inhibitory activities of two novel racemic tetracyclic aromatic heterocycles produced by two fungal species. *Tetrahedron Lett.* **2002**, *43* (13), 2351–2354. DOI: 10.1016/S0040-4039(02)00265-4.
- (43) Liu, D.; Li, Y.; Li, X.; Cheng, Z.; Huang, J.; Proksch, P.; Lin, W. Chartarolides A-C, novel meroterpenoids with antitumor activities. *Tetrahedron Lett.* **2017**, *58* (19), 1826–1829. DOI: 10.1016/j.tetlet.2017.03.079.
- (44) More, A. A.; Ramana, C. V. Total Synthesis of Integrastatin B Enabled by a Benzofuran Oxidative Dearomatization Cascade. *Org. Lett.* **2016**, *18* (6), 1458–1461. DOI: 10.1021/acs.orglett.6b00404.
- (45) Foot, J. S.; Giblin, G. M. P.; Taylor, R. J. K. Synthesis of the integrastatin nucleus using the Ramberg-Bäcklund reaction. *Org. Lett.* **2003**, *5* (23), 4441–4444. DOI: 10.1021/ol035786v.
- (46) Ramana, C. V.; Nageswara Reddy, C.; Gonnade, R. G. An expeditious one-step entry to the tetracyclic core of integrastatins. *Chem. Commun. (Cambridge, U. K.)* **2008** (27), 3151–3153. DOI: 10.1039/b801755g.
- (47) Tadross, P. M.; Bugga, P.; Stoltz, B. M. A rapid and convergent synthesis of the integrastatin core. *Org. Biomol. Chem.* **2011**, *9* (15), 5354–5357. DOI: 10.1039/C10B05725A.
- (48) More, A. A.; Ramana, C. V. o-Quinone Methides via Oxone-Mediated Benzofuran Oxidative Dearomatization and Their Intramolecular Cycloaddition with Carbonyl Groups: An Expeditious Construction of the Central Tetracyclic Core of Integrastatins, Epicoccolide A, and Epicocconigrone A. *Org. Lett.* **2016**, *18* (3), 612–615. DOI: 10.1021/acs.orglett.5b03707.
- (49) Jeong, J. Y.; Sperry, J.; Brimble, M. A. Synthesis of the Tetracyclic Cores of the Integrastatins, Epicoccolide A and Epicocconigrone A. *J. Org. Chem.* **2019**, *84* (18), 11935–11944. DOI: 10.1021/acs.joc.9b01796.
- (50) Dedenbach, S. Contributions to the Total Synthesis of Epicoccolide B. ongoing dissertation, Rheinische Friedrich-Wilhelms-Universität Bonn, Bonn, 2016.
- (51) Li, W.-S. Contributions to the Total Synthesis of Epicoccolide B. Master thesis, Rheinische Friedrich-Wilhelms-Universität Bonn, Bonn, 2021.
- (52) Abd El-Salam, M.; Bastos, J. K.; Han, J. J.; Previdi, D.; Coelho, E. B.; Donate, P. M.; Romero, M. F.; Lieske, J. The Synthesized Plant Metabolite 3,4,5-Tri-O-Galloylquinic Acid Methyl Ester Inhibits Calcium Oxalate Crystal Growth in a Drosophila Model, Downregulates Renal Cell Surface Annexin A1 Expression, and Decreases Crystal Adhesion to Cells. *J. Med. Chem.* **2018**, *61* (4), 1609–1621. DOI: 10.1021/acs.jmedchem.7b01566.
- (53) Mulholland, G. K.; Zheng, Q.-H. A Direct Iodination Method with Iodine and Silver Triflate for the Synthesis of Spect and Pet Imaging Agent Precursors. *Synth. Commun.* **2001**, *31* (20), 3059–3068. DOI: 10.1081/SCC-100105877.

- (54) Herbert, J. M. Negishi-type coupling of bromoarenes with dimethylzinc. *Tetrahedron Lett.* **2004**, *45* (4), 817–819. DOI: 10.1016/j.tetlet.2003.11.018.
- (55) Perry, G. J. P.; Quibell, J. M.; Panigrahi, A.; Larrosa, I. Transition-Metal-Free Decarboxylative Iodination: New Routes for Decarboxylative Oxidative Cross-Couplings. *J. Am. Chem. Soc.* **2017**, *139* (33), 11527–11536. DOI: 10.1021/jacs.7b05155.
- (56) Adrio, L. A.; Nguyen, B. N.; Guilera, G.; Livingston, A. G.; Hii, K. K. Speciation of Pd(OAc) 2 in ligandless Suzuki–Miyaura reactions. *Catal. Sci. Technol.* **2012**, *2* (2), 316–323. DOI: 10.1039/C1CY00241D.
- (57) Zhu, L.; Duquette, J.; Zhang, M. An improved preparation of arylboronates: application in one-pot Suzuki biaryl synthesis. *J. Org. Chem.* **2003**, *68* (9), 3729–3732. DOI: 10.1021/jo0269114.
- (58) Liu, C.; Ji, C.-L.; Hong, X.; Szostak, M. Palladium-Catalyzed Decarbonylative Borylation of Carboxylic Acids: Tuning Reaction Selectivity by Computation. *Angew. Chem., Int. Ed. Engl.* **2018**, *57* (51), 16721–16726. DOI: 10.1002/anie.201810145.
- (59) Ohsawa, K.; Yoshida, M.; Doi, T. A direct and mild formylation method for substituted benzenes utilizing dichloromethyl methyl ether-silver trifluoromethanesulfonate. *J. Org. Chem.* **2013**, *78* (7), 3438–3444. DOI: 10.1021/jo400056k.
- (60) Mal, D.; Pahari, P.; De, S. R. Regiospecific synthesis of 3-(2,6-dihydroxyphenyl)phthalides: application to the synthesis of isopestacin and cryphonectric acid. *Tetrahedron* **2007**, *63* (47), 11781–11792. DOI: 10.1016/j.tet.2007.08.048.
- (61) Newman, S. G.; Aureggi, V.; Bryan, C. S.; Lautens, M. Intramolecular cross-coupling of gem-dibromoolefins: a mild approach to 2-bromo benzofused heterocycles. *Chem. Commun. (Cambridge, U. K.)* **2009** (35), 5236–5238. DOI: 10.1039/b912093a.
- (62) Kempfle, J. S.; Nguyen, K.; Hamadani, C.; Koen, N.; Edge, A. S.; Kashemirov, B. A.; Jung, D. H.; McKenna, C. E. Bisphosphonate-Linked TrkB Agonist: Cochlea-Targeted Delivery of a Neurotrophic Agent as a Strategy for the Treatment of Hearing Loss. *Bioconjugate Chem.* **2018**, *29* (4), 1240–1250. DOI: 10.1021/acs.bioconjchem.8b00022.
- (63) Akiyama, T.; Hirofuji, H.; Ozaki, S. AlCl3-N,N-dimethylaniline: A new benzyl and allyl ether cleavage reagent. *Tetrahedron Lett.* **1991**, *32* (10), 1321–1324. DOI: 10.1016/S0040-4039(00)79656-0.
- (64) Okano, K.; Okuyama, K.; Fukuyama, T.; Tokuyama, H. Mild Debenzylation of Aryl Benzyl Ether with BCl 3 in the Presence of Pentamethylbenzene as a Non-Lewis-Basic Cation Scavenger. *Synlett* **2008**, *2008* (13), 1977–1980. DOI: 10.1055/s-2008-1077980.
- (65) Buck, E.; Song, Z. J.; Tschaen, D.; Dormer, P. G.; Volante, R. P.; Reider, P. J. Ullmann diaryl ether synthesis: rate acceleration by 2,2,6,6-tetramethylheptane-3,5-dione. *Org. Lett.* **2002**, *4* (9), 1623–1626. DOI: 10.1021/ol025839t.

- (66) Maiti, D.; Buchwald, S. L. Cu-catalyzed arylation of phenols: synthesis of sterically hindered and heteroaryl diaryl ethers. *J. Org. Chem.* **2010**, *75* (5), 1791–1794. DOI: 10.1021/jo9026935.
- (67) Sivaraman, A.; Kim, J. S.; Harmalkar, D. S.; Min, K. H.; Park, J.-W.; Choi, Y.; Kim, K.; Lee, K. Synthesis and Cytotoxicity Studies of Bioactive Benzofurans from Lavandula agustifolia and Modified Synthesis of Ailanthoidol, Homoegonol, and Egonol. *J. Nat. Prod.* **2020**, *83* (11), 3354–3362. DOI: 10.1021/acs.jnatprod.0c00697.
- (68) Miller, A. E. G.; Biss, J. W.; Schwartzman, L. H. Reductions with Dialkylaluminum Hydrides. *J. Org. Chem.* **1959**, *24* (5), 627–630. DOI: 10.1021/jo01087a013.
- (69) Reetz, M. T.; Drewes, M. W.; Schwickardi, R. Preparation of Enantiomerically Pure a-N,N-Dibenzylamino Aldehydes: S-2-(N,N-Dibenzylamino)-3-Phenylpropanal. *Org. Synth.* **1999**, *76*, 110. DOI: 10.15227/orgsyn.076.0110.
- (70) More, J. D.; Finney, N. S. A simple and advantageous protocol for the oxidation of alcohols with O-iodoxybenzoic acid (IBX). *Org. Lett.* **2002**, *4* (17), 3001–3003. DOI: 10.1021/ol026427n.
- (71) Sajiki, H.; Kuno, H.; Hirota, K. Suppression effect of the Pd/C-catalyzed hydrogenolysis of a phenolic benzyl protective group by the addition of nitrogen-containing bases. *Tetrahedron Lett.* **1998**, *39* (39), 7127–7130. DOI: 10.1016/S0040-4039(98)01514-7.
- (72) Brückner, R. *Reaktionsmechanismen*; Springer Berlin Heidelberg, 2004. DOI: 10.1007/978-3-662-45684-2.
- (73) Pal, R.; Sarkar, T.; Khasnobis, S. Amberlyst-15 in organic synthesis. *Arkivoc (Gainesville, FL, U. S.)* **2012**, *2012* (1), 570–609. DOI: 10.3998/ark.5550190.0013.114.
- (74) Wise, H. Mechanisms of Catalyst Poisoning by Sulfur Species. In *Catalyst Deactivation 1991, Proceedings of the 5th International Symposium*; Studies in Surface Science and Catalysis; Elsevier, 1991; pp 497–504. DOI: 10.1016/S0167-2991(08)62676-2.
- (75) Fuji, K.; Ichikawa, K.; Node, M.; Fujita, E. Hard acid and soft nucleophile system. New efficient method for removal of benzyl protecting group. *J. Org. Chem.* **1979**, *44* (10), 1661–1664. DOI: 10.1021/jo01324a017.
- (76) Paliakov, E.; Strekowski, L. Boron tribromide mediated debenzylation of benzylamino and benzyloxy groups. *Tetrahedron Lett.* **2004**, *45* (21), 4093–4095. DOI: 10.1016/j.tetlet.2004.03.139.
- (77) Fürstner, A.; Davies, P. W. Heterocycles by PtCl2-catalyzed intramolecular carboalkoxylation or carboamination of alkynes. *J. Am. Chem. Soc.* **2005**, *127* (43), 15024–15025. DOI: 10.1021/ja055659p.
- (78) Nakamura, M.; Ilies, L.; Otsubo, S.; Nakamura, E. 2,3-disubstituted benzofuran and indole by copper-mediated C-C bond extension reaction of 3-zinciobenzoheterole. *Org. Lett.* **2006**, *8* (13), 2803–2805. DOI: 10.1021/ol060896y.
- (79) Tyagi, A.; Reshi, N. U. D.; Daw, P.; Bera, J. K. Palladium complexes with an annellated mesoionic carbene (MIC) ligand: catalytic sequential Sonogashira coupling/cyclization reaction for one-pot

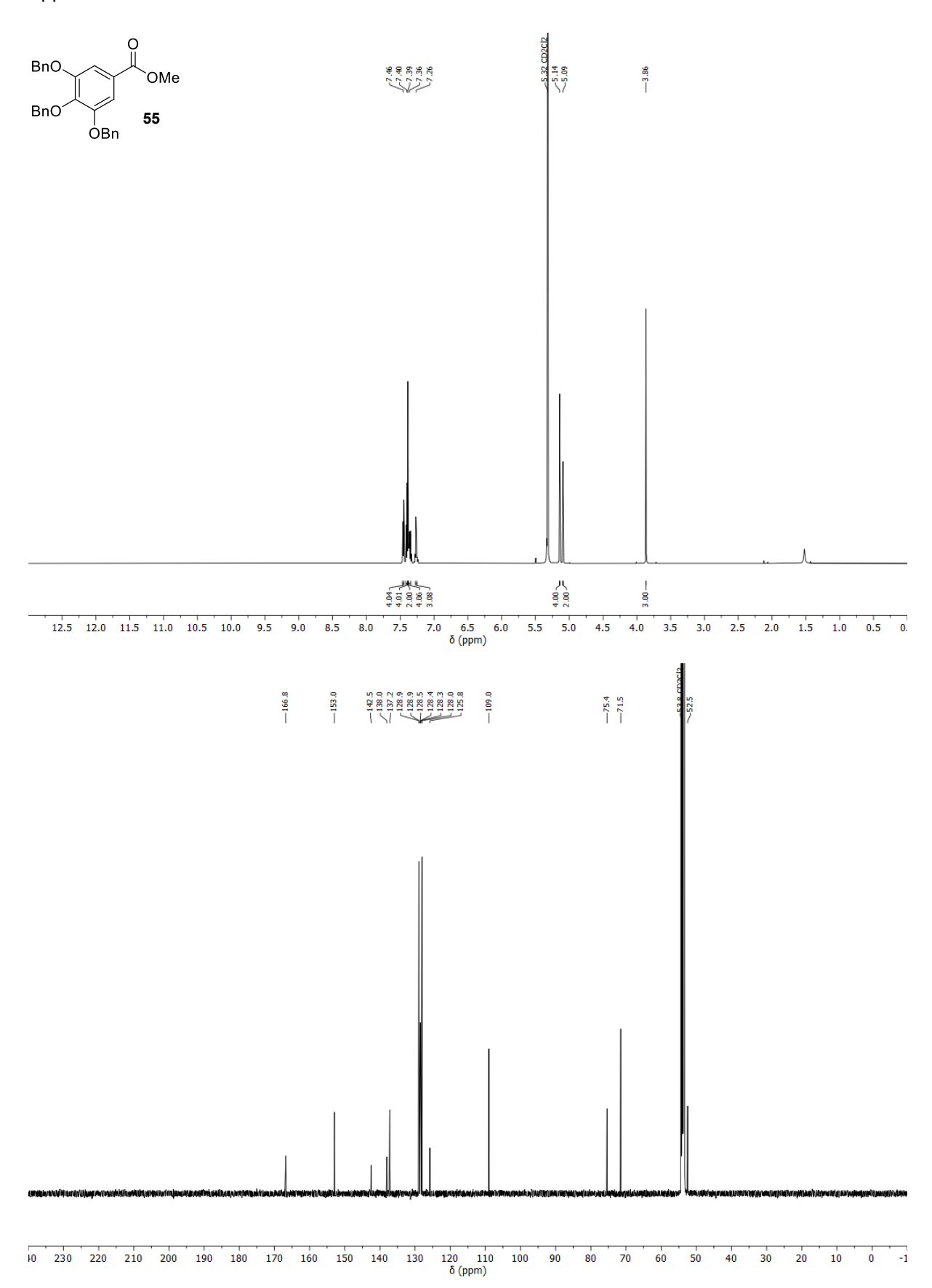
- synthesis of benzofuran, indole, isocoumarin and isoquinolone derivatives. *Dalton Trans.* **2020**, *49* (43), 15238–15248. DOI: 10.1039/d0dt02918a.
- (80) Rong, Z.; Gao, K.; Zhou, L.; Lin, J.; Qian, G. Facile synthesis of 2-substituted benzobfurans and indoles by copper-catalyzed intramolecular cyclization of 2-alkynyl phenols and tosylanilines. *RSC Adv.* **2019**, *9* (31), 17975–17978. DOI: 10.1039/c9ra01260e.
- (81) Müller, S.; Liepold, B.; Roth, G. J.; Bestmann, H. J. An Improved One-pot Procedure for the Synthesis of Alkynes from Aldehydes. *Synlett* **1996**, *1996* (06), 521–522. DOI: 10.1055/s-1996-5474.
- (82) Li, Y.; Zhang, J.; Wang, W.; Miao, Q.; She, X.; Pan, X. Efficient synthesis of tribenzohexadehydro12annulene and its derivatives in the ionic liquid. *J. Org. Chem.* **2005**, *70* (8), 3285–3287. DOI: 10.1021/jo047836v.
- (83) Li, X.; Liu, L.; Huang, T.; Tang, Z.; Li, C.; Li, W.; Zhang, T.; Li, Z.; Chen, T. Palladium-Catalyzed Decarbonylative Sonogashira Coupling of Terminal Alkynes with Carboxylic Acids. *Org. Lett.* **2021**, *23* (9), 3304–3309. DOI: 10.1021/acs.orglett.1c00768.
- (84) Liu, C.; Szostak, M. Decarbonylative Sonogashira Cross-Coupling of Carboxylic Acids. *Org. Lett.* **2021**, *23* (12), 4726–4730. DOI: 10.1021/acs.orglett.1c01445.
- (85) Okita, T.; Kumazawa, K.; Takise, R.; Muto, K.; Itami, K.; Yamaguchi, J. Palladium-catalyzed Decarbonylative Alkynylation of Aromatic Esters. *Chem. Lett.* **2017**, *46* (2), 218–220. DOI: 10.1246/cl.161001.
- (86) Papaplioura, E.; Mercier, M.; Jerhaoui, S.; Schnürch, M. The Vinyl Group: Small but Mighty Transition Metal Catalyzed and Non-Catalyzed Vinylation Reactions. *ChemCatChem* **2024**, *16* (24). DOI: 10.1002/cctc.202400513.
- (87) Willand-Charnley, R.; Fisher, T. J.; Johnson, B. M.; Dussault, P. H. Pyridine is an organocatalyst for the reductive ozonolysis of alkenes. *Org. Lett.* **2012**, *14* (9), 2242–2245. DOI: 10.1021/ol300617r.
- (88) Yu, W.; Mei, Y.; Kang, Y.; Hua, Z.; Jin, Z. Improved procedure for the oxidative cleavage of olefins by OsO4-NaIO4. *Org. Lett.* **2004**, *6* (19), 3217–3219. DOI: 10.1021/ol0400342.
- (89) VanRheenen, V.; Kelly, R. C.; Cha, D. Y. An improved catalytic OsO4 oxidation of olefins to -1,2-glycols using tertiary amine oxides as the oxidant. *Tetrahedron Lett.* **1976**, *17* (23), 1973–1976. DOI: 10.1016/S0040-4039(00)78093-2.
- (90) Prasad, K. R.; Anbarasan, P. Stereoselective formal synthesis of (–)-centrolobine. *Tetrahedron* **2007**, *63* (5), 1089–1092. DOI: 10.1016/j.tet.2006.11.062.
- (91) Adam, W.; Hadjiarapoglou, L.; Peters, K.; Sauter, M. Dimethyldioxirane epoxidation of benzofurans: reversible thermal and photochemical valence isomerization between benzofuran epoxides, quinone methides, and benzoxetenes. *J. Am. Chem. Soc.* **1993**, *115* (19), 8603–8608. DOI: 10.1021/ja00072a012.
- (92) Kothari, V. Selective autoxidation of some phenols using salcomines and metal phthalocyanines*1. *J. Catal.* **1976**, *41* (1), 180–189. DOI: 10.1016/0021-9517(76)90214-1.

- (93) Brückner, R. *Advanced organic chemistry:Reaction mechanisms*; Advanced organic chemistry series; Harcourt/Academic Press, 2002.
- (94) Dzyurkevich, M. S.; Shtyrlin, N. V.; Shtyrlin, Y. G. Synthetic route optimization of Sumepirin antiepileptic drug candidate. *Chim.Tech.Acta* **2020**, *7* (4), 159–168. DOI: 10.15826/chimtech.2020.7.4.04.
- (95) Gilmore, K.; Mohamed, R. K.; Alabugin, I. V. The Baldwin rules: revised and extended. *Wiley Interdiscip. Rev.:Comput. Mol. Sci.* **2016**, *6* (5), 487–514. DOI: 10.1002/wcms.1261.
- (96) Corey, E. J.; Kang, J.; Kyler, K. Activation of methylenetriphenylphosphorane by reaction with butyl- or -butyllithium. *Tetrahedron Lett.* **1985**, *26* (5), 555–558. DOI: 10.1016/S0040-4039(00)89146-7.
- (97) Cummins, C. H. Synthesis of symmetrical diarylalkynes by double stille coupling of bis(tributylstannyl)acetylene. *Tetrahedron Lett.* **1994**, *35* (6), 857–860. DOI: 10.1016/S0040-4039(00)75982-X.
- (98) Wagner, F. A. Contributions to the Total Synthesis of Epicocconigrone A. ongoing master thesis, Rheinische Friedrich-Wilhelms-Universität Bonn, Bonn, 2025.
- (99) Lott, R. S.; Chauhan, V. S.; Stammer, C. H. Trimethylsilyl iodide as a peptide deblocking agent. *J. Chem. Soc., Chem. Commun.* **1979** (11), 495. DOI: 10.1039/c39790000495.
- (100) Wagner, F. A. Fragmentsynthese von Epicoccolid A und Epicocconigron A. Bachelor thesis, Rheinische Friedrich-Wilhelms-Universität Bonn, Bonn, 2022.
- (101) Gröbel, B.-T.; Seebach, D. Umpolung of the Reactivity of Carbonyl Compounds Through Sulfur-Containing Reagents. *Synthesis* **1977**, *1977* (06), 357–402. DOI: 10.1055/s-1977-24412.
- (102) Lin, E. S.; Yang, Y. S. Colorimetric determination of the purity of 3'-phospho adenosine 5'-phosphosulfate and natural abundance of 3'-phospho adenosine 5'-phosphate at picomole quantities. *Anal. Biochem.* **1998**, *264* (1), 111–117. DOI: 10.1006/abio.1998.2800.
- (103) Mikula, H.; Svatunek, D.; Lumpi, D.; Glöcklhofer, F.; Hametner, C.; Fröhlich, J. Practical and Efficient Large-Scale Preparation of Dimethyldioxirane. *Org. Process Res. Dev.* **2013**, *17* (2), 313–316. DOI: 10.1021/op300338q.
- (104) Frigerio, M.; Santagostino, M.; Sputore, S. A User-Friendly Entry to 2-lodoxybenzoic Acid (IBX). J. Org. Chem. 1999, 64 (12), 4537–4538. DOI: 10.1021/jo9824596.
- (105) Fulmer, G. R.; Miller, A. J. M.; Sherden, N. H.; Gottlieb, H. E.; Nudelman, A.; Stoltz, B. M.; Bercaw, J. E.; Goldberg, K. I. NMR Chemical Shifts of Trace Impurities: Common Laboratory Solvents, Organics, and Gases in Deuterated Solvents Relevant to the Organometallic Chemist.

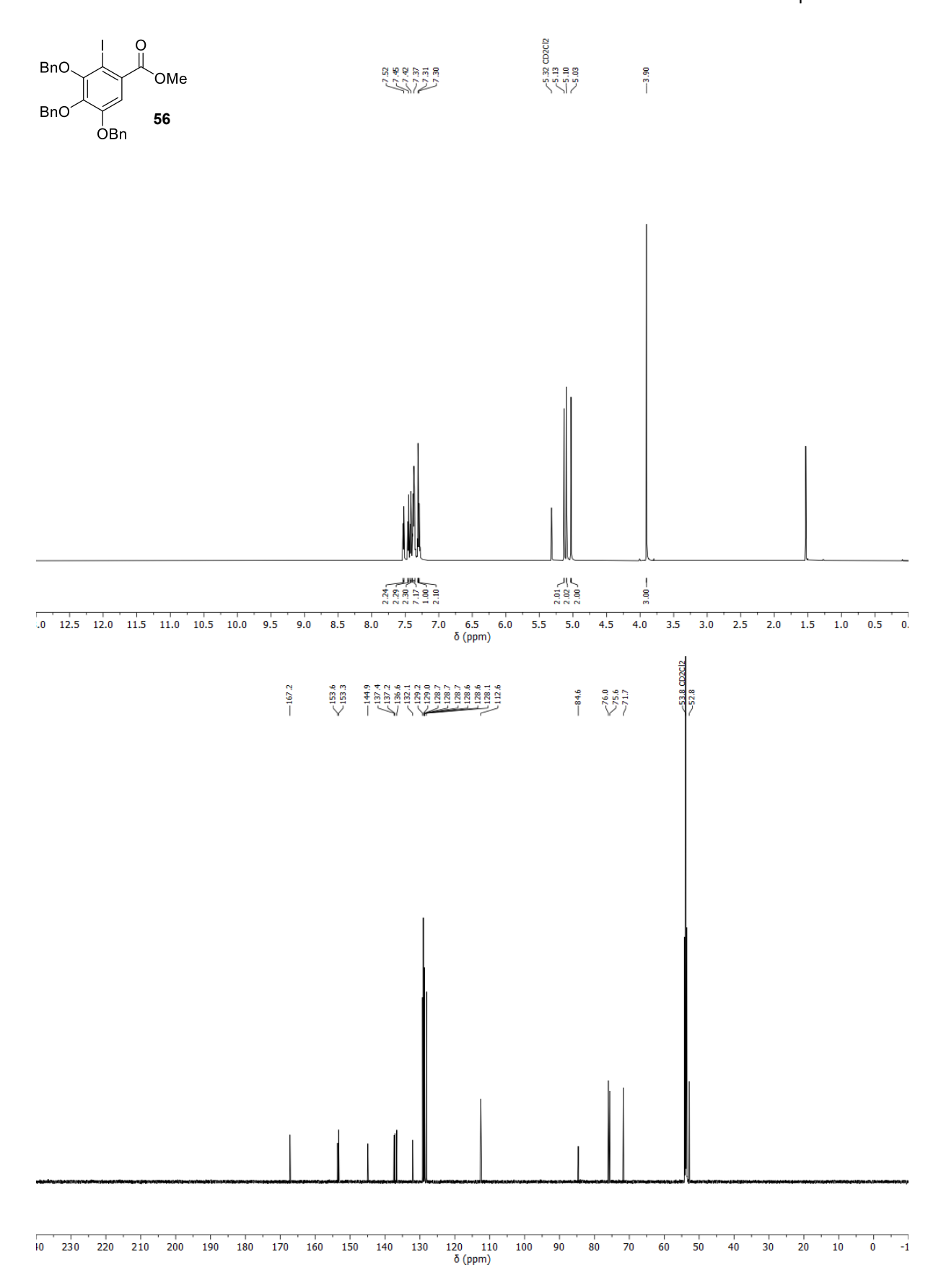
 Organometallics 2010, 29 (9), 2176–2179. DOI: 10.1021/om100106e.

Appendix

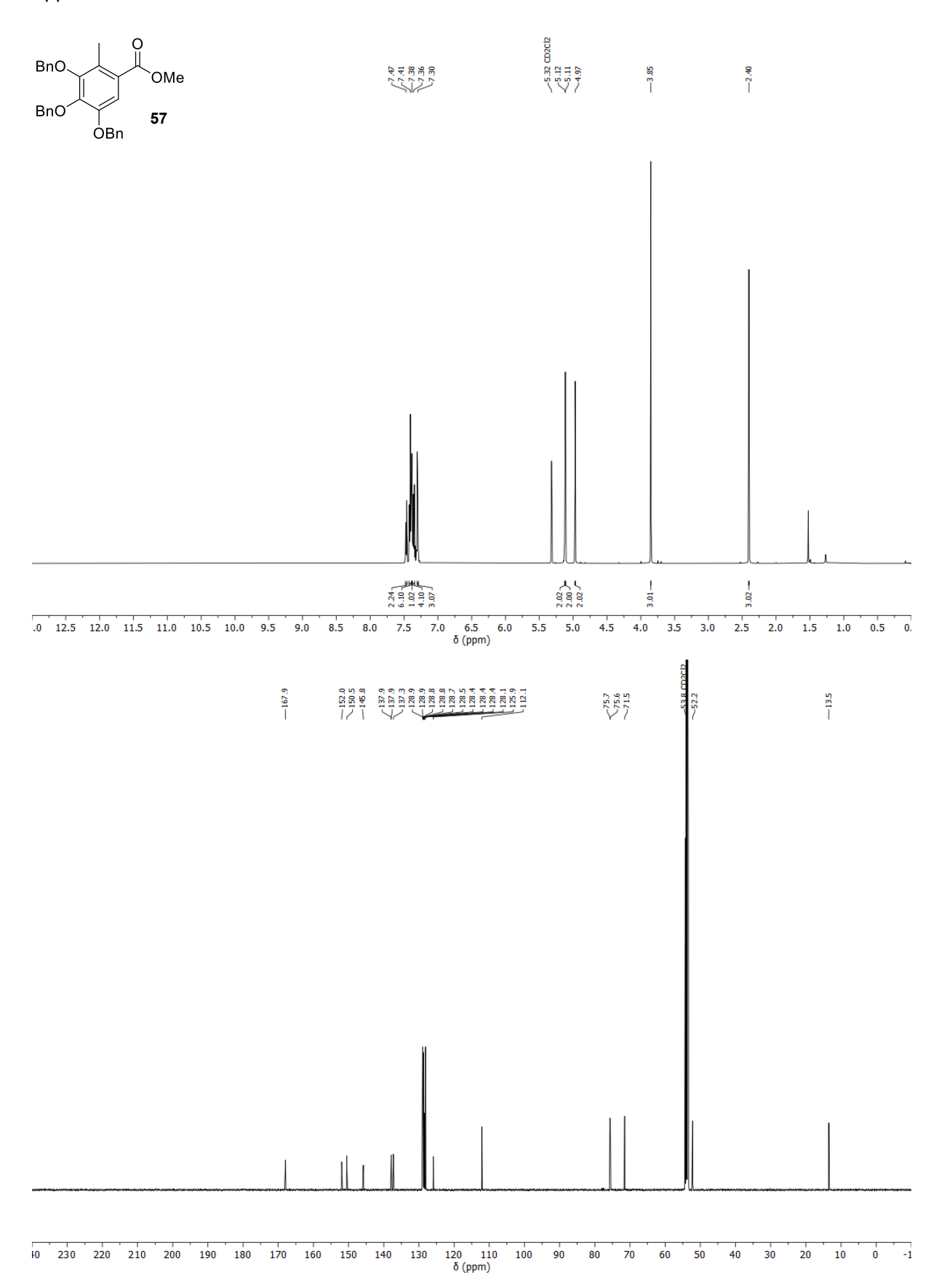
NMR-Spectra



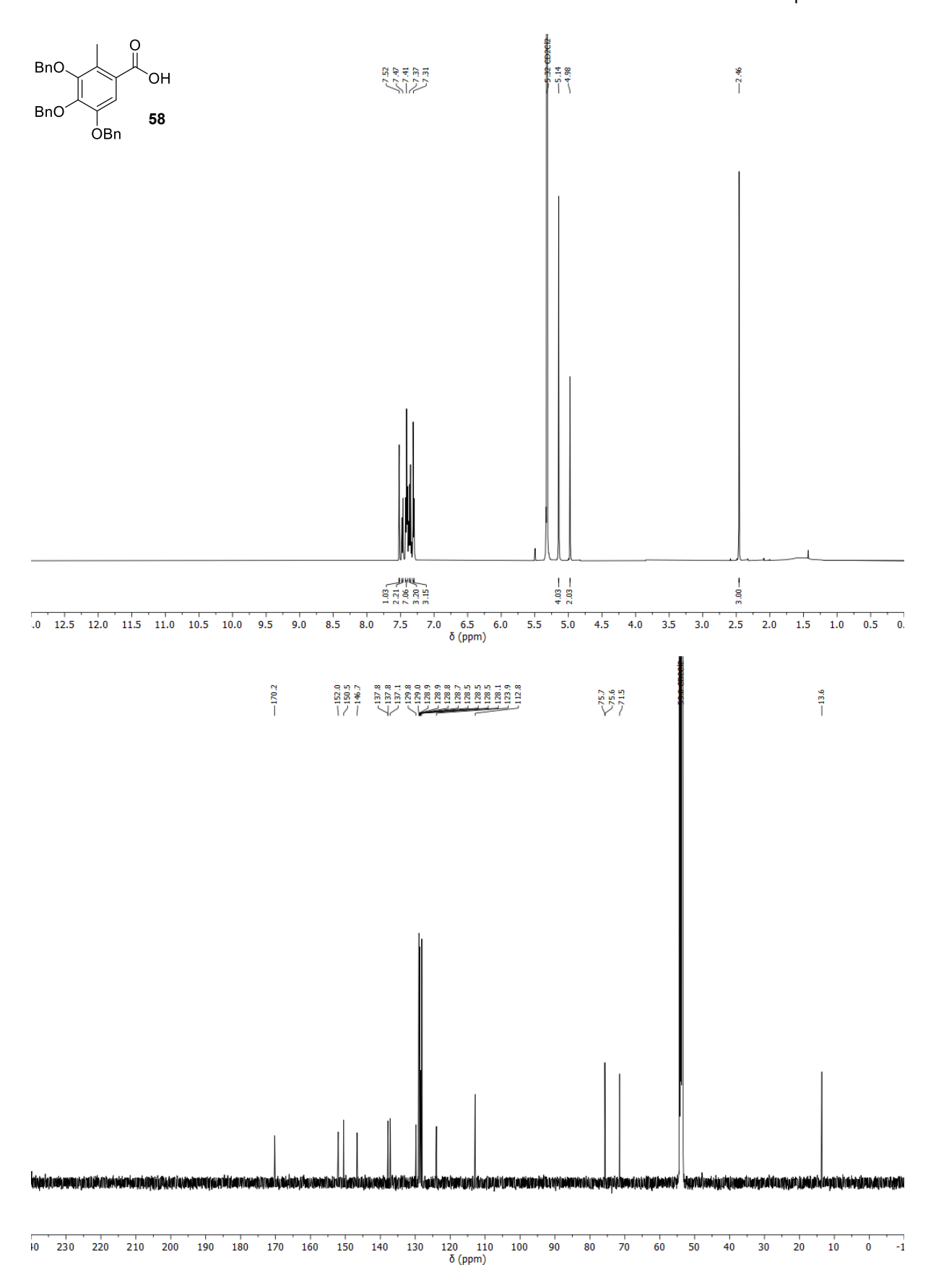
Appendix 1: ¹H- (top, 500 MHz) and ¹³C-NMR (bottom, 126 MHz) spectra of compound **55**, CD₂Cl₂, 298 K.



Appendix 2: ¹H- (top, 700 MHz) and ¹³C-NMR (bottom, 176 MHz) spectra of compound **56**, CD₂Cl₂, 298 K.

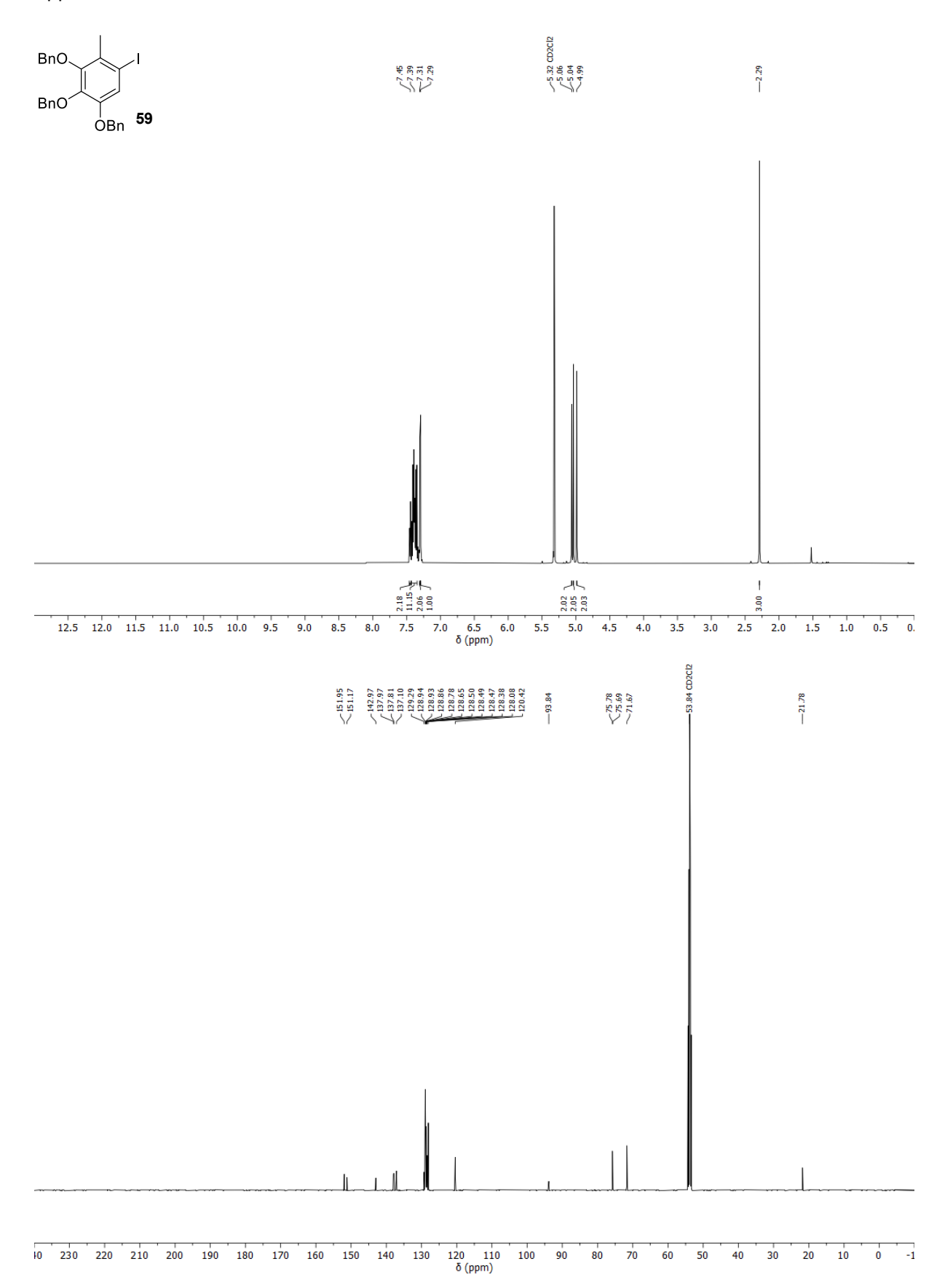


Appendix 3: ¹H- (top, 500 MHz) and ¹³C-NMR (bottom, 126 MHz) spectra of compound **57**, CD₂Cl₂, 298 K.

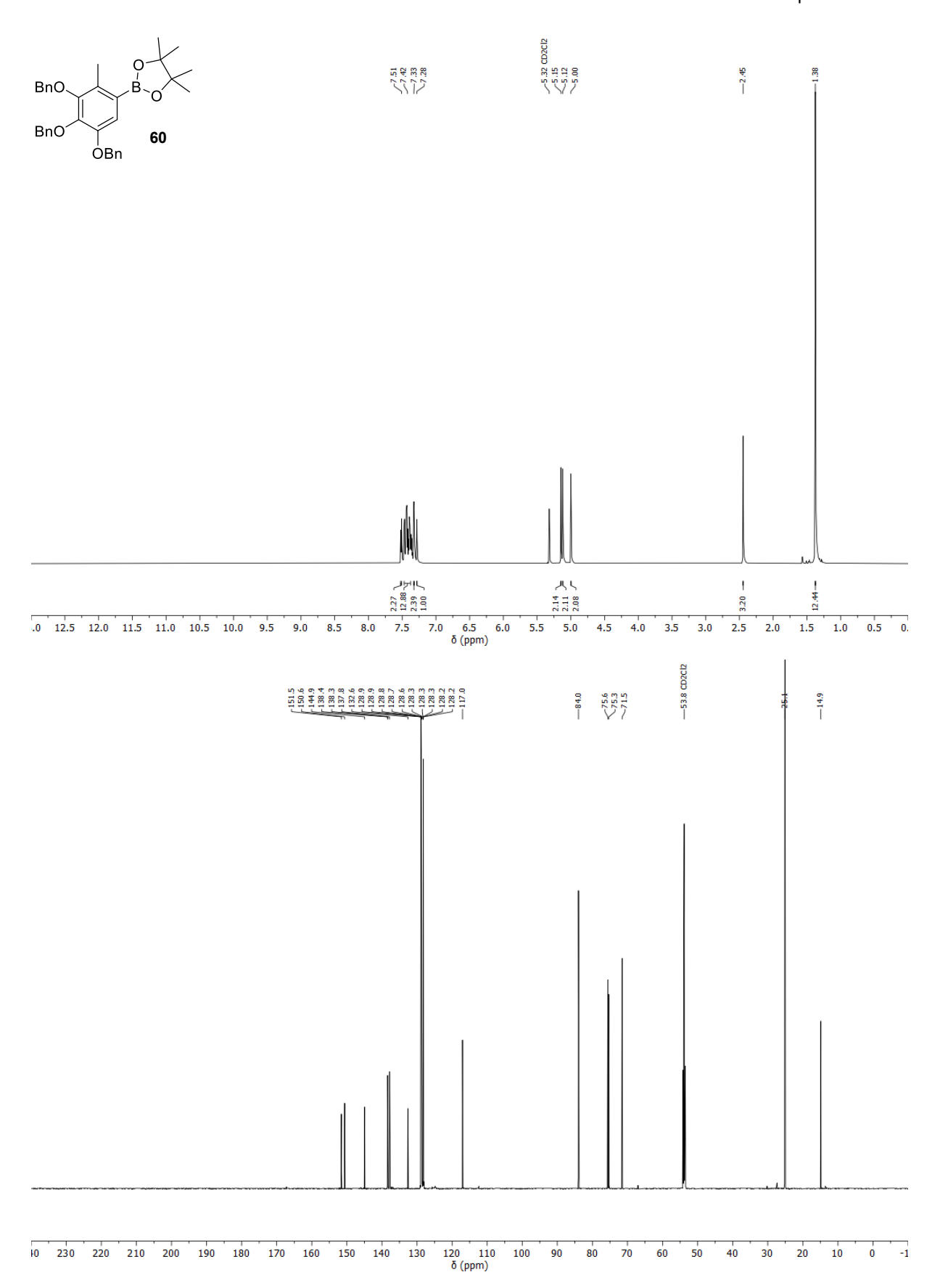


Appendix 4: ¹H- (top, 500 MHz) and ¹³C-NMR (bottom, 126 MHz) spectra of compound **58**, CD₂Cl₂, 298 K.

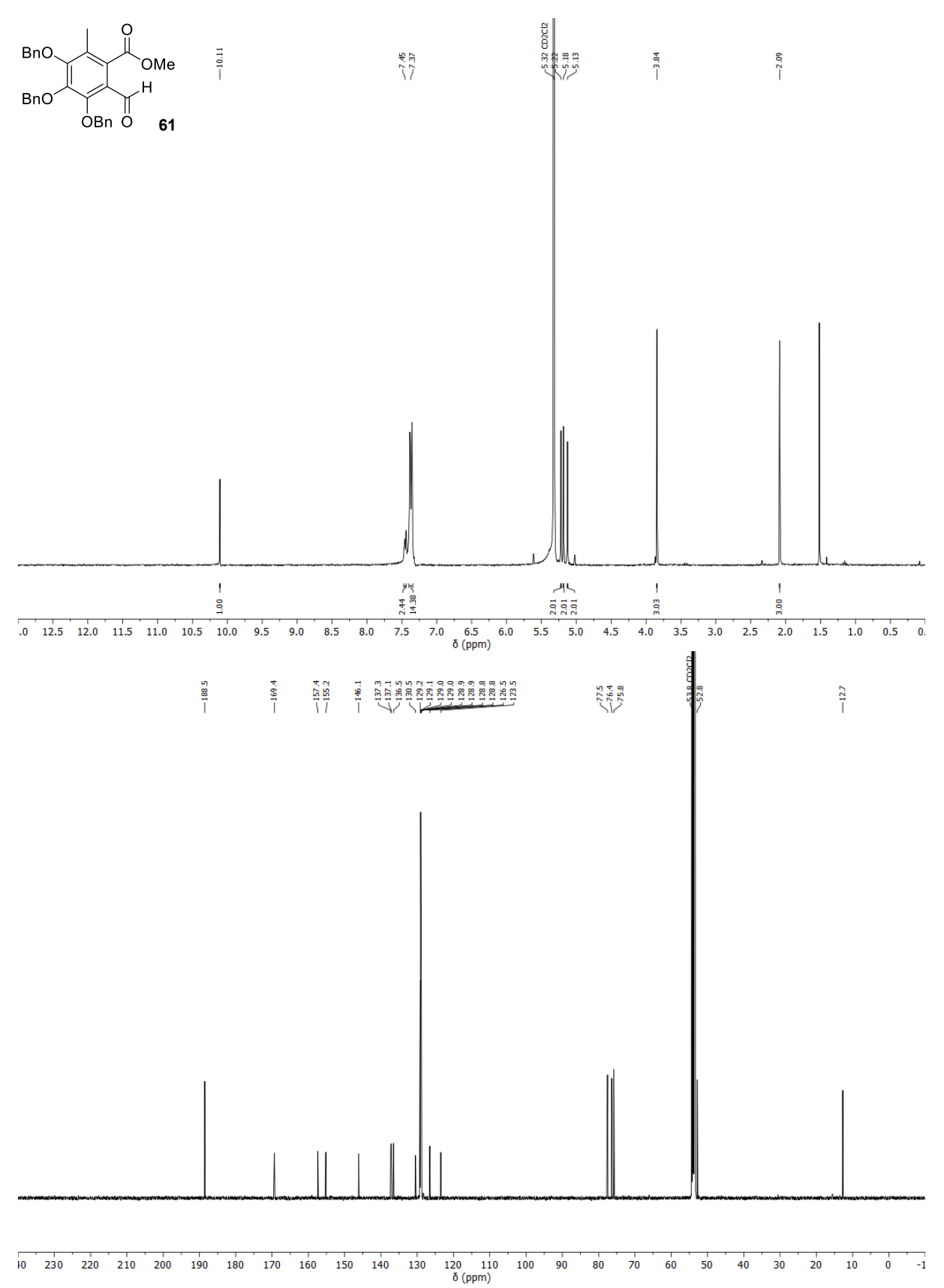




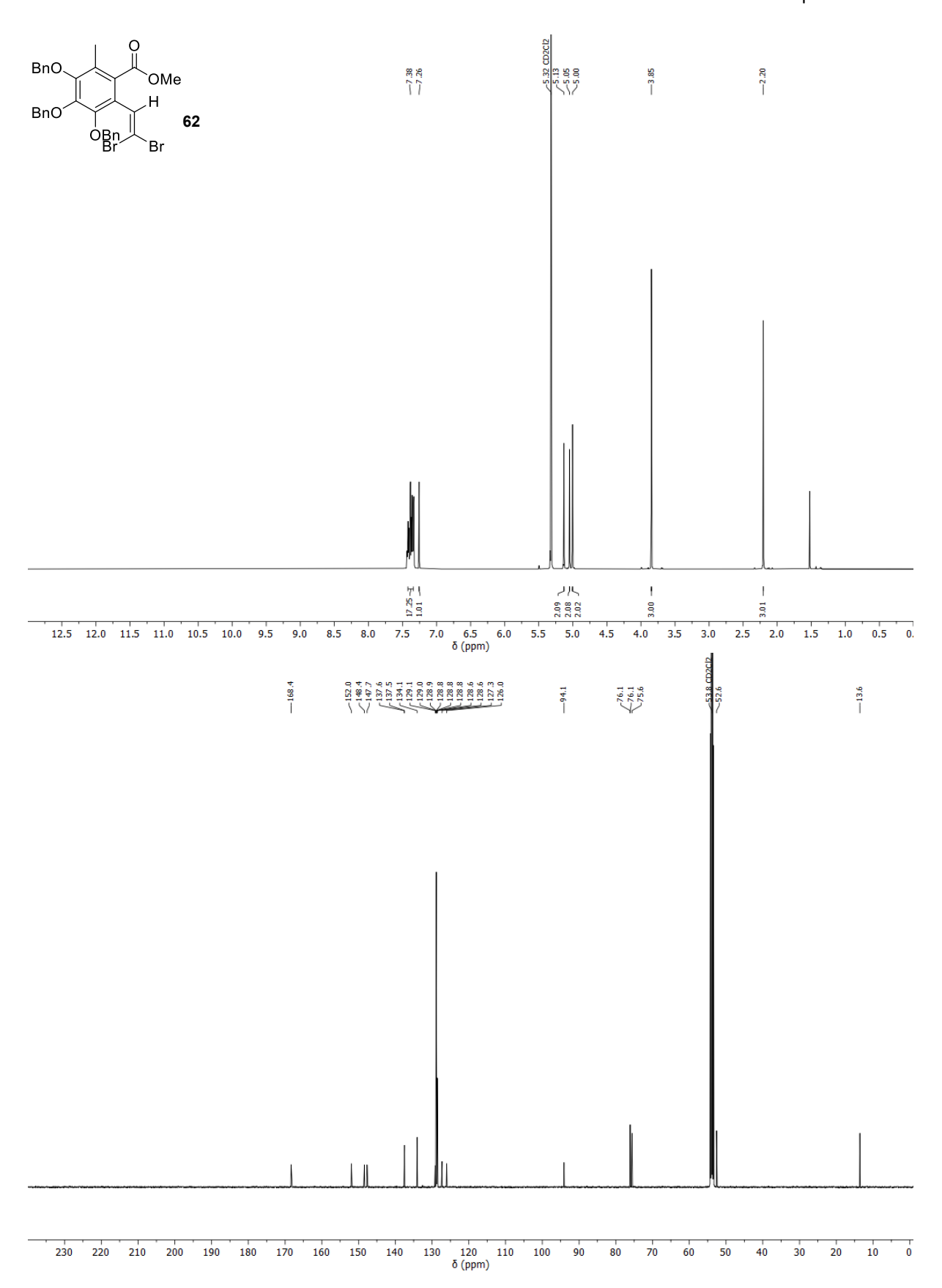
Appendix 5: ¹H- (top, 500 MHz) and ¹³C-NMR (bottom, 126 MHz) spectra of compound **59**, CD₂Cl₂, 298 K.



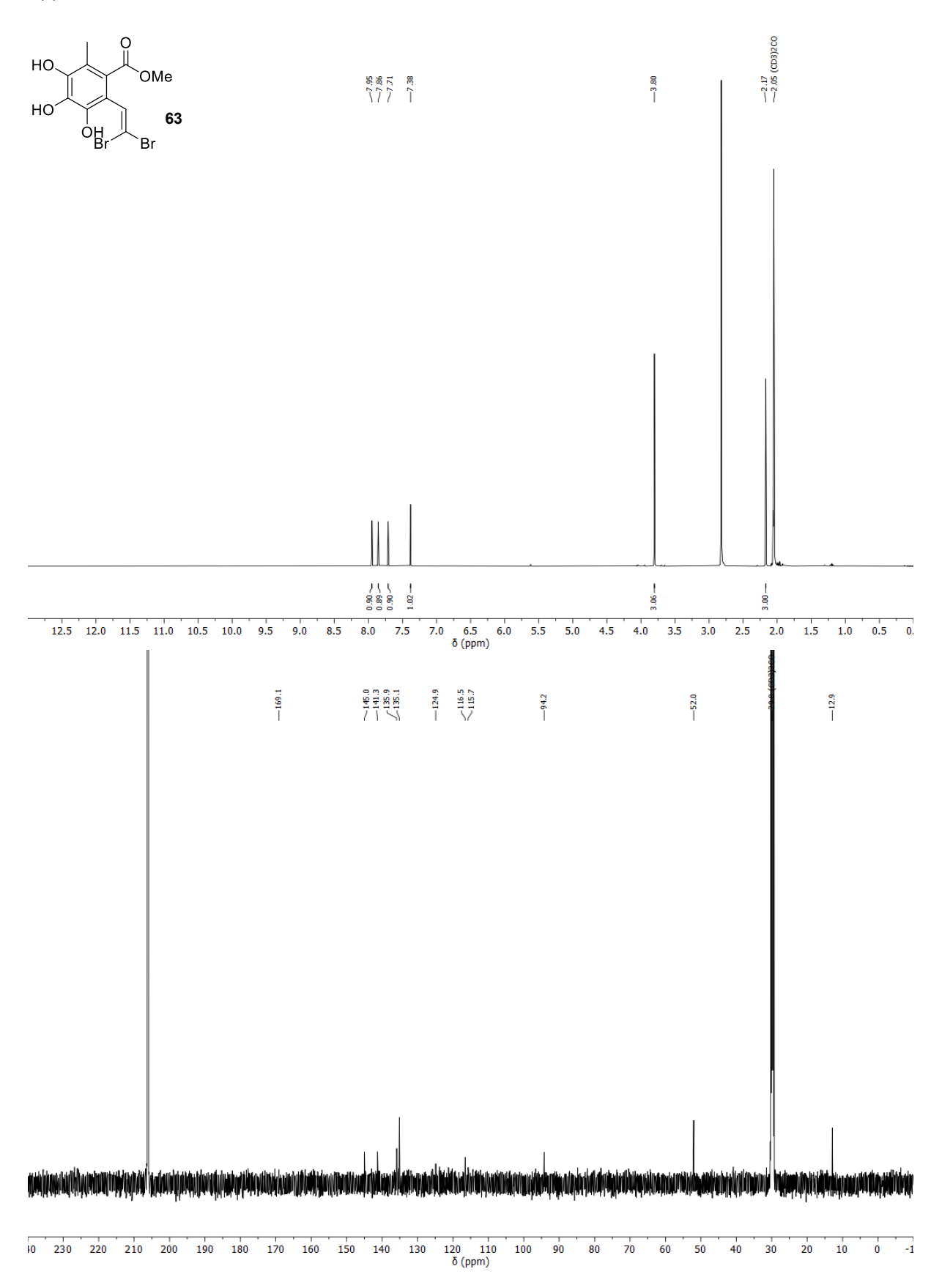
Appendix 6: ¹H- (top, 700 MHz) and ¹³C-NMR (bottom, 176 MHz) spectra of compound **60**, CD₂Cl₂, 298 K.



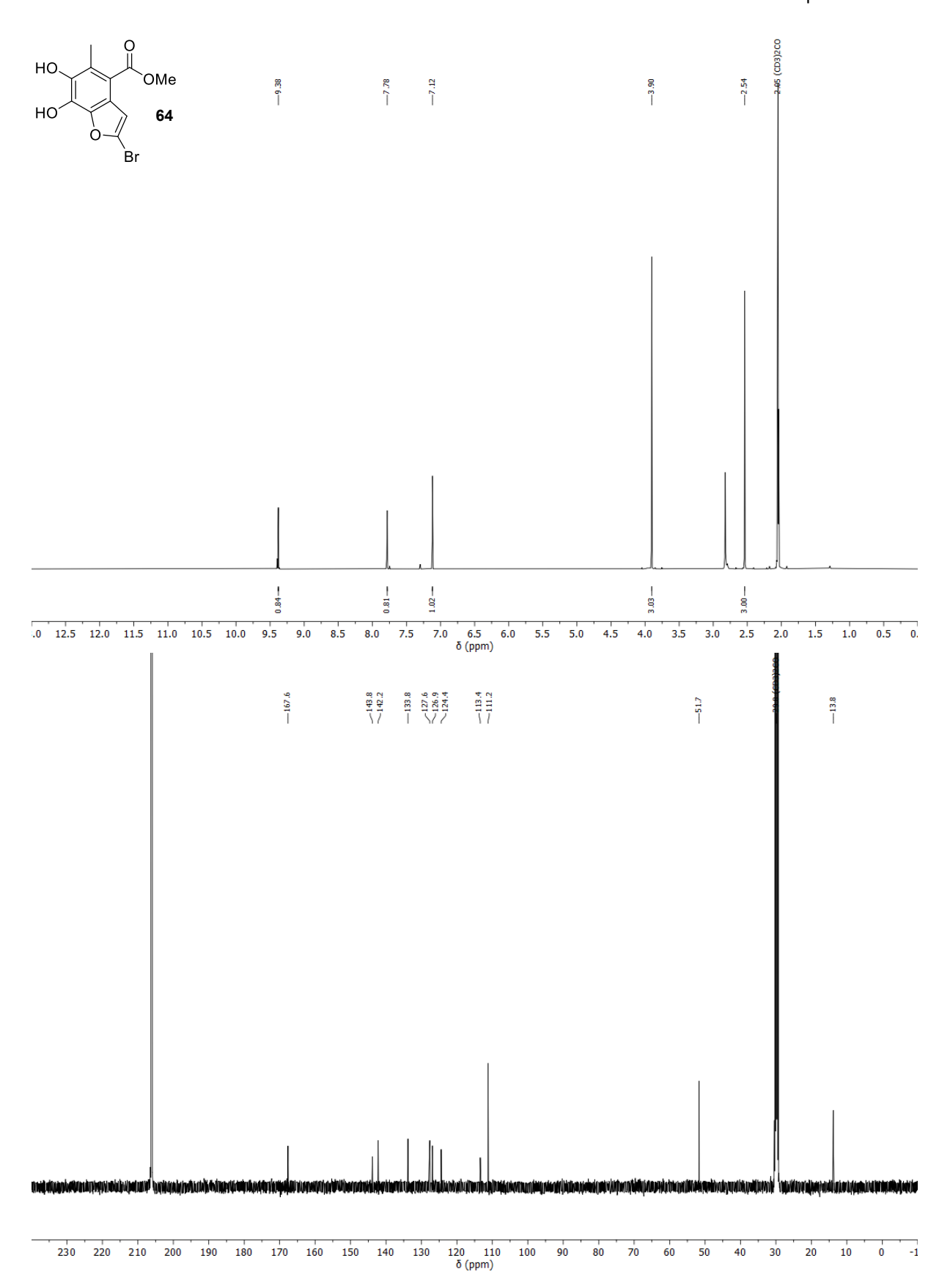
Appendix 7: ¹H- (top, 300 MHz) and ¹³C-NMR (bottom, 126 MHz) spectra of compound **61**, CD₂Cl₂, 298 K.



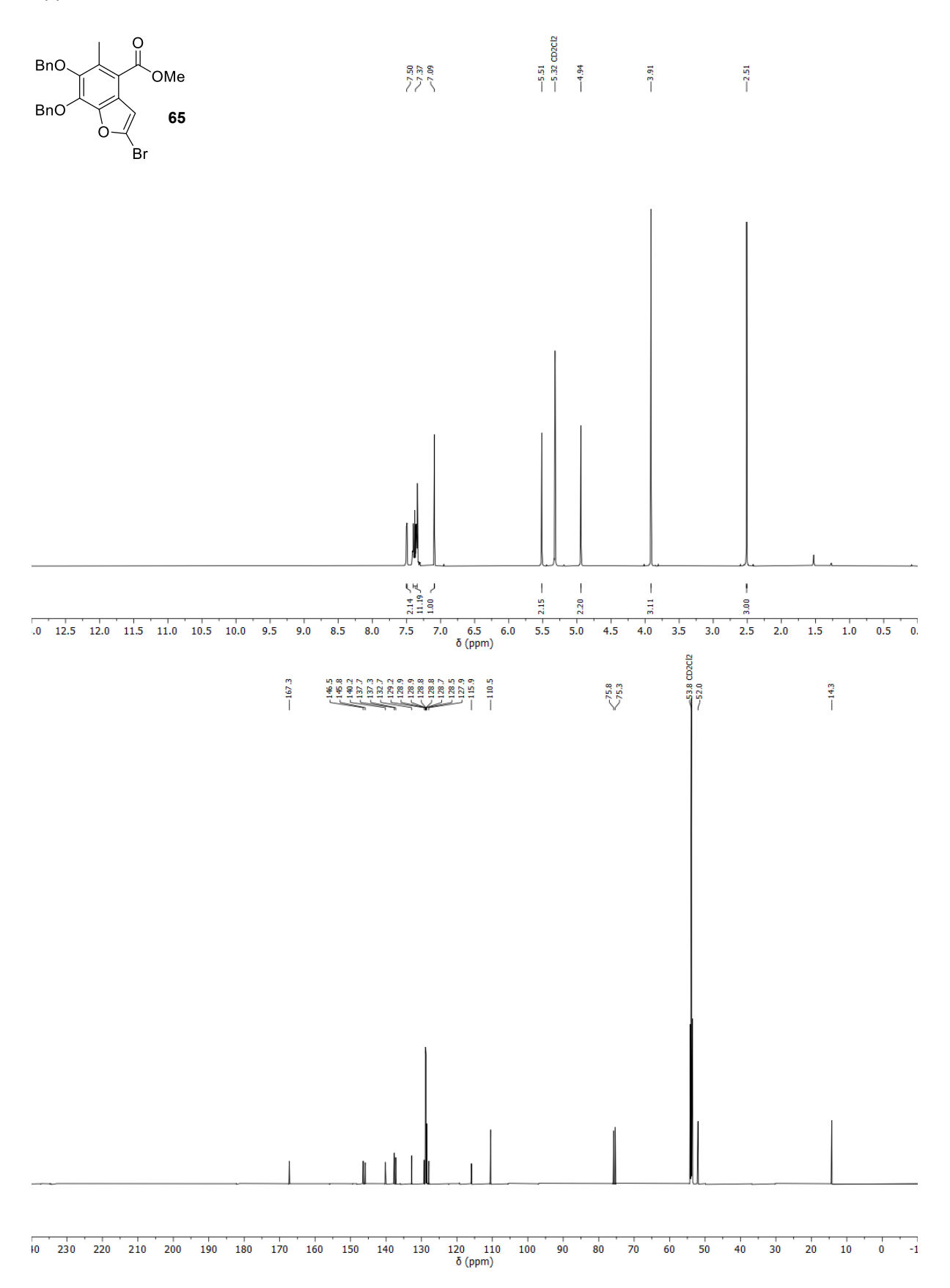
Appendix 8: ¹H- (top, 500 MHz) and ¹³C-NMR (bottom, 126 MHz) spectra of compound **62**, CD₂Cl₂, 298 K.



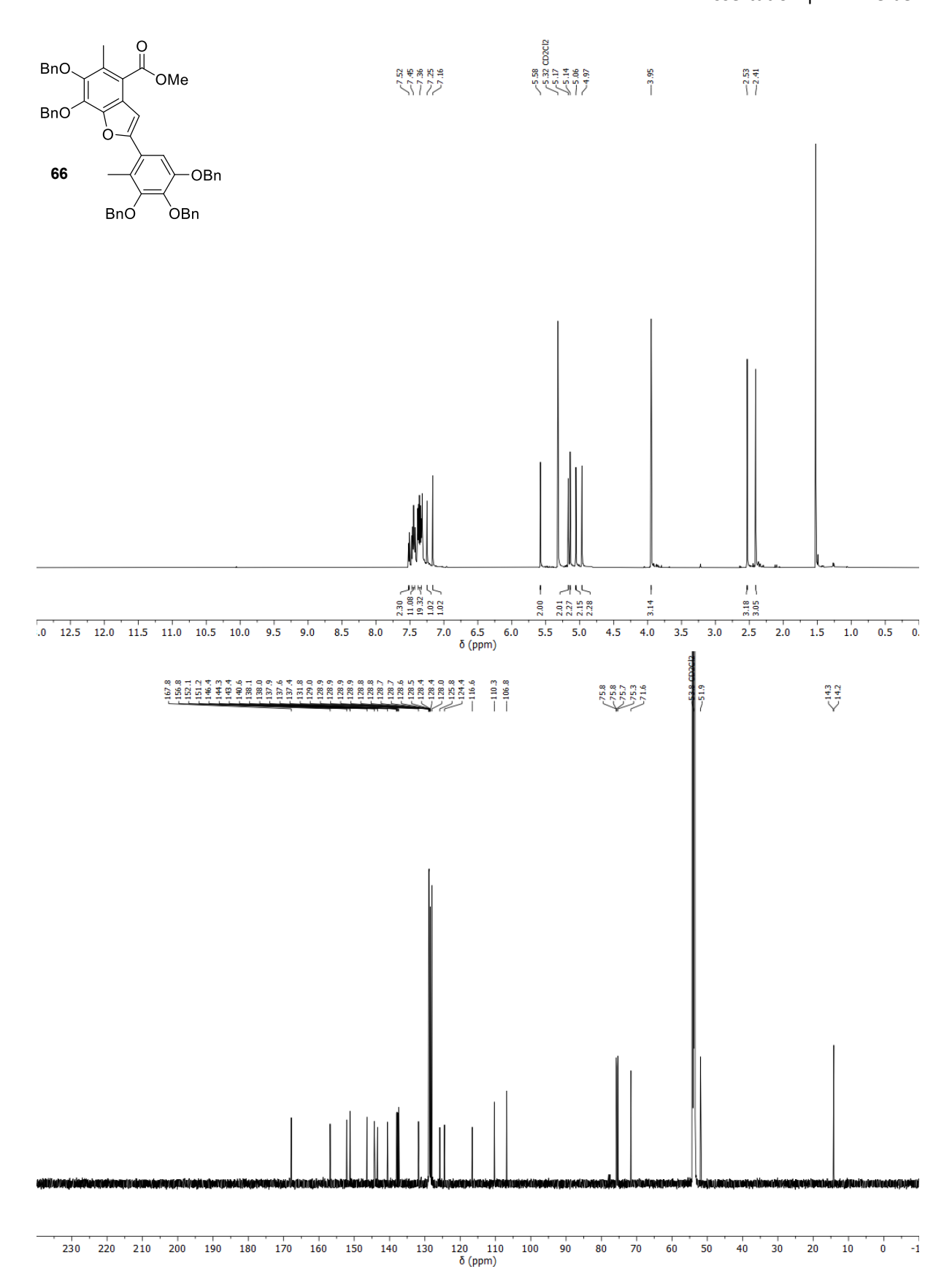
Appendix 9: ¹H- (top, 500 MHz) and ¹³C-NMR (bottom, 126 MHz) spectra of compound **63**, acetone-d6, 298 K.



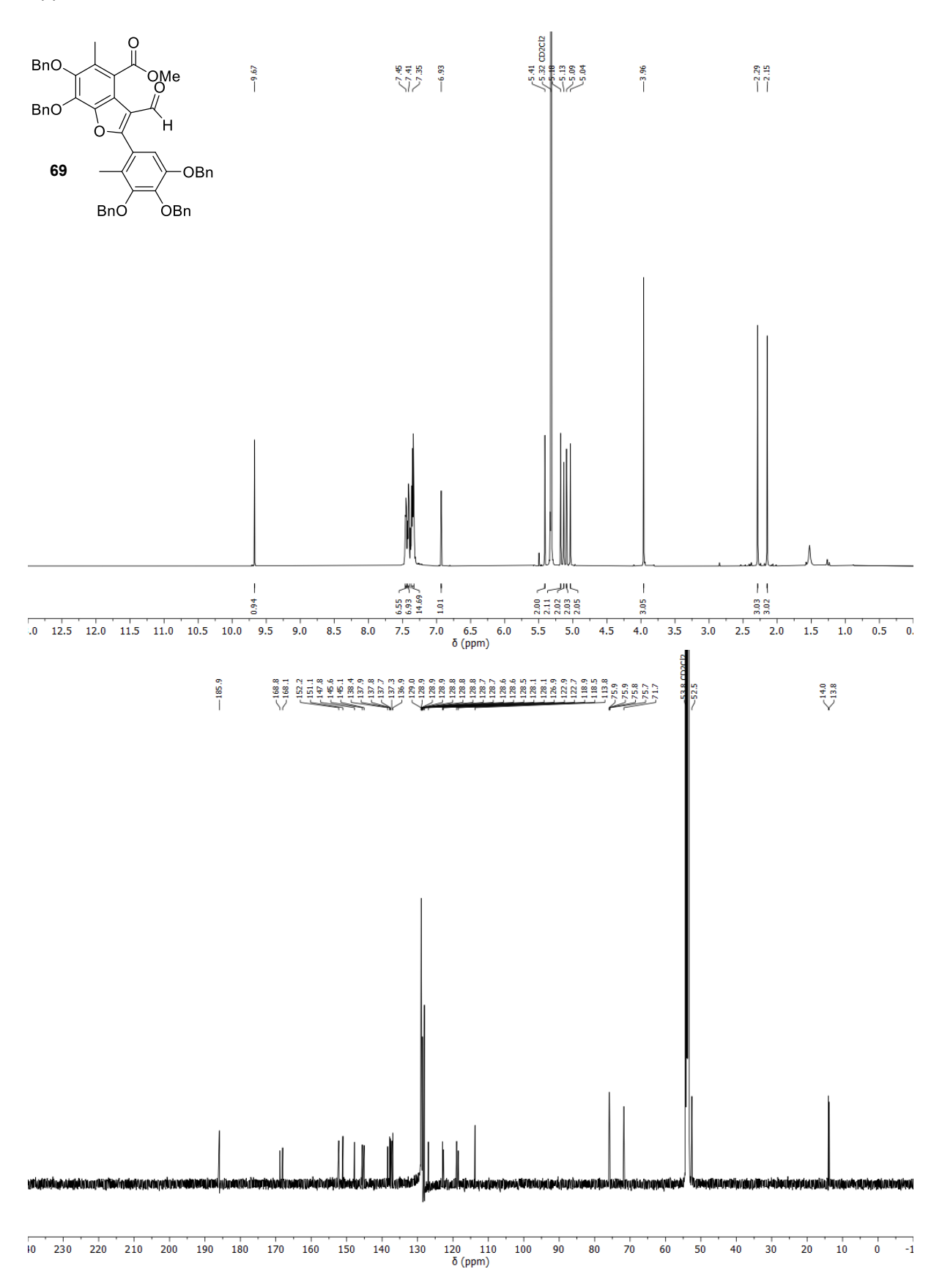
Appendix 10: ¹H- (top, 500 MHz) and ¹³C-NMR (bottom, 126 MHz) spectra of compound **64**, acetone-d6, 298 K.



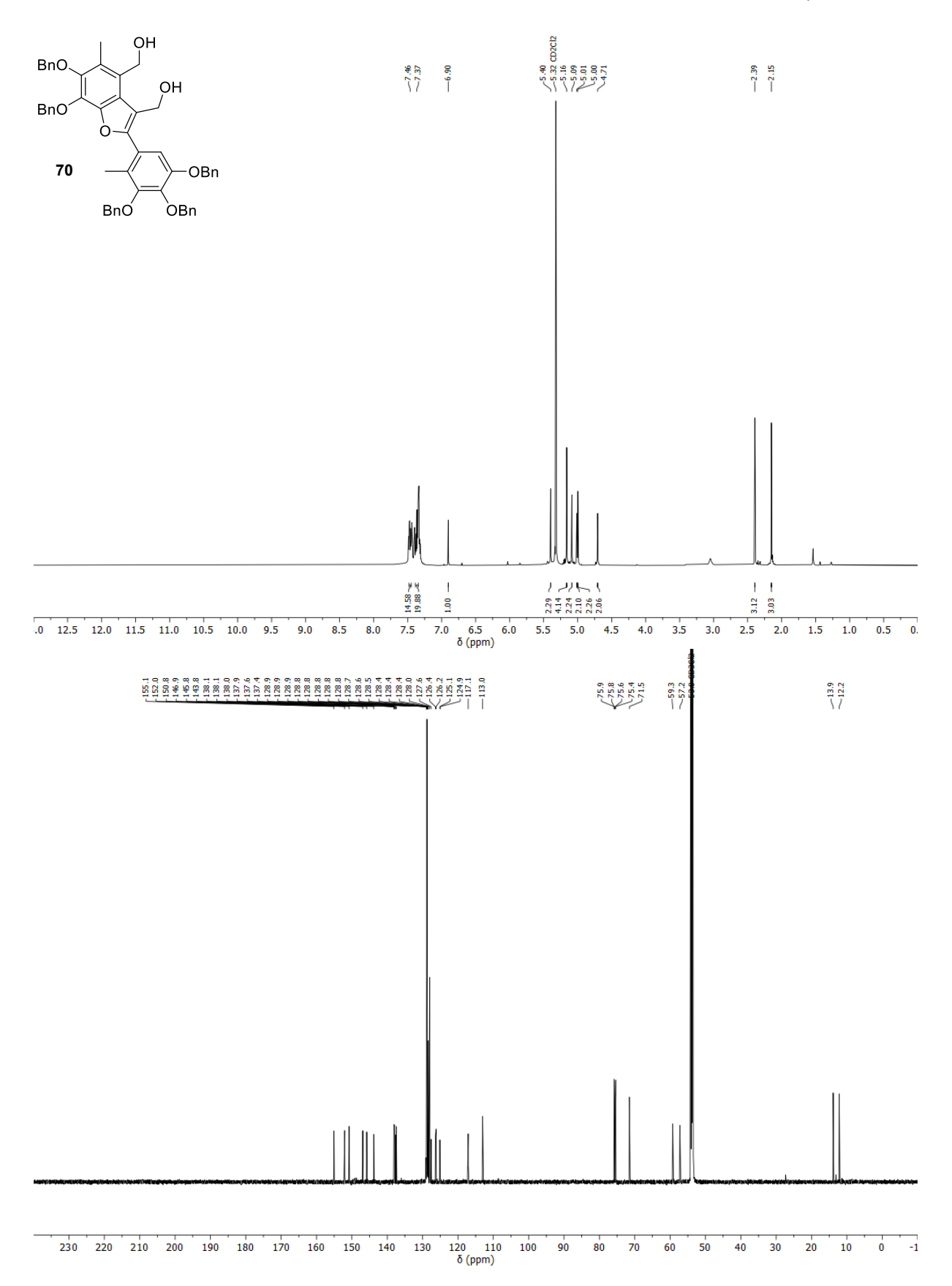
Appendix 11: ¹H- (top, 700 MHz) and ¹³C-NMR (bottom, 176 MHz) spectra of compound **65**, CD₂Cl₂, 298 K.



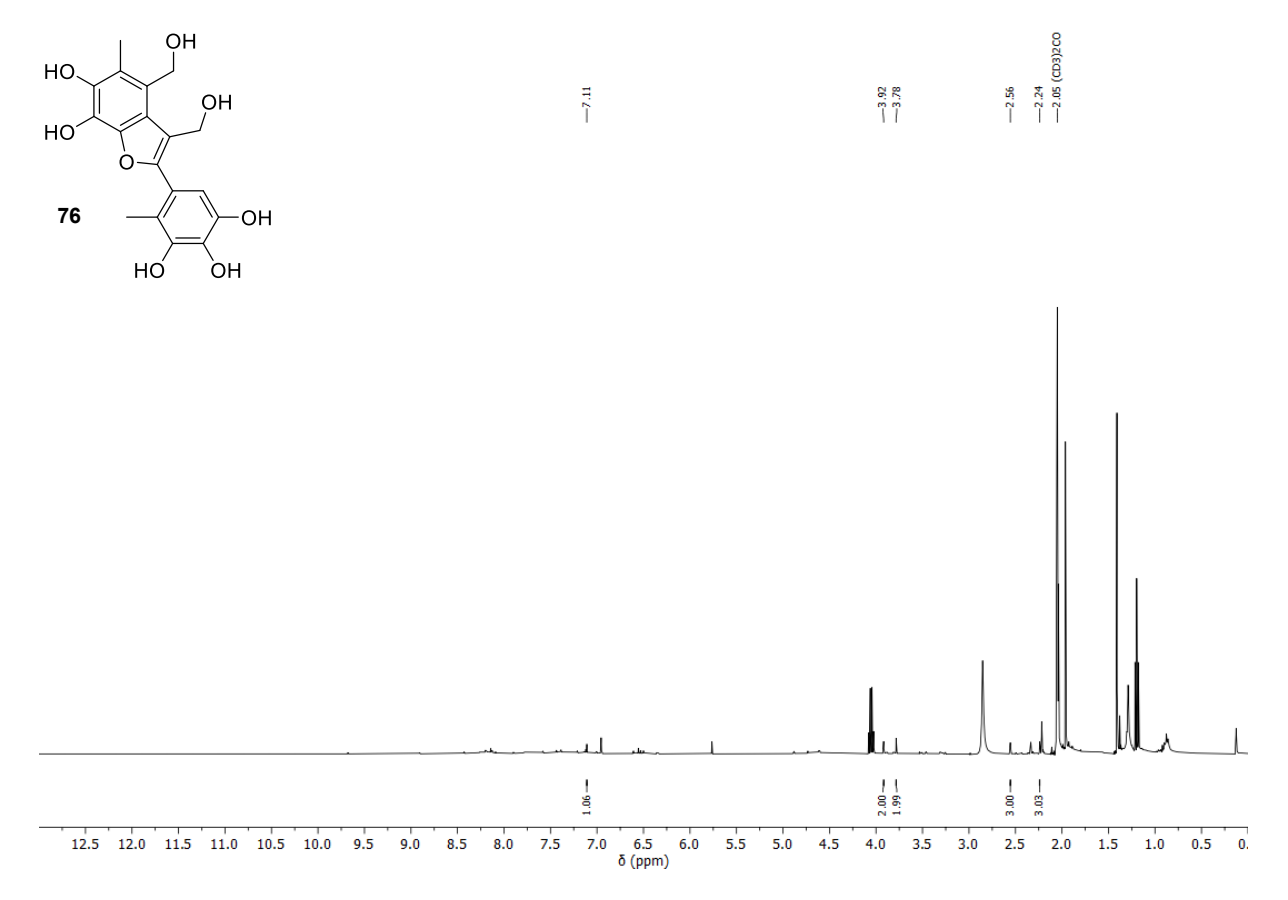
Appendix 12: ¹H- (top, 700 MHz) and ¹³C-NMR (bottom, 176 MHz) spectra of compound **66**, CD₂Cl₂, 298 K.



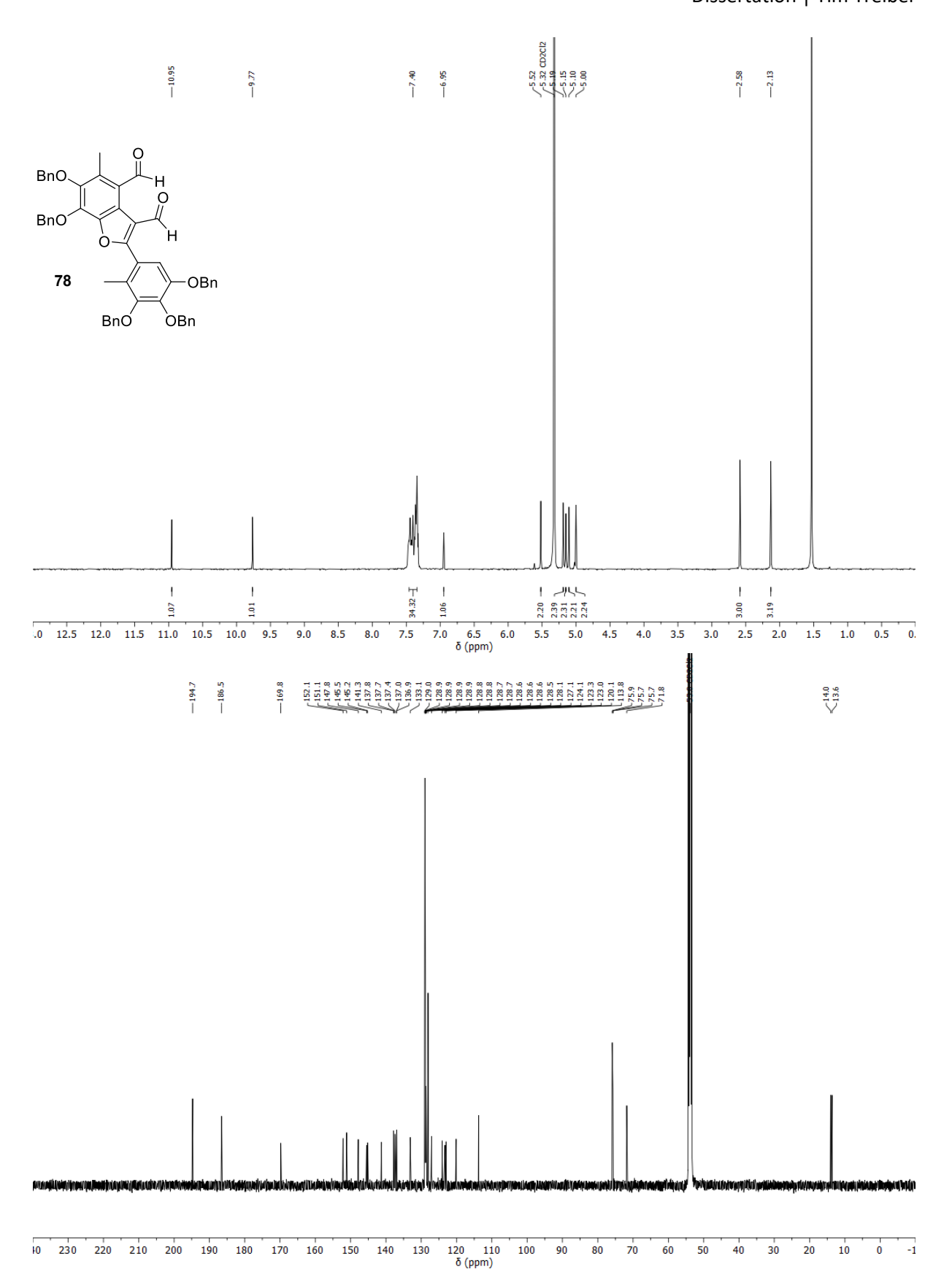
Appendix 13: ¹H- (top, 500 MHz) and ¹³C-NMR (bottom, 126 MHz) spectra of compound **69**, CD₂Cl₂, 298 K.



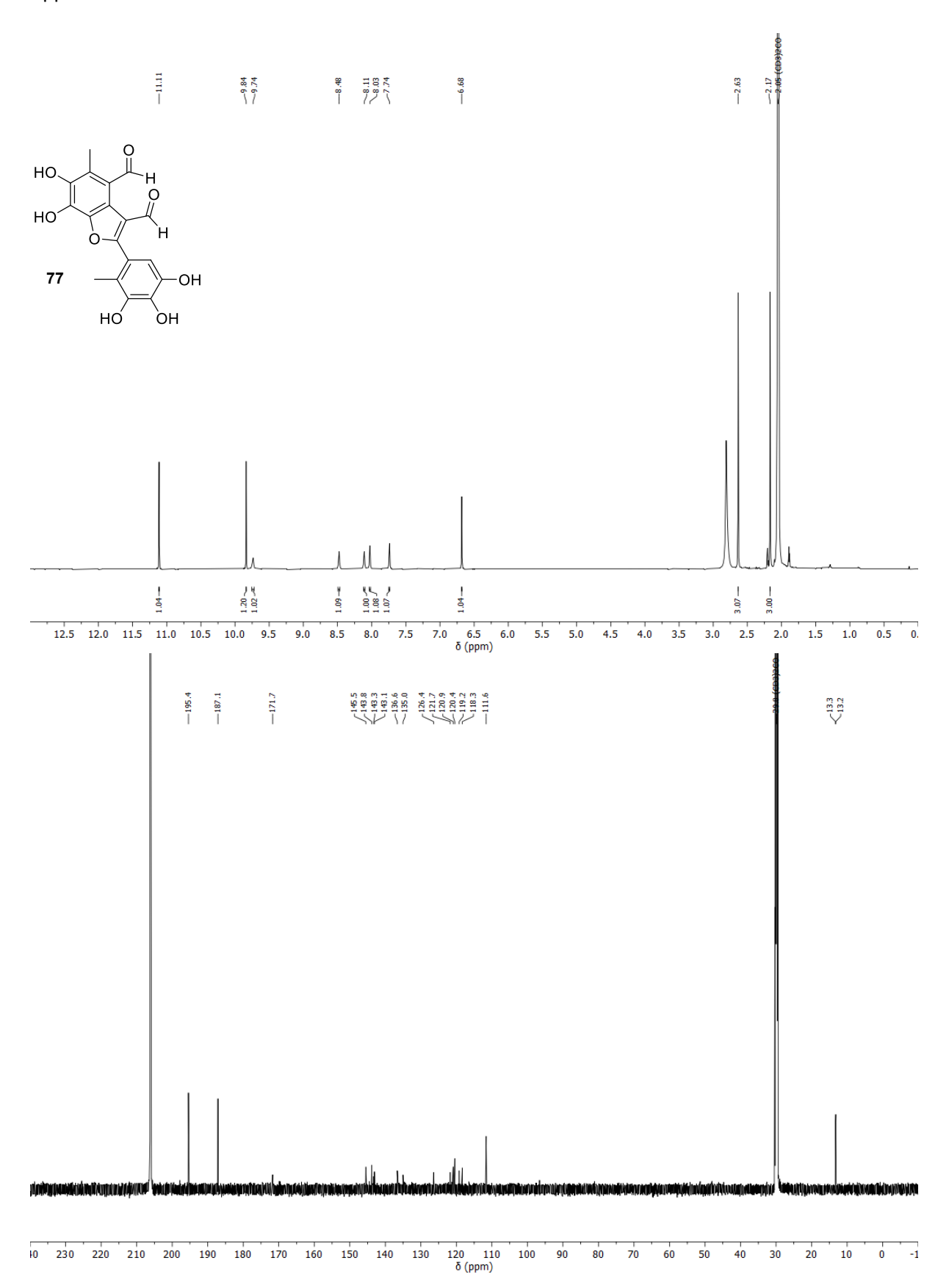
Appendix 14: ¹H- (top, 700 MHz) and ¹³C-NMR (bottom, 176 MHz) spectra of compound **70**, CD₂Cl₂, 298 K.



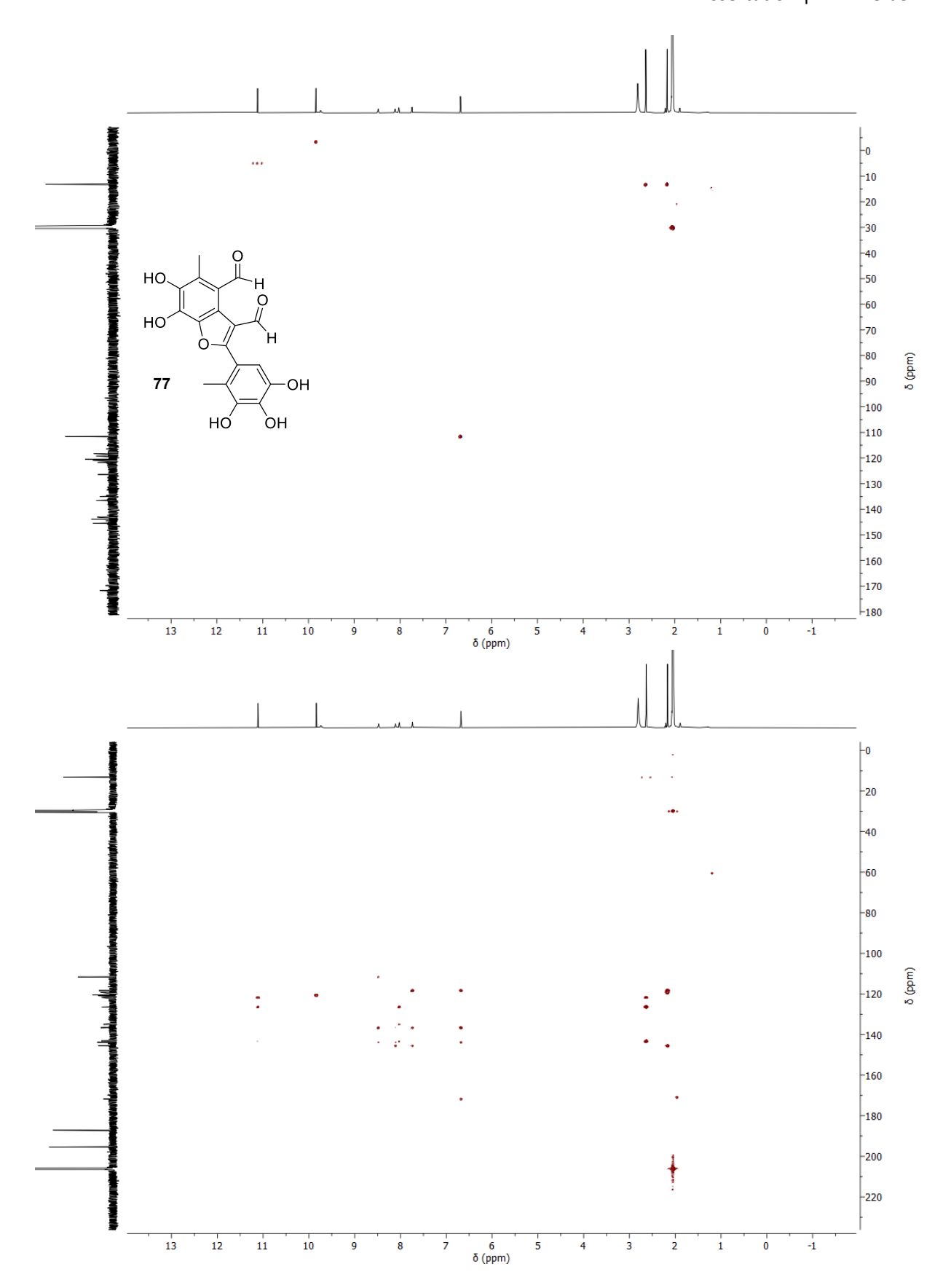
Appendix 15: $^1\text{H-NMR}$ (400 MHz) spectrum of compound **76**, CD₂Cl₂, 298 K.



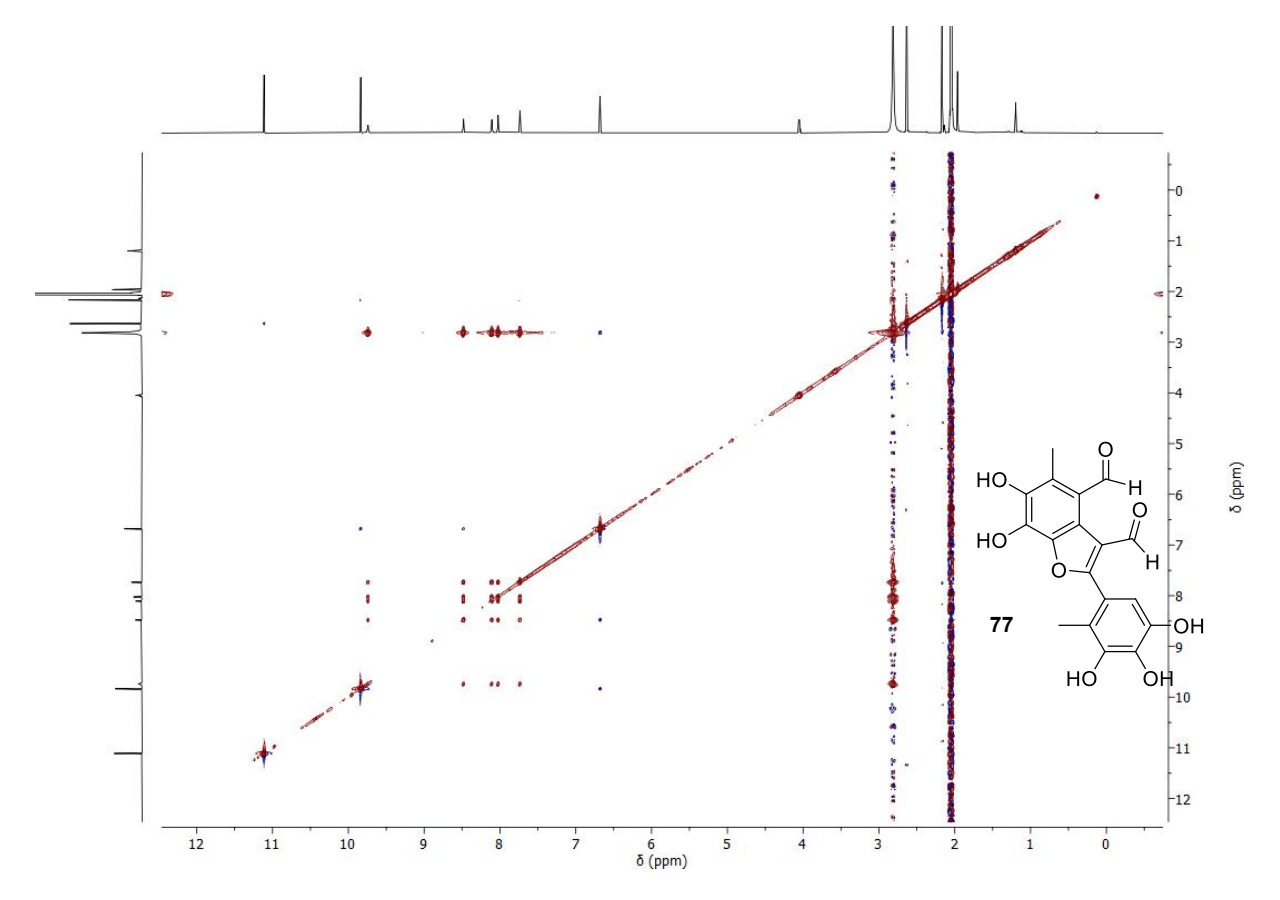
Appendix 16: ¹H- (top, 300 MHz) and ¹³C-NMR (bottom, 126 MHz) spectra of compound **78**, CD₂Cl₂, 298 K.



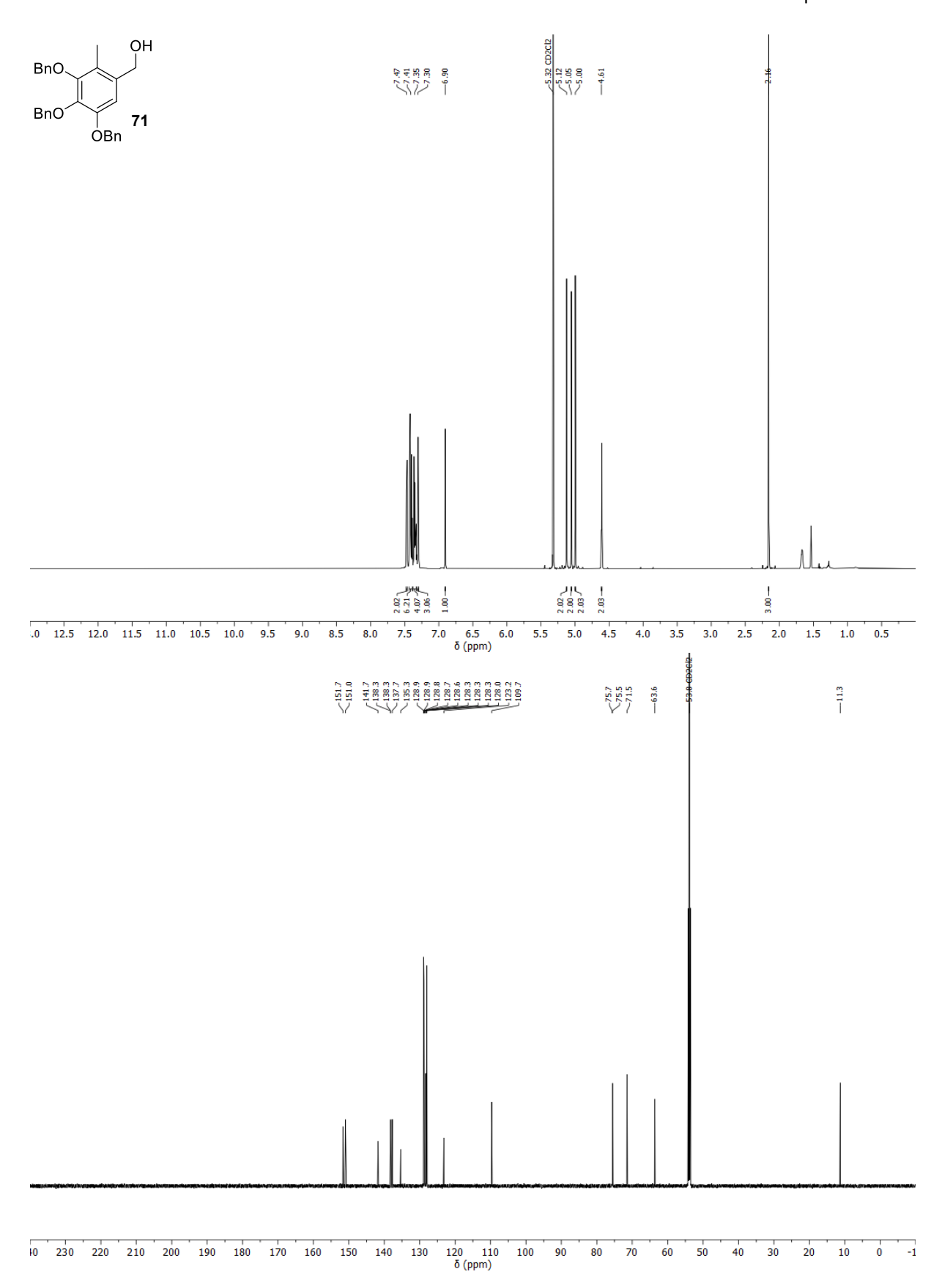
Appendix 17: ¹H- (top, 400 MHz) and ¹³C-NMR (bottom, 176 MHz) spectra of compound **77**, acetone-d6, 298 K.



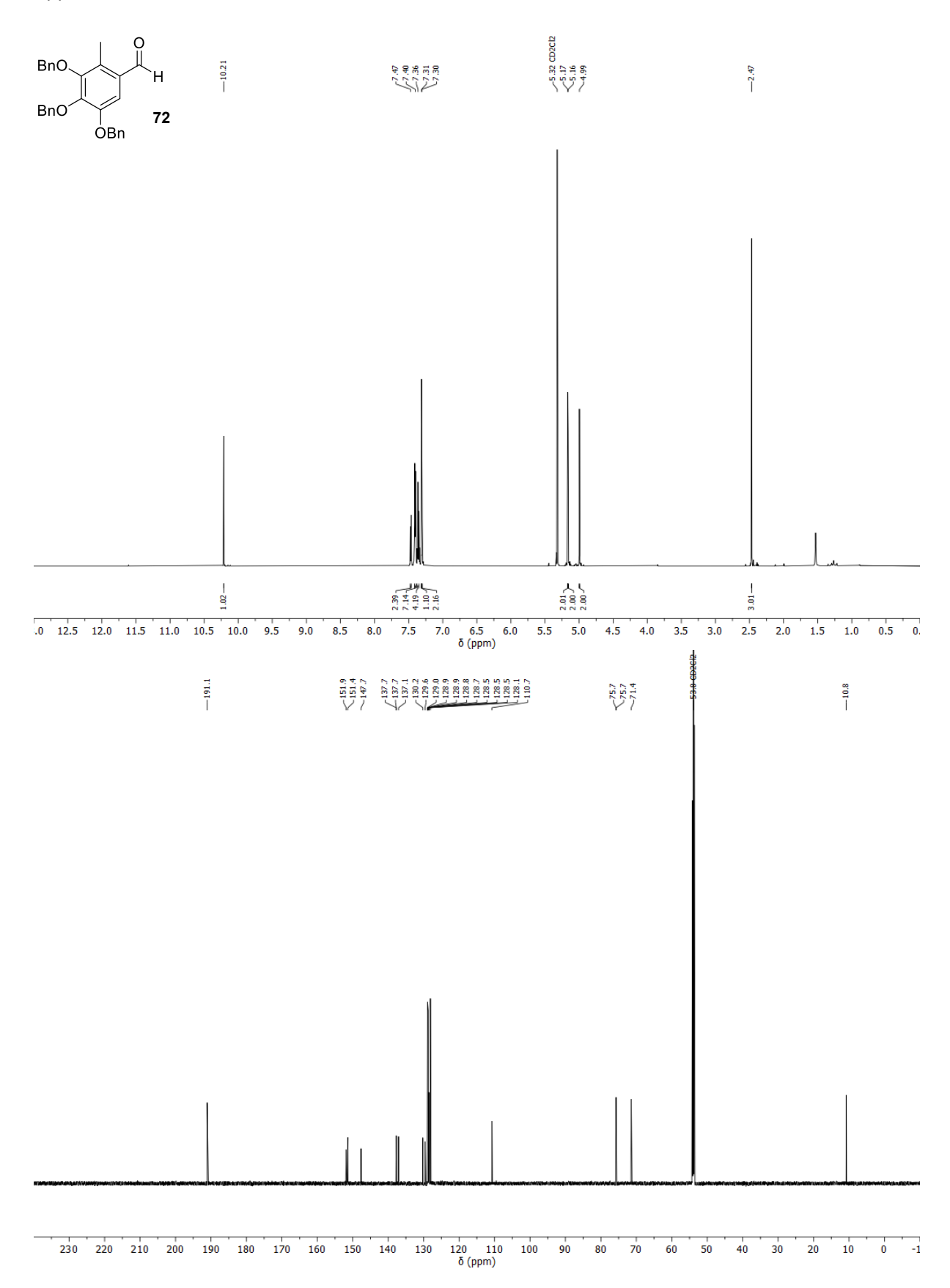
Appendix 18: HSQC- (top, 700, 176 MHz) and HMBC-NMR (bottom, 700, 176 MHz) spectra of compound **77**, acetone-d6, 298 K.



Appendix 19: NOESY-NMR (700, 700 MHz) spectrum of compound 77, acetone-d6, 298 K.

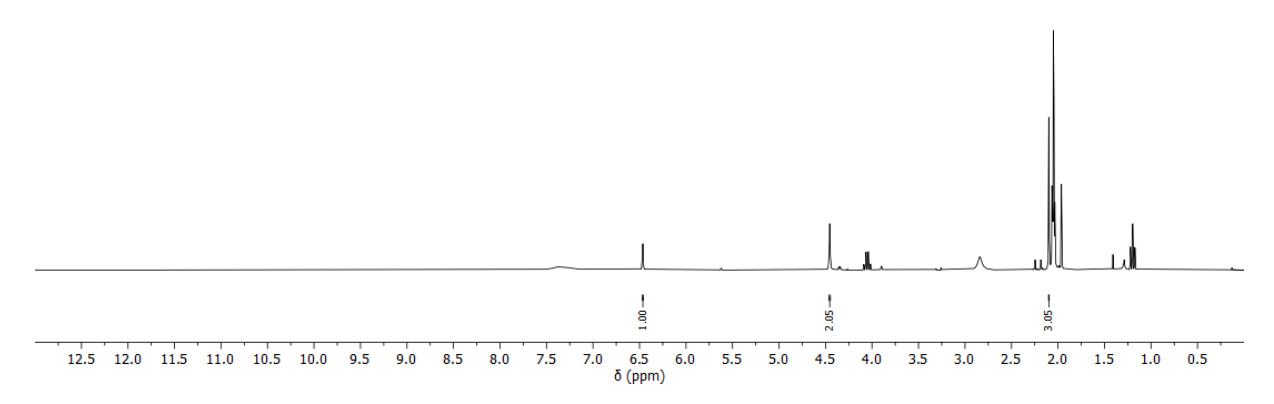


Appendix 20: ¹H- (top, 700 MHz) and ¹³C-NMR (bottom, 176 MHz) spectra of compound **71**, CD₂Cl₂, 298 K.



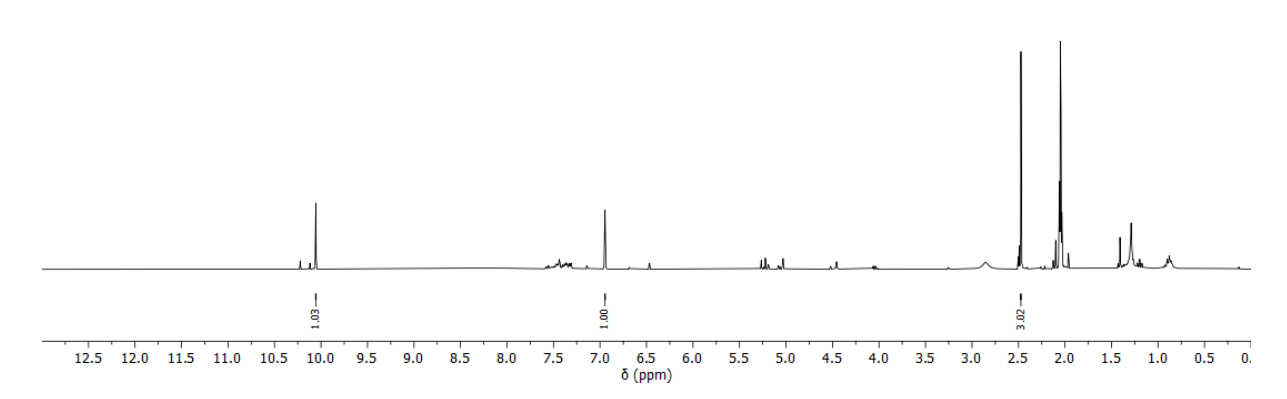
Appendix 21: ¹H- (top, 700 MHz) and ¹³C-NMR (bottom, 176 MHz) spectra of compound **72**, CD₂Cl₂, 298 K.



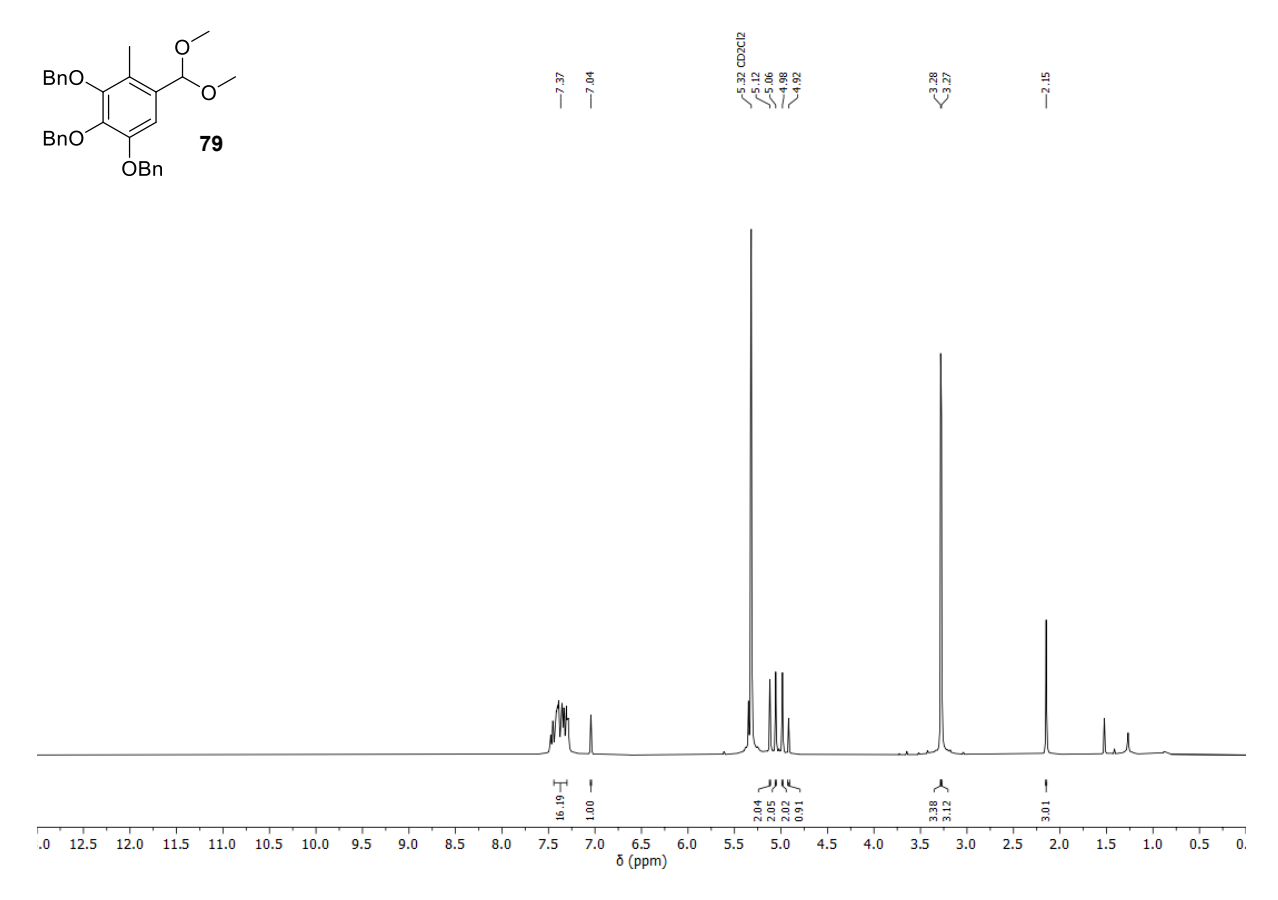


Appendix 22: ¹H-NMR (300 MHz) spectrum of compound **74**, acetone-d6, 298 K.



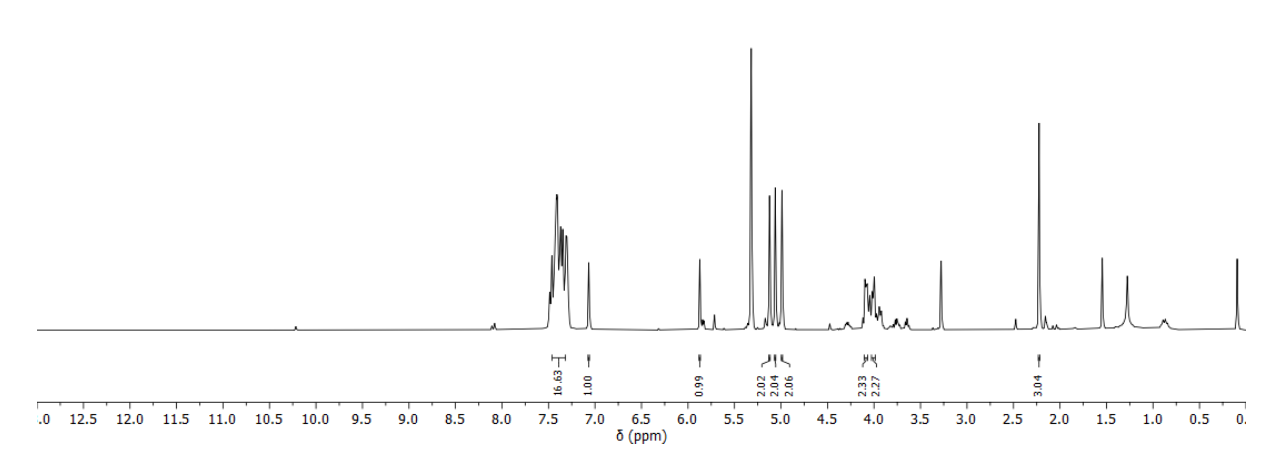


Appendix 23: ¹H-NMR (300 MHz) spectrum of compound **75**, acetone-d6, 298 K.

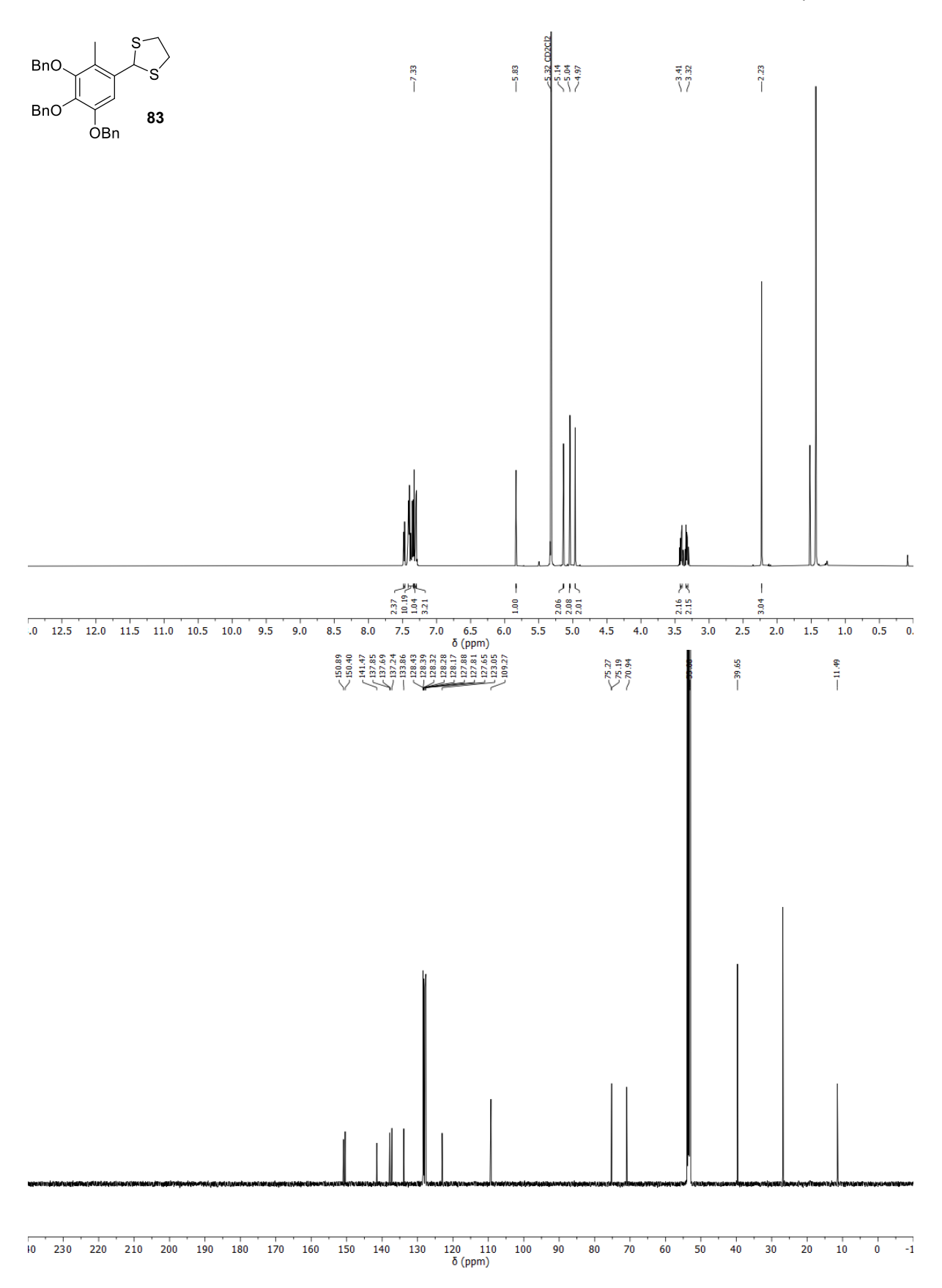


Appendix 24: ¹H-NMR (300 MHz) spectrum of compound **79**, CD₂Cl₂, 298 K.





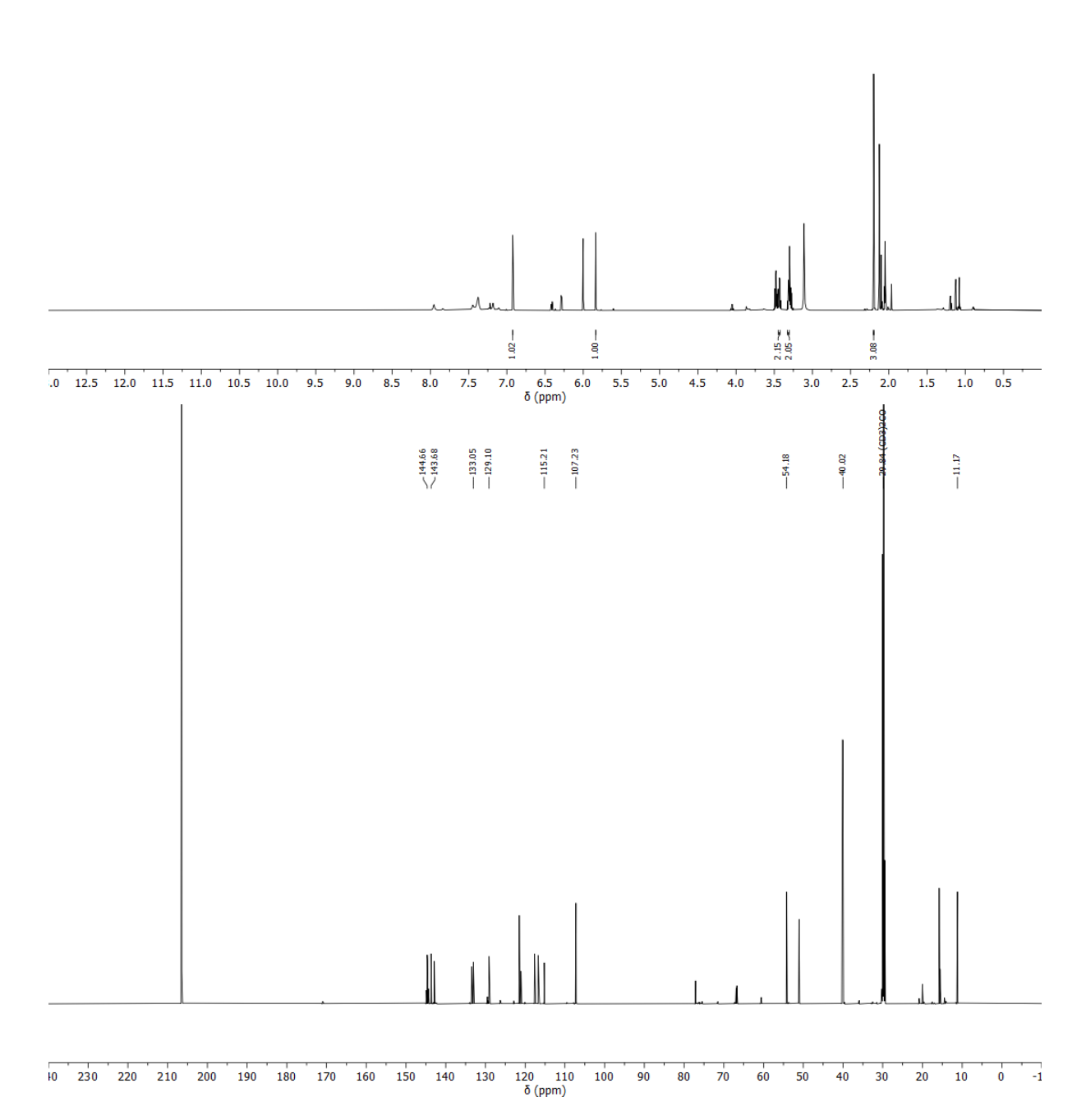
Appendix 25: ¹H-NMR (300 MHz) spectrum of compound **81**, CD₂Cl₂, 298 K.



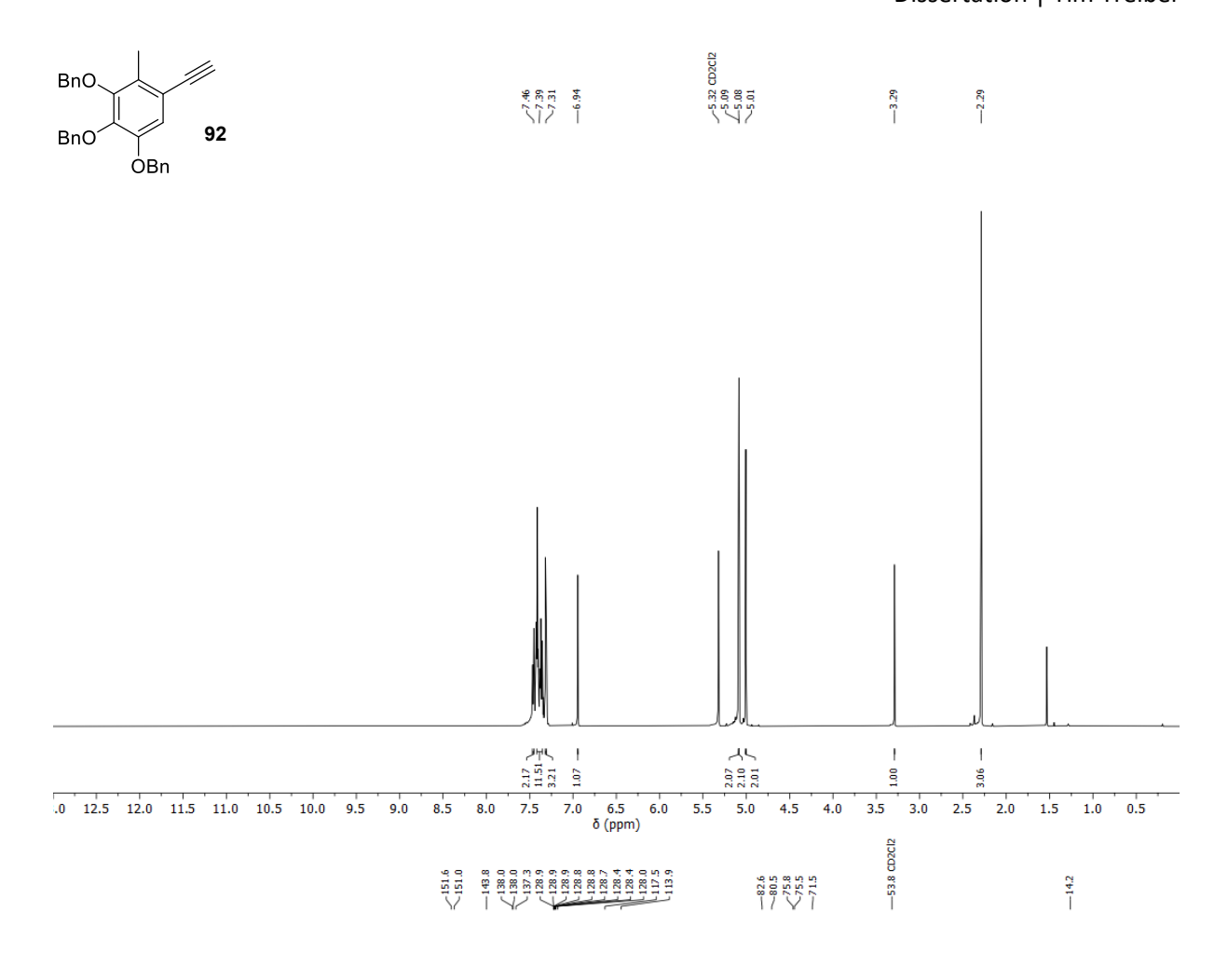
Appendix 26: ¹H- (top, 500 MHz) and ¹³C-NMR (bottom, 126 MHz) spectra of compound **83**, CD₂Cl₂, 298 K.

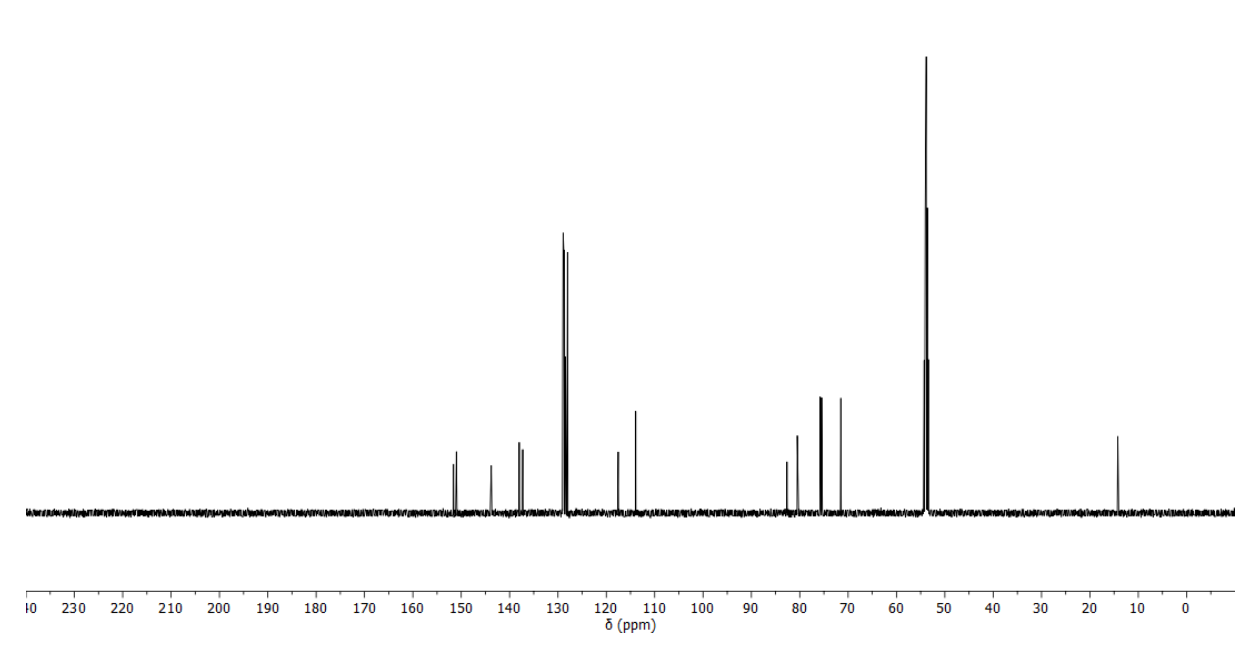




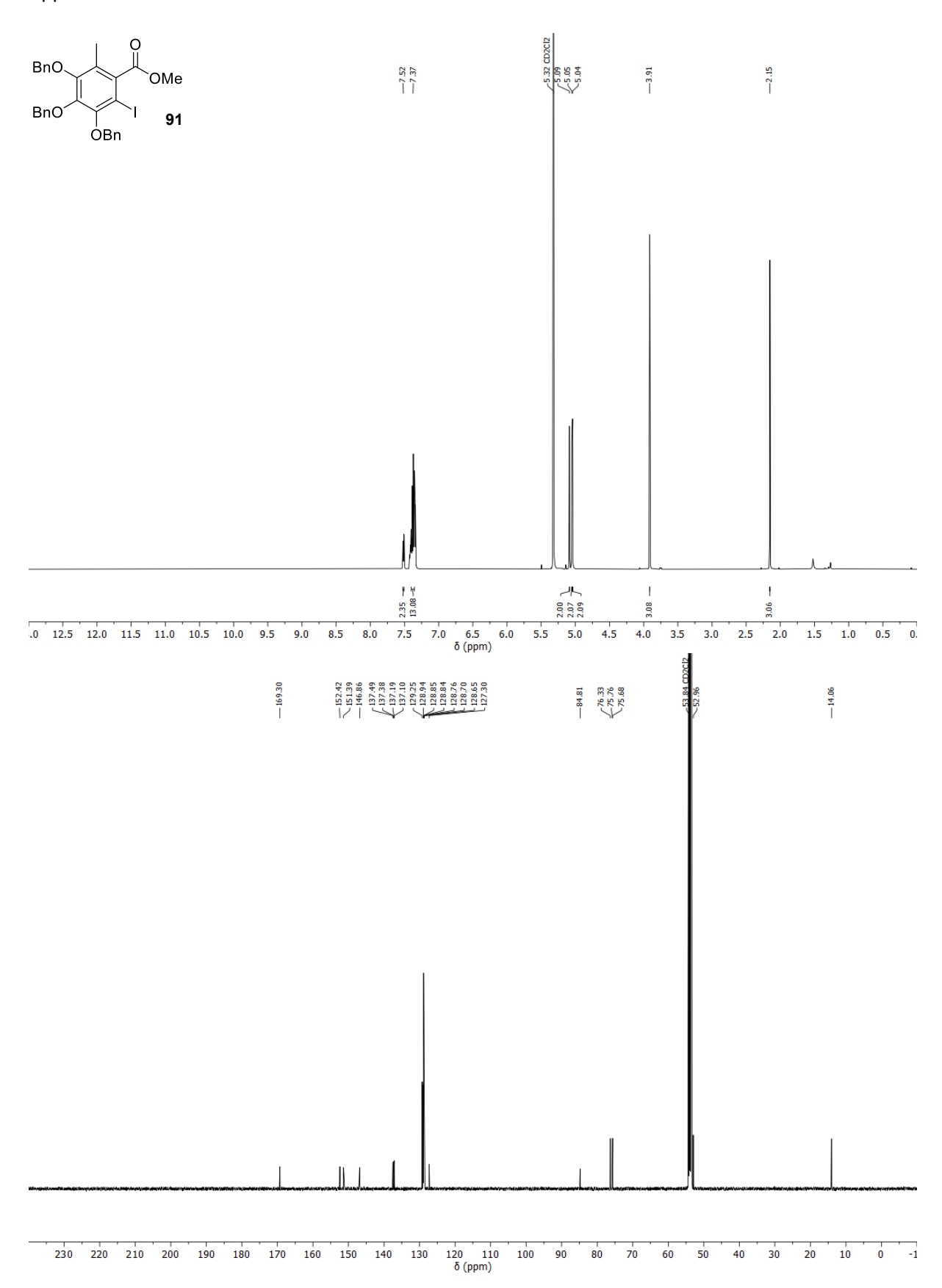


Appendix 27: ¹H- (top, 700 MHz) and ¹³C-NMR (bottom, 176 MHz) spectra of compound **84**, acetone-d6, 298 K.

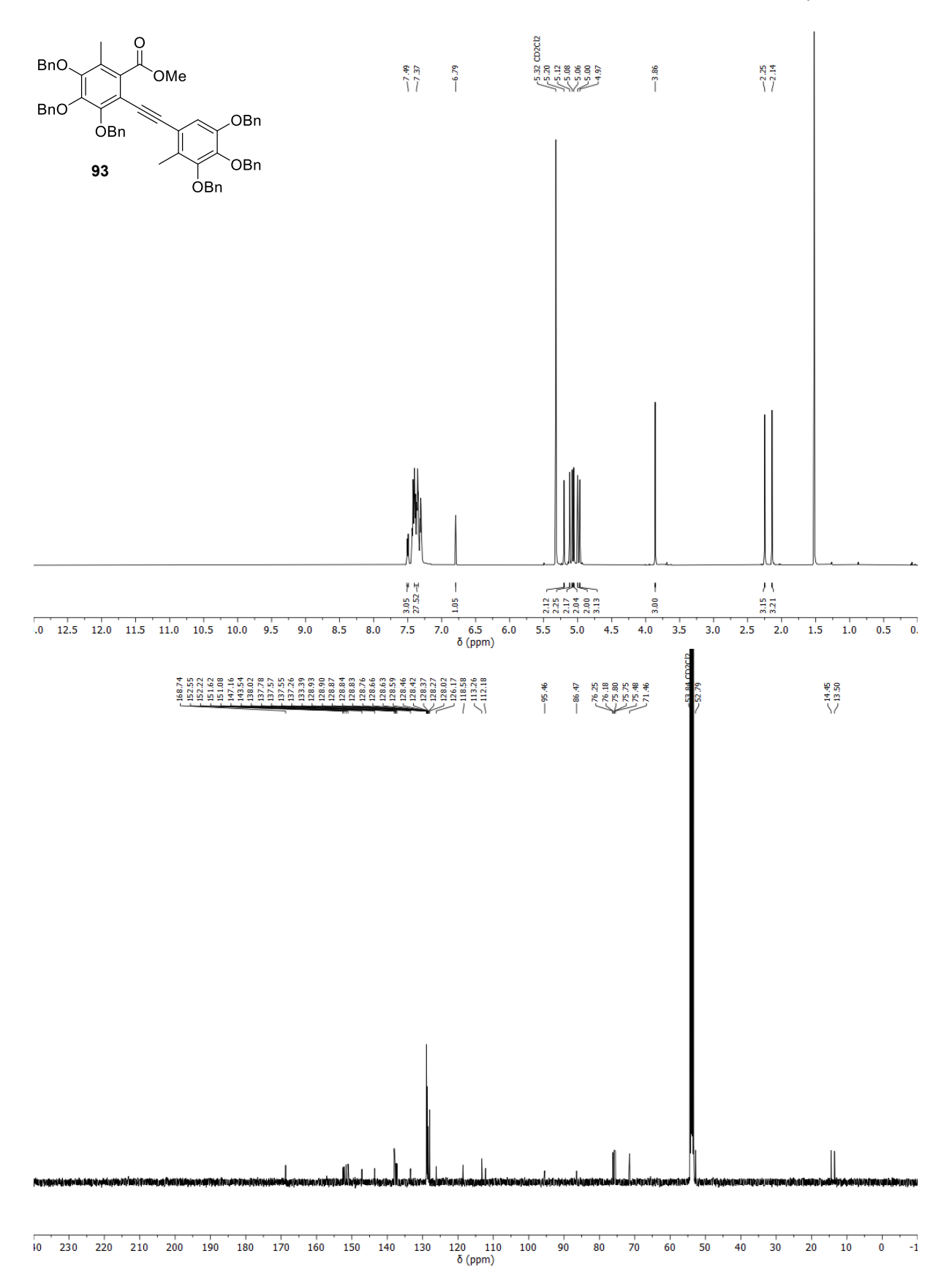




Appendix 28: ¹H- (top, 500 MHz) and ¹³C-NMR (bottom, 126 MHz) spectra of compound **92**, CD₂Cl₂, 298 K.

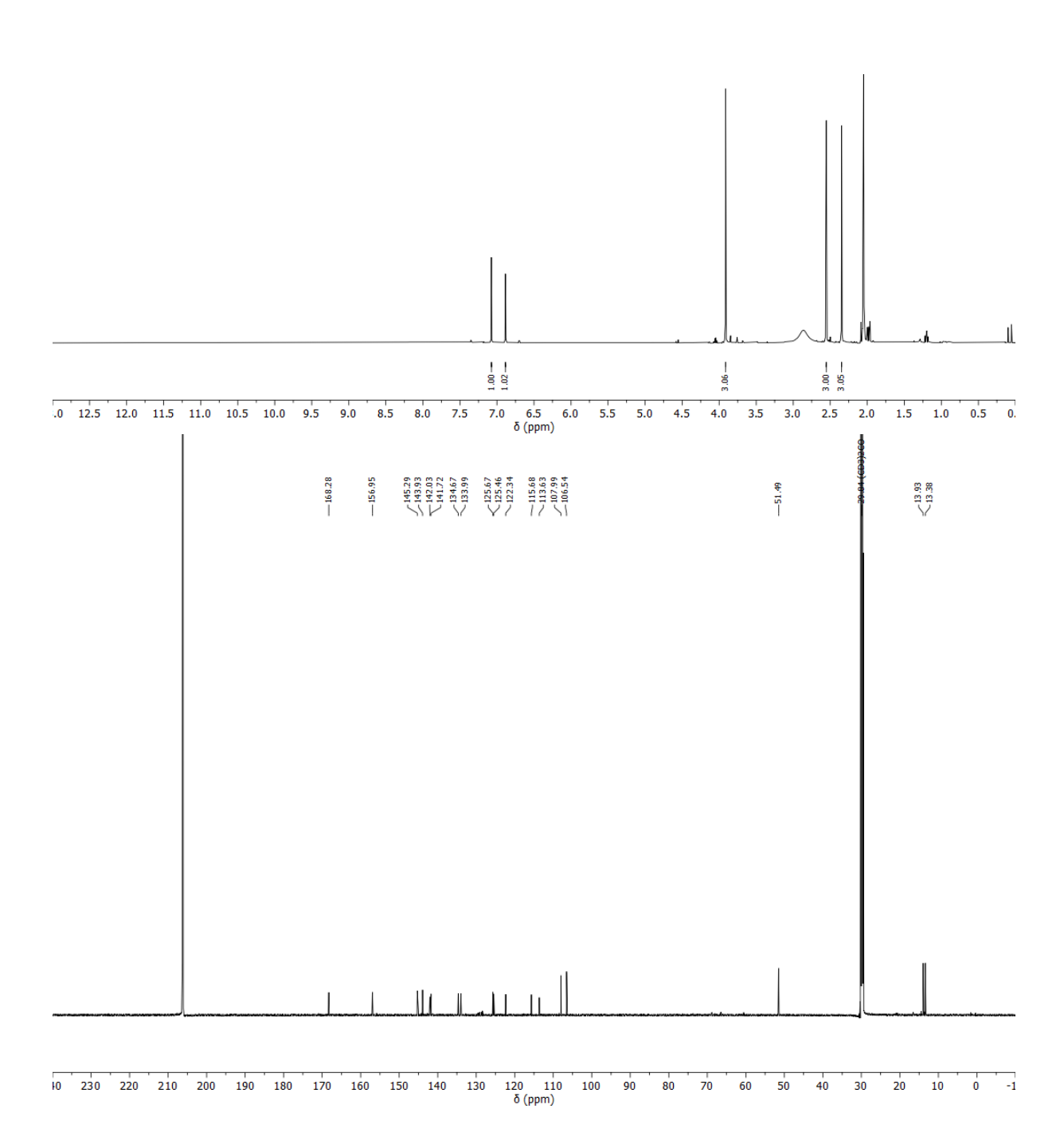


Appendix 29: ¹H- (top, 500 MHz) and ¹³C-NMR (bottom, 126 MHz) spectra of compound **91**, CD₂Cl₂, 298 K.

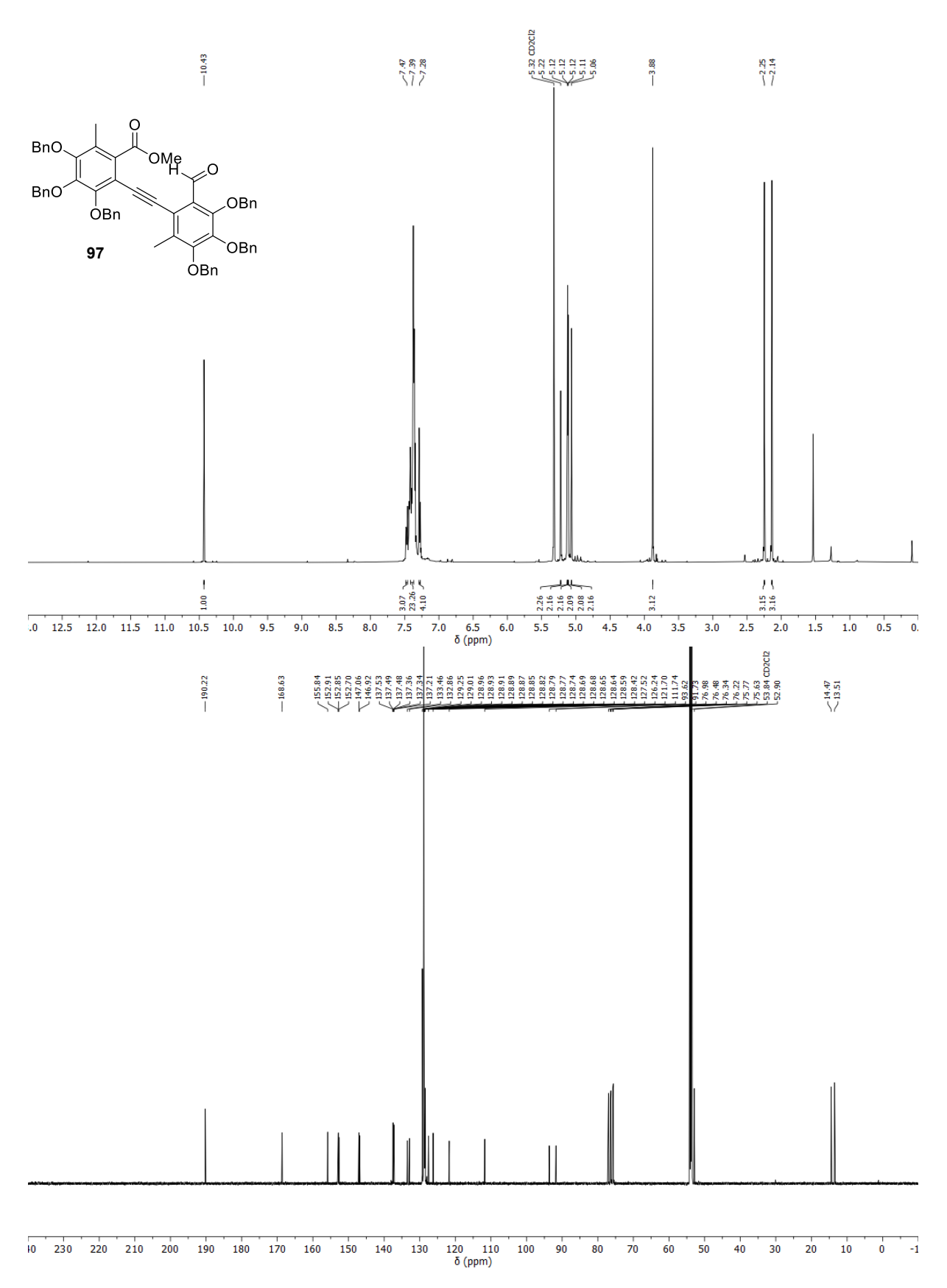


Appendix 30: ¹H- (top, 500 MHz) and ¹³C-NMR (bottom, 126 MHz) spectra of compound **93**, CD₂Cl₂, 298 K.

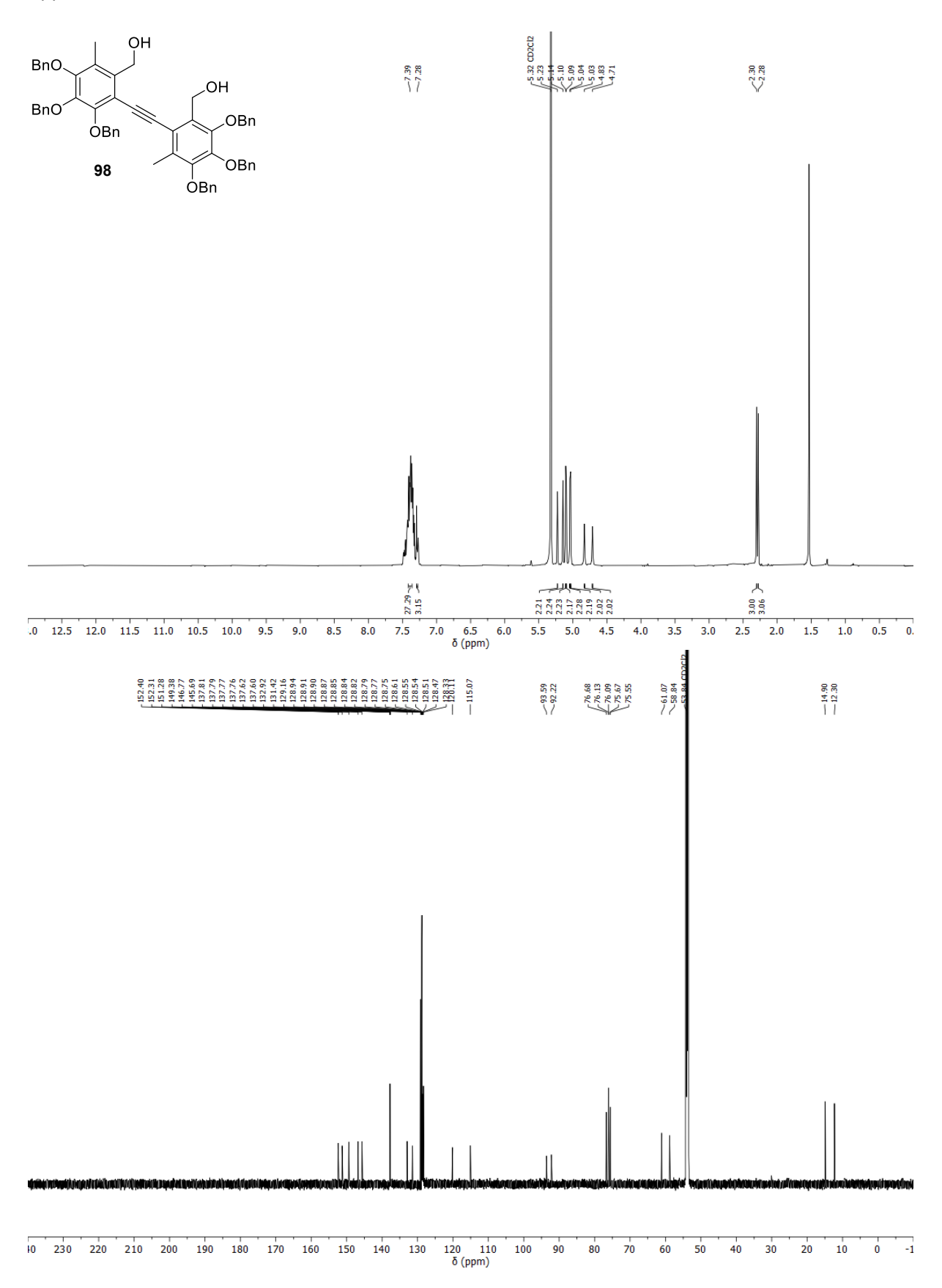




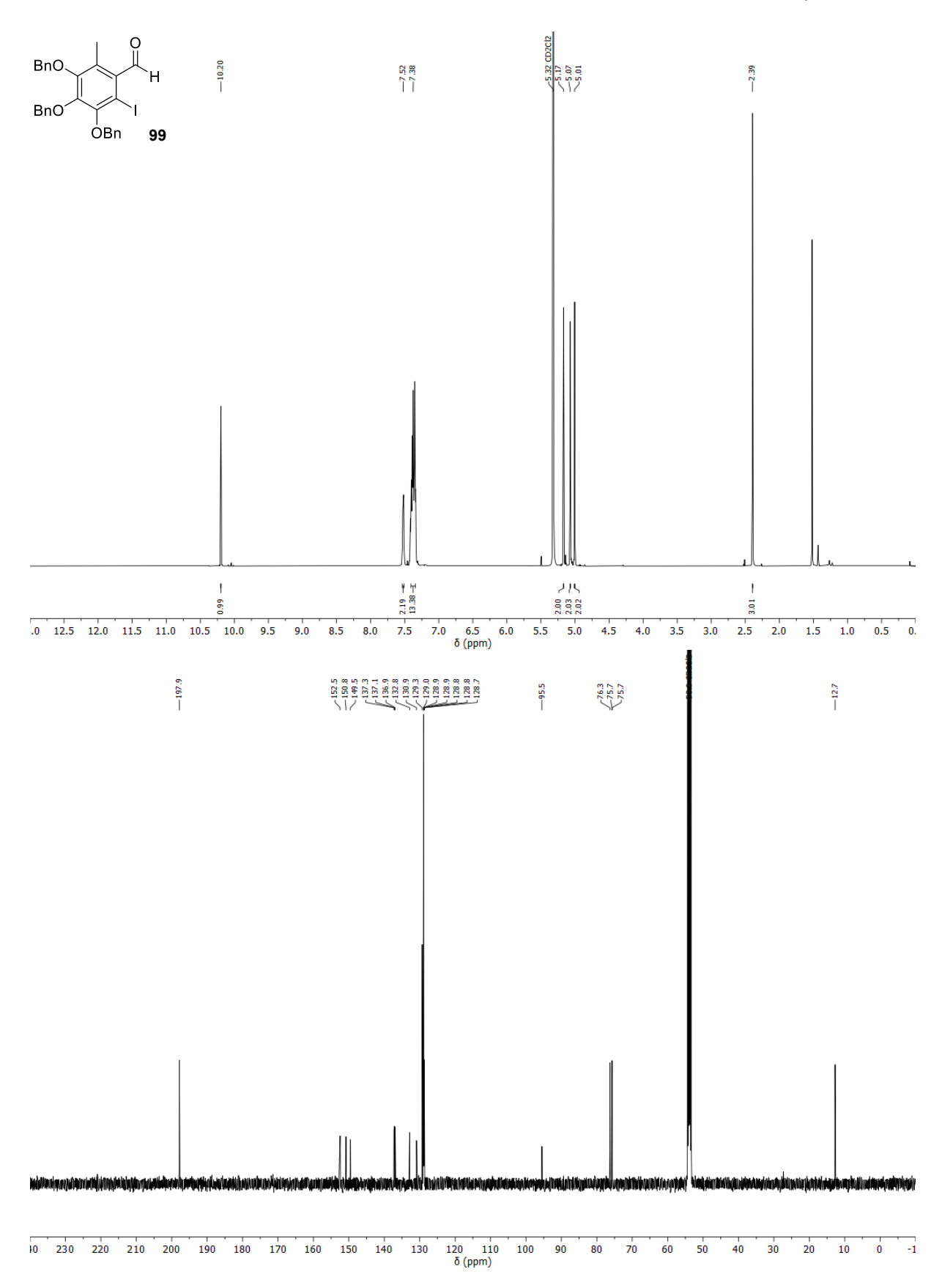
Appendix 31: ¹H- (top, 500 MHz) and ¹³C-NMR (bottom, 176 MHz) spectra of compound **95**, acetone-d6, 298 K.



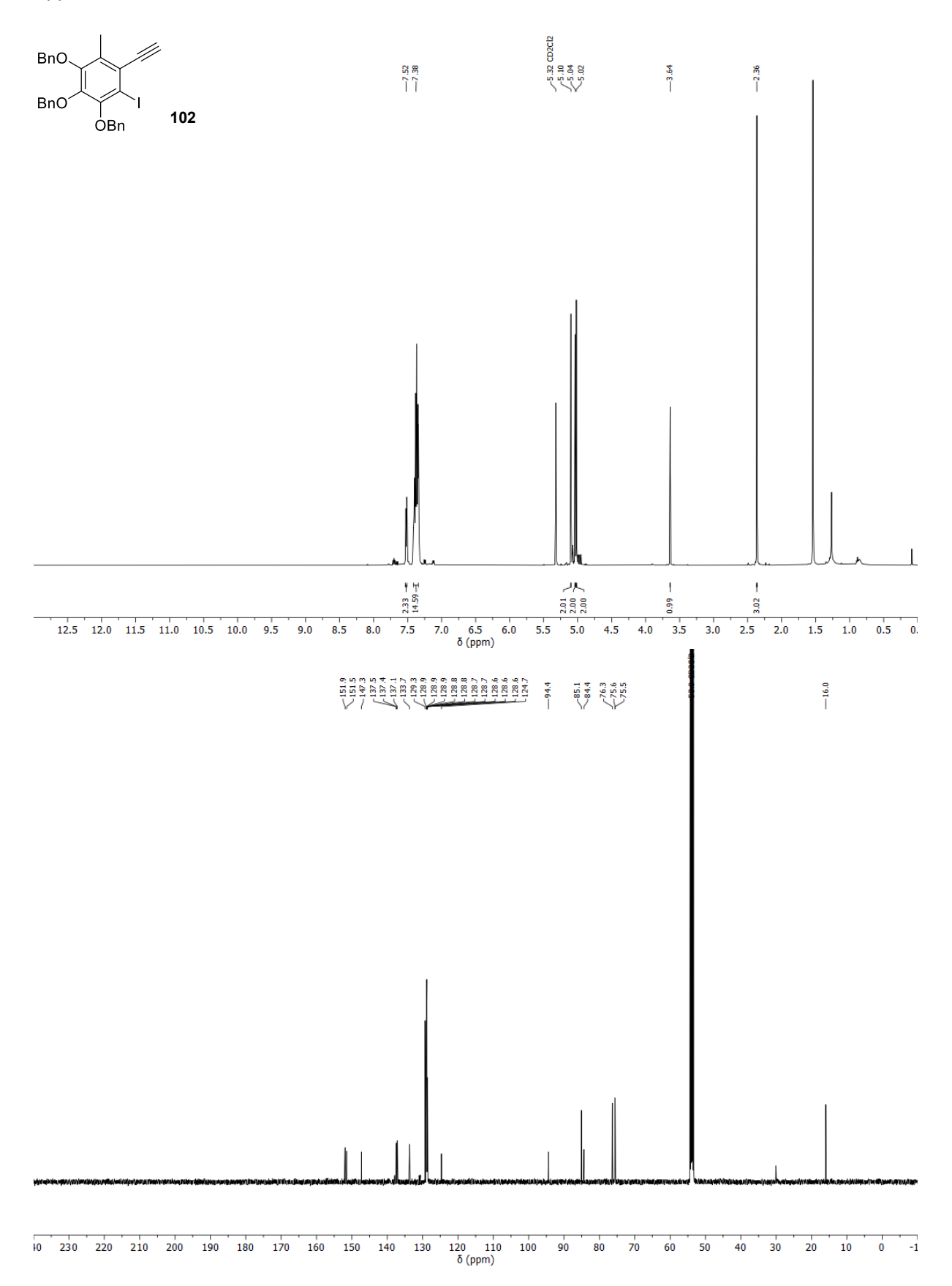
Appendix 32: ¹H- (top, 400 MHz) and ¹³C-NMR (bottom, 176 MHz) spectra of compound **97**, CD₂Cl₂, 298 K.



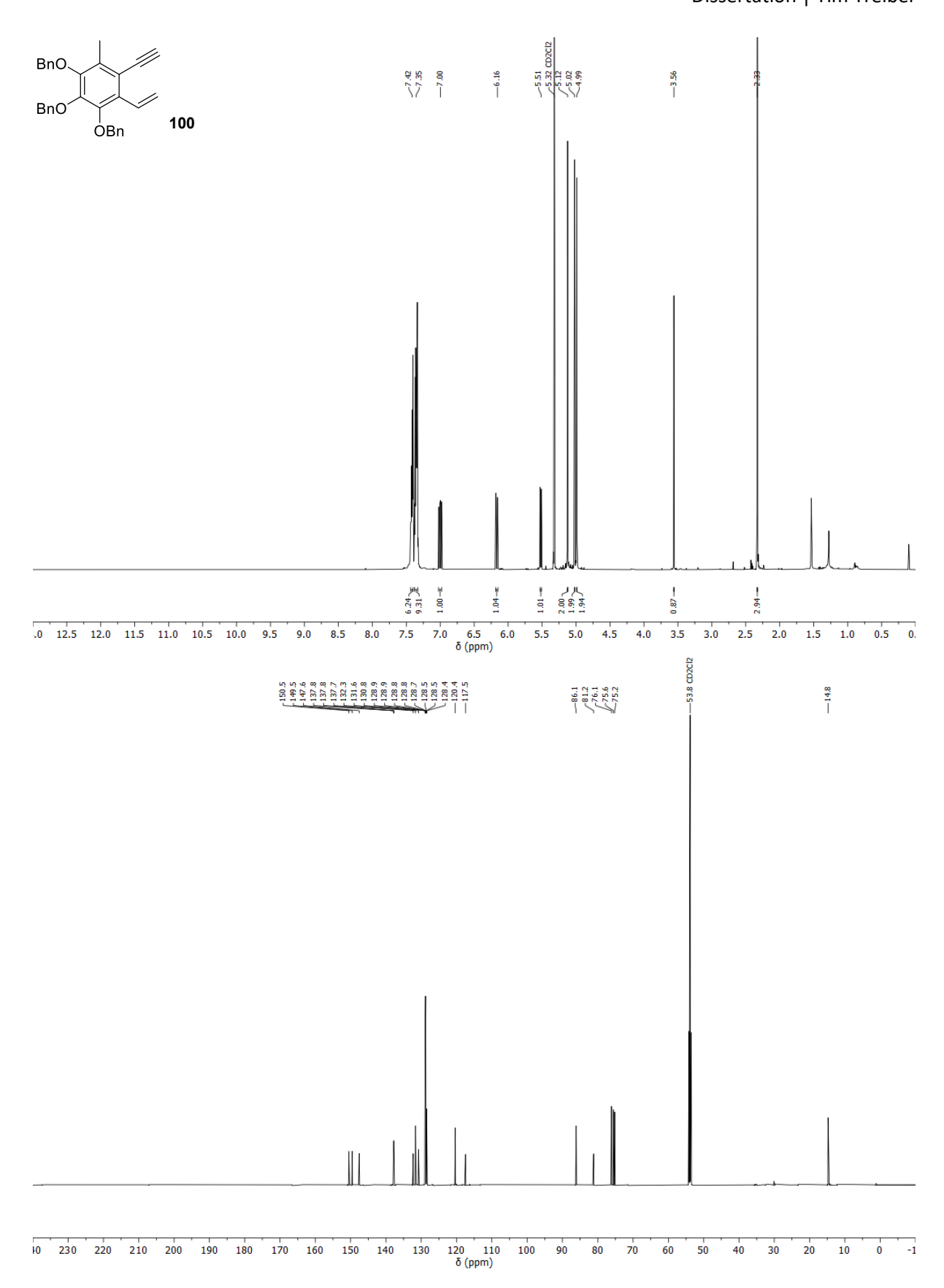
Appendix 33: ¹H- (top, 400 MHz) and ¹³C-NMR (bottom, 176 MHz) spectra of compound **98**, CD₂Cl₂, 298 K.



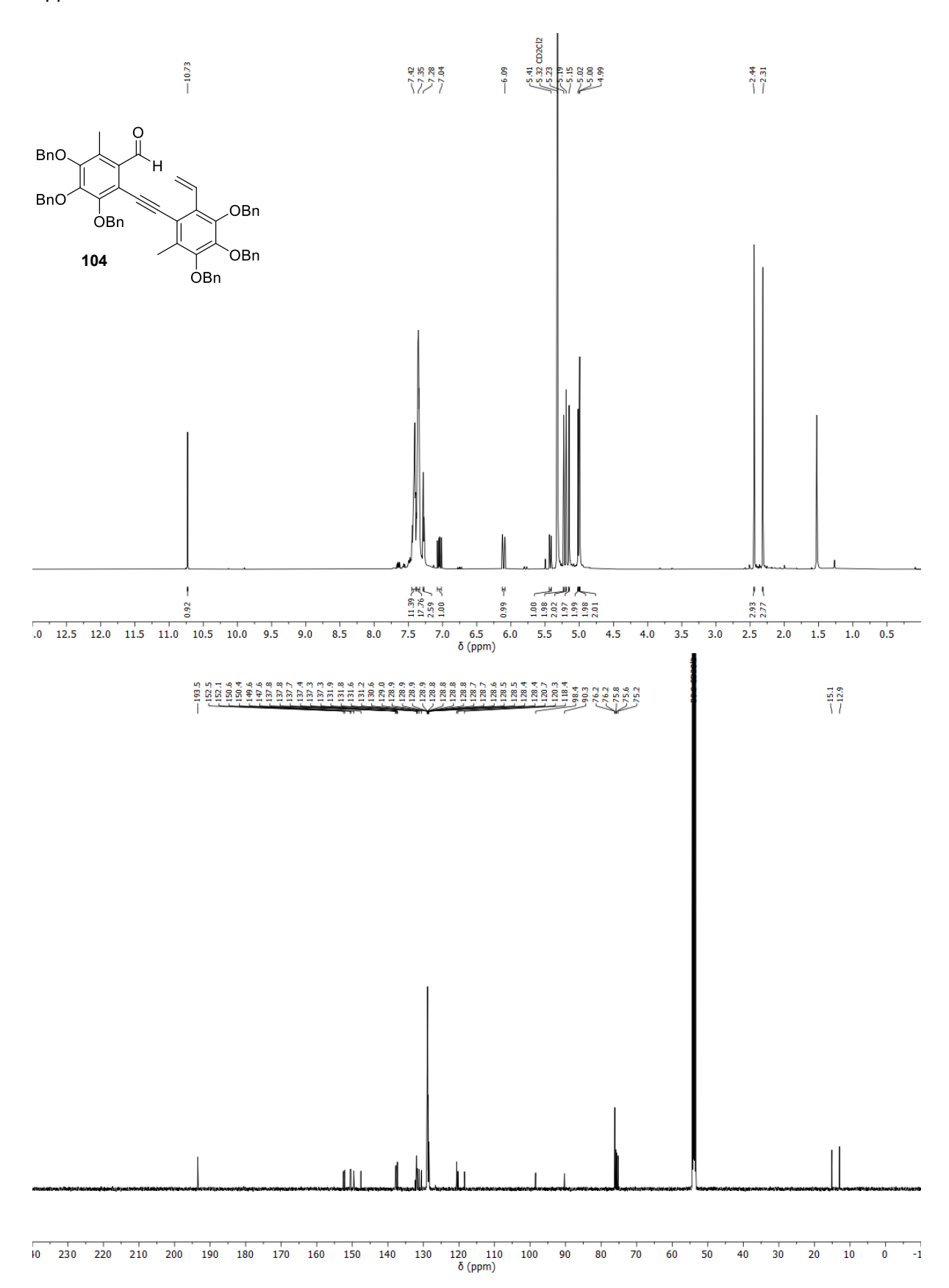
Appendix 34: ¹H- (top, 500 MHz) and ¹³C-NMR (bottom, 126 MHz) spectra of compound **99**, CD₂Cl₂, 298 K.



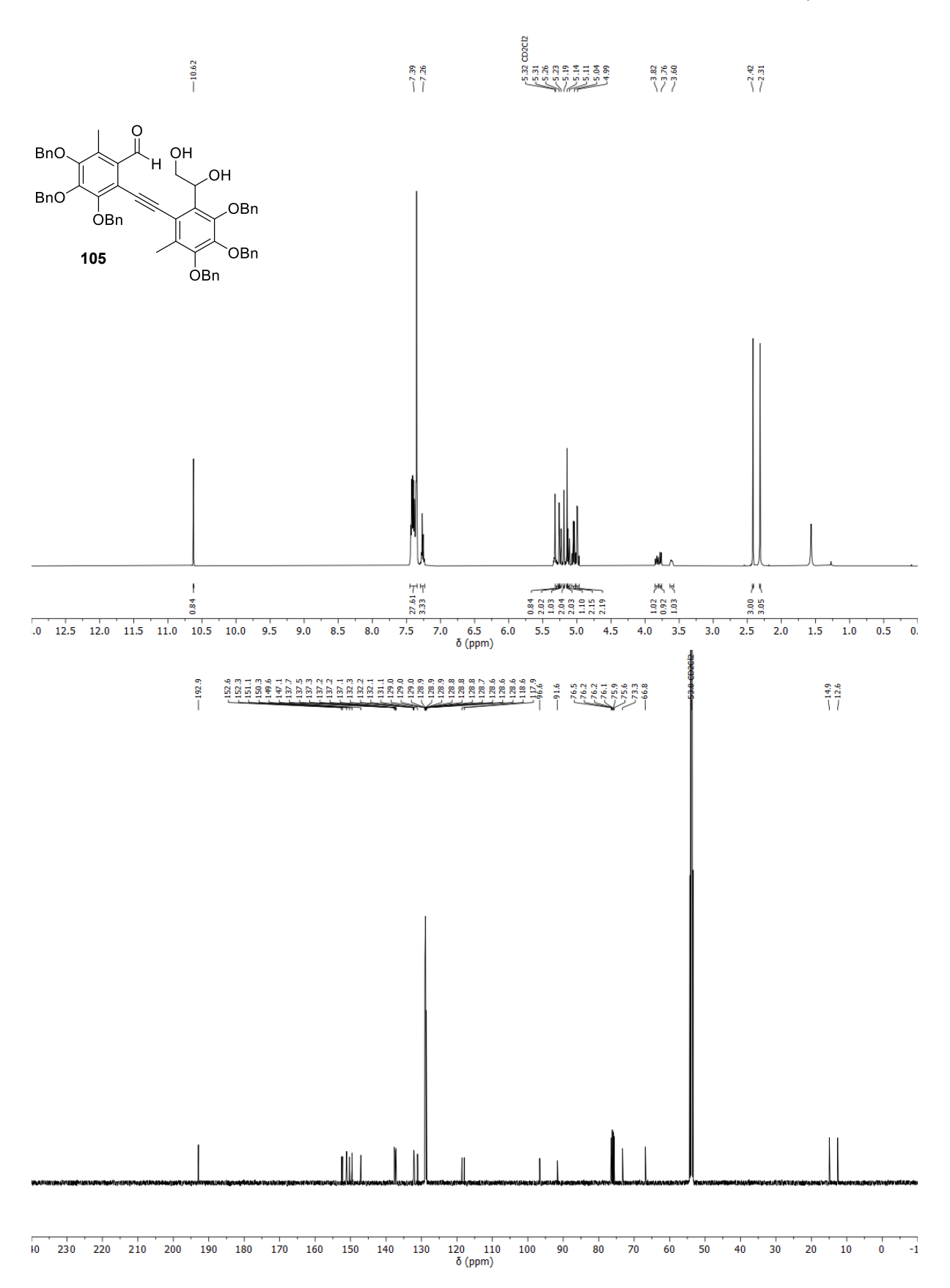
Appendix 35: ¹H- (top, 500 MHz) and ¹³C-NMR (bottom, 126 MHz) spectra of compound **102**, CD₂Cl₂, 298 K.



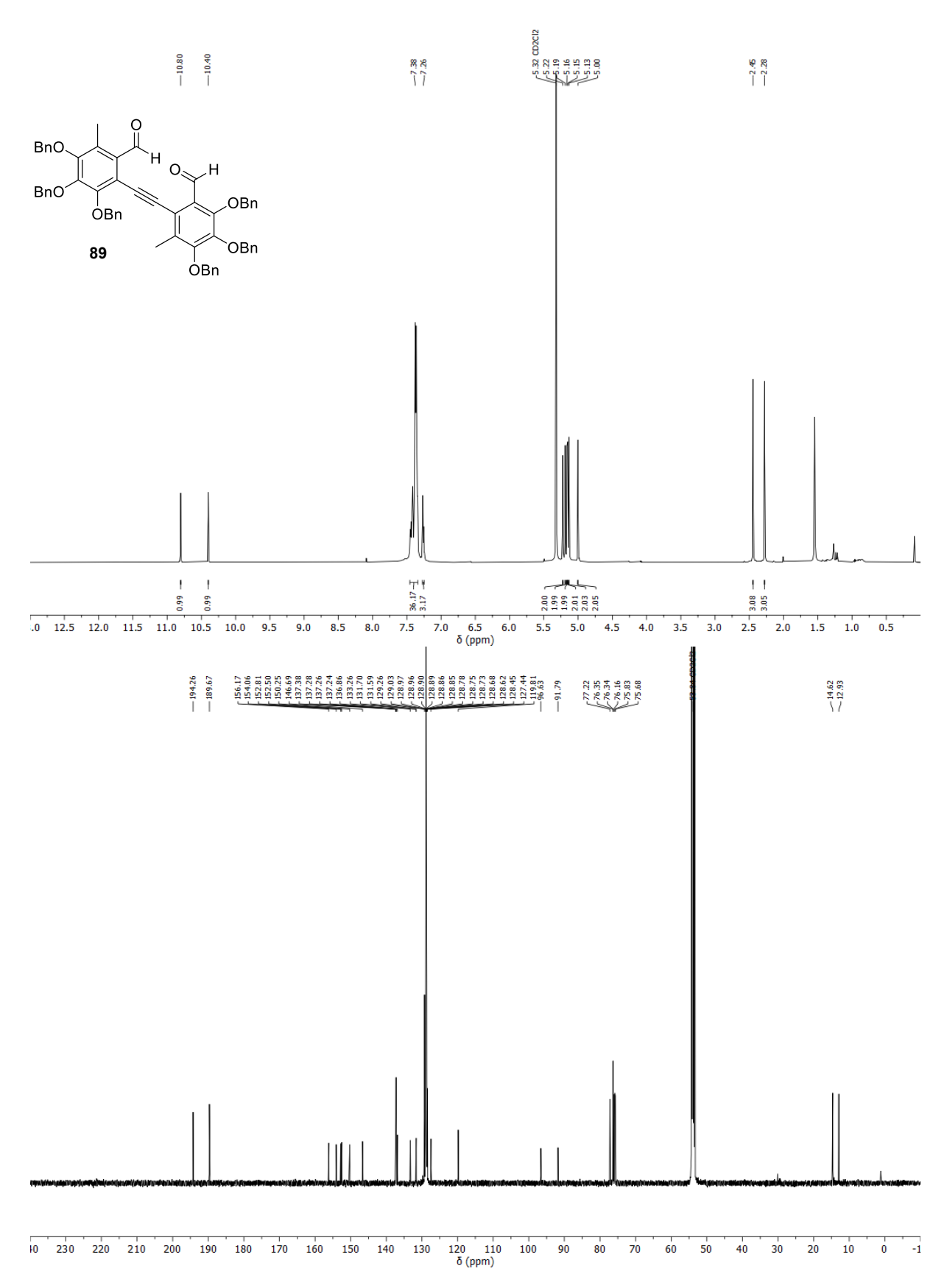
Appendix 36: ¹H- (top, 700 MHz) and ¹³C-NMR (bottom, 176 MHz) spectra of compound **100**, CD₂Cl₂, 298 K.



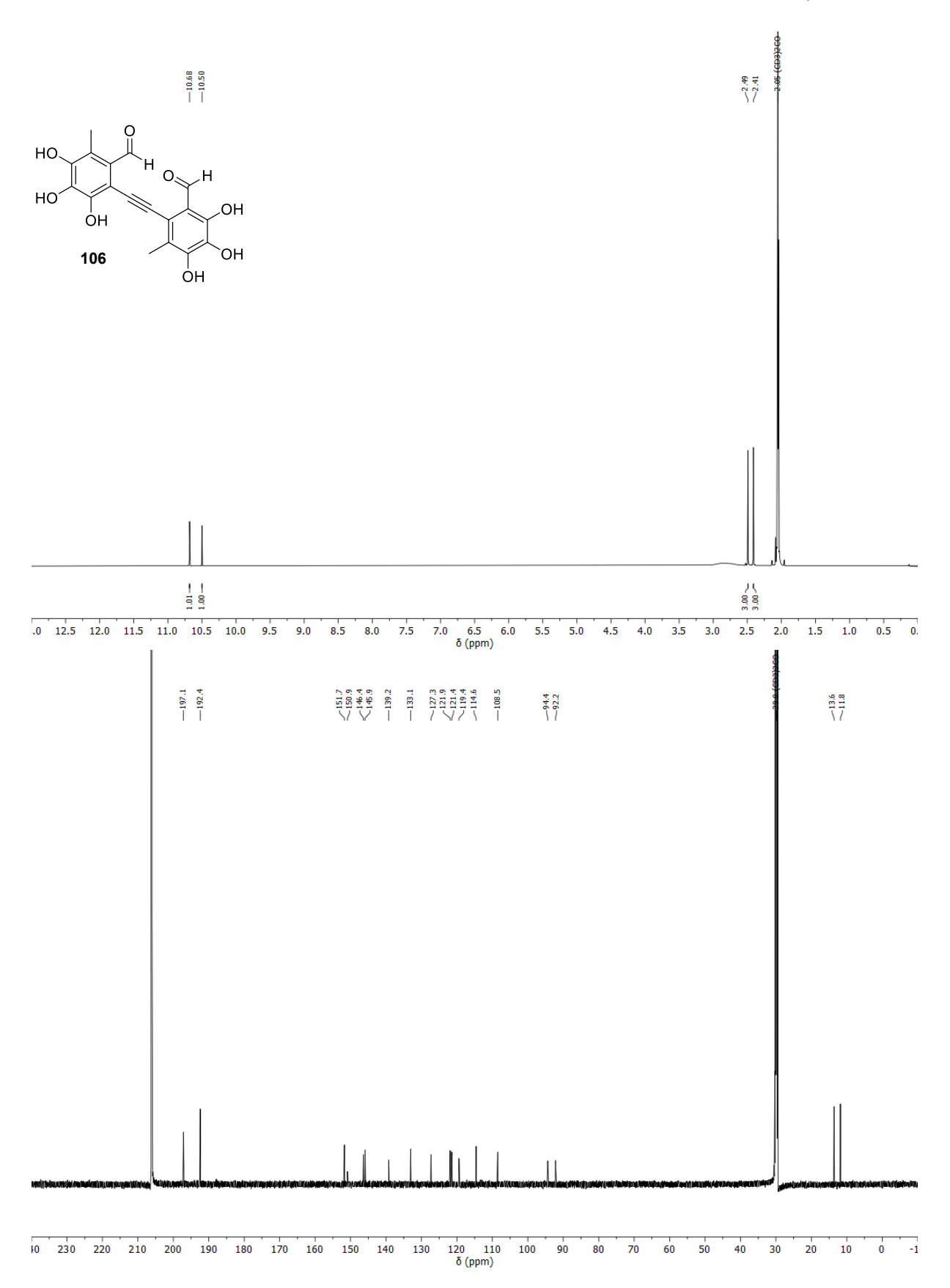
Appendix 37: ¹H- (top, 500 MHz) and ¹³C-NMR (bottom, 126 MHz) spectra of compound **104**, CD₂Cl₂, 298 K.



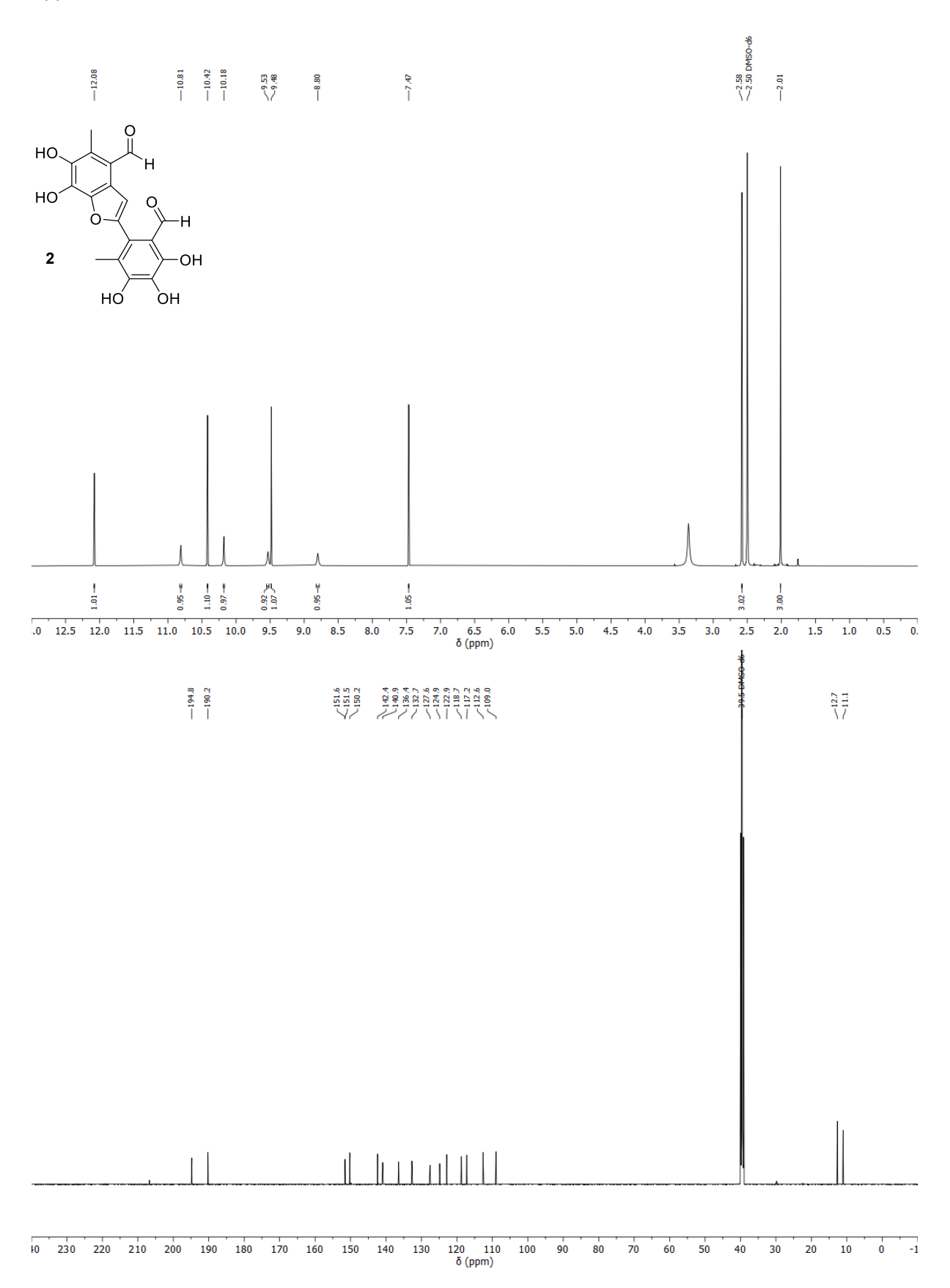
Appendix 38: ¹H- (top, 500 MHz) and ¹³C-NMR (bottom, 126 MHz) spectra of compound **105**, CD₂Cl₂, 298 K.



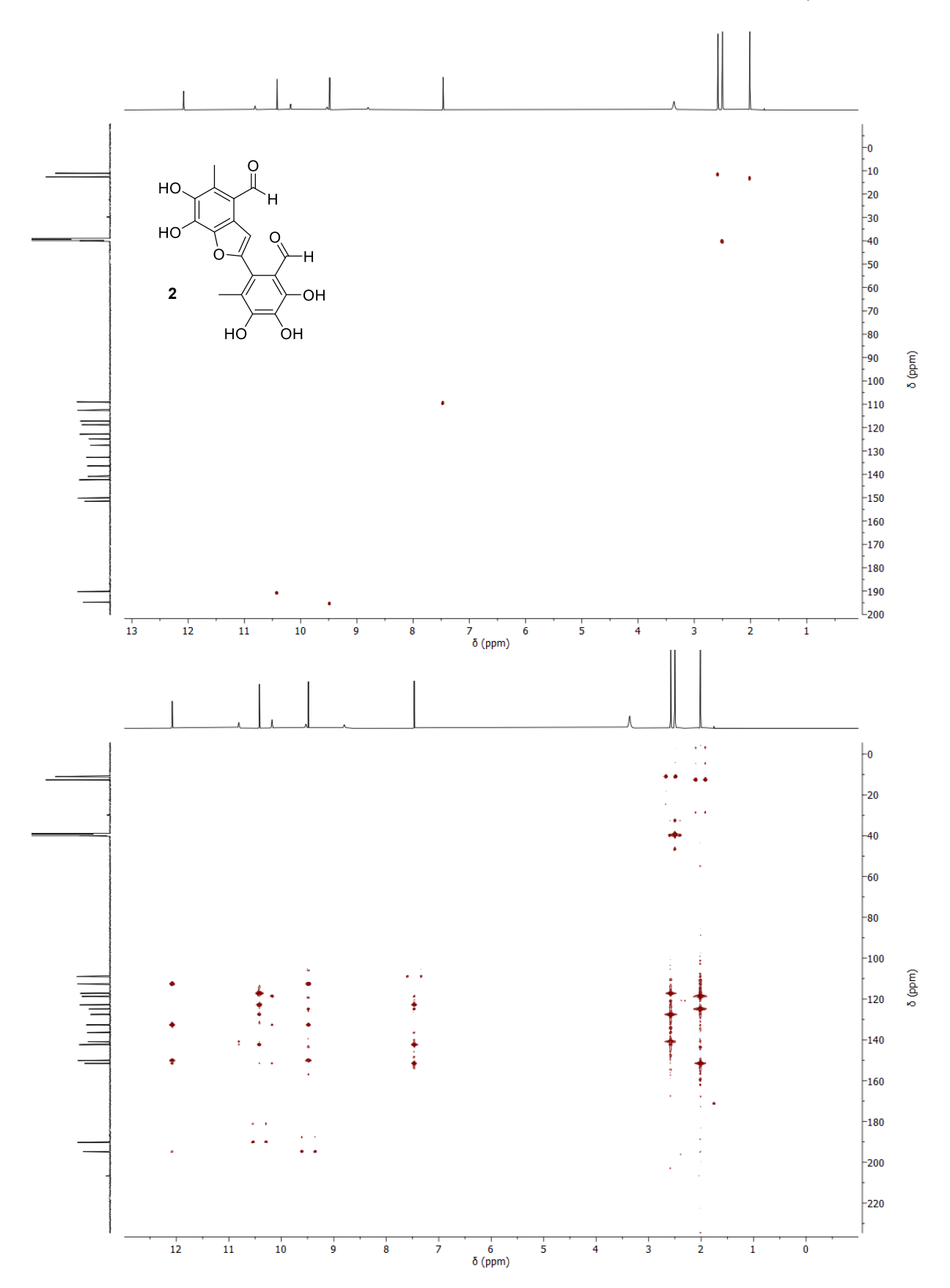
Appendix 39: ¹H- (top, 500 MHz) and ¹³C-NMR (bottom, 126 MHz) spectra of compound **89**, CD₂Cl₂, 298 K.



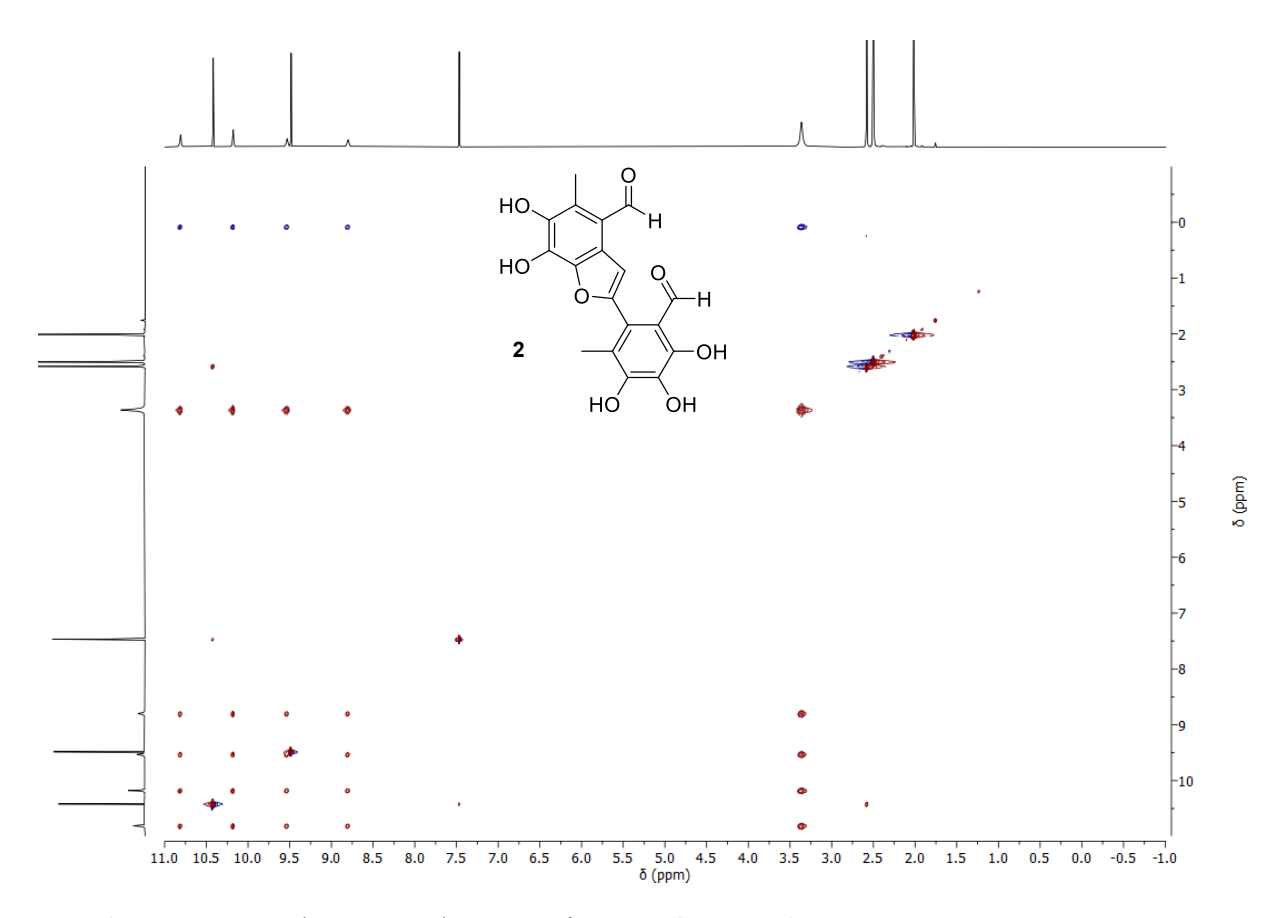
Appendix 40: ¹H- (top, 700 MHz) and ¹³C-NMR (bottom, 176 MHz) spectra of compound **106**, acetone-d6, 298 K.



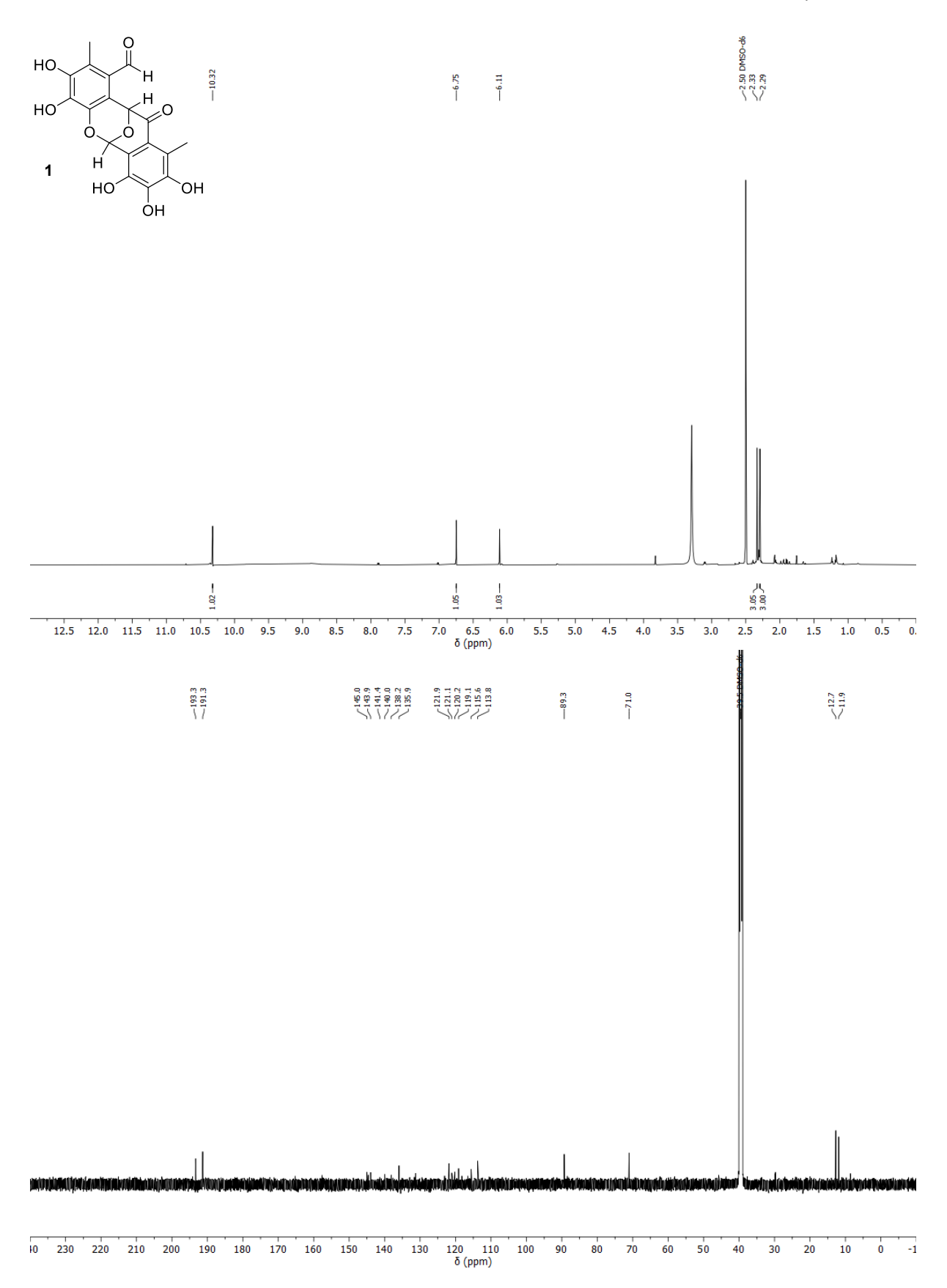
Appendix 41: ¹H- (top, 700 MHz) and ¹³C-NMR (bottom, 176 MHz) spectra of compound **2**, DMSO-d6, 298 K.



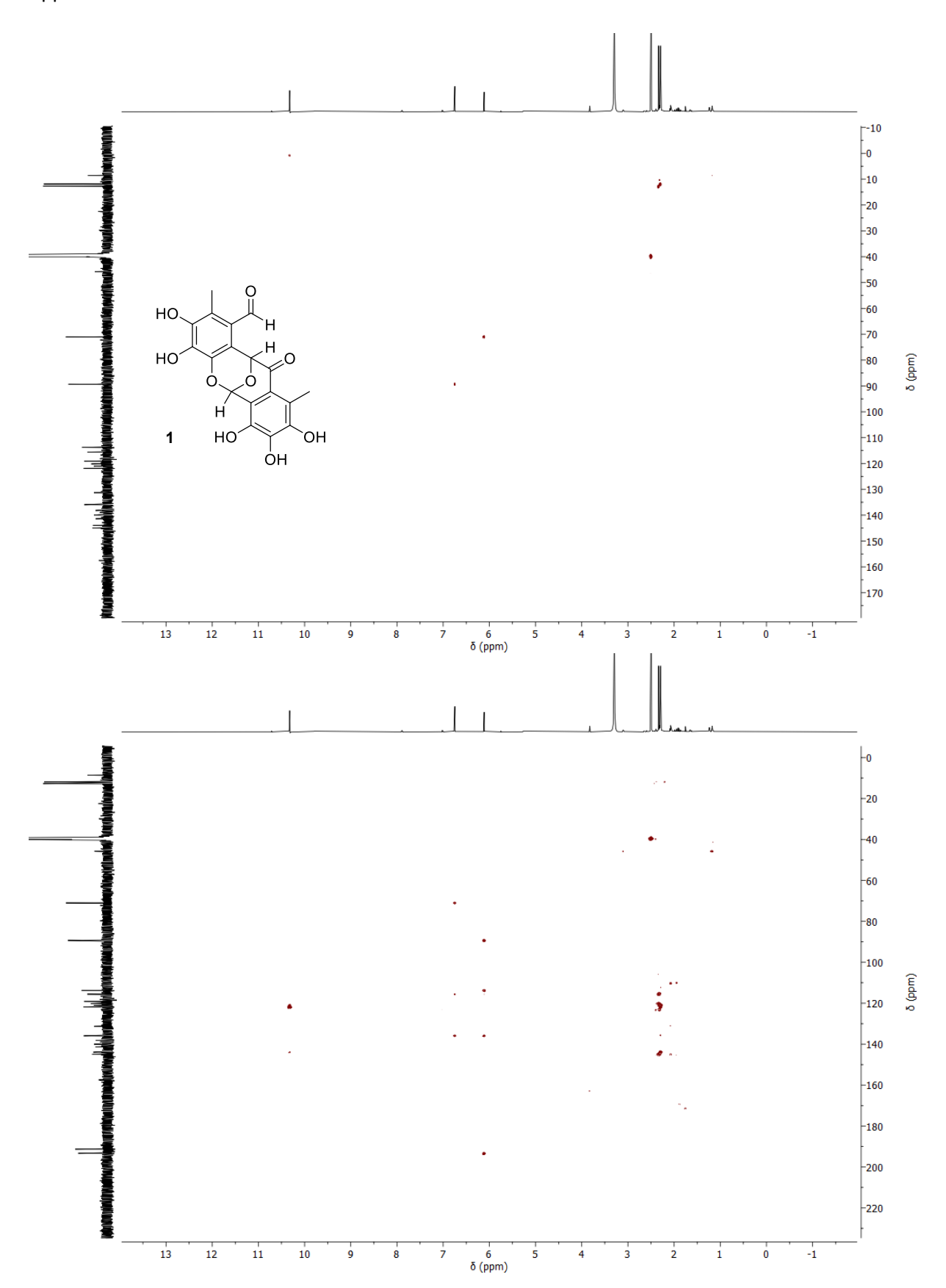
Appendix 42: HSQC (top, 700, 176 MHz) and HMBC-NMR (bottom, 700, 176 MHz) spectra of compound 2, DMSO-d6, 298 K.



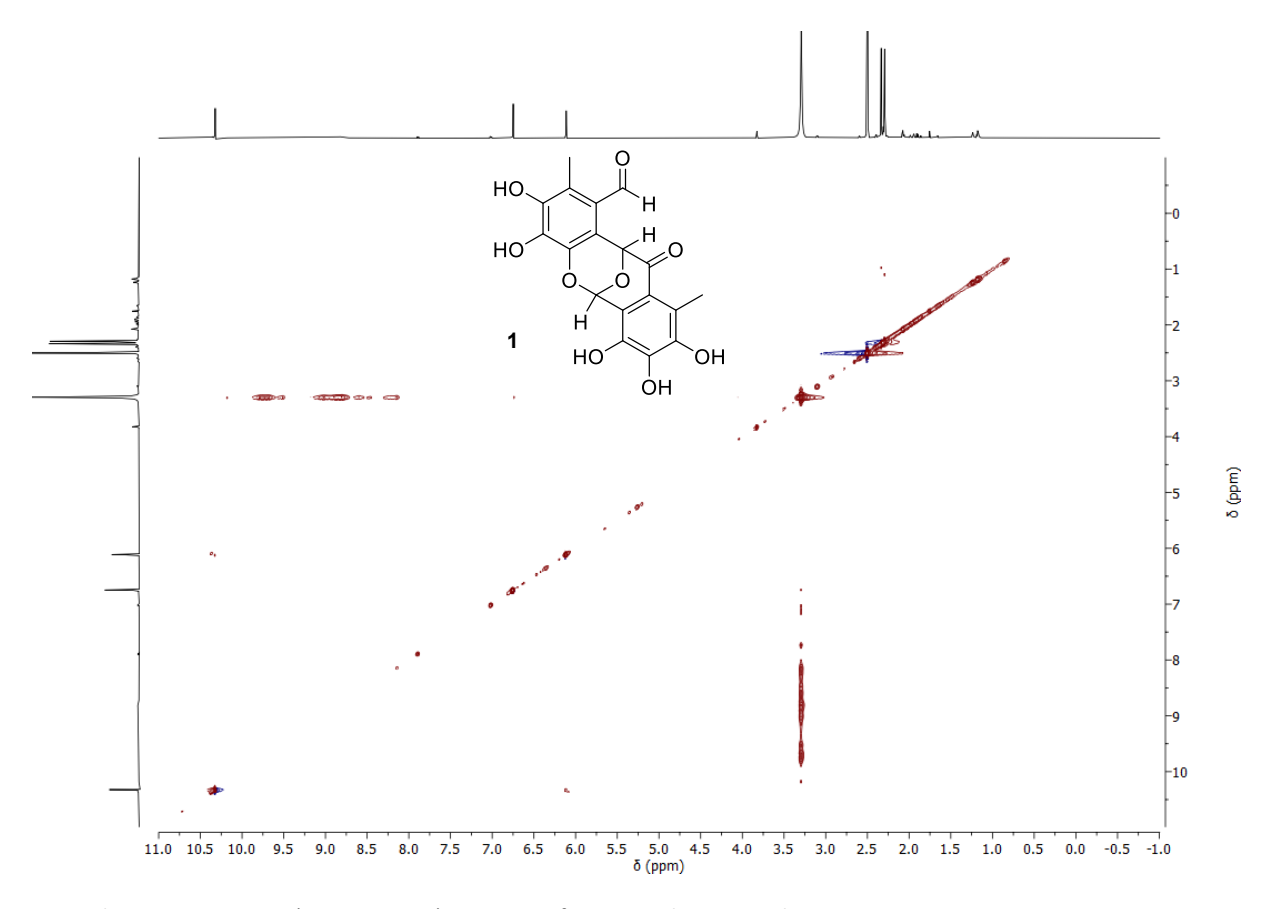
Appendix 43: NOESY-NMR (700, 700 MHz) spectrum of compound **2**, DMSO-d6, 298 K.



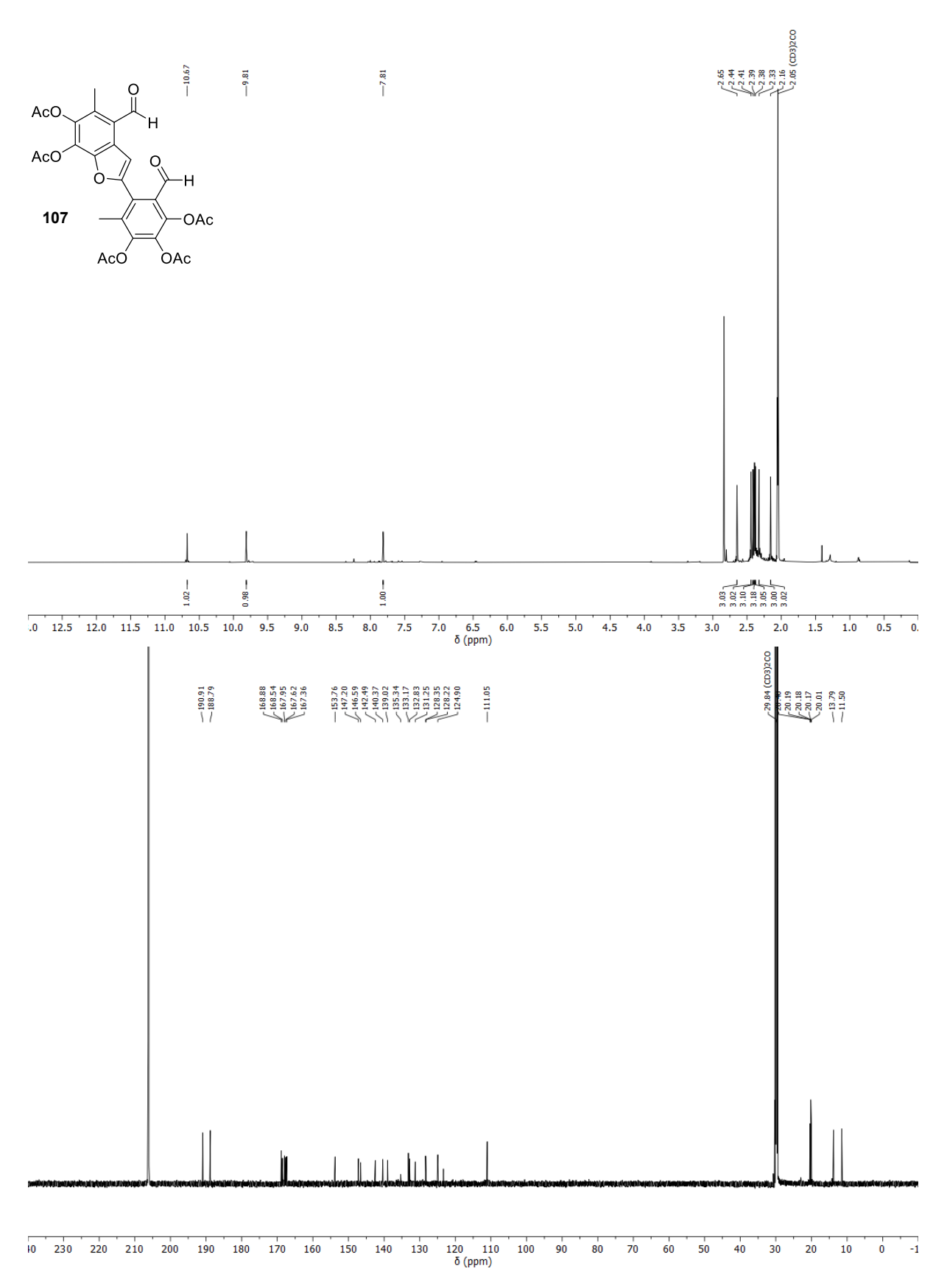
Appendix 44: ¹H- (top, 700 MHz) and ¹³C-NMR (bottom, 176 MHz) spectra of compound **1**, DMSO-d6, 298 K.



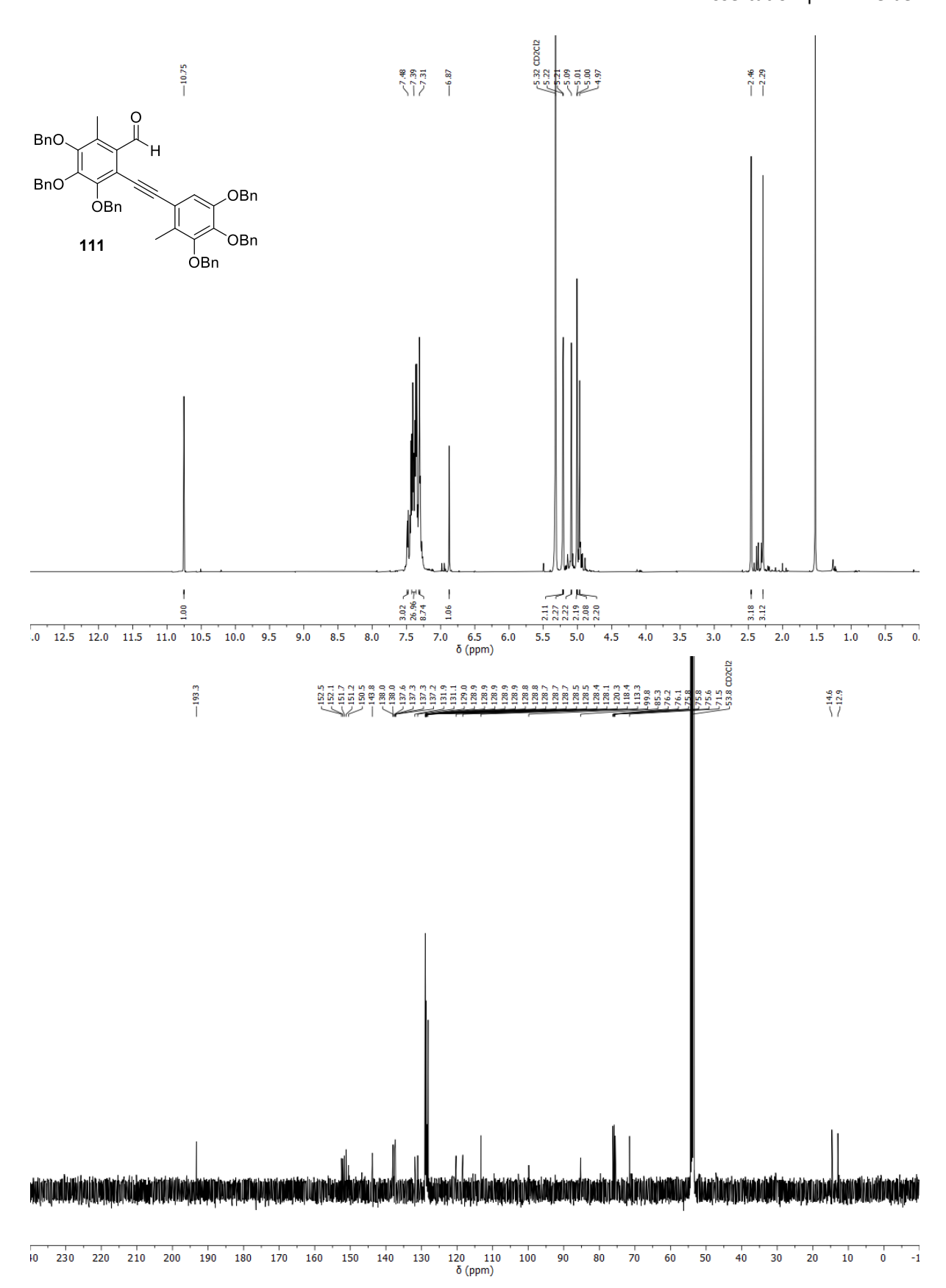
Appendix 45: HSQC (top, 700, 176 MHz) and HMBC-NMR (bottom, 700, 176 MHz) spectra of compound 1, DMSO-d6, 298 K.



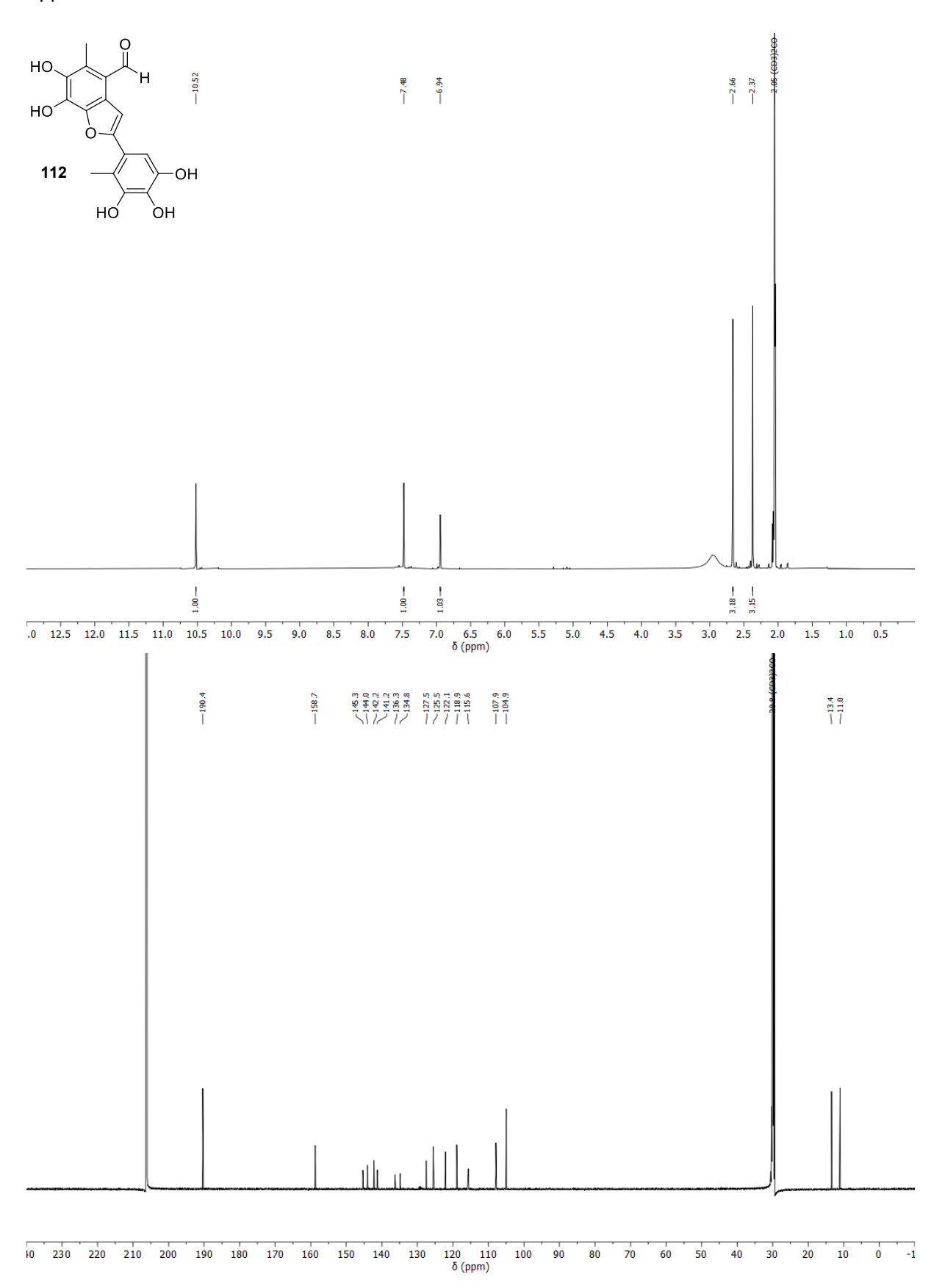
Appendix 46: NOESY-NMR (700, 700 MHz) spectrum of compound 1, DMSO-d6, 298 K.



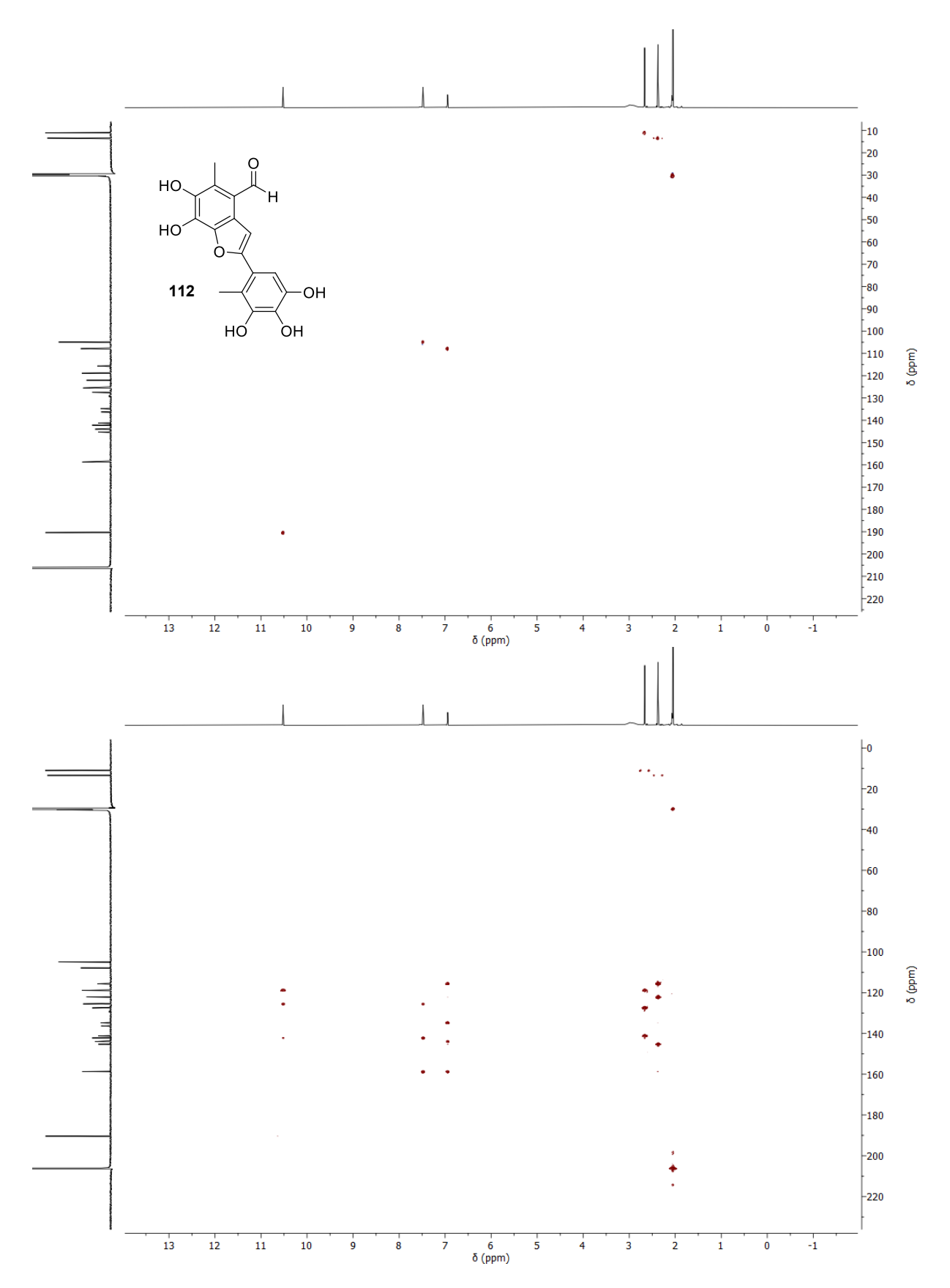
Appendix 47: ¹H- (top, 700 MHz) and ¹³C-NMR (bottom, 176 MHz) spectra of compound **107**, aceton-d6, 298 K.



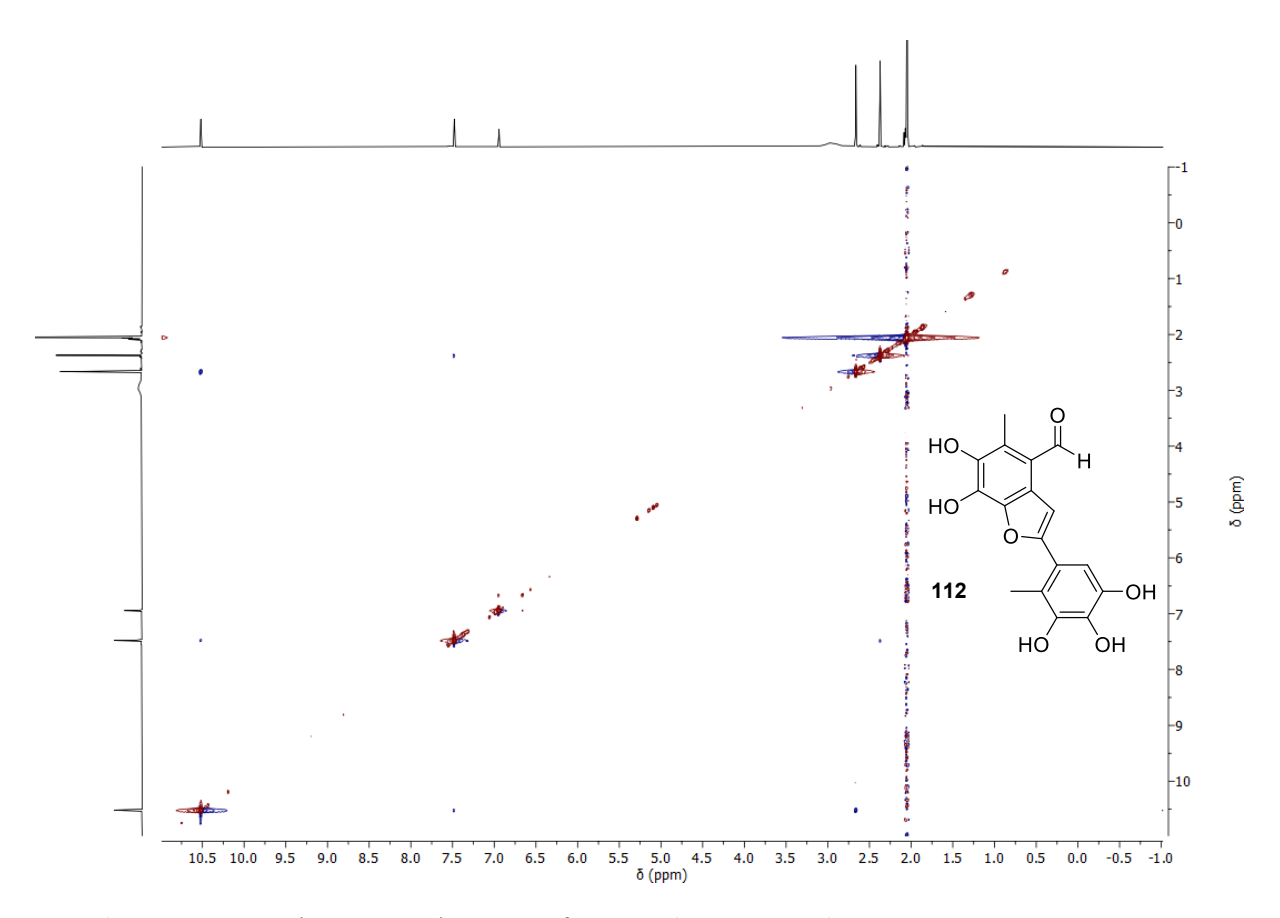
Appendix 48: ¹H- (top, 500 MHz) and ¹³C-NMR (bottom, 126 MHz) spectra of compound **111**, CD₂Cl₂, 298 K.



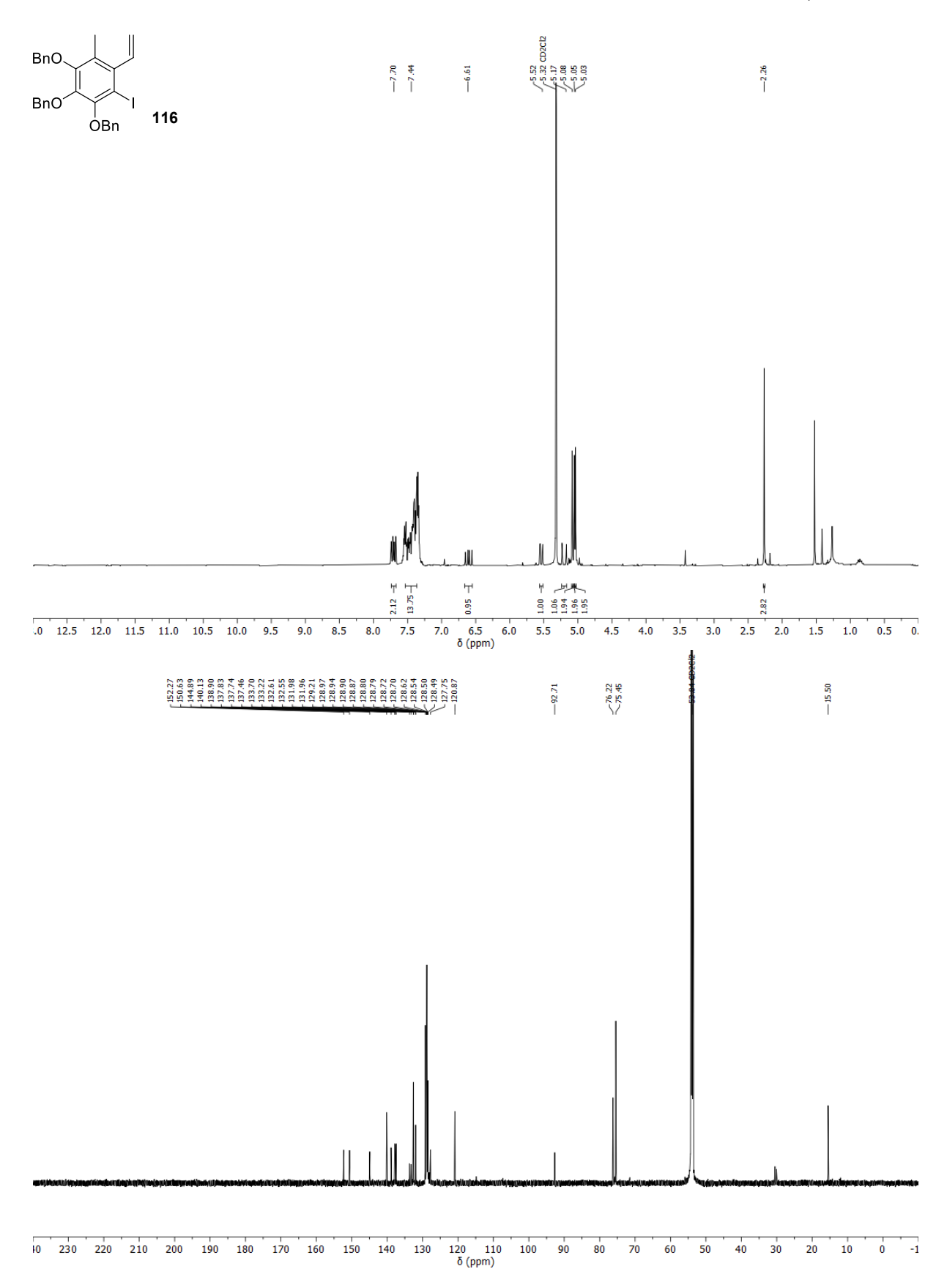
Appendix 49: ¹H- (top, 700 MHz) and ¹³C-NMR (bottom, 176 MHz) spectra of compound **112**, acetone-d6, 298 K.



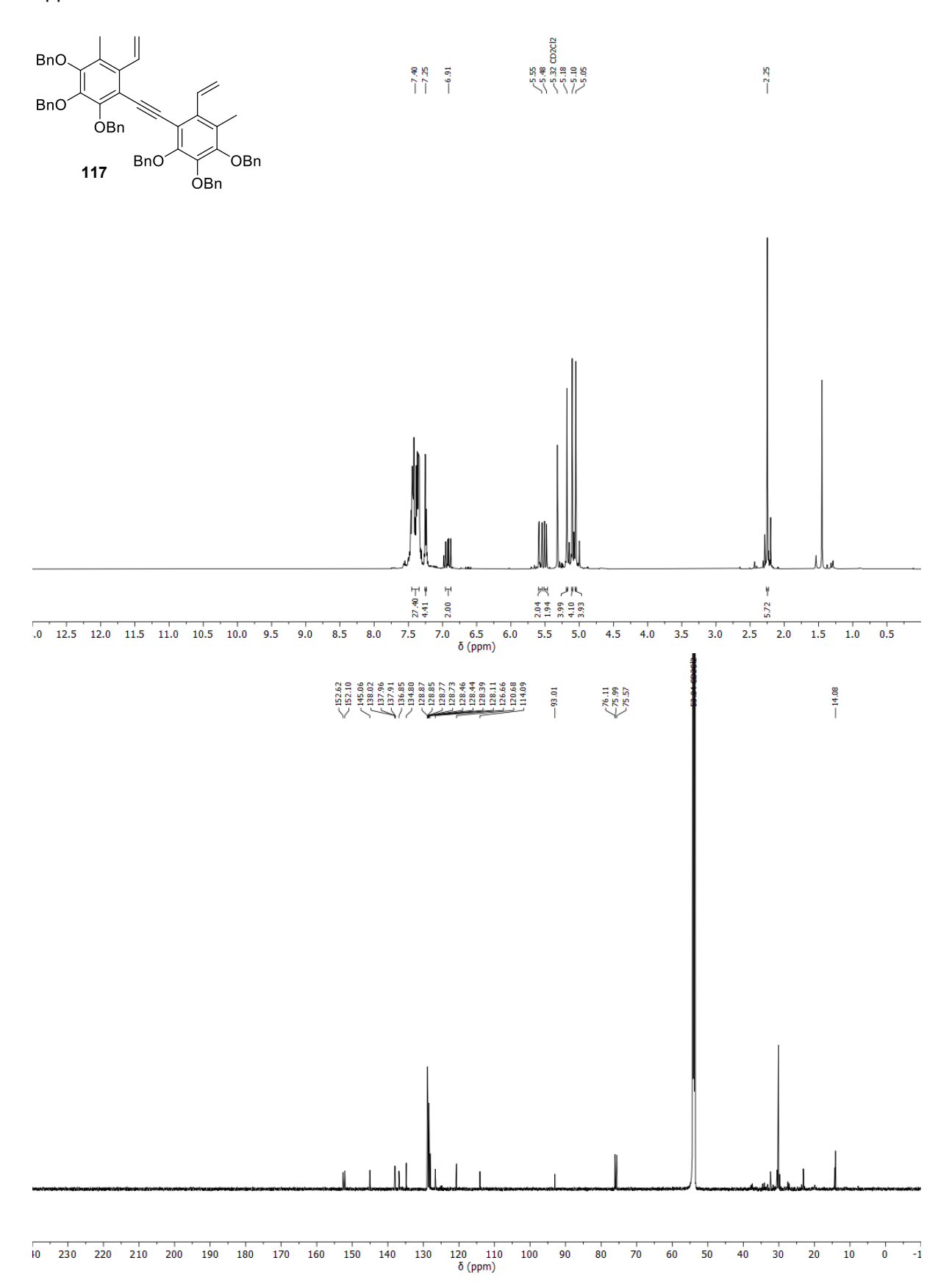
Appendix 50: HSQC (top, 700, 176 MHz) and HMBC-NMR (bottom, 700, 176 MHz) spectra of compound **112**, acetone-d6, 298 K.



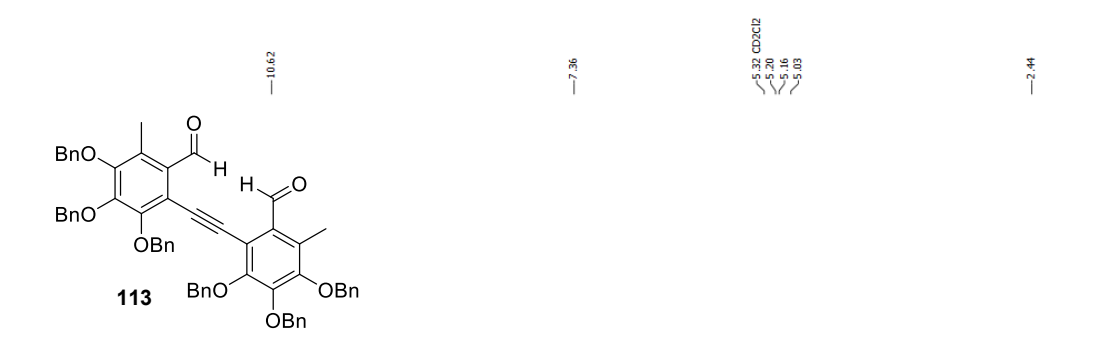
Appendix 51: NOESY-NMR (700, 700 MHz) spectrum of compound **112**, acetone-d6, 298 K.

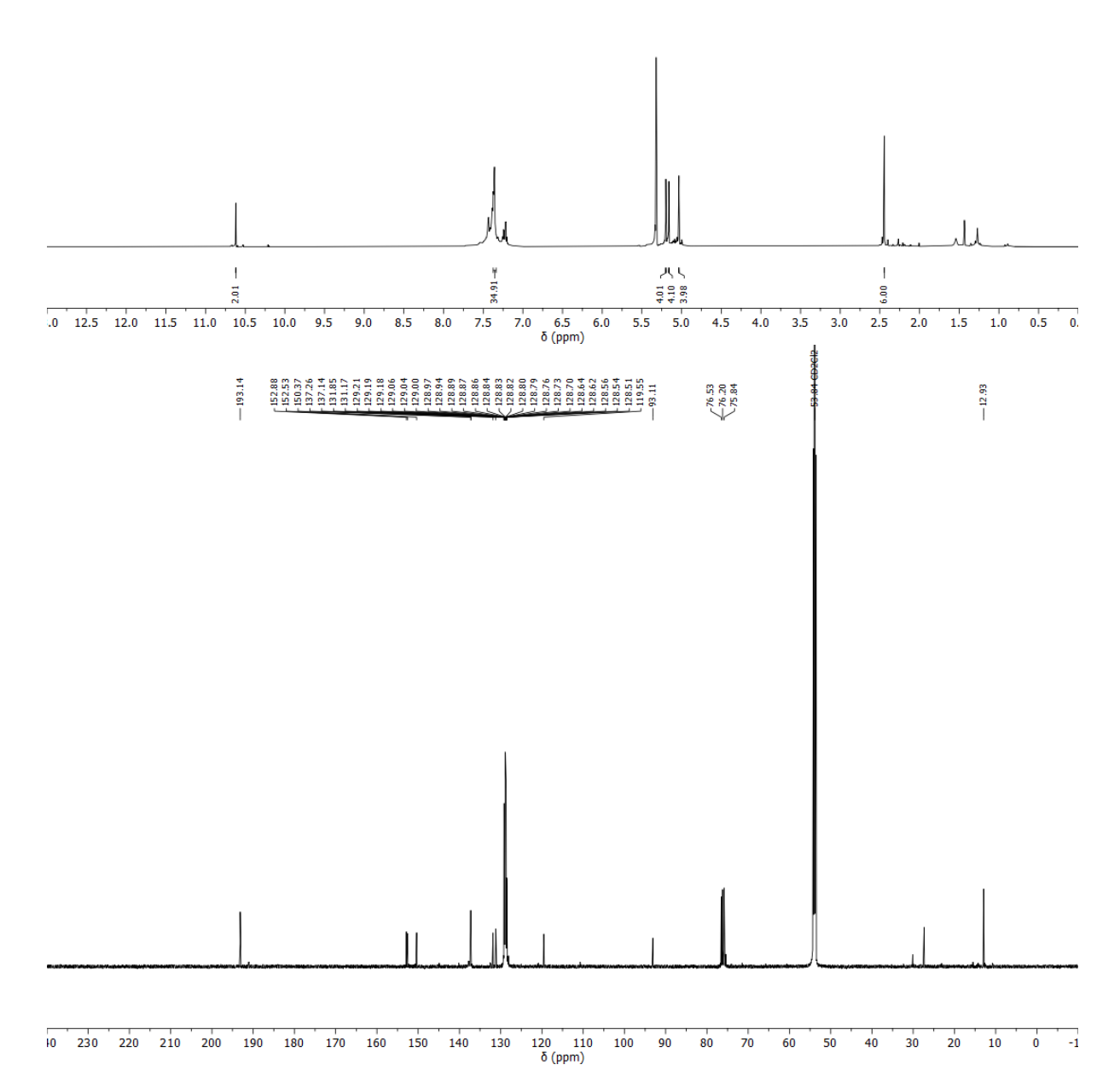


Appendix 52: ¹H- (top, 300 MHz, CD₂Cl₂) and ¹³C-NMR (bottom, 176 MHz, acetone-d6) spectra of compound **116**, 298 K.



Appendix 53: ¹H- (top, 400 MHz) and ¹³C-NMR (bottom, 176 MHz) spectra of compound **117**, CD₂Cl₂, 298 K.





Appendix 54: ¹H- (top, 700 MHz) and ¹³C-NMR (bottom, 176 MHz) spectra of compound **113**, CD₂Cl₂, 298 K.